AFRPL TR-82-092 AD:

Final Report

# Bondline Infrared Spectroscopy

January 1983

Thiokol Corporation
Huntsville Division
Huntsville, AL 35807

Thiokol Report U-82-14B
Contract F04611-80-C-0034

**Approved for Public Release**

Distribution unlimited. The AFRPL Technical Services Office has reviewed this report, and it is releasable to the National Technical Information Service, where it will be available to the general public including foreign nationals



Prepared for the: **Air Force Rocket Propulsion Laboratory**

Air Force Space Technology Center
Space Division, Air Force Systems Command
Edwards Air Force Base,
California 93523

## NOTICE



## FOREWORD

This Technical Report was prepared by the Thiokol/Hunstville Division, Thiokol Corporation, Hunstville, AL 35807 in partial fulfillment of the requirements of Contract F04611-80-C-0034, Job Order No. 57013LJ with the Air Force Rocket Propulsion Laboratory, Edwards AFB, CA 93523.

This Technical Report is approved for release and distribution in accordance with the distribution statement on the cover and on the DD Form 1473.

R. John Moss

R. JOHN MOSS, CAPT, USAF
Project Manager

Francisco Q. Roberto

FRANCISCO Q. ROBERTO
Chief, Propellant Development Branch

FOR THE DIRECTOR

Thomas C. Meier

THOMAS C. MEIER, LT COL, USAF
Director, Solid Rocket Divsion

UNCLASSIFIED

SECURITY CLASSIFICATION OF THIS PAGE (When Data Entered)

| REPORT DOCUMENTATION PAGE | | READ INSTRUCTIONS BEFORE COMPLETING FORM |
|---|---|---|
| 1. REPORT NUMBER AFRPL-TR-82-92 | 2. GOVT ACCESSION NO. A124 728 | 3. RECIPIENT'S CATALOG NUMBER |
| 4. TITLE (and Subtitle) Bondline Infrared Spectroscopy (BIS), Final Report | | 5. TYPE OF REPORT & PERIOD COVERED Final Report 80 Sep 01 - 82 Nov 30 |
| | | 6. PERFORMING ORG. REPORT NUMBER U-82-14B |
| 7. AUTHOR(s) W. W. Schwarz, et al | | 8. CONTRACT OR GRANT NUMBER(s) AFRPL F04611-80-C-0034 |
| 9. PERFORMING ORGANIZATION NAME AND ADDRESS Thiokol Corporation Huntsville Division Huntsville, Alabama 35807 | | 10. PROGRAM ELEMENT, PROJECT, TASK AREA & WORK UNIT NUMBERS JON: 573013LJ EEIC: 588 |
| 11. CONTROLLING OFFICE NAME AND ADDRESS Air Force Rocket Propulsion Laboratory/MKPB Edwards Air Force Base, California 93523 | | 12. REPORT DATE January 1983 |
| | | 13. NUMBER OF PAGES 227 |
| 14. MONITORING AGENCY NAME & ADDRESS(if different from Controlling Office) | | 15. SECURITY CLASS. (of this report) Unclassified |
| | | 15a. DECLASSIFICATION/DOWNGRADING SCHEDULE N/A |

16. DISTRIBUTION STATEMENT (of this Report)

Approved for Public Release. Distribution Unlimited.

17. DISTRIBUTION STATEMENT (of the abstract entered in Block 20, if different from Report)

Approved for Public Release. Distribution Unlimited.

18. SUPPLEMENTARY NOTES

Principal Investigator was W. W. Schwarz. R. J. Schorr was Computer Programmer. W. I. Dale, Jr. was Program Manager, Significant technical contributions were made by J. W. Blanks.

19. KEY WORDS (Continue on reverse side if necessary and identify by block number)

Solid propellant rocket motor, aging and surveillance, service life, HTPB propellant, minimum smoke propellant, Fourier transform infrared spectroscopy, FTIS, FTIR, bondline, bond aging


20. ABSTRACT (Continue on reverse side if necessary and identify by block number)

Laboratory procedures for making the IR spectrum of propellant, liner, and insulation were established. Samples of an HTPB propellant bond system and a minimum smoke propellant bond system were aged for 32 weeks at up to 165°F. Changes in the absorption (peak height) of certain IR wave lengths in the spectra of the binders of the propellants, liners, and insulations were correlated to changes in the strengths of the bond between the various substrates. Computer programs were written to perform the IR data reduction, correlate the changes taking place in IR absorption and bond strength, compute (over)


DD FORM 1 JAN 73 1473 EDITION OF 1 NOV 65 IS OBSOLETE

UNCLASSIFIED

SECURITY CLASSIFICATION OF THIS PAGE (When Data Entered)

20. (continued)

reaction rate constants, reaction activation energy and predict bond strengths at some future times at selected temperatures.

## TABLE OF CONTENTS


| Title | Page No. |
|---|---|
| List of Tables | 4 |
| List of Figures | 7 |
| INTRODUCTION | 14 |
| OBJECTIVE | 14 |
| BACKGROUND | 14 |
| PROJECT OUTLINE | 15 |
| SUMMARY OF ACCOMPLISHMENTS | 17 |
| TECHNICAL ACCOMPLISHMENTS | 19 |
| GENERAL REMARKS | 19 |
| PHASE I - ANALYTICAL DEVELOPMENT | 19 |
| Task 1 - IR Data Acquisition Methodology | 19 |
| Selection of Bond Systems | 19 |
| Preparation of Bond Systems | 19 |
| Thermal Shock Debonding | 24 |
| "Bond Zone" Study | 24 |
| Gel/Sol Separation Procedures for Insulation & Liner | 33 |
| Insulation | 33 |
| Liner | 35 |
| Statistical Evaluation of the Harrick ATR Unit | 35 |
| IR Spectrum of Minimum Smoke Propellant | 41 |
| IR Data Collection Parameters | 44 |
| Evaluation of FTS-10 "Collect" Parameters | 44 |
| Sample Thickness | 56 |
| Torque Level | 59 |
| IRE Cleaning Procedure | 59 |
| Final Procedure for Taking IR Spectra | 64 |
| Task 2 - Computer Programming | 64 |
| Task 3 - Correlation of IR and Bond Properties | 67 |
| Selected Bond Systems | 67 |
| Aging Plan | 67 |
| Aging Data | 67 |
| Data Analysis | 70 |
| HTPB Propellant | 70 |
| HTPB TL-H755A | 74 |

Table of Contents (Continued)


| Title | Page No. |
|---|---|
| Data Analysis (Continued) | |
| TI-R300 Insulation | 80 |
| Minimum Smoke Propellant Gel Fraction | 96 |
| Conclusions from Phase I Work | 106 |
| PHASE II - SERVICE LIFE | 107 |
| Task 1 - Future Properties Programming | 107 |
| Summary of Programs | 107 |
| E410 - Propellant Properties Computer Program Description | 109 |
| E490 - IR Data Reduction Computer Program Description | 111 |
| E571 - Activation Energy Computer Program Description | 111 |
| E572 - Multiple Regression Computer Program Description | 113 |
| E575 - Future Properties Computer Program Description | 114 |
| Rationale for Future Bond Property Prediction | 115 |
| Task 2 - Bond System Aging and Data Analysis | 117 |
| Preparation of Bond Samples for Aging | 117 |
| Aging Plan | 120 |
| Aging Data | 120 |
| Bond Data | 120 |
| IR Data | 120 |
| Analysis of TP-H8288 Data | 129 |
| IR Data and Time/Temperature | 129 |
| IR Data and Bond Properties | 133 |
| Analysis of TP-Q7030 Data | 140 |
| IR Data and Time/Temperature | 140 |
| IR Data and Bond Properties | 143 |
| Prediction of Bond Strength | 148 |
| Analysis of MSL-303 Propellant Data | 150 |
| Mechanical Properties and Time/Temperature | 150 |
| IR Data and Time | 153 |
| IR Data and Mechanical Properties | 163 |
| CONCLUSIONS AND RECOMMENDATIONS | 169 |
| CONCLUSIONS | 169 |
| RECOMMENDATIONS | 169 |

Table of Contents (Continued)


| Title | Page No. |
|---|---|
| APPENDIX A - Correlation of Spectral Changes with Sample Location | 170 |
| APPENDIX B - Infrared Testing Procedures | 181 |
| HTPB Propellant Bondline Infrared Testing Procedure | 182 |
| Minimum Smoke Propellant Bondline Infrared Testing Procedure | 183 |
| APPENDIX C - Correlations Among Mechanical Properties, Hardness, Gel Fraction and Time for HTPB Bond System Aged 16 Weeks | 185 |
| APPENDIX D - Correlations Among Mechanical Properties, Hardness, Gel Fraction and Time for Minimum Smoke Propellant Bond System Aged 16 Weeks | 201 |
| APPENDIX E - Data Plots for MSL-303 Propellant | 219 |

## LIST OF TABLES


| Number | Title | Page No. |
|---|---|---|
| 1 | HTPB Propellant Bond System (AMRAAM) | 20 |
| 2 | Minimum Smoke Propellant Bond System | 21 |
| 3 | Bond Samples - HTPB Propellant | 22 |
| 4 | Bond Samples - Minimum Smoke Propellant | 23 |
| 5 | Gel/Sol Separation of TI-R300 | 34 |
| 6 | Gel/Sol Separation of Liner (TL-H755A/RL-05680) | 36 |
| 7 | Gel/Sol Separation of Liner (TL-H763A/LM-23926) | 37 |
| 8 | FTIS Precision Study | 38 |
| 9 | FTIS Study - Summary of Averages | 39 |
| 10 | FTIS Study - Summary of Standard Deviations | 39 |
| 11 | Standard Deviation and General Ranking of Various ATR/IRE Combinations | 40 |
| 12 | Experiment Design for Analysis of FTS-10 "Collect" Parameters | 46 |
| 13 | FTIS Precision Study (ATR by Barnes Engineering) | 48 |
| 14 | FTIS Study - Summary of Averages | 49 |
| 15 | FTIS Study - Summary of Standard Deviations | 49 |
| 16 | Absorption Data for Variance Analysis | 54 |
| 17 | Variance of IR Spectra | 55 |
| 18 | Variance of IR Spectra | 57 |
| 19 | Sample-To-Sample Variance | 65 |
| 20 | Data Acquisition Procedures for HTPB Propellant | 66 |
| 21 | Composition of Bond Samples (Phase I, Task 3) | 68 |
| 22 | Aging Plan - Phase I, Task 3 | 69 |
| 23 | Test Results, HTPB Propellant/Liner/Insulation 165°F Bond Aging | 71 |
| 24 | Test Results, Minimum Smoke Propellant/Liner/Insulation | 72 |

List of Tables (Continued)


| Number | Title | Page No. |
|---|---|---|
| 25 | Correlation Coefficients: Peak Heights and Liner Properties | 83 |
| 26 | Summary of Project Computer Programs | 108 |
| 27 | HTPB Type Bond System Aging | 118 |
| 28 | Minimum Smoke Type Bond System Aging | 119 |
| 29 | AIM-9L Aging Test Matrix | 121 |
| 30 | Minimum Smoke Aging Test Matrix | 122 |
| 31 | HTPB Propellant Bond System Aging (Mix T-1161) | 123 |
| 32 | Minimum Smoke Propellant Bond System Aging | 124 |
| 33 | Correlation of IR Peak Height and Time. IR of Propellant at Bond Interface. | 132 |
| 34 | Correlation of IR ln Peak Height and Time. IR of Propellant at Bond Interface. | 132 |
| 35 | Correlation of ln Reaction Rate Constant and 1/Temperature | 134 |
| 36 | Correlation of IR Peak Height and Time. IR of Propellant 0.5 Inch from Interface | 134 |
| 37 | Correlation of ln IR Peak Height and Time. IR of Propellant 0.5 Inch from Interface. | 135 |
| 38 | Correlation of ln Reaction Rate Constant and 1/Temperature | 136 |
| 39 | Correlation of IR Peak Height and Peel. IR of Propellant at Bond Interface. | 137 |
| 40 | Correlation of IR Peak Height and Adhesion. IR of Propellant at Bond Interface. | 138 |
| 41 | Correlation of IR Peak Height and Peel. IR of Propellant 0.5 Inch from Interface. | 139 |
| 42 | Correlation of IR Peak Height and Adhesion. IR of Propellant 0.5 Inch from Interface. | 139 |
| 43 | Correlation of IR Peak Height and Time. IR of Propellant 0.5 Inch from Interface. | 142 |

List of Tables (Continued)


| Number | Title | Page No. |
|---|---|---|
| 44 | Correlation of ln IR Peak Height and Time. IR of Propellant 0.5 Inch from Interface. | 142 |
| 45 | Correlation of ln Reaction Rate Constant and 1/Temperature | 144 |
| 46 | Correlation of IR Peak Height and Time. IR of Propellant at the Interface. | 144 |
| 47 | Correlation of ln IR Peak Height and Time. IR of Propellant at the Interface. | 145 |
| 48 | Correlation of ln Reaction Rate Constant and 1/Temperature | 145 |
| 49 | Correlation of IR Peak Height and Peel. IR of Propellant at 0.5 Inch from Interface. | 146 |
| 50 | Correlation of IR Peak Height and Adhesion. IR of Propellant 0.5 Inch from Interface. | 146 |
| 51 | Correlation of IR Peak Height and Peel. IR of Propellant at Interface. | 147 |
| 52 | Correlation of IR Peak Height and Adhesion. IR of Propellant at Interface. | 147 |
| 53 | Predicted Peel Strength for 100°F Aging (MSL-303 Prop.) | 151 |
| 54 | MSL-303 Propellant - Pershing P1a | 152 |
| 55 | Correlation of IR Peak Height and Time (MSL-303 Propellant) | 158 |
| 56 | Correlation of ln IR Peak Height and Time (MSL-303 Propellant) | 158 |
| 57 | ln Height of IR Peak at 911.5 $cm^{-1}$ and Its Variation with Time and Temperature | 159 |
| 58 | Correlation of ln Reaction Rate Constant ($K_1$) and 1/Temperature | 159 |
| 59 | Correlation of IR Peak Height and Propellant Modulus, Max. Stress, and Strain at Max. Stress (MSL-303) | 165 |
| 60 | Correlation of IR Peak Height and Propellant Stress | 166 |
| 61 | Correlation of IR Peak Height and Strain at Max. Stress (MSL-303 Propellant) | 167 |

List of Tables (Continued)


| Number | Title | Page No. |
|---|---|---|
| C-1 | Gradient Hardness of Insulation/Liner/Propellant | 192 |
| C-2 | Gel Fraction of Binders in the HTPB Propellant Bond Samples | 195 |
| D-1 | Gradient Hardness of Insulation/Liner/Propellant | 206 |
| D-2 | Minimum Smoke Propellant Binder Gel Fraction | 210 |


## LIST OF FIGURES


| | | |
|---|---|---|
| 1 | Work Flow Diagram | 16 |
| 2 | Spectrum of TP-H8279 Propellant at Propellant/Liner Interface with Teflon Bond Release Subtracted. | 25 |
| 3 | Spectrum of TL-H755A Liner at Propellant/Liner Interface with Teflon Bond Release Subtracted. | 26 |
| 4 | Spectrum of TP-H8279 Propellant 1mm from Liner Bond Inhibited Sample. Ambient Storage. | 28 |
| 5 | Spectrum of TP-H8279 Normal Propellant 15 mm from Liner, No Bond Release, Ambient Storage. | 29 |
| 6 | Spectrum of TP-H8279 Propellant at Liner Surface, Teflon Bond Release Scraped off. Ambient Storage. | 30 |
| 7 | Spectrum of TP-H8279 Propellant at Propellant/Liner Interface with Mold Release (Teflon). | 31 |
| 8 | Spectrum of TL-H755A Liner at Propellant/Liner Interface with Mold Release | 32 |
| 9 | Transmissivity of Various ATR/IRE Combinations | 42 |
| 10 | Infrared Spectrum of TP-Q7029 Propellant | 43 |
| 11 | IR Spectrum of the Gel Fraction of TP-Q7029 Propellant | 45 |
| 12 | Spectral Region 870-640 $cm^{-1}$ at RES-2, WDS-SP, NSS-250 (Plots are not Normalized). | 50 |
| 13 | Infrared Spectrum of AMRAAM Propellant; for "Collect" Parameters Study | 52 |

List of Figures (Continued)


| Number | Title | Page No. |
|---|---|---|
| 14 | Infrared Spectrum of AMRAAM Propellant; for "Collect" Parameters Study | 53 |
| 15 | Effect of Sample Thickness and Torque on Spectral Amplitude | 58 |
| 16 | Effect of Wait Time and Torque on Spectral Amplitude | 60 |
| 17 | Effect of Wait Time and Torque on Spectral Amplitude | 61 |
| 18 | Effect of Heat on Wait Time and Spectral Amplitude | 62 |
| 19 | Effect of Torquing Procedure on Wait Time and Spectral Amplitude | 63 |
| 20 | Typical IR Spectrum of Whole TP-H8279 Propellant | 73 |
| 21 | Correlation of Peak at 3008 $cm^{-1}$ with Distance from Liner Interface. TP-H8279 Propellant. | 75 |
| 22 | Change in Peak Height at 1734 $cm^{-1}$ with Time and Distance from Liner. TP-H8279 Propellant. | 76 |
| 23 | Change in Peak Height at 1641 $cm^{-1}$ with Time and Distance from Liner. HTPB Propellant. | 77 |
| 24 | HTPB Propellant Correlation of Gel Fraction and Absorbance at 1641 $cm^{-1}$ | 78 |
| 25 | Correlation Between Propellant/Liner Peel Strength and Peak Height at 3008 $cm^{-1}$ at the Interface. HTPB Propellant. | 79 |
| 26 | IR Spectrum of TL-H755A Liner Sol Fraction at Start of Aging. | 81 |
| 27 | IR Spectrum of TL-H755A Liner Sol Fraction at End of Aging. | 82 |
| 28 | Correlation Between Peak Height at 969 $cm^{-1}$ and Liner Tensile Stress | 84 |
| 29 | Change in Peak at 915 $cm^{-1}$ with Age Time | 85 |
| 30 | Correlation Between Peak H ight at 915 $cm^{-1}$ and Liner Tensile Stress | 86 |
| 31 | Correlation Between Peak Height at 1737 $cm^{-1}$ and Propellant/Liner Peel | 87 |

List of Figures (Continued)


| Number | Title | Page No. |
|---|---|---|
| 32 | Correlation Between Peak Height at 2962 $cm^{-1}$ and Propellant/Liner Peel Strength | 88 |
| 33 | Infrared Spectrum of TI-R300 Insulation Sol Fraction. Age 0 Weeks. | 89 |
| 34 | Infrared Spectrum of TI-R300 Insulation Sol Fraction. Aged 16 Weeks at 165°F. | 90 |
| 35 | AMRAAM Insulation Sol - TI-R300 - Change in Peak at 1737 $cm^{-1}$ with Age Time | 92 |
| 36 | AMRAAM Insulation Sol - TI-R300 - Change in Peak at 1380 $cm^{-1}$ with Age Time | 93 |
| 37 | AMRAAM Insulation Sol - TI-R300 - Change in Peak at 2734 $cm^{-1}$ with Age Time | 94 |
| 38 | AMRAAM Insulation Sol - TI-R300 - Correlation Between Peak Height at 1380 $cm^{-1}$ and Composite Tensile Adhesion | 95 |
| 39 | AMRAAM Insulation Sol - TI-R300 - Correlation Between Peak Height at 1737 $cm^{-1}$ and Gel Fraction | 97 |
| 40 | Variation with Time of Peak at 1656 $cm^{-1}$ in Sol Fraction of TI-R300 Aged 0 to 16 Weeks | 98 |
| 41 | AMRAAM TI-R300 Insulation Sol Aged 0 to 16 Weeks at 165°F | 99 |
| 42 | Minimum Smoke Propellant (TP-Q7029), Gel Fraction. Aged 0 Weeks. | 100 |
| 43 | Minimum Smoke Propellant (TP-Q7029), Gel Fraction. Aged 16 Weeks. | 101 |
| 44 | Minimum Smoke Propellant Correlation Between Propellant/Liner Peel and Peak at 1521 $cm^{-1}$ | 102 |
| 45 | Minimum Smoke Propellant Correlation Between Gel Fraction and Peak at 1726 $cm^{-1}$ | 103 |
| 46 | Minimum Smoke Propellant Correlation Between Composite Tensile Stress and Peak at 1726 $cm^{-1}$ | 104 |
| 47 | Minimum Smoke Propellant Correlation Between Propellant/Liner Peel and Peak at 1726 $cm^{-1}$ | 105 |
| 48 | Interrelationships Among Project Computer Programs | 110 |

List of Figures (Continued)


| Number | Title | Page No. |
|---|---|---|
| 49 | Variation in Tensile Adhesion with Time and Temperature. | 125 |
| 50 | Variation of Peel Strength with Time and Temperature | 126 |
| 51 | Variation of Tensile Adhesion with Time and Temperature | 127 |
| 52 | Variation of Peel Strength with Time and Temperature | 128 |
| 53 | IR Spectra of TP-H8288 Propellant 0.5 Inch from Liner Interface | 130 |
| 54 | IR Spectra of TP-H8288 Propellant Near Interface with Liner | 131 |
| 55 | Infrared Spectrum of the Gel Fraction of TP-Q7030 Propellant (Mix X-27). | 141 |
| 56 | Peel Strength as Identified from Peaks at 1563 and 1235 $cm^{-1}$ | 149 |
| 57 | Variation in Modulus with Age Time (MSL-303) | 154 |
| 58 | Variation in Strain at Max. Stress with Age Time (MSL-303) | 155 |
| 59 | Variation in Max. Stress with Age Temperature (MSL-303) | 156 |
| 60 | IR Spectrum of MSL-303 Propellant at Zero Age Time | 157 |
| 61 | Variation in 911 $cm^{-1}$ Peak Height with Age Time at 75° and 150°F (MSL-303 Propellant) | 160 |
| 62 | Variation in 911 $cm^{-1}$ Peak Height with Age Time at 110° and 130°F (MSL-303 Propellant) | 161 |
| 63 | Variation in 911 $cm^{-1}$ Peak Height with Age Time at 170° and 190°F (MSL-303 Propellant) | 162 |
| 64 | Activation Energy Plot for the Peak at 911 $cm^{-1}$ | 164 |
| 65 | Correlation of Max. Stress with Peak at 911 $cm^{-1}$ (MSL-303) | 168 |
| A-1 | Absorbance at 3008 $cm^{-1}$ As A Function of Distance Into the Propellant from the Liner Interface. Sample Aged 3 Months at 77°F. | 173 |

List of Figures (Continued)


| Number | Title | Page No. |
|---|---|---|
| A-2 | Absorbance at 1737 $cm^{-1}$ As A Function of Distance Into the Propellant from the Liner Interface. Sample Aged 3 Months at 77°F. | 174 |
| A-3 | Absorbance at 1640 $cm^{-1}$ As A Function of Distance Into the Propellant from the Liner Interface. Sample Aged 3 Months at 77°F. | 175 |
| A-4 | Absorbance at 1243 $cm^{-1}$ As A Function of Distance Into the Propellant from the Liner Interface. Sample Aged 3 Months at 77°F. | 176 |
| A-5 | Absorbance at 3008 $cm^{-1}$ As A Function of Distance Into the Propellant from the Liner Interface. Sample Aged 3 Months at 170°F. | 177 |
| A-6 | Absorbance at 1737 $cm^{-1}$ As A Function of Distance Into the Propellant from the Liner Interface. Sample Aged 3 Months at 170°F. | 178 |
| A-7 | Absorbance at 1640 $cm^{-1}$ As A Function of Distance Into the Propellant from the Liner Interface. Sample Aged 3 Months at 170°F. | 179 |
| A-8 | Absorbance at 1243 $cm^{-1}$ As A Function of Distance Into the Propellant from the Liner Interface. Sample Aged 3 Months at 170°F. | 180 |
| C-1 | Liner-to-Insulation Peel Strength | 188 |
| C-2 | Propellant-to-Liner Peel Strength | 189 |
| C-3 | Composite Bond Tensile Strength | 190 |
| C-4 | TL-H755A Liner Tensile Properties | 191 |
| C-5 | Liner and Insulation Hardness As A Function of Age Time at 165°F | 193 |
| C-6 | Propellant Hardness As A Function of Distance from Liner and Aging Time | 194 |
| C-7 | Gel Fraction As A Function of Age Time | 196 |
| C-8 | Correlation Between Hardness and Peel Strength of Liner and Propellant | 197 |
| C-9 | Correlation Between Propellant Hardness and Propellant/Liner Peel Strength | 198 |

List of Figures (Continued)


| Number | Title | Page No. |
|---|---|---|
| C-10 | Correlation of Gel Fraction and Propellant/Liner Peel Strength | 199 |
| C-11 | Correlation Between Liner Gel Fraction and Stress and Strain | 200 |
| D-1 | Minimum Smoke Propellant Liner-to-Insulation Peel Strength | 202 |
| D-2 | Minimum Smoke Propellant Propellant-to-Liner Peel Strength | 203 |
| D-3 | Minimum Smoke Propellant Composite Bond Tensile Strength | 204 |
| D-4 | Minimum Smoke Propellant TL-H774 Liner Tensile Properties | 205 |
| D-5 | Minimum Smoke Propellant Liner and Insulation Hardness | 207 |
| D-6 | Minimum Smoke Propellant - Propellant Hardness | 208 |
| D-7 | Minimum Smoke Propellant - Propellant Hardness | 209 |
| D-8 | Minimum Smoke Propellant Change in Propellant Gel Fraction with Time and Distance from Liner Interface | 211 |
| D-9 | Minimum Smoke Propellant Change in Propellant Gel Fraction with Time and Distance from Liner Interface | 212 |
| D-10 | Minimum Smoke Propellant Correlation Between Hardness and Liner/Insulation Peel Strength | 213 |
| D-11 | Minimum Smoke Propellant Correlation Between Propellant Hardness and Propellant/Liner Peel Strength | 214 |
| D-12 | Minimum Smoke Propellant Correlation Between Liner Hardness and Propellant/Liner Peel Strength | 215 |
| D-13 | Minimum Smoke Propellant Correlation of Propellant Gel Fraction at 0.00 Inch from Liner with Propellant/Liner Peel Strength | 216 |
| D-14 | Minimum Smoke Propellant Correlation of Propellant Gel Fraction at 0.00 Inch from Liner with Composite Adhesion Max. Stress | 217 |
| D-15 | Minimum Smoke Propellant Correlation of Gel Fraction with Hardness | 218 |

List of Figures (Continued)


| Number | Title | Page No. |
|---|---|---|
| E-1 | Activation Energy Plot for the Peak at 3014 $cm^{-1}$ | 220 |
| E-2 | Activation Energy Plot for the Peak at 1638.3 $cm^{-1}$ | 221 |
| E-3 | Activation Energy Plot for the Peak at 1506.9 $cm^{-1}$ | 222 |
| E-4 | Activation Energy Plot for the Peak at 965.6 $cm^{-1}$ | 223 |
| E-5 | Variation of Strain at Max. Stress with Log Age Time | 224 |
| E-6 | Variation of Strain at Max. Stress with Age Time | 225 |
| E-7 | Variation of Max. Stress with Age Time | 226 |
| E-8 | Variation of Max. Stress with Log Age Time | 227 |

# INTRODUCTION

## OBJECTIVE

The objectives of this program were to establish the relationship between infrared spectra and aging of the propellant/liner/insulator bond and to demonstrate the applicability of the relationship to service life prediction.

## BACKGROUND

This project called for a study of rocket motor bond lines and the development of procedures to determine their integrity without sacrificing the rocket motor. Furthermore, the project called for the development of a technique whereby the bond line strength (or integrity) could be measured directly without reliance upon indirect or secondary means such as testing a sample stored with the rocket motor. In this project (and, thus, this report), the term "bondline" includes all interfaces among materials used in a rocket motor from the motor case inward to the propellant....insulation, liner, migration barriers, and propellant.

Previous procedures for determining the integrity of bondlines involved taking a sample from a rocket motor or sectioning a rocket motor and testing the bond lines thus removed. The methods were generally destructive to the rocket motor and, thus, were not totally satisfactory. Where small rocket motors are concerned, and the cost of such motors not prohibitively high, sacrificing a motor to determine the condition of the remainder of a lot or batch of motors is not a totally unacceptable procedure. This procedure, however, applied to a very large rocket motor was totally unacceptable simply because of the cost involved. An alternate method used was to store samples of the bond system along with the motor and then test those bond samples; from that information, then determine the integrity of the bond system within the motor. While this procedure was considerably less costly, the measure of bond strength was indirect and did not reveal the absolute condition of the bond system within the large rocket motor.

Thiokol/Huntsville had recently completed the FTIS project (AFRPL Contract F04611-78-C-0027). which demonstrated the feasibility of determining the mechanical properties of propellant using infrared (IR) spectroscopy. Also during that program, techniques were established for projecting, based on changes in mechanical properties and corresponding changes in the infrared spectral characteristics of the propellant, the mechanical properties of propellant to some future time.

This program was based on the idea that any changes in the mechanical properties at or near the bond line during aging are the result of chemical changes either in the propellant, the liner, or the insulator. These chemical changes are reactions that result in changes to the network structure of the polymers in the propellant, liner, or insulation or could be the result of migration of some chemical specie from one layer to another. Whatever the chemical changes are, they are detectable by infrared spectroscopy and these changes can be correlated to changes in the mechanical properties of the bond system. This basic premise had been demonstrated in Thiokol/Huntsville's

previous FTIS project. It remained in this project to demonstrate:

1) that the detected changes in infrared spectra were related to what was occurring in the bond system,

2) that the changes in the chemistry of the bond system were of sufficient magnitude to be observed in the infrared, and

3) that the infrared spectra could be obtained in a manner such that the infrared data were quantitative.

Each bond system used in a rocket motor will have its own chemical characteristics, these being a result of the particular insulation, liner, and propellant used. Types and quantities of materials employed in making the insulation, liner, and propellant have a profound effect upon the chemical reactivity and chemical stability of the entire bond system.

While there are some basic similarities between bond systems used in a great many rocket motors, the specific details of each bond system will cause its chemistry to be slightly different from every other bond system. The fact that a polyisoprene insulator, an HTPB-type liner, and an HTPB-type propellant are used gives rocket motors having these components some features in common, but the specific correlations between chemical changes and mechanical property changes must be determined for each individual bond system employed.

Correlation of infrared spectral changes with bond system mechanical property changes is most easily accomplished through the use of a computer program. Such a computer program was written and checked out on the previous FTIS project. The computer program accomplishes reduction of the raw infrared spectral data and then correlates that reduced infrared spectral data with the mechanical property data, establishing the relationship between the two phenomena.

## PROJECT OUTLINE

The project consisted of two phases, with each phase subdivided in three tasks.

### Phase I - Analytical Development

Task 1 - IR Data Acquisition Methodology
Task 2 - Computer Programming
Task 3 - Correlation of IR and Bond Properties

### Phase II - Service Life

Task 1 - Future Properties Programming
Task 2 - Bond System Aging and Data Analysis
Task 3 - Computer Program Transfer and User's Workshop

A detailed diagrammatic view of the entire project is presented in Figure 1, Work Flow Diagram.

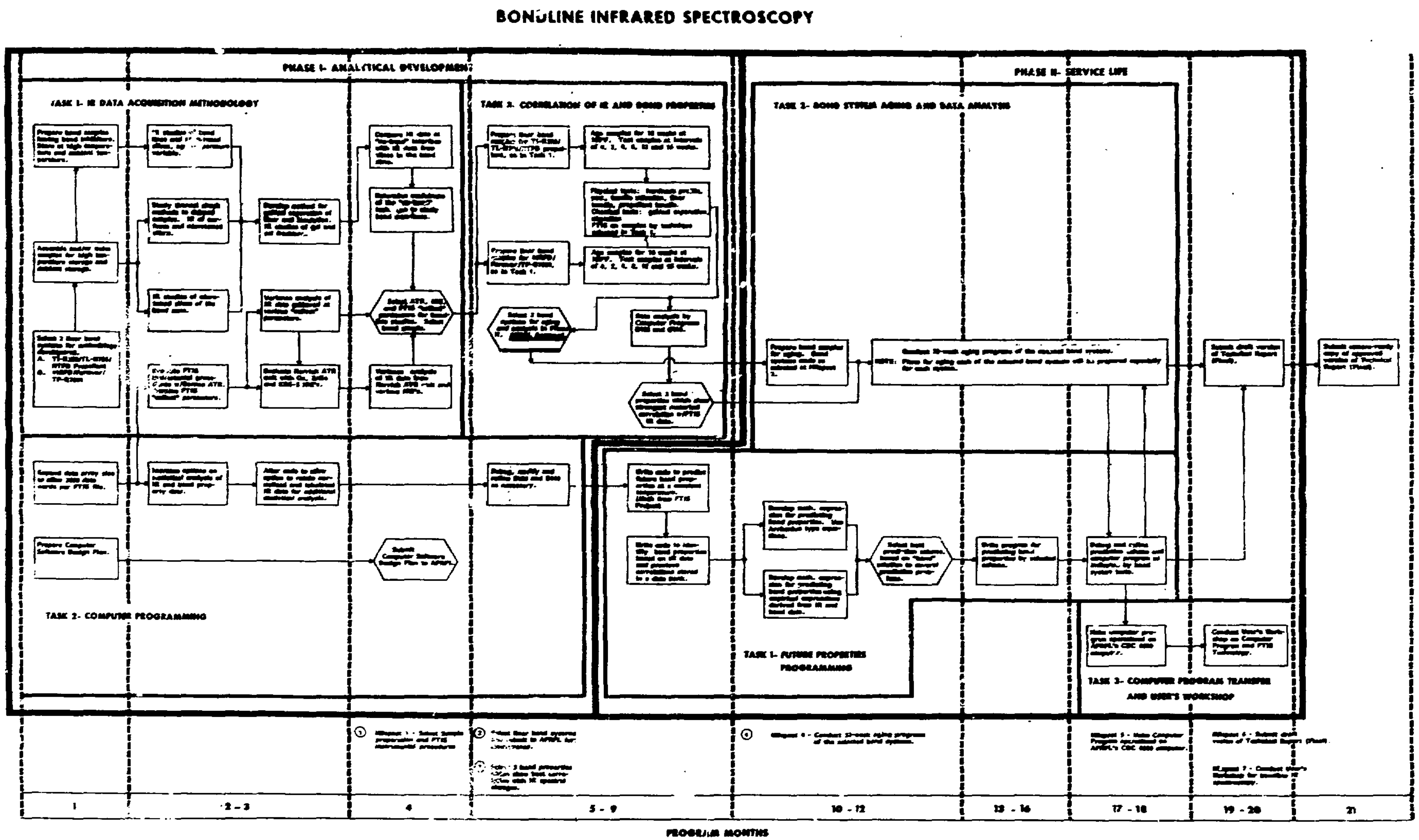


FIGURE 1. WORK FLOW DIAGRAM

As the outline implies, Phase I was devoted to development of analytical techniques for accumulating the infrared data on bond systems. Task 1, IR Data Acquisition Methodology, was to select bond systems to study and then examine several methods for physically reaching these bondlines so that their chemical structure could be examined in the infrared. Several different procedures and apparatus for acquiring the infrared data were examined. Task 2, Computer Programming, was devoted to improving the computer programs developed in the FTIS project (AFRPL Contract F04611-78-C-0027) to make these programs more useful by expanding their capabilities. Task 3 in this phase was concerned with the short-term, high-temperature aging of two bond systems and testing the Task 1 techniques for acquiring the infrared data. This task was also concerned with evaluation of several mechanical bond tests and other parameters that describe "bond" and the selection of the best of these tests for later use in Phase II.

Phase II - Service Life was divided into three tasks also. Task 1 was a continuation of the computer programming begun in Phase I. The concern here was to write a program for predicting the properties of a bond system based upon infrared information and the correlation of that infrared data with bond properties. Several techniques for predicting were examined, a selection made of the best technique and that particular prediction scheme programmed. Task 2 - Bond System Aging and Data Analysis, was concerned with the conduct of an aging program for two bond systems, one involving an HTPB propellant and liner while the other was a minimum smoke-type propellant with an HTPB liner. Both aging programs proceeded for 32 weeks with the measurement of bond properties as identified in Phase I. IR data on the chemical changes occurring in the bond system were accumulated using the technique selected in Phase I. Data analysis was performed after all of the aging had taken place. Task 3 in this phase was the transfer of the computer program to RPL so that it was operable on the AFRPL CDC 6600 computer. Also included was a presentation of the techniques developed in the program at an industry-wide workshop.

## SUMMARY OF ACCOMPLISHMENTS

During Phase I of the project, the IR data acquisition methodology was worked out. Laboratory procedures were established for acquiring the infrared spectra of propellant, liner, and insulation. It was found that the best quantitative data could be obtained for insulation and liner by using the sol fraction of those materials. For HTPB propellant, infrared spectra were made by an ATR technique with procedures for preparing samples, etc., worked out in detail. To avoid the overwhelming influence of RDX on the IR spectrum of minimum smoke propellant and to allow us to examine the binder of that propellant, it was found that the gel fraction of the minimum smoke propellant provided the best data. Procedures for using a Harrick ATR unit were worked out, as were all of the parameters to use in acquiring the IR spectra on a Digilab FTS-10 IR spectrophotometer. Small modifications were made to existing computer programs which increased the utility of these programs and allowed the reduction of IR data where the data were acquired at a resolution of 2, 4, or 8 wave numbers. Also during this phase, a 16-week aging program was conducted wherein a variety of physical property tests of the bond specimens for HTPB propellant and for minimum smoke propellant were examined. These bond tests included hardness profile, peel, tensile adhesion,

liner tensile, and chemical tests involving gel/sol separation of several of the substrates. Data from these tests were correlated with infrared spectral information and the selection made of the tests to use in the Phase II, long-term aging program.

During Phase II of the project, a 32-week aging program was conducted on an HTPB propellant bond system and a minimum smoke propellant bond system. Peel and adhesion were the tests conducted on samples aged at temperatures up to 165°F. Computer programs were written which permitted the computation of reaction rate constants, activation energy, and the prediction of bond properties from changes in the infrared spectra of the materials in the aging studies.

Correlations were found with the changes in the IR characteristics of the propellant with each of the two bond systems examined. These correlations were used to predict bond strength at a future time and temperature. The predictions correlated quite well with the actual bond strengths measured in the project.

## TECHNICAL ACCOMPLISHMENTS

### GENERAL REMARKS

The technical accomplishments of the project are presented below by phase and task. An outline of the project was presented in the Introduction of the report. Details of the experimental procedures developed during the course of the project are given in separate appendices located at the end of this report.

### PHASE I - ANALYTICAL DEVELOPMENT

### Task 1 - IR Data Acquisition Methodology

#### Selection of Bond Systems

In order to study IR data acquisition techniques, it was necessary, first, to select bond systems to study and to prepare the samples that would be used in the acquisition technology studies. To assure that techniques developed would be applicable to the current HTPB propellant systems and to the new minimum smoke propellant bond systems, a sample of each type bond system was selected to represent state-of-the-art propellants, liners and insulators. TP-H8279 was selected as the HTPB propellant, while propellant TP-Q7029 was selected as the minimum smoke propellant for the study. Liners and insulations used in preparing the bond systems were also state-of-the-art and they, along with the propellant formulations, are shown in Table 1 for the HTPB propellant bond system and in Table 2 for the minimum smoke propellant bond system.

#### Preparation of Bond Systems

Bond samples for each of the types of propellant were prepared. Samples employed liners of different thicknesses and in some samples the liner was bonded to the propellant and in others the bond between liner and propellant was inhibited by a very thin layer of a Teflon® powder spray-applied to the precured liner just prior to casting the propellant. Separate samples of the liner and of the insulation were prepared for independent infrared studies. A complete list of samples prepared from each of the types of propellant is displayed in Tables 3 and 4. Samples were aged at 165°F to provide some readily-observable change and at 77°F to provide a "no-change" environment so that IR techniques could be checked out.

The purpose of preparing bond samples wherein the bond was inhibited with Teflon powder was to have ready access to the actual bonding interfaces to determine whether it is necessary to examine that interface in order to measure the effect of aging on that interface. The bond inhibition technique worked quite well and the propellant and liner separated easily.

Previous tests showed that the very thin coating of sprayed-on Teflon powder did not prevent migration of mobile chemical species across the interface. That could be important to establishing a good bond. IR examination of the propellant at the bond line showed the presence of Teflon powder.

## TABLE 1

## HTPB PROPELLANT BOND SYSTEM

Insulation: TI-R300 (polyisoprene/asbestos)

Liner: TL-H755A

| Ingredient | Wt. % |
|---|---|
| R-45M | 41.85 |
| DDI | 12.15 |
| HX-868 | 6.00 |
| Carbon Black | 40.00 |
| | 100.00 |

Propellant: TP-H8279 (Mix G-195, 16 September 1980)

| Ingredient | Wt. % |
|---|---|
| R-45M/DDI | This information is classified confidential. Data are available under Contract F08635-78-C-0073. |
| DOA | |
| HX-752 | |
| ZrC | |
| $Al_2O_3$ | |
| AP | |

TABLE 2

## MINIMUM SMOKE PROPELLANT BOND SYSTEM

**Insulation:** TI-R701 (polyisoprene/Kevlar/Hi Sil)

**Liner:** TL-H763A

| Ingredient | Wt. % |
|---|---|
| R-45HT (Flexzone 6H/DTBH) | 45.501 |
| DDI | 10.094 |
| HX-868 | 4.000 |
| Carbon | 40.000 |
| $\phi_3$Bi | 0.135 |
| M. A. | 0.135 |
| MgO | 0.135 |
| | 100.000 |

**Propellant:** TP-Q7029 ($\rho$ = 0.06125 lb./in.$^3$) (Mix 18Q-647)

| Ingredient | Wt. % |
|---|---|
| Minimum Smoke Binders | 7.50 |
| Nitrate Plasticizers | 26.00 |
| Nitramine Oxidizer | 65.00 |
| Ballistic Additives | 1.50 |
| | 100.00 |

TABLE 3

BOND SAMPLES - HTPB PROPELLANT

| TYPE | TI-R300 Thickness | TL-H744A Thickness | TP-H8279 Thickness | Age Temp. 77°F | Age Temp. 165°F | Cure/Migration by FTIS | Total No. Samples |
|---|---|---|---|---|---|---|---|
| "A" | 0.200 | 0.020 | 0.875 | 5 | 5 | | 10 |
| bonded | | 0.040 | 0.875 | 5 | 5 | | 10 |
| 2x2x7/8 | | 0.100 | 0.875 | 5 | 5 | | 10 |
| composite | | | | | | | |
| "B" | 0.200 | 0.020 | 0.875 | 5 | 5 | 5 | 15 |
| bond inhib. | | 0.040 | 0.875 | 5 | 5 | 5 | 15 |
| 2x2x7/8 | | 0.100 | 0.875 | 5 | 5 | 5 | 15 |
| | | | | | | TOTAL | 75 |
| "C" | - | 0.05 | - | 3 | 3 | | 6 |
| liner sheet | | 0.10 | - | 3 | 3 | | 6 |
| 6x6 in. | | | | | | | |
| "D" | 0.05 | - | - | 3 | 3 | | 6 |
| TI-R300 | 0.10 | - | - | 3 | 3 | | 6 |
| sheet | 0.20 | - | - | 3 | 3 | | 6 |
| 6x6 in. | | | | | | | |
| vulcanized | | | | | | | |
| "E" | | | 3 lbs | | | | |
| block of | | | | | | | |
| propellant | | | | | | | |

TABLE 4

BOND SAMPLES - MINIMUM SMOKE PROPELLANT

| Sample Type | TI-R701 Thickness | TL-H763 Thickness | TP-Q7029 Thickness | Age Temp. 77°F | Age Temp. 165°F | Total No. Samples |
|---|---|---|---|---|---|---|
| "A" bonded 2x2x7/8 Composite | 0.200 | 0.020 | 0.875 | 5 | 5 | 10 |
| | | 0.060 | 0.875 | 5 | 5 | 10 |
| "B" bond inhib. 2x2x7/8 composite | 0.200 | 0.020 | 0.875 | 5 | 5 | 10 |
| | | 0.060 | 0.875 | 5 | 5 | 10 |
| | | | | | | 40 |
| "C" TI-R701 sheet - 6x6 in. vulcanized | 0.05 | - | - | 3 | 3 | 6 |
| | 0.10 | - | - | 3 | 3 | 6 |
| | 0.20 | - | - | 3 | 3 | 6 |
| | | | | | | 18 |
| "D" block of propellant | - | - | place used mat'l.in a mold | | | |

Electronic subtraction of a Teflon spectrum from the propellant spectrum was satisfactory and that propellant data was considered quantitative.

Thermal Shock Debonding

In addition to the bond inhibition technique for examining the actual interface between propellant and liner, another technique was investigated for separating liner and propellant. A study of this method revealed that it is only partially effective in giving a "clean" separation of propellant and liner. If insulation is left on the liner so that the sample is composed of insulation, liner and propellant, then the thermal shock method will fracture the sample in the propellant. If the insulation is removed, then no separation at all is achieved. Thermal shock procedure is to submerge the sample in liquid nitrogen and then remove the sample from the liquid nitrogen in a few minutes.

Where the sample did fracture, the break was always in the propellant with the break occurring at about 0.5 mm into the propellant. Fracture appears to be occurring between a hard layer and a layer of normal, unaffected propellant; the hard layer being formed by migration of HX-868 from the liner into the propellant. This hard layer phenomena has been observed in other propellant/liner systems where the liner contains HX-868. The surface of the fracture, where fracture does occur, is rough and the infrared spectrum shows large AP peaks and small binder peaks such that the IR spectrum has only marginal quantitative value.

"Bond Zone" Study

At the outset of this project, one of the basic premises was that there was a "zone" in which bond between liner and propellant was established. The "zone" extends into the propellant some finite distance beyond the actual interface between liner and propellant. This premise is based upon the ingredients in liner having some influence on the strength of the propellant immediately adjacent to the bond interface and for some small finite distance into the propellant. Such an effect is normally attributed to a migratable, polymerizable specie such as an aziridine, principally, HX-868. This influence of liner on propellant has been identified by hardness measurements and by mechanical property measurements in other programs. (The effect is readily observed in the data presented here.) The principal thought here was that, if the chemistry of this "liner-affected" zone is identical from the interface into the propellant for some measurable distance, then it is not necessary to actually sample propellant at the precise interface, but that propellant may be sampled some small distance away and knowledge of the chemical characteristics of the actual interface obtained by analyzing this propellant. Following are the results of that portion of this project which was designed to investigate this bond zone.

A sample in which the bond had been inhibited by Teflon powder was separated at the bond line and the infrared spectra of both the propellant and liner taken. These spectra are shown on Figures 2 and 3. Figure 2 is the propellant at that interface; Figure 3 is the spectrum of the liner at that interface. The influence of the liner on the propellant binder can readily be seen in Figure 2 with three peaks, appearing between 1700 and 1400 wave numbers, that are not normally a part of the propellant binder spectrum or are a very minor part of that spectrum. In both the liner and the propellant, these three peaks were very prominent. This very strongly infers that the

Date: 80 Nov 04
Sample: TP-H8279 Propellant at Propellant/Liner Interface
with Teflon bond release subtracted.
MNY: 0.67
MXY: 78.70
STP: 4000
ENP: 400
Tape/File: 101/MTO:40-MTO:18
Mode: ATR

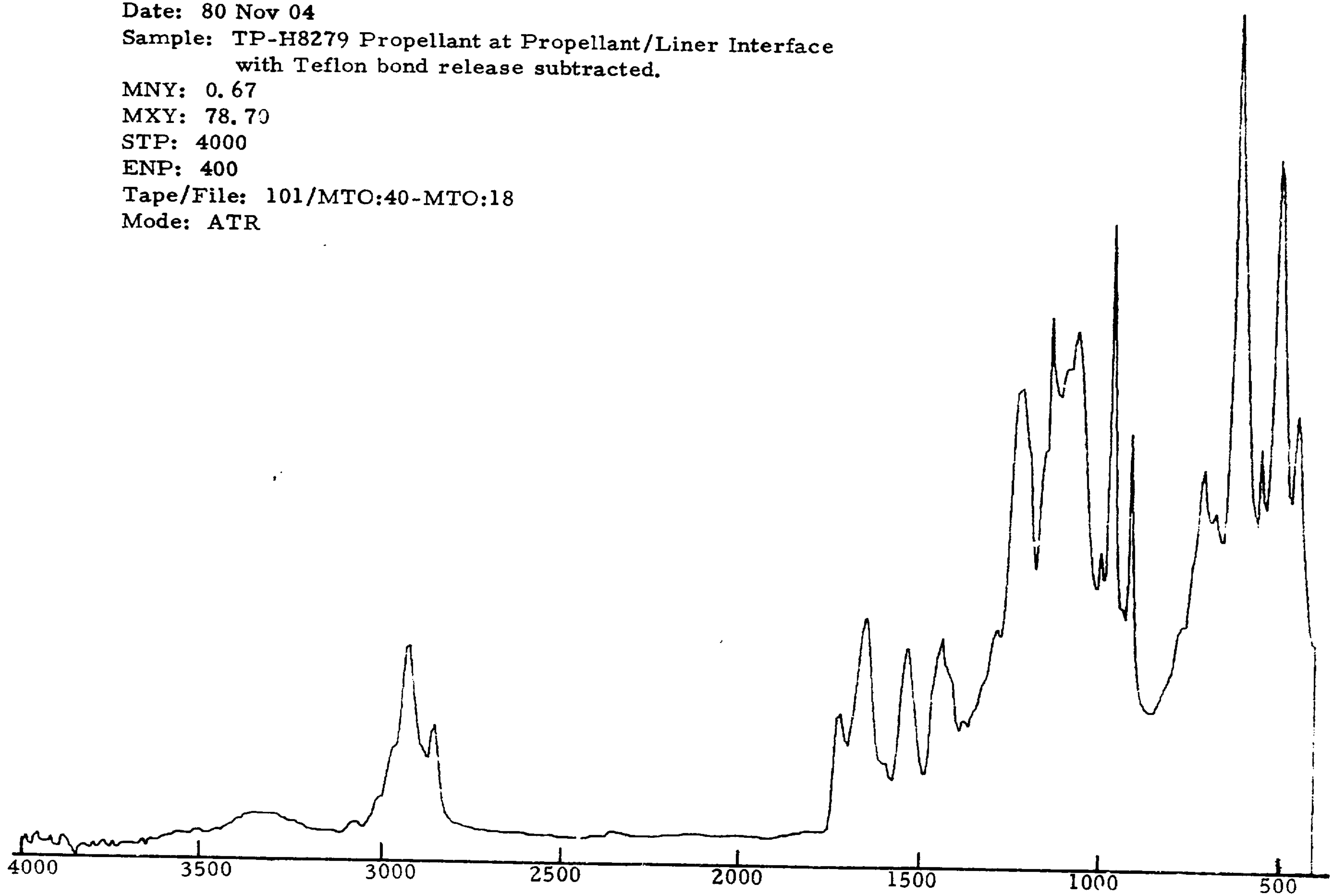


Figure 2. Spectrum of TP-H8279 Propellant at Propellant/Liner Interface with Teflon Bond Release Subtracted

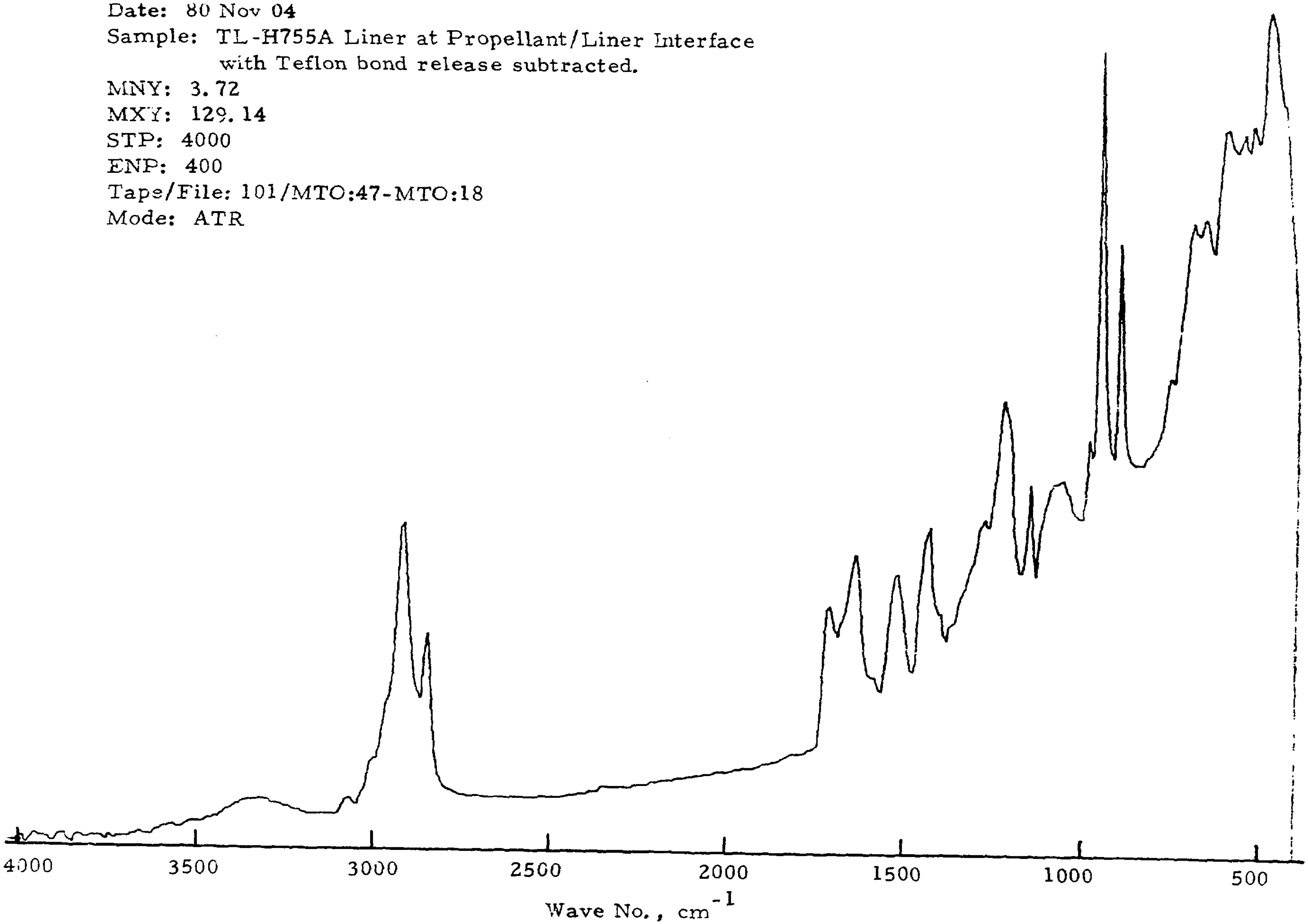


Figure 3. Spectrum of TL-H755A Liner at Propellant/Liner Interface with Teflon Bond Release Subtracted

chemistries on both sides near the bond line between propellant and liner are very close to the same and that HX-868 (from the liner) has migrated into the propellant. This is certainly not a new revelation but there is now spectral evidence of that migration.

The spectral influence of Teflon has been subtracted from the spectra of propellant and liner in Figures 2 and 3. Subtraction of the Teflon is more cleanly accomplished with propellant than with liner.

Infrared spectrum of the propellant at 1 mm from the bond line (where the bond was inhibited) reveals that most of the liner influence on the binder spectrum has disappeared (see Figure 4). IR spectrum, Figure 5, of the same propellant 15 mm from the liner/propellant interface reveals approximately the same chemistry in the "liner influence region" as the propellant at 1 mm from the propellant/liner interface. The relative amounts of plasticizer, DOA, in the propellant at 1 mm and at 15 mm from the liner are considerably different with there being less DOA in the propellant at 1 mm from the liner.

Rather than electronically subtracting the spectral influence of Teflon from the spectrum of propellant, an alternate method would be to scrape the Teflon from the sample before the spectrum is taken. This technique does work and the Teflon can be removed from the propellant; but, in the process, the AP particles at the surface of the propellant are disturbed and broken, thereby leaving a very thin layer of AP powder on the surface of the propellant and the AP then dominates the infrared spectrum of propellant. This is revealed in Figure 6, where the organic portions of that spectrum are very small while the AP contribution into the spectrum is exceedingly large. The actual surface of propellant at the bond interface, where a mold release has been used, leaves the propellant in a binder-rich condition. This binder film is exceedingly thin, but it does furnish an excellent spectrum of the binder as displayed in Figure 2. Scraping the surface with a razor blade disturbs the binder-rich film and breaks AP particles and deposits a thin film of very small particle AP on the surface, thus reducing the spectrum of the organic portion of the propellant. This is not a good technique to use for removing Teflon from the surface.

The spectral influence of Teflon on propellant can be seen in Figure 7. The two very large peaks located at 1150 and 1200 $cm^{-1}$ are the major peaks of Teflon with smaller peaks being located at 510, 550, and 640 $cm^{-1}$. Teflon does not have a spectral absorption in the region above 1300 $cm^{-1}$; therefore, it does not interfere with the spectrum of propellant in the "liner influence" area which occurs between 1400 and 1700 $cm^{-1}$.

A spectrum of propellant at the propellant/liner interface where the bond was inhibited with Teflon powder is given in Figure 8. This spectrum shows the influence of Teflon and should be compared with the spectrum shown on Figure 2. As can be seen, subtraction of a Teflon spectrum from the spectrum of propellant is uncertain and should not be done if the spectrum is to be used quantitatively. An electronic subtraction is certainly acceptable for qualitative data.

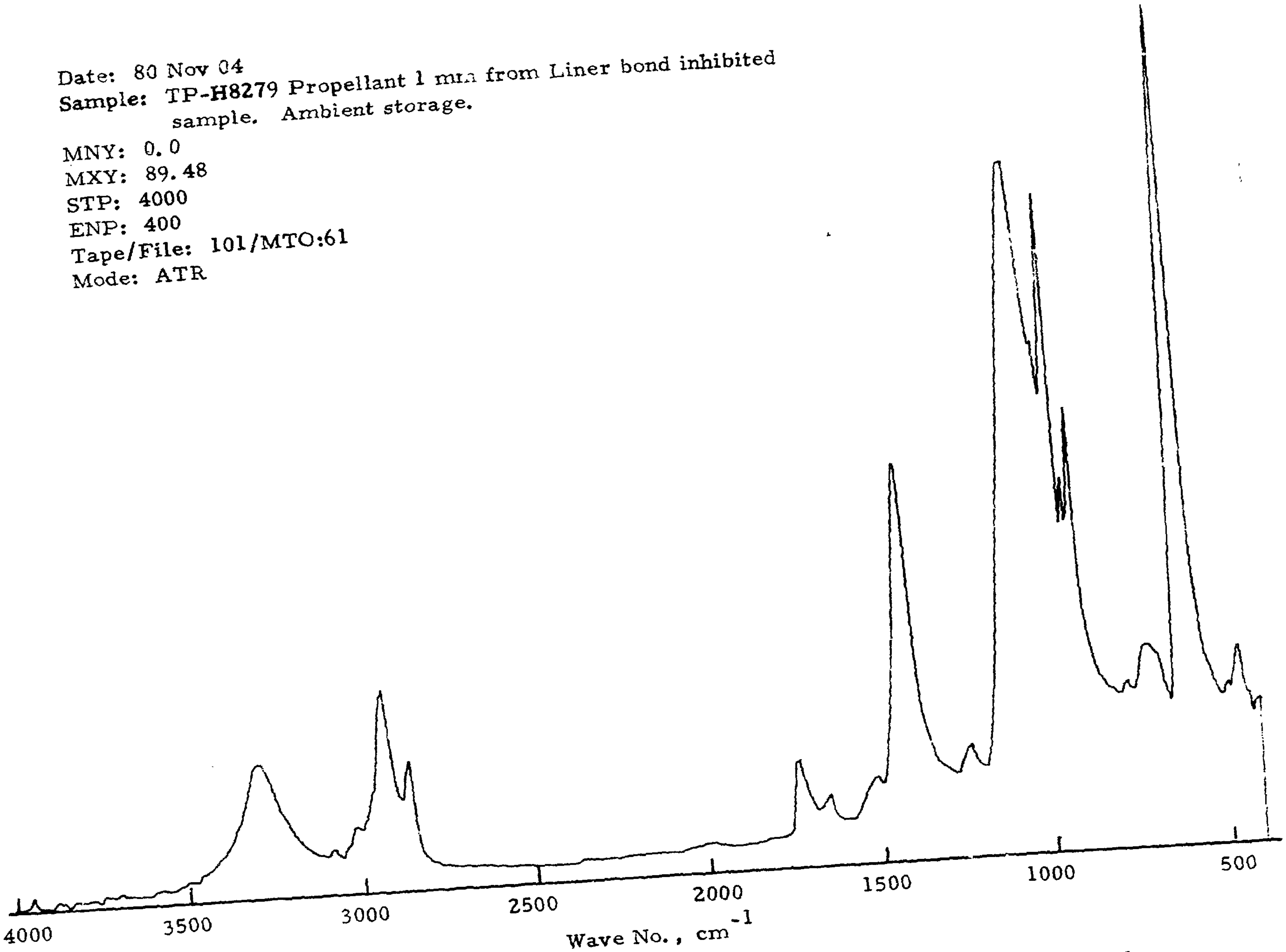


Figure 4. Spectrum of TP-H8279 Propellant 1mm from Liner Bond Inhibited Sample. Ambient Storage.

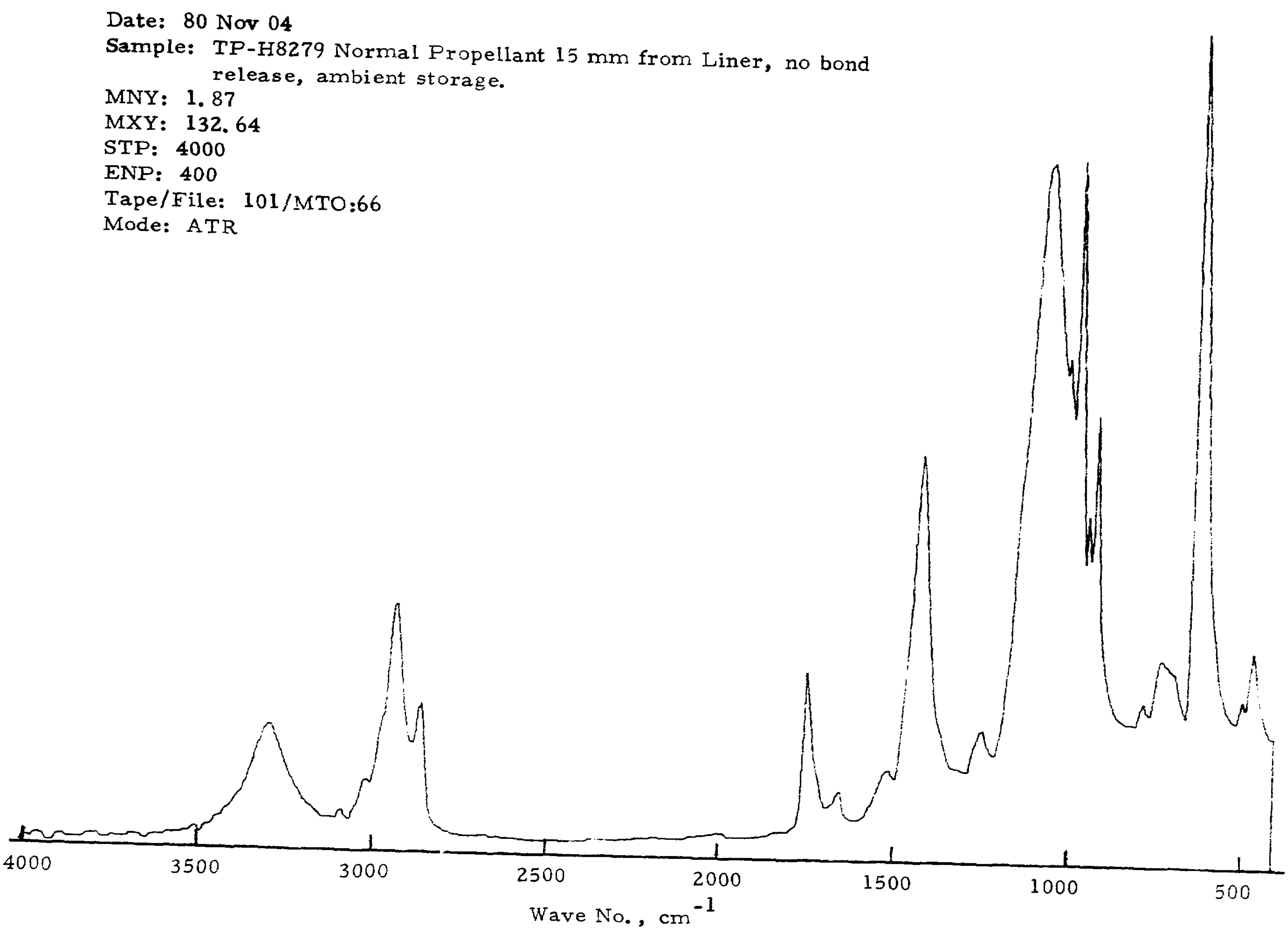


Figure 5. Spectrum of TP-H8279 Normal Propellant 15 mm from Liner, No Bond Release, Ambient Storage.

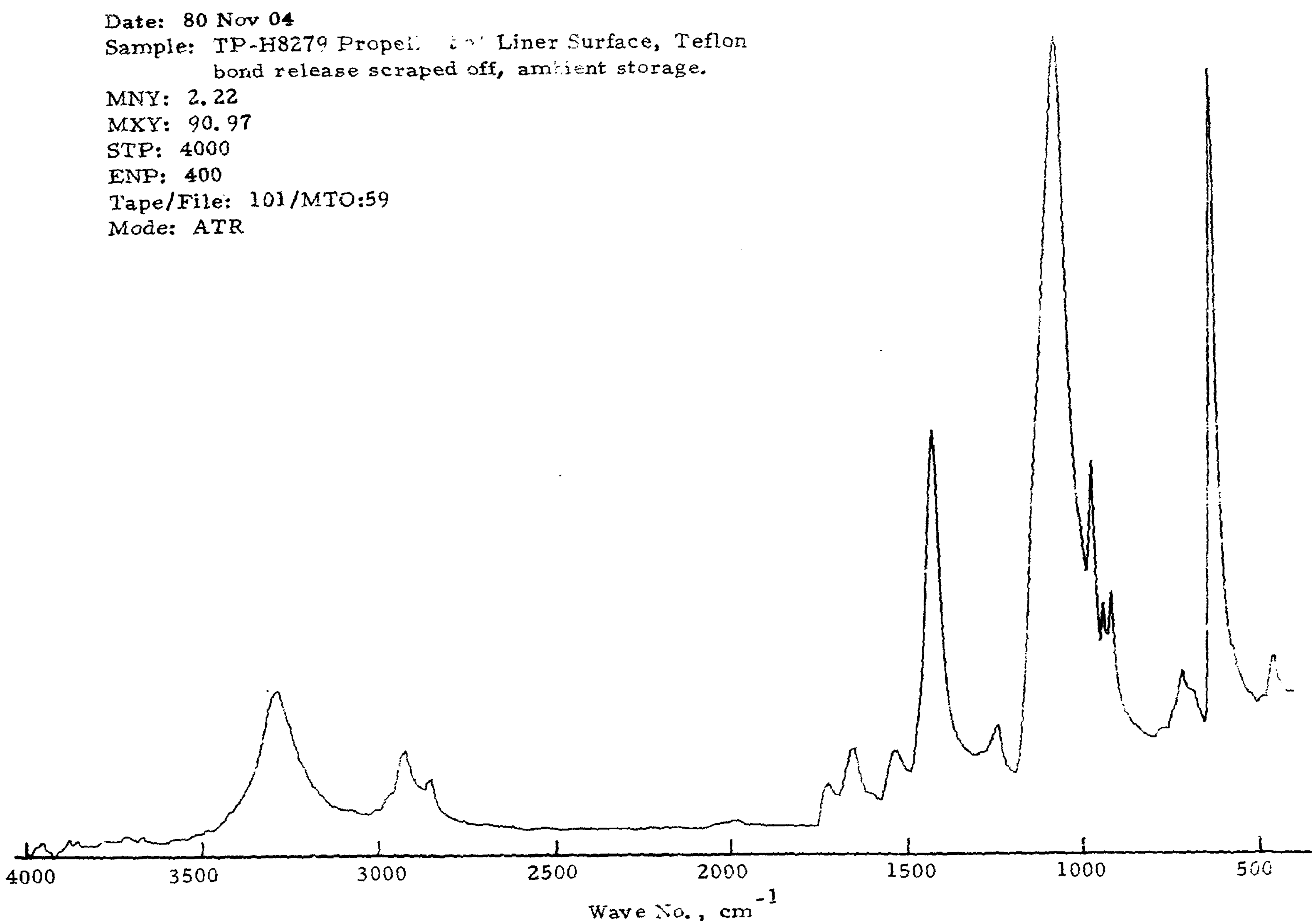


Figure 6. Spectrum of TP-H8279 Propellant at Liner Surface, Teflon Bond Release Scraped off. Ambient Storage.

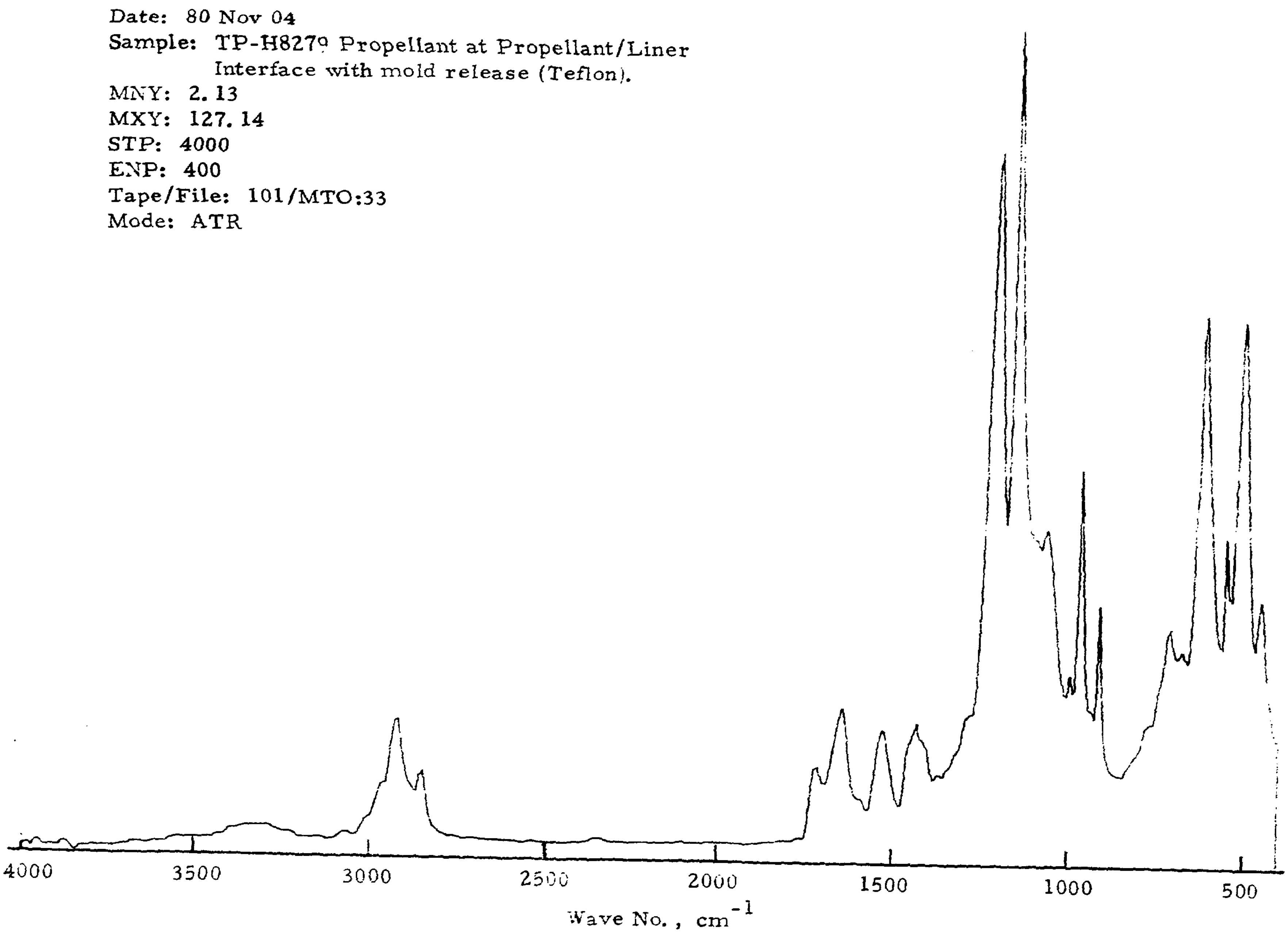


Figure 7. Spectrum of TP-H8279 Propellant at Propellant/Liner Interface with Mold Release (Teflon).

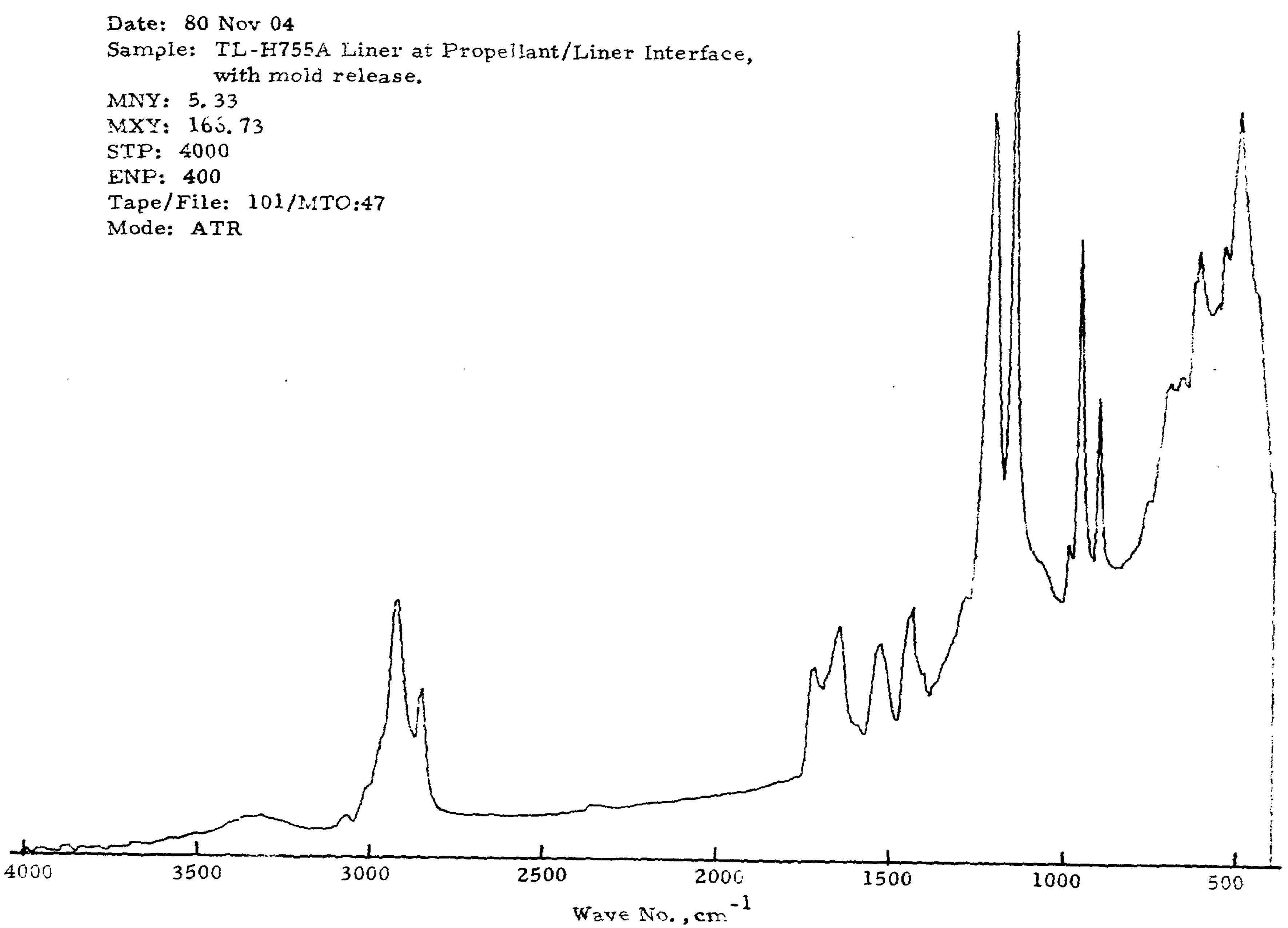


Figure 8. Spectrum of TL-H755A Liner at Propellant/Liner Interface with Mold Release

The removal of Teflon by scraping the liner side removed the Teflon as effectively as it did from propellant, but it also disturbed the thin binder rich film at the interface and exposed carbon particles at that surface. The carbon particles are very strong infrared absorbers and this resulted in a very weak spectrum with almost no detail. Almost all of the infrared energy was absorbed and/or dispersed by the carbon particles.

Infrared spectra were also made of samples of propellant taken from those bond specimens where the liner/propellant bond had been allowed to form. Propellant 0.5 mm away from the bond line where the liquid nitrogen-thermal shock method was used and where a sample was microtomed, revealed approximately the same spectral influence of the liner. Where the thermal shock method had been used to separate the propellant from the liner, the spectral influence of ammonium perchlorate was exceedingly large because fracture had taken place such that AP particles were exposed over the entire surface. Where the propellant was microtomed, the spectral influence of AP was much less and the binder part of the propellant was more easily observed. Infrared spectra of these samples and of the propellant where the liner/propellant bond had been inhibited all showed approximately the same spectral influence of the liner. There is an indication that the Teflon powder promoted the migration of HX-868 from liner into propellant. This conclusion is reached by comparing the heights of the peaks in the "liner influence" area in the two types of samples; i.e., the bond-inhibited and the bonded samples at identical locations from the liner/propellant interface.

## Gel/Sol Separation Procedures for Insulation and Liner

### Insulation

Insulation is an integral part of the structure making up the rocket motor. Examination of vulcanized insulation by infrared is not possible using a see-through technique, for obvious reasons, and is also not possible using an ATR technique because invariably the surface of insulation is too rough to present enough surface to the IRE of the ATR unit for a useful spectrum. The modulus of insulation is also generally too high to allow the insulation to be "squeezed" against an IRE so that a useful infrared spectrum can be made. It is then essential that a technique be developed wherein some portion of the insulation could be examined to determine the effect of aging upon the insulation and its chemistry.

A technique for determining the sol/gel fraction of TI-R300 insulation was developed. The technique is identical to that used for propellant wherein the sample of insulation is extracted continuously for 24-hour period in a Sohxlet extractor using methylene chloride as the solvent. Table 5 gives the results of the gel/sol separation experiments and shows that the binder recovery for the insulation is quite good and is equivalent to binder recovery applying the same technique to propellant. Both the vulcanized and the unvulcanized insulation gave identical or nearly identical binder recovery fractions. During vulcanization, the sol fraction of the insulation went from approximately 41% down to approximately 1.9%.

In addition to giving information on changes to the gel/sol ratio during aging, this procedure also furnished the sol fraction, a portion of the insulation that could be used for IR examination and, thus, for correlation of IR changes with bond property changes.

TABLE 5

GEL/SOL SEPARATION OF TI-R300

Formulation Binder Quantity = 51.72%
Formulation Filler Quantity = 48.28%
100.00%

| Unvulcanized TI-R300 | 1 | 2 | 3 |
|---|---|---|---|
| Sol, % | 40.76 | 40.93 | 41.27 |
| Gel, % | 10.36 | 10.55 | 10.44 |
| Total Binder, % | 51.12 | 51.48 | 51.71 |
| Binder Recovery, % | 98.84 | 99.52 | 99.98 |

Vulcanized TI-R300
(Vulcanized 2 hours at 225°F
plus bake-out 5 days at 170°F)

| | 1 | 2 | 3 | 4 |
|---|---|---|---|---|
| Sol, % | 1.87 | 1.79 | 1.97 | 2.25 |
| Gel, % | 49.44 | 49.43 | 49.43 | 49.49 |
| Total Binder, % | 51.31 | 51.22 | 51.40 | 51.74 |
| Binder Recovery, % | 99.21 | 99.03 | 99.38 | 100.04 |

## Liner

The two liners being used in this program, TL-H755A and TL-H763A, were subjected to a gel/sol separation in order to assure that our current techniques would give satisfactory results. Results of the gel/sol separation for these two liners are given in Tables 6 and 7. The technique for separating the sol and the gel fractions of liner works well and gives quite reproducible results. These experiments conclude our planned effort for gel/sol separation studies and we have identified a satisfactory method for accomplishing this separation.

## Statistical Evaluation of the Harrick ATR Unit

A set of experiments was run to evaluate the Harrick ATR unit and three internal reflection elements (IRE). Internal reflection elements were made of KRS-5, zinc selenide, and germanium. In this experiment, three specimens were taken from the same sample of propellant and one specimen used with one IRE in the Harrick ATR unit. Six replicate spectra were made with each of the IRE's. All spectra were made at resolution 4 with 1000 scans per spectrum and the data collected in double precision. Spectra were reduced using computer program E490 and the spectra normalized at 2850 $cm^{-1}$. Four peaks were selected in each of the spectra and the heights of those peaks used in the statistical analysis. The data employed in the statistical analysis is displayed in Table 8. The averages and standard deviations of replicates for the Harrick ATR data of Table 8 are summarized in Tables 9 and 10. Since each of the IRE's has its own characteristic spectral influence, there is no reason why the averages of a given wave number should be the same for the different types of IRE's so that the data are not cross-correlatable but are correlatable within a group for a single IRE. The results of this analysis are summarized as follows:

1) The precision of units with the zinc selenide and germanium IRE's is generally better than that with the KRS-5. For the two lower wave number groups, the differences are statistically significant.

2) With the KRS-5 unit, the precision degrades (relative variation becomes larger) with decreasing wave number (increasing wave length). This was not apparent with the other two IRE's, nor was it with the Barnes Engineering ATR unit.

3) The precision of the Harrick ATR with the germanium or zinc selenide IRE is comparable to the Barnes ATR unit with the "collect" parameters set at resolution 4, double precision and 1000 scans (i.e., coefficient of variation is from 0.20% to 1.5% depending upon wave number or height).

Since we had equivalent data taken at the same set of conditions for the Barnes ATR unit with its KRS-5 prism, it was of interest to compare the standard deviation of this Barnes/KRS-5 unit with the three sets of data taken with the Harrick ATR unit. A summary of the standard deviations at the four wave numbers is given in Table 11. These data reveal which of

TABLE 6

## GEL/SOL SEPARATION OF LINER
(TL-H755A/RL-05680)

| Sample No. | Recovery % | Sol in Liner, % | Sol in Binder, % | Gel in Liner, % | Gel in Binder, % |
|---|---|---|---|---|---|
| 1 | 100.43 | 7.16 | 12.85 | 48.58 | 87.15 |
| 2 | 99.30 | 6.77 | 12.28 | 48.34 | 87.72 |
| 3 | 99.68 | 6.91 | 12.50 | 48.41 | 87.50 |
| Average | 99.80 | 6.95 | 12.54 | 48.44 | 87.46 |

TL-H755A Formulation

| | |
|---|---|
| R-45M | 42.44% |
| DDI | 11.56 |
| HX-868 | 6.00 |
| Thermax | 40.00 |
| | 100.00% |

| | | |
|---|---|---|
| Binder | 55.50% | (includes 25% of HX-868) |
| Extractable | 4.50 | (75% of HX-868) |
| Solids | 40.00 | |
| | 100.00% | |

TABLE 7

## GEL/SOL SEPARATION OF LINER

(TL-H763A/LM-23926)

| Sample No. | Recovery, % | Sol in Liner, % | Sol in Binder, % | Gel in Liner, % | Gel in Binder, % |
|---|---|---|---|---|---|
| 1 | 100.18 | 14.74 | 20.84 | 55.97 | 79.16 |
| 2 | 99.45 | 14.38 | 20.48 | 55.81 | 79.52 |
| 3 | 99.49 | 14.15 | 20.15 | 56.07 | 79.85 |
| 4 | 99.43 | 14.29 | 20.36 | 55.89 | 79.64 |
| Average | 99.64 | 14.39 | 20.46 | 55.94 | 79.54 |

TL-H763A Formulation

| | |
|---|---|
| R-45HT | 56.53% |
| DDI | 13.05 |
| HX-868 | 4.00 |
| Thermax | 26.00 |
| DQC | 0.42 |
| | 100.00 |

| | | |
|---|---|---|
| Binder | 70.58% | (includes 25% of HX-868) |
| Extractables | 3.28 | (includes 75% of HX-868 and 67% of DQC) |
| | 26.14 | (includes 33% of DQC) |
| | 100.00% | |

TABLE 8

FTIS PRECISION STUDY
(Harrick ATR, Resolution 4, Double Precision, 1000 Scans per Sample)

| IRE Type | Replicate | Wave Number, $cm^{-1}$ 2923-2929 | 1737-1739 | 1236-1239 | 909-912 |
|---|---|---|---|---|---|
| | | Peak Heights | | | |
| KRS-5 | 1 | 21.720 | 16.889 | 5.424 | 14.081 |
| | 2 | 21.776 | 17.223 | 5.406 | 14.295 |
| | 3 | 21.599 | 17.199 | 5.244 | 14.504 |
| | 4 | 21.538 | 17.200 | 5.216 | 14.486 |
| | 5 | 21.542 | 17.187 | 5.170 | 14.814 |
| | 6 | 21.641 | 17.229 | 5.158 | 14.964 |
| ZnSe | 1 | 58.495 | 42.860 | 9.423 | 36.089 |
| | 2 | 58.538 | 43.213 | 9.499 | 36.218 |
| | 3 | 58.550 | 43.232 | 9.352 | 35.671 |
| | 4 | 58.350 | 43.255 | 9.435 | 35.454 |
| | 5 | 58.631 | 43.478 | 9.460 | 35.870 |
| | 6 | 58.356 | 43.489 | 9.480 | 35.695 |
| Ge | 1 | 49.082 | 38.254 | 8.575 | 35.862 |
| | 2 | 49.036 | 39.162 | 8.695 | 35.755 |
| | 3 | 49.250 | 39.486 | 8.738 | 35.851 |
| | 4 | 49.031 | 39.631 | 8.786 | 36.030 |
| | 5 | 48.710 | 39.645 | 8.802 | 35.868 |
| | 6 | 48.907 | 39.926 | 8.859 | 35.988 |

TABLE 9

FTIS STUDY - SUMMARY OF AVERAGES

(Harrick ATR - 6 Replicates per Average)

| Wave Number, $cm^{-1}$ | KRS-5 $\overline{X}_{\ell n}$ | KRS-5 $\overline{X}$ | ZnSe $\overline{X}_{\ell n}$ | ZnSe $\overline{X}$ | Ge $\overline{X}_{\ell n}$ | Ge $\overline{X}$ |
|---|---|---|---|---|---|---|
| 2923-2929 | 3.0744 | 21.637 | 4.0688 | 58.487 | 3.8919 | 49.004 |
| 1737-1739 | 2.8422 | 17.153 | 3.7671 | 43.254 | 3.6724 | 39.346 |
| 1236-1239 | 1.6618 | 5.269 | 2.2451 | 9.441 | 2.1681 | 8.742 |
| 909- 912 | 2.6756 | 14.521 | 3.5788 | 35.831 | 3.5805 | 35.891 |

TABLE 10

FTIS STUDY - SUMMARY OF STANDARD DEVIATIONS

(Harrick ATR - 6 Replicates per Group)

IRE TYPE

| Wave Number, $cm^{-1}$ | KRS-5 Std. Dev. $\ell n$ units x $10^2$ | Zn Se Std. Dev. $\ell n$ units x $10^2$ | Ge Std. Dev. $\ell n$ units x $10^2$ |
|---|---|---|---|
| 2923-2929 | 0.445 | 0.192 | 0.370 |
| 1737-1739 | 0.768 | 0.531 | 1.517 |
| 1236-1239 | 2.208 | 0.552 | 1.140 |
| 909- 912 | 2.237 | 0.793 | 0.279 |

TABLE 11

STANDARD DEVIATION AND GENERAL RANKING OF VARIOUS ATR/IRE COMBINATIONS

| | Standard Deviation at Wave Number | | | | General Ranking |
|---|---|---|---|---|---|
| | $2929\ cm^{-1}$ | $1738\ cm^{-1}$ | $1236\ cm^{-1}$ | $912\ cm^{-1}$ | |
| B/KRS-5 | 0.315 | 2.154 | 0.788 | 0.364 | 3 |
| H/KRS-5 | 0.445 | 0.768 | 2.208 | 2.237 | 4 |
| H/ZnSe | 0.192 | 0.531 | 0.552 | 0.793 | 1 |
| H/Ge | 0.370 | 1.517 | 1.140 | 0.279 | 2 |

Shere: RES = 4
NSS = 1000
WDS = DP

the four combinations of IRE and ATR unit can be expected to give the spectra with the least variance. The general ranking is shown in the table and places the Harrick unit with zinc selenide as the first choice, followed closely by the Harrick unit with germanium and the Barnes unit with KRS-5. There is statistically little or no difference in these three units, but the Harrick unit with the KRS-5 IRE is last in this general ranking by a large margin.

One of the conclusions concerning the effect of peak height on the variance of spectra was that the greater the peak height, the less the variance; i.e., the less influence the electronic noise in the FTS-10 had upon the spectrum. Since the noise is more or less a fixed value, then the greater the energy passing through the instrument, the less the relative proportion the noise contributes to the spectrum. It was then of interest to see which of the four combinations of ATR and IRE's would pass the greatest amount of energy. A single-beam spectrum was made from each of the four combinations. These four single-beam spectra are plotted on Figure 9 and reveal that the Harrick unit with the zinc selenide passes the most energy and it is followed by the Harrick unit with the germanium and the KRS-5 IRE's. The least amount of energy was transmitted by the Barnes unit with the KRS-5 prism. Since the amount of energy transmitted through an IRE is a characteristic of the material of construction and directly proportional to the surface condition of the IRE, it is understandable that the Barnes unit with its KRS-5 prism should pass the least amount of energy. That particular KRS-5 prism has been used the most and its surface condition is the poorest; i.e., it is scratched and dented. The Harrick IRE's have not been used and they are, by far, in the best condition of the four units. However, the ranking among the Harrick IRE's is significant in that they are arranged in the same order as the standard deviation/general ranking on Table 11.

Based on the data in Figure 9 and on Table 11, we selected the Harrick ATR unit with the zinc selenide IRE as the standard. Zinc selenide as an IRE material has one other distinct advantage; it is approximately four times harder than KRS-5 and is, therefore, less subject to scratches and dents.

## IR Spectrum of Minimum Smoke Propellant

Figure 10 is an infrared spectrum of TP-Q7029 propellant made by the standard ATR technique. A study of this spectrum revealed several serious problems to resolve before the IR spectra of minimum smoke propellant would be quantitatively useful for correlations with mechanical property changes.

The most serious problem was that of normalizing the spectrum. The usual procedure for HTPB propellants was to normalize using a peak in the $-CH_2-$ region; i.e., around 2900 $cm^{-1}$. This peak in the spectrum on Figure 10 is only 11 units while the peaks in the low wave number end of the spectrum are near 200 magnitude. IR peaks for quantitative purposes should have a magnitude between 20 and 80 absorbance units and not beyond 100. Peaks in the Figure 10 spectrum that are near 200 absorbance units are well beyond the quantitative limits, while in the usual normalizing region (2900 $cm^{-1}$) the peak is only 11 units so that it, too, was not useful.

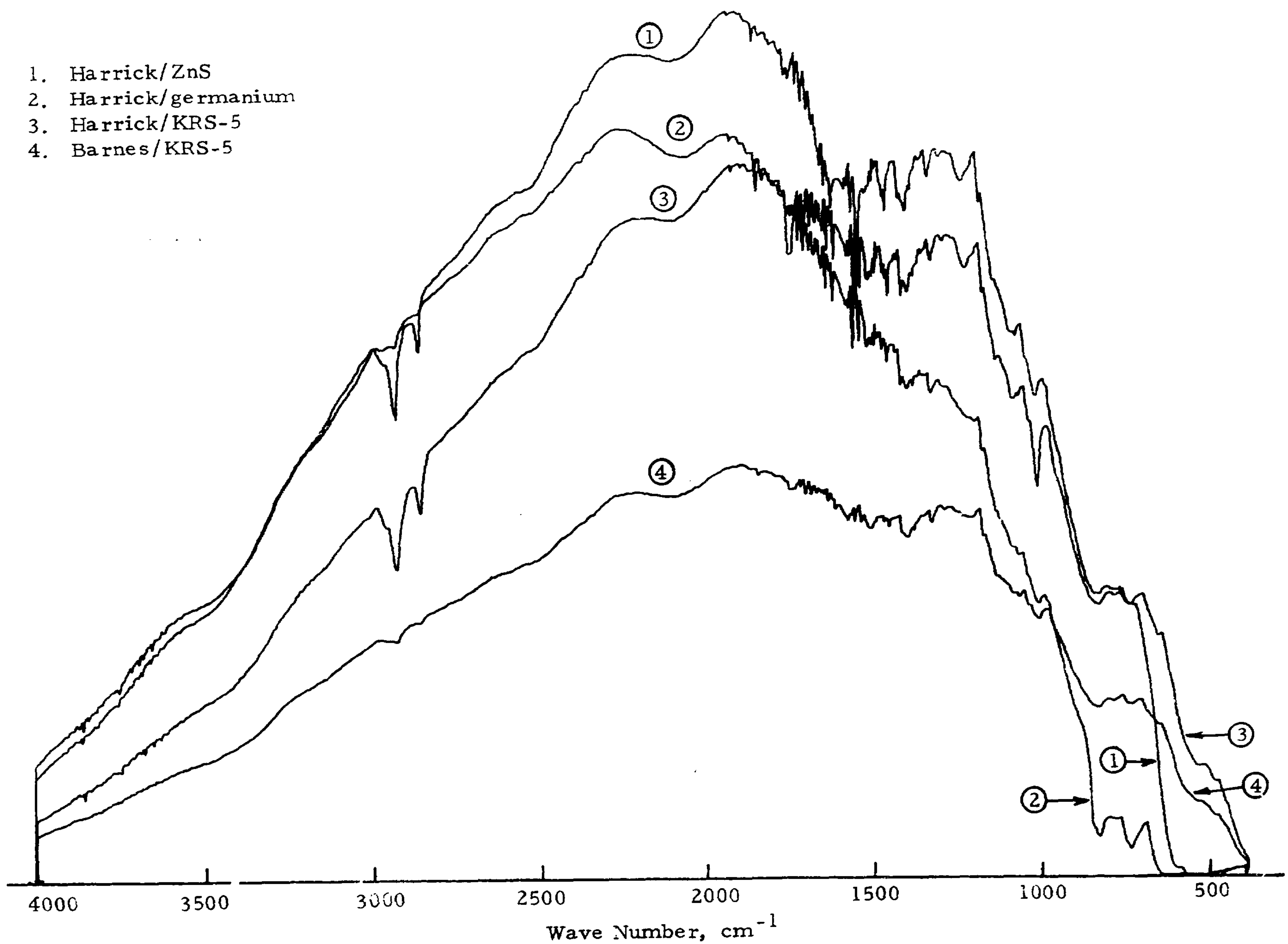


Figure 9. Transmissivity of Various ATR/IRE Combinations.

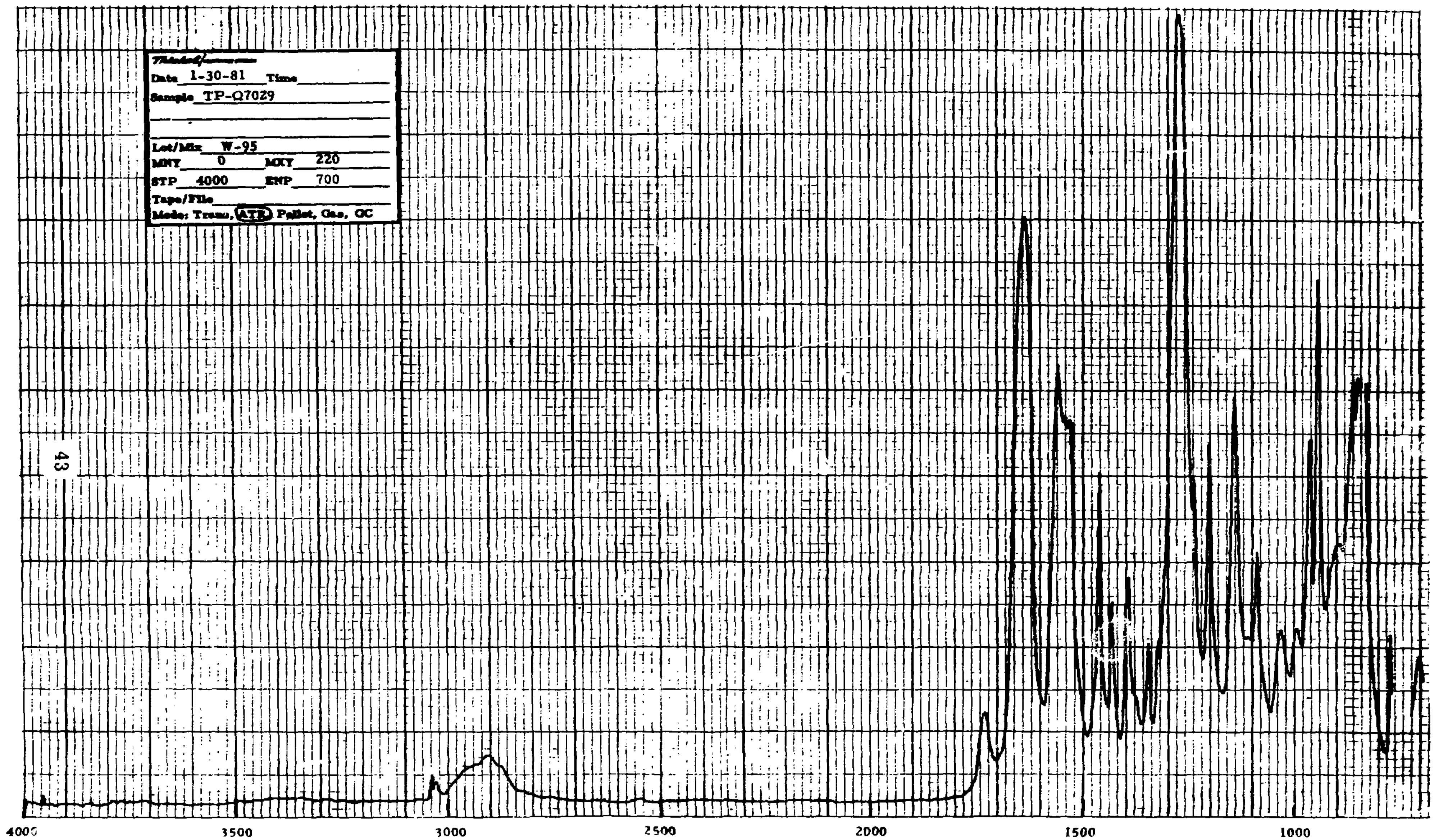


Figure 10. Infrared Spectrum of TP-Q7029 Propellant.

Another serious problem was that there were apparently no binder peaks which were free of the influence of HMX and nitratoplasticizer.

Potential solutions were:

1) Locate binder peaks where the nitratoplasticizers and nitramine oxidizers do not interfere.

2) Make the IR spectrum of the propellant gel fraction after a gel/sol separation has been performed.

An infrared spectrum was made of a small piece of minimum smoke propellant, TP-Q7029, that had been through a gel/sol extraction using acetone. HMX and the three nitratoplasticizers present in TP-Q7029 propellant are soluble in acetone. The spectrum of the gel fraction is displayed in Figure 11. Comparing this spectrum with Figure 10 reveals that there are some outstanding differences and it appears that the spectrum shown on Figure 11 is free of the spectral influences of HMX and the plasticizers. The separation was effective and this technique for taking the infrared spectra of the aging minimum smoke propellant was chosen.

IR Data Collection Parameters

Evaluation of FTS-10 "Collect" Parameters

One of the work items of Task 1 was to perform a statistical analysis of the "collect" parameters used for accumulating the infrared information and to establish the set of parameters which will give statistically sound data. FTS-10 collect parameters examined were: resolution, word size, and number of scans to be co-added by the computer. Three resolutions values were selected for evaluation: 2, 4, and 8 $cm^{-1}$. In the word size category, there were two levels of variable, single precision and double precision. For the number of scans to be co-added, we selected 250, 500, and 1000. These variables were input to a computer program, entitled "COED", that designed an experiment to determine the interactions among the three variables and to aid in selecting the set of conditions to provide the best spectral information. The experiment designed by COED is given in Table 12.

The first four experiments constituted the minimum effort, and those four experiments were performed.

Infrared spectra of propellant TP-H8279 were run using the Barnes Engineering attenuated total reflectance (ATR) unit with its KRS-5 internal

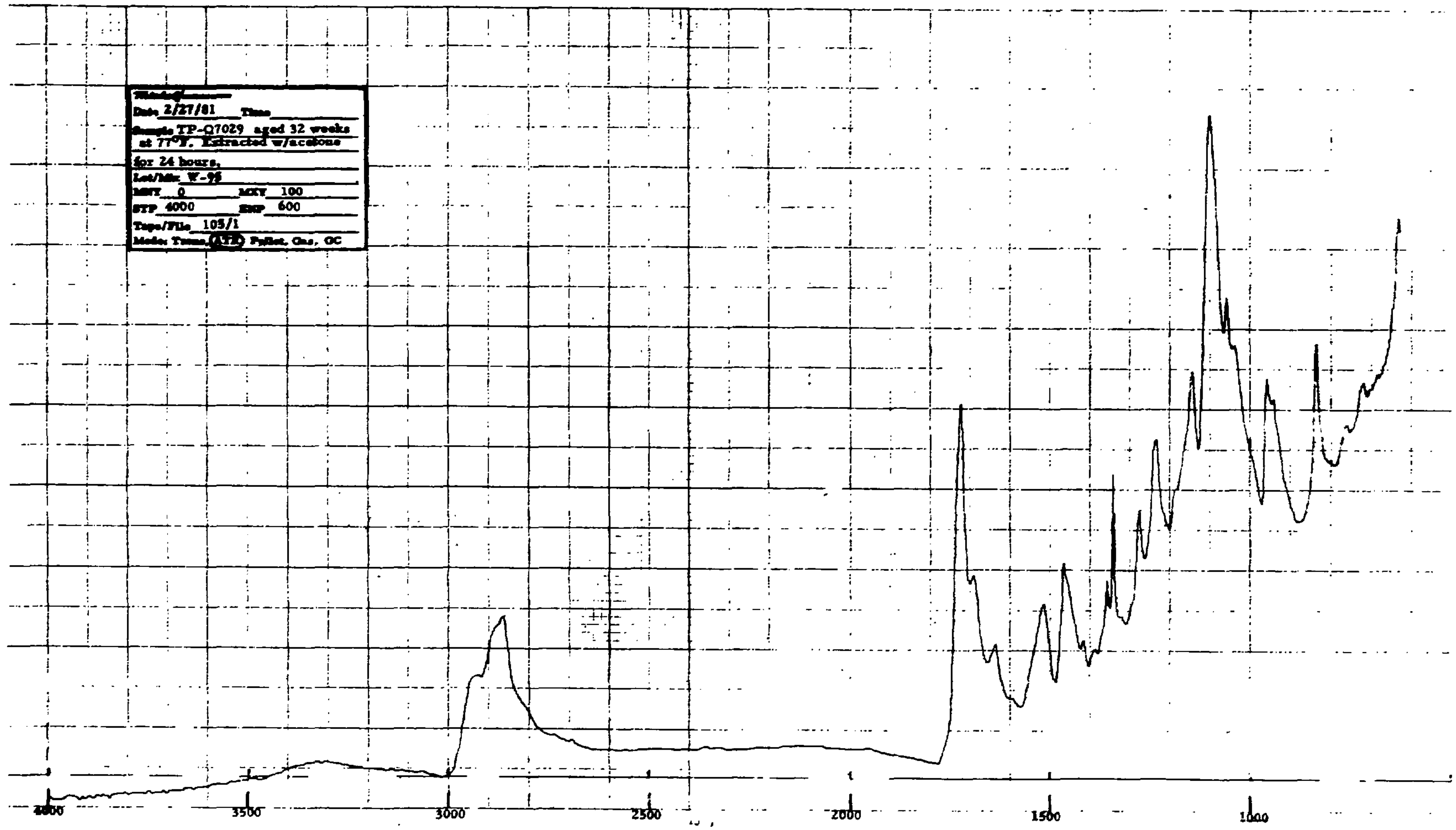


Figure 11. IR Spectrum of the Gel Fraction of TP-Q7029 Propellant.

## TABLE 12

## EXPERIMENT DESIGN FOR ANALYSIS OF FTS-10 "COLLECT" PARAMETERS

Number of Variables: 3

Independent Variable Names:

| | |
|---|---|
| Variable No. 1 | Resolution (RES) |
| Variable No. 2 | Word Size (WDS) |
| Variable No. 3 | Number of Scans (NSS) |

Design Space and Levels:

For each variable, specify number of levels:

| | |
|---|---|
| RES | 2 4 8 |
| WDS | 0 1* |
| NSS | 250 500 1000 |

The first 4 Expts. constitute minimum effort.

| | RES = $X_1$ | WDS = $X_2$ | NSS = $X_3$ |
|---|---|---|---|
| 1 | 8 | 0 | 1000 |
| 2 | 2 | 0 | 250 |
| 3 | 4 | 1 | 1000 |
| 4 | 8 | 1 | 250 |
| 5 | 4 | 0 | 250 |
| 6 | 4 | 0 | 500 |
| 7 | 8 | 0 | 250 |
| 8 | 2 | 0 | 1000 |
| 9 | 8 | 1 | 1000 |
| 10 | 4 | 1 | 500 |
| 11 | 4 | 1 | 250 |

*0 = Single Precision; 1 = Double Precision

reflectance element (IRE). The resolution, word size, and number of scans per sample were varied in the test series to measure their effect, if any, on the precision of the data from the FTIS instrument. Four sets of conditions were examined and for each set of conditions a separate sample of propellant was used such that, within each set there were six replicate spectra made, all at identical conditions. The digital spectral data were all reduced using computer program E490 that had been modified to accept and reduce data at resolutions of 2 and 4 wave numbers in double as well as single precision. The height of peaks at five wave numbers were analyzed to determine the reproducibility of peak height among each of the sets of six replicate spectra. Peak heights and variables employed for this set of tests are shown in Table 13.

An analysis of variance and a regression analysis on the standard deviation of the replicates were calculated from the data of Table 13 to measure the effect of resolution, word size, and number of scans on the peak height within a wave number and the precision as measured by the within-group standard deviation. Averages for the values at each of the wave numbers are summarized on Table 14 and the standard deviations for these values are given in Table 15. Natural logarithms were used in the calculation so that direct relative comparisons can be made.

Note on Table 13 that there are some abnormally low values for the peak in the 772-776 $cm^{-1}$ region in data set 2 (that set having resolution of 2, single precision, and 250 scans). This was somewhat puzzling, so the infrared spectra in this region were plotted to determine why these three values are so greatly different from the other three values. All six samples in this data set were plotted in the region 640-870 $cm^{-1}$ and the plots are shown in Figure 12. Data tabulated in Table 13 show that replicates 2, 3, and 6 had abnormally low values. Examination of these three spectra in Figure 12 reveals that they are greatly different from the spectra for replicates 1, 4, and 5...the difference being that the peak at the 775 $cm^{-1}$ region is split in the case of spectra 2, 3, and 6 and not split for the other three spectra. The infrared data reduction program (E490) establishes a baseline for each peak for the purpose of measuring peak height by "drawing a line" from minimum to minimum on either side of the peak or from minimum to tangency point on either side of the peak. If one draws baseline for each of the six spectra in Figure 12, it is obvious why the 776 $cm^{-1}$ peak in spectra 2, 3, and 6 will have very small peak heights while the peak height for spectra 1, 4, and 5 will be of significantly greater magnitude. This not only explains why there were two families of peak heights in that data, but also points out an undesirable condition that would exist with spectra made at resolution 2 at a relatively small number of scans. The split in the peak height at 776 $cm^{-1}$ occurred 50% of the time and <u>not</u> 50% of the time. The magnitude of the "split" peaks is approximately the magnitude of the electronic noise that occurs elsewhere in the spectrum. This is apparent by examining the variation among the six spectra in the 800-825 $cm^{-1}$ region.

The results of this analysis are summarized as follows:

1) The effect, if any, of word size (double or single precision) could not be distinguished from experimental error.

TABLE 13

FTIS PRECISION STUDY
(ATR by Barnes Engineering)

| | Experimental Variables | | | | Wave Number, $cm^{-1}$ | | | | |
|---|---|---|---|---|---|---|---|---|---|
| | Resolution | Word Size | No. of Scans | Replicate | 2923-2929 | 1737-1739 | 1236-1239 | 909-912 | 772-776 |
| | | | | | Peak Heights | | | | |
| 1) | 8 | Single | 1000 | 1 | 36.990 | 26.240 | 5.419 | 32.025 | 2.478 |
| | | | | 2 | 37.038 | 26.581 | 5.490 | 32.135 | 2.530 |
| | | | | 3 | 37.104 | 26.703 | 5.615 | 32.034 | 2.540 |
| | | | | 4 | 37.169 | 26.745 | 5.574 | 31.994 | 2.509 |
| | | | | 5 | 36.925 | 26.671 | 5.536 | 31.847 | 2.516 |
| | | | | 6 | 37.009 | 26.587 | 5.540 | 31.876 | 2.513 |
| 2) | 2 | Single | 250 | 1 | 34.836 | 23.316 | 5.150 | 29.388 | 2.682 |
| | | | | 2 | 34.943 | 23.858 | 5.238 | 27.330 | 0.936 |
| | | | | 3 | 34.917 | 24.406 | 5.101 | 28.430 | 0.658 |
| | | | | 4 | 35.172 | 25.570 | 5.410 | 28.103 | 2.834 |
| | | | | 5 | 35.171 | 24.689 | 5.236 | 27.874 | 2.174 |
| | | | | 6 | 35.128 | 24.558 | 5.321 | 26.758 | 0.847 |
| 3) | 4 | Double | 1000 | 1 | 37.599 | 26.210 | 5.835 | 33.014 | 2.819 |
| | | | | 2 | 37.760 | 26.856 | 5.892 | 32.844 | 2.771 |
| | | | | 3 | 37.854 | 27.338 | 5.925 | 32.771 | 2.844 |
| | | | | 4 | 37.899 | 27.577 | 5.809 | 32.827 | 2.802 |
| | | | | 5 | 37.929 | 27.682 | 5.828 | 32.658 | 2.770 |
| | | | | 6 | 37.796 | 27.644 | 5.896 | 32.746 | 2.671 |
| 4) | 8 | Double | 250 | 1 | 38.870 | 27.070 | 5.651 | 35.779 | 2.624 |
| | | | | 2 | 39.065 | 27.909 | 5.778 | 35.213 | 2.693 |
| | | | | 3 | 39.035 | 28.050 | 5.815 | 35.185 | 2.485 |
| | | | | 4 | 39.380 | 28.784 | 5.796 | 35.462 | 2.625 |
| | | | | 5 | 39.450 | 28.781 | 5.912 | 35.798 | 2.735 |
| | | | | 6 | 39.497 | 28.895 | 5.949 | 35.654 | 2.716 |

TABLE 14

FTIS STUDY - SUMMARY OF AVERAGES

(Barnes ATR, 6 Replicates per Average)

| ID | Wave Number, $cm^{-1}$ 2923-2929 $\overline{X}\,\ell n$ | 2923-2929 $\overline{X}$ | 1737-1739 $\overline{X}\,\ell n$ | 1737-1739 $\overline{X}$ | 1236-1239 $\overline{X}\,\ell n$ | 1236-1239 $\overline{X}$ | 909-912 $\overline{X}\,\ell n$ | 909-912 $\overline{X}$ | 772-776 $\overline{X}\,\ell n$ | 772-776 $\overline{X}$ |
|---|---|---|---|---|---|---|---|---|---|---|
| Res 8, SP, 1000 | 3.6120 | 37.040 | 3.2804 | 26.586 | 1.7099 | 5.528 | 3.4652 | 31.983 | 0.9220 | 2.514 |
| Res 2, SP, 250 | 3.5561 | 35.026 | 3.1942 | 24.391 | 1.6566 | 5.241 | 3.3311 | 27.969 | 0.9349* | 2.547* |
| Res 4, DP, 1000 | 3.6325 | 37.807 | 3.3037 | 27.213 | 1.7688 | 5.864 | 3.4907 | 32.809 | 1.0221 | 2.779 |
| Res 8, DP, 250 | 3.6691 | 39.216 | 3.3408 | 28.242 | 1.7606 | 5.816 | 3.5699 | 35.513 | 0.9721 | 2.643 |

*Deleting three abnormally low values.

TABLE 15

FTIS STUDY - SUMMARY OF STANDARD DEVIATIONS

(Barnes ATR, 6 Replicates per Group)

| ID | Wave Number, $cm^{-1}$ 2923-2929 Std. Dev. $\ell n$ units x $10^2$ | 1737-1739 Std. Dev. $\ell n$ units x $10^2$ | 1236-1239 Std. Dev. $\ell n$ units x $10^2$ | 909-912 Std. Dev. $\ell n$ units x $10^2$ | 772-776 Std. Dev. $\ell n$ units x $10^2$ |
|---|---|---|---|---|---|
| Res 8, SP, 1000 | 0.233 | 0.687 | 1.235 | 0.335 | 0.847 |
| Res 2, SP, 250 | 0.418 | 3.144 | 2.134 | 3.238 | 13.990* |
| Res 4, DP, 1000 | 0.315 | 2.154 | 0.788 | 0.364 | 2.189 |
| Res 8, DP, 250 | 0.661 | 2.539 | 1.823 | 0.768 | 3.442 |

*Deleting three abnormally low values.

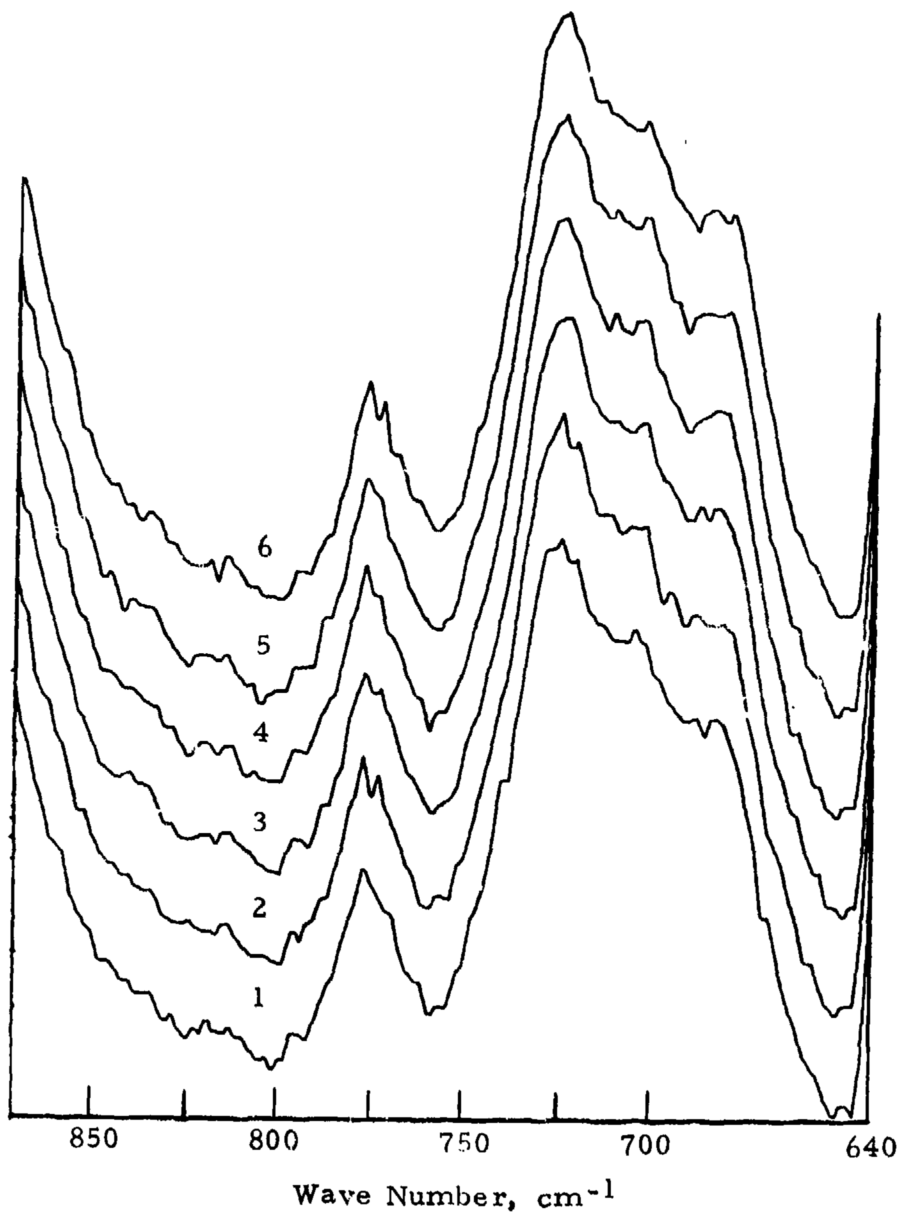


Figure 12. Spectral Region 870-640 $cm^{-1}$ at RES - 2, WDS - SP, NSS - 250 (Plots are not normalized).

2) The best precision occurs when there are 1000 scans per sample (this is supported by regression analyses where "scans per sample" was the only statistically significan factor).

3) There is evidence (although not highly significant) that the higher numbered resolutions improved the test precision.

4) The relative precision depends upon the peak height or wave number. The best precision occurs with the highest average height, while the worst is with the lowest average height. The coefficient of variation at heights of 35 to 39 ranged from 0.23% to 0.66%, while those at heights of 2.5 to 2.8 ranged from 0.85% to about 15% (set 2 at 772-776 $cm^{-1}$).

Based on this summary, we concluded that resolution 2 should not be considered in accumulating infrared data for the purposes of this project or for the purposes of following the aging of propellant. The reasoning here is there are too many data to conveniently analyze and, based upon the statistical analysis, these data are more subject to the effects of electronic noise and unknown variability than data gathered at a lesser resolution. Word size of double precision will not be employed since there seems to be no benefit from using double precision word size.

There is no clear-cut distinction between resolution 4 and resolution 8, so additional experimentation was performed to make this decision. A two-variable experiment was run in which the two variables were resolution (4 and 8) and number of scans per sample (250, 500, and 1000). This six-experiment matrix was replicated six times.

Data for this statistical analysis were collected using the Harrick ATR unit with its zinc selenide (ZnSe) internal reflection element (IRE). Other fixed conditions of the data collection were word size of single precision; UDR = 2; ZFF = 1; DPM = P. Four wave numbers were selected and peak heights at these wave numbers were statistically compared. Examples of the spectra used in this analysis are shown on Figures 13 and 14. On Figure 13, the spectrum is at a resolution of 8, while on Figure 14 the resolution of the spectrum is at 4. Infrared peaks from which the data were taken for the statistical analysis are identified by arrows. All of the raw data used in the analysis are displayed in Table 16. An analysis of this data is presented in Table 17.

A review of those data revealed that the greatest change in the magnitude of any peak occurred prior to the third replicate in each of the sets, although there were some exceptions to this observation. This change in magnitude was due to "flow" of the sample in the ATR unit. In order to obtain a good spectrum of a solid, using an ATR technique, the sample is placed next to the IRE and pressure is applied to the sample retaining plate to hold the sample firmly against the IRE. Because propellant is visco-elastic, it will cold-flow and as it does so, the binder, and particularly the sol portion, will flow around ammonium perchlorate particles so that the magnitude of the organic portion of the spectrum increases slightly with time.

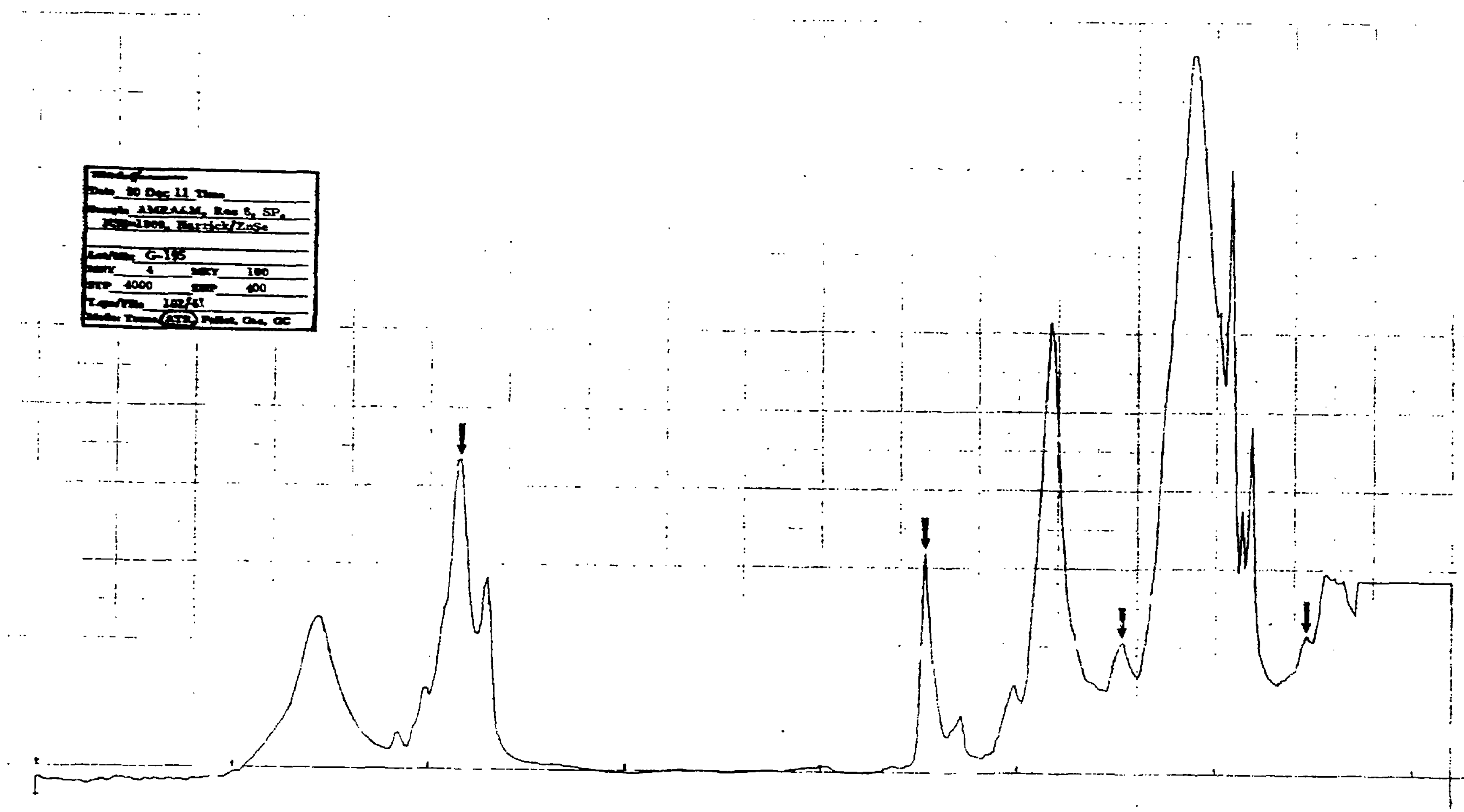

Figure 13. Infrared Spectrum of AMRAAM Propellant; for "Collect" Parameters Study.

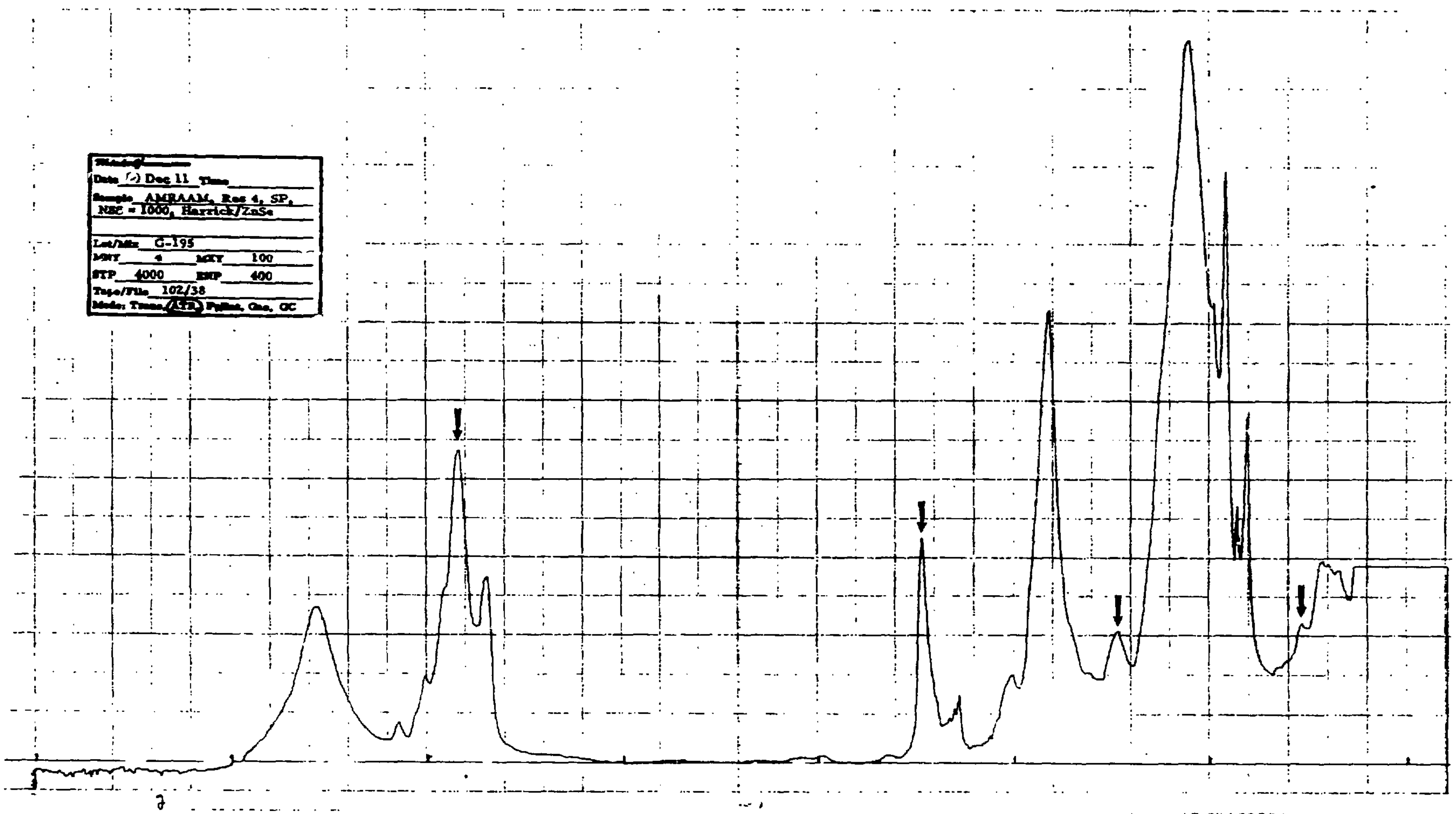


Figure 14. **Infrared Spectrum of AMRAAM Propellant; for "Collect" Parameters Study.**

TABLE 16

ABSORPTION* DATA FOR VARIANCE ANALYSIS

| NSS | RES | Replicate | Absorption at Wave Number 2923-2929 | 1737-1739 | 1236-1244 | 772-776 |
|---|---|---|---|---|---|---|
| 250 | 8 | 1 | 36.818 | 24.705 | 5.041 | 1.910 |
| | | 2 | 36.960 | 25.089 | 5.177 | 1.842 |
| | | 3 | 36.780 | 25.018 | 5.114 | 1.548 |
| | | 4 | 36.718 | 25.121 | 5.121 | 2.061 |
| | | 5 | 36.854 | 25.135 | 5.250 | 1.941 |
| | | 6 | 36.861 | 25.153 | 5.184 | 2.000 |
| 500 | 8 | 1 | 36.878 | 24.565 | 4.949 | 1.795 |
| | | 2 | 36.837 | 25.150 | 5.181 | 1.995 |
| | | 3 | 37.074 | 25.230 | 5.178 | 2.010 |
| | | 4 | 36.846 | 25.189 | 5.187 | 1.906 |
| | | 5 | 36.871 | 25.233 | 5.178 | 1.786 |
| | | 6 | 36.888 | 25.254 | 5.203 | 2.057 |
| 1000 | 8 | 1 | 36.782 | 24.653 | 4.932 | 1.958 |
| | | 2 | 36.857 | 25.144 | 5.124 | 1.953 |
| | | 3 | 36.919 | 25.205 | 5.179 | 2.034 |
| | | 4 | 36.860 | 25.217 | 5.188 | 1.577 |
| | | 5 | 36.785 | 25.203 | 5.222 | 1.496 |
| | | 6 | 36.832 | 25.253 | 5.211 | 1.720 |
| 250 | 4 | 1 | 37.377 | 25.082 | 5.087 | 1.018 |
| | | 2 | 37.494 | 25.860 | 5.277 | 1.950 |
| | | 3 | 37.586 | 26.011 | 5.225 | 1.852 |
| | | 4 | 37.603 | 26.045 | 5.180 | 2.013 |
| | | 5 | 37.784 | 26.164 | 5.260 | 2.041 |
| | | 6 | 37.650 | 26.128 | 5.141 | 2.340 |
| 500 | 4 | 1 | 37.189 | 25.154 | 4.988 | 2.087 |
| | | 2 | 37.447 | 25.796 | 5.130 | 1.052 |
| | | 3 | 37.525 | 25.938 | 5.179 | 1.320 |
| | | 4 | 37.505 | 25.978 | 5.254 | 1.681 |
| | | 5 | 37.555 | 26.003 | 5.134 | 1.895 |
| | | 6 | 37.557 | 26.027 | 5.217 | 1.886 |
| 1000 | 4 | 1 | 37.329 | 25.294 | 4.936 | 2.493 |
| | | 2 | 37.367 | 25.829 | 5.121 | 1.861 |
| | | 3 | 37.431 | 25.900 | 5.143 | 1.841 |
| | | 4 | 37.451 | 25.963 | 5.138 | 1.942 |
| | | 5 | 37.463 | 25.978 | 5.162 | 2.018 |
| | | 6 | 37.472 | 26.025 | 5.198 | 1.850 |

*Harrick ATR/ZnSe IRE
WDS = SP; UDR = 2; ZFF = 1; DPM = P

TABLE 17

VARIANCE OF IR SPECTRA
(All 6 spectra included in each set)

| NSS | RES | Identification of Value | Value at Wave Number 2923-2929 | 1737-1739 | 1236-1244 | 772-776 |
|---|---|---|---|---|---|---|
| 250 | 8 | Avg. absorp. | 36.832 | 25.037 | 5.148 | 1.884 |
| | | Std. deviation | 0.08198 | 0.16935 | 0.07194 | 0.18076 |
| | | % Std. Deviat. | 0.222 | 0.676 | 1.397 | 9.596 |
| 500 | 8 | Avg. absorp. | 36.899 | 25.103 | 5.146 | 1.925 |
| | | Std. deviation | 0.08789 | 0.2664 | 0.0970 | 0.1150 |
| | | % Std. Deviat. | 0.238 | 1.061 | 1.884 | 5.975 |
| 1000 | 8 | Avg. absorp. | 36.839 | 25.112 | 5.143 | 1.790 |
| | | Std. deviation | 0.0517 | 0.2278 | 0.1087 | 0.2241 |
| | | % Std. Deviat. | 0.140 | 0.907 | 2.113 | 12.520 |
| 250 | 4 | Avg. absorp. | 37.582 | 25.882 | 5.195 | 1.869 |
| | | Std. deviation | 0.1383 | 0.4059 | 0.0730 | 0.4479 |
| | | % Std. Deviat. | 0.368 | 1.568 | 1.405 | 23.966 |
| 500 | 4 | Avg. absorp. | 37.463 | 25.816 | 5.150 | 1.654 |
| | | Std. deviation | 0.1402 | 0.3344 | 0.0928 | 0.3935 |
| | | % Std. Deviat. | 0.374 | 1.295 | 1.802 | 23.796 |
| 1000 | 4 | Avg. absorp. | 37.419 | 25.832 | 5.116 | 2.001 |
| | | Std. deviation | 0.0578 | 0.2720 | 0.0922 | 0.2505 |
| | | % Std. Deviat. | 0.155 | 1.053 | 1.801 | 12.521 |

In gathering the IR spectra, replicate No. 1 for each set of conditions was taken, then replicate 2 for each set of conditions, then replicate 3, and so forth to replicate 6. The first spectrum was taken at the conditions where NSS = 250 and RES = 8 and the last of the No. 1 replicates was taken where NSS = 1000 and RES = 4. A review of the data also reveals the least variability in replicates 1 and 2 at the conditions NSS = 1000 and RES = 4. That is simply because the sample had greater time to cold-flow and equilibrate from the first to the last spectrum in the replicate 1 series.

Because of this cold-flow characteristic of the propellant, an analysis was made of only the last four replicates in each data set. That revealed a greatly improved reproducibility of the spectra and, thus, was a more true representation of the variance due to electronic noise and other equipment vagaries inherent in the FTS-10. The variance analysis involving the last four spectra in each set is given in Table 18. As a group, those spectra accumulated at resolution 4 have a lower standard deviation than those spectra taken at resolution 8. Thus, resolution 4 is preferred over resolution 8. Of the spectra taken at resolution 4, those where NSS = 1000 had a lower standard deviation than those taken where the number of scans was 250. Thus, 1000 scans of the samples is preferable to 250 or 500 scans of the sample.

## Sample Thickness

Thickness of the propellant sample for the Bondline Infrared studies was felt to be an important parameter, having some control over the reproducibility of the infrared data. Thicknesses of 0.005, 0.010, and 0.020 inch were employed in this study. Samples of a single piece of HTPB propellant that had not been subjected to high-temperature aging were cut and used in the Harrick ATR unit with a zinc selenide IRE. Torque level (i.e., pressure) holding the sample against the IRE was varied, and the spectrum of the propellant taken. As a measure of the effect of thickness and torque level on spectral amplitude, the amplitude of the peak at 2920 $cm^{-1}$ was measured. A plot of the accumulated data is shown on Figure 15.

Propellant cut to a thickness of 0.005 inch was found to be too difficult to handle. These samples were very easily torn, and the difficulty in handling the propellant at this thickness is compounded by the fact that the sample for the Harrick ATR unit is very small (50 mm x 6 mm). Of the other two thicknesses of propellant, we concluded that a thickness of 0.010 inch is preferred over a thickness of 0.020 inch, although the preference is not very strong. The sample cut to 0.010 inch underwent less change as torque level was increased than did the sample cut to a thickness of 0.020 inch. Growth of the spectral amplitude as torque level is increased is merely the result of cold-flow of the viscoelastic binder in the propellant. As torque level is increased, the binder flows around AP particles and more of the binder material is pressed against the IRE so that the organic portion of the propellant is more clearly displayed. This is a definite advantage, but with that also comes the problem of selective migration or movement of plasticizer and binder sol fraction in the propellant to the point where it is preferentially present at the IRE surface. The less change there is in the spectral amplitude, i.e., the less cold flow there is, the more representative the spectrum will be of the true composition of the propellant.

TABLE 18

VARIANCE OF IR SPECTRA
(Last 4 spectra included in each set)

| NSS | RES | Identification of Value | Value at Wave Number 2923-2929 | 1737-1739 | 1236-1244 | 772-776 |
|---|---|---|---|---|---|---|
| 250 | 8 | Avg. absorp. | 36.803 | 25.107 | 5.167 | 1.888 |
| | | Std. deviation | 0.0676 | 0.0606 | 0.0[illegible]25 | 0.2316 |
| | | % Std. Deviat. | 0.184 | 0.241 | 1.210 | 12.269 |
| 500 | 8 | Avg. absorp. | 36.920 | 25.226 | 5.187 | 1.940 |
| | | Std. deviation | 0.1043 | 0.0272 | 0.0118 | 0.1204 |
| | | % Std. Deviat. | 0.282 | 0.108 | 0.227 | 6.204 |
| 1000 | 8 | Avg. absorp. | 36.849 | 25.220 | 5.200 | 1.707 |
| | | Std. deviation | 0.0560 | 0.0232 | 0.0199 | 0.2370 |
| | | % Std. Deviat. | 0.152 | 0.092 | 0.383 | 13.885 |
| 250 | 4 | Avg. absorp. | 37.656 | 26.087 | 5.202 | 2.062 |
| | | Std. deviation | 0.0897 | 0.0711 | 0.0519 | 0.2035 |
| | | % Std. Deviat. | 0.238 | 0.272 | 0.999 | 9.869 |
| 500 | 4 | Avg. absorp. | 37.535 | 25.987 | 5.196 | 1.696 |
| | | Std. deviation | 0.0251 | 0.0380 | 0.0514 | 0.2691 |
| | | % Std. Deviat. | 0.067 | 0.146 | 0.999 | 15.874 |
| 1000 | 4 | Avg. absorp. | 37.454 | 25.966 | 5.160 | 1.913 |
| | | Std. deviation | 0.0177 | 0.0516 | 0.0272 | 0.0837 |
| | | % Std. Deviat. | 0.047 | 0.199 | 0.527 | 4.376 |

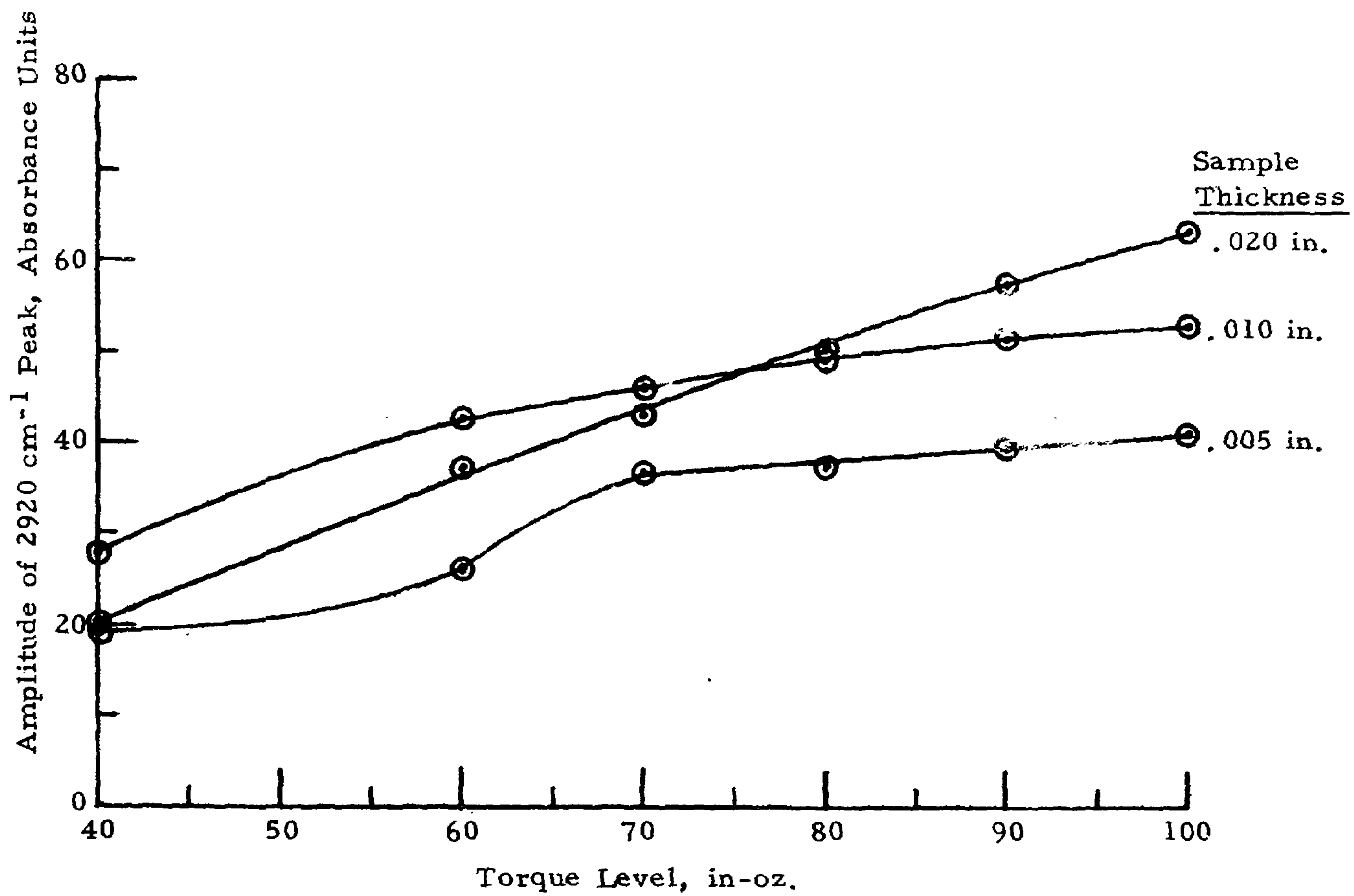


Figure 15. **Effect of Sample Thickness and Torque on Spectral Amplitude.**

## Torque Level

Reproducibility studies revealed that the smaller the magnitude of any given peak, the greater the variability in that peak; variability coming from electronic noise and other uncontrolled sources. In order to reduce the coefficient of variation in the spectral information, we decided that the 2920 $cm^{-1}$ peak in the spectrum should be near an amplitude of 50 absorbance units, and with the HTPB propellant, this required a torque level on the ATR pressure plate assembly bolts of 60 to 100 in-oz. With other propellants, this torque level will be different. The amplitude of the spectrum in the 2920 $cm^{-1}$ region (also all other regions of the spectrum), is also a function of the length of time one waits from the initial torquing of the ATR unit until the spectrum is taken.

We thought that it would be important to establish the relationship between wait time, torque level, and the amplitude of the resulting spectrum so that if wait time were an important parameter that it, too, could be specified as a part of the standard IR data acquisition procedure. To this end, we employed samples at a thickness of 0.010 and 0.020 inch and torqued these samples to levels of 60 and 100 in-oz. The influence of wait-time and torque level on spectral amplitude is plotted on Figures 16 and 17. A review of these two plots will show that the amplitude does not stop changing, but continued to change for as long as we conducted the test. As can be seen on Figure 17, with the 0.020-inch sample, most of the change occurred within 20 minutes.

In order to identify a procedure whereby we could reach an equilibrium spectral amplitude in a short time, we took one of the propellant samples at a thickness of 0.010 inch and assembled it into the ATR unit which had been preheated to 77°C. It was thought that by warming the sample, it would flow quickly and reach a point where it would stop flowing; however, this supposition was incorrect, as can be seen on Figure 18. Changes in spectral amplitude continued for a period of 18 hours. As a matter of fact, it appears that the procedure created more flow than a sample and ATR unit at nominal room temperature. Heat, therefore, is not an effective way to quickly bring the sample to flow equilibrium.

A second method investigated for quickly establishing flow equilibrium was to torque the sample initially to a high value, loosen the clamping screw, and then retorque the sample to a lower value. The results of this experiment are plotted on Figure 19 and show that the procedure was totally ineffective in stopping cold flow. On the basis of these experiments, we conclude that there is no way to stop the cold flow. It is going to occur, and therefore, we must live with it. It is one of the "uncontrolled" variables that will have some influence on reproducibility of the IR data.

## IRE Cleaning Procedure

In the course of running these experiments, we found at one point that we were getting a large variation in the magnitude of the $-CH_2-$ peaks in the 2900 $cm^{-1}$ region. The variance was considerably larger than we had experienced previously when we had been using the same sample over and over again for the reproducibility studies. Several experiments revealed the source to be the procedure for cleaning the IRE after each use.

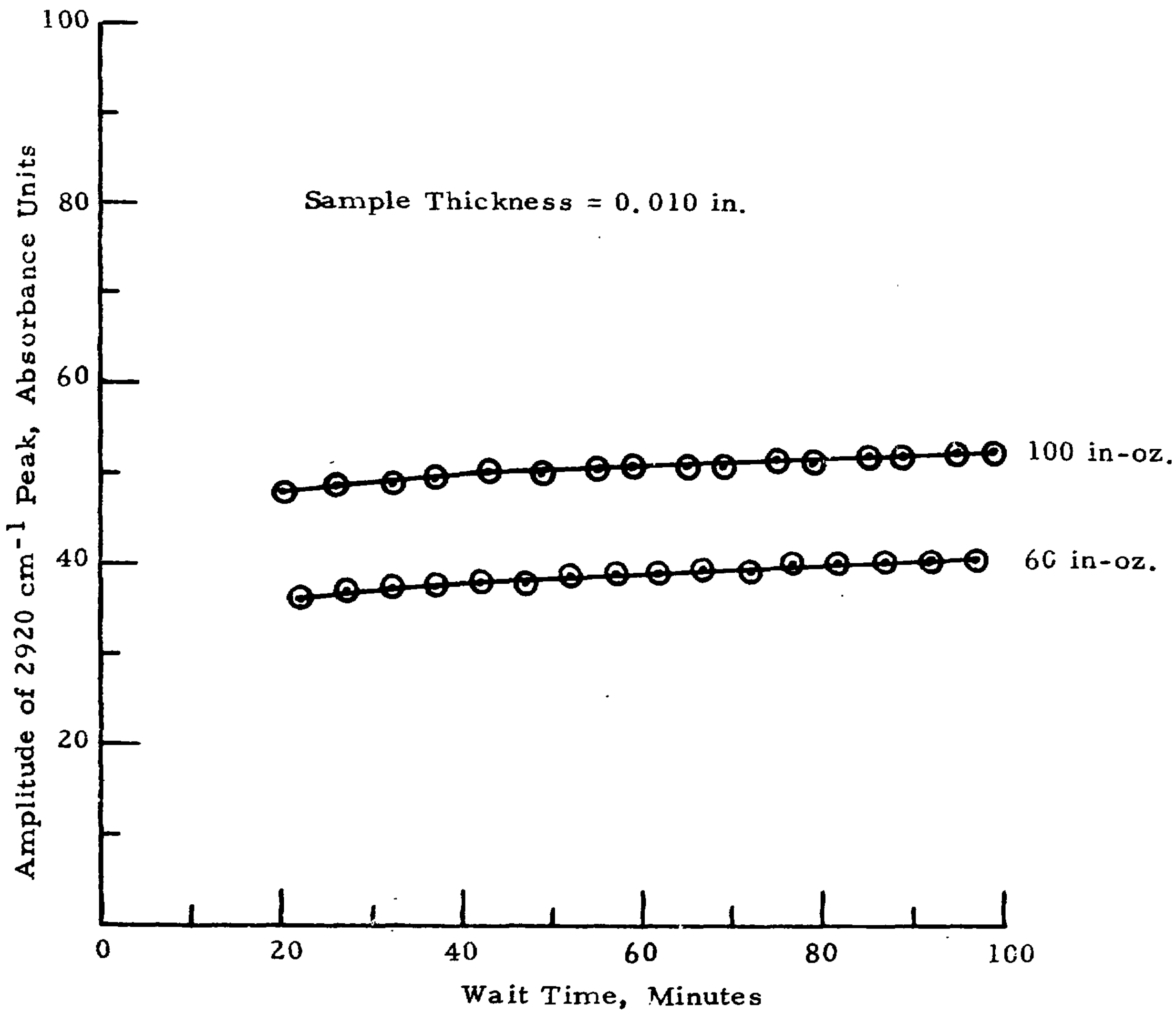


Figure 16. Effect of Wait Time and Torque on Spectral Amplitude.

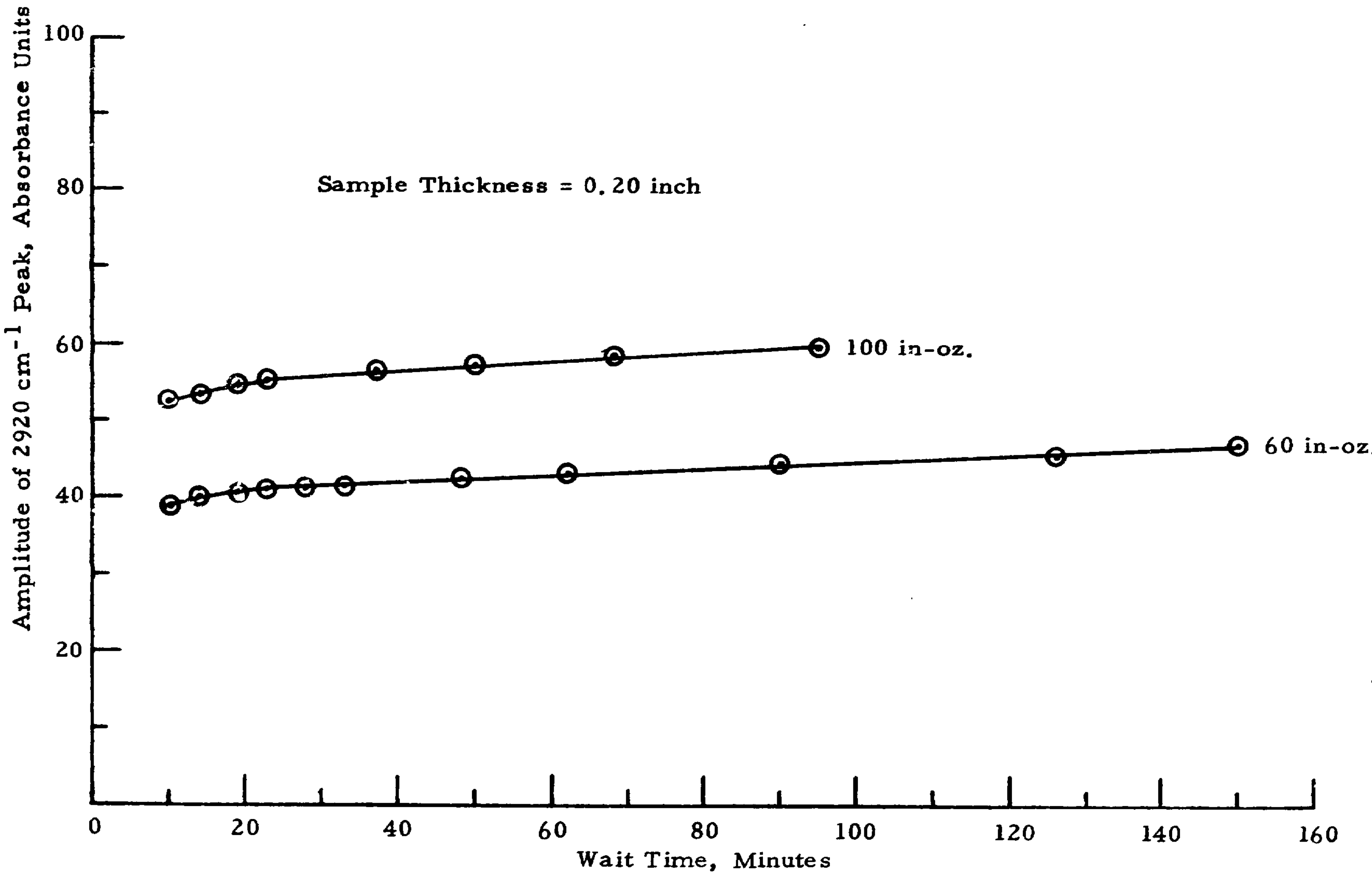


Figure 17. **Effect of Wait Time and Torque on Spectral Amplitude.**

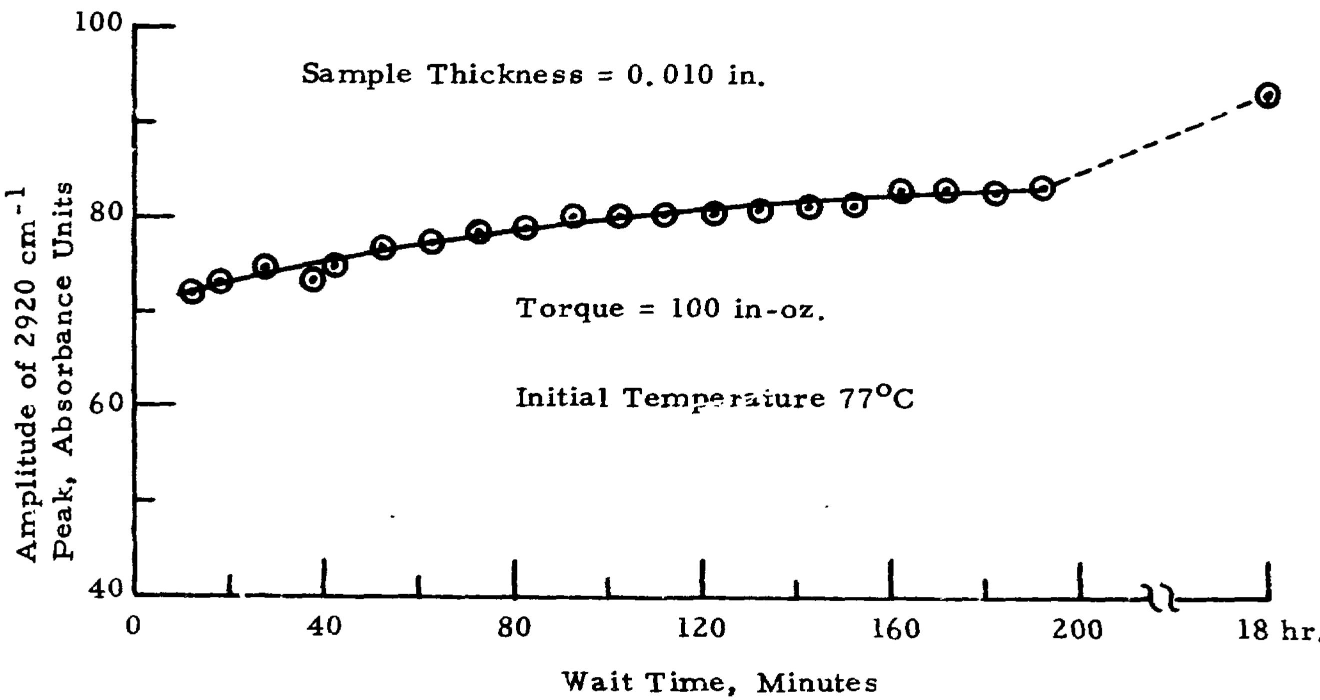


Figure 18. Effect of Heat on Wait Time and Spectral Amplitude.

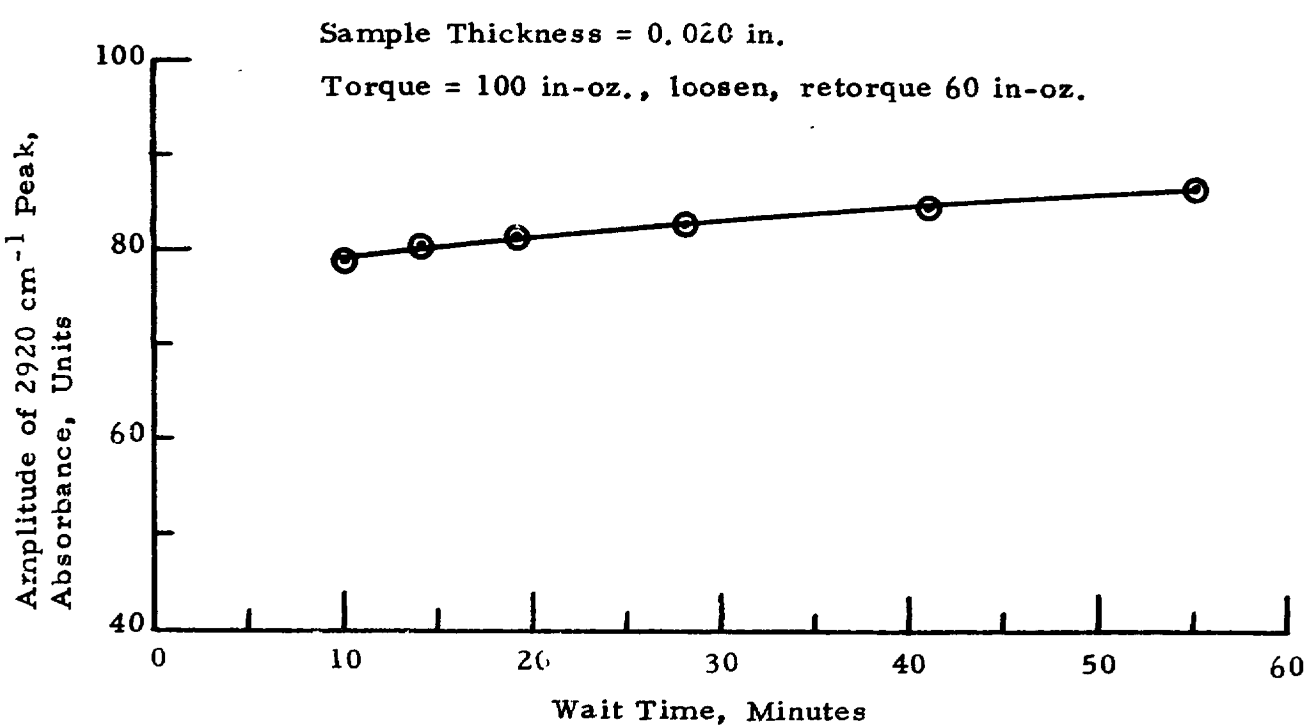


Figure 19. Effect of Torquing Procedure on Wait Time and Spectral Amplitude.

When we found this variation, our cleaning procedure was to rinse the IRE with methylene chloride, then with ethanol and dry the IRE using a lens tissue. It turned out that the lens tissue was depositing organic material on the IRE and the amount of organic material deposited was a function of how hard and how long the IRE was rubbed. A few experiments revealed as much as 5% variation in the height of the $-CH_2-$ peaks. A change in the cleaning and drying procedure reduced that variation to 0.

The standard cleaning procedure is: Rinse the IRE with a stream of methylene chloride, rinse with a stream of ethanol, rinse again with methylene chloride, and then dry the IRE in warm air from a heat gun or hair-dryer.

Final Procedure for Taking IR Spectra

A reproducibility test series was run to establish the variation that could be expected employing all of the selected data acquisition procedures and parameters. In this experiment series, a single sample of the HTPB propellant was used and the propellant cut to a thickness of 0.010 inch. Six samples were selected and the IR spectra of each sample made using the standard procedure. Data collected in this series are displayed in Table 19 and are typical of the variance that can be expected. Standard procedures for acquiring IR data are given in Table 20.

Task 2 - Computer Programming

Modifications were made to the computer program developed as a part of the FTIS project. Modifications were made for the express purpose of improving the utility of the computer program to allow improved data reduction and to make the use of the program easier for the persons employing the program for IR data reduction and analysis. Specifically, three things were to be accomplished: (1) Expand the data array to 1872 data words from the original limit of 468 data words; (2) increase the data analysis options; and (3) retain the tabulated IR data in a form in the computer that would allow it to be used for correlations and data analysis.

At the end of the FTIS project, the computer code E490 would read IR spectra from magnetic tape and reduce the data to a numerical spectrum, as an option it would plot that spectrum. Its limit, however, was 468 data words, which permitted a spectrum made at a resolution of 8 wave numbers with data accumulated in single precision over the spectral range of 4000-400 $cm^{-1}$. That data handling capability was improved by reprogramming so that now the computer program handles 1872 data words per file for a total of 40 files. The expanded capability now permits spectra to be accumulated at a resolution of 2 wave numbers in single precision data words or a resolution of 4 wave numbers in double precision data words.

Computer program E490, at the end of the FTIS project, would do single and multiple correlations of data in linear form or transform to the squared function. Data analysis options have been increased such that the following can now be accomplished:

TABLE 19

SAMPLE-TO-SAMPLE VARIANCE

| Sample | Absorbance at Wave Number 2920 $cm^{-1}$ | 1736 $cm^{-1}$ | 1236 $cm^{-1}$ | 772 $cm^{-1}$ |
|---|---|---|---|---|
| 1 | 53.261 | 36.952 | 8.508 | 3.562 |
| 2 | 52.438 | 36.328 | 8.325 | 3.329 |
| 3 | 52.723 | 36.455 | 8.736 | 3.438 |
| 4 | 52.566 | 36.643 | 8.594 | 3.453 |
| 5 | 52.501 | 36.612 | 8.275 | 3.372 |
| 6 | 52.933 | 36.904 | 8.750 | 3.540 |
| Avg. Value | 52.737 | 36.649 | 8.531 | 3.449 |
| Std. Deviation | 0.3123 | 0.2445 | 0.2012 | 0.0911 |
| Coef. of Variation | 0.592 | 0.667 | 3.417 | 2.642 |

Data Acquisition Conditions:

Harrick ATR/ZnSe

RES = 4

WDS = SP

NSS = 1000

Sample Thickness = 0.010

Wait Time = 15 Minutes

Torque = 100 in-oz.

TABLE 20

## DATA ACQUISITION PROCEDURES FOR HTPB PROPELLANT

### Sample Preparation

ATR Unit: Harrick, 4X Beam Condenser, 60° Angle of Incidence

IRE: Irtran 4 (Zn Se)

Sample Thickness: 0.010 to 0.020 inch

Torque Level: Sufficient to Make 2920 $cm^{-1}$ Peak Have An Amplitude of About 50 Absorbance Units at the Highest Possible SEN setting.

Wait Time: About 15 Minutes

### Spectrum COL (Collect) Parameters for the FTS-10

RES = 4

NSS = 500

UDR = 2

ZFF = 1

SEN = Max., w/o an "overflow" in the A to D converter

WDS = SP (Single Precision)

### IRE Clean-Up

1) Wash (rinse) with stream of $CH_2Cl_2$
2) Rinse with a stream of $CH_2OH$
3) Rinse with a stream of $CH_2Cl_2$
4) Dry in a warm air stream (hair dryer) to prevent moisture condensation.

1) Simple linear correlation;

2) Multiple linear correlations;

3) Nonlinear (squared term) correlations;

4) Simple linear correlations with log of dependent variables;

5) Multiple correlations with log of dependent variables;

6) Simple correlations with log of independent variables;

7) Multiple correlations with log of independent variables;

8) Simple correlations with log of independent and dependent variables;

and, 9) Multiple correlations with log of independent and dependent variables.

One of the shortcomings of the E490 program as it existed at the start of the Bondline Infrared Spectroscopy project was that once the E490 spectral data had been employed in a correlation, the data were lost within the computer; i.e., the data were printed and then all memory of the data in the computer erased. This created problems if one wished to do a different correlation using a transform of one of the dependent or independent variables. The entire E490 IR spectral data reduction needed to be rerun to reassemble the IR data; a time-consuming process. The obvious solution to the problem was to have the IR spectral data stored on disc or on mag tape so that it would be recalled and used as needed. To that end, two changes were made in the E490 computer program: (1) Valid peaks are retained in temporary storage; and, (2) depending upon the user's system, this tabulation can be permanently stored on tape or disc.

Task 3 - Correlation of IR and Bond Properties

Task 3 of Phase I called for the aging of HTPB and minimum smoke propellant bond systems in order to evaluate : (1) The IR data acquisition procedures, (2) several measured properties of the bond systems, and (3) correlations, if any, between (1) and (2). The end product of this task was to be selection of bond properties to measure in a 32-week aging program to be conducted in Phase II.

Selected Bond Systems

Propellant, liner, and insulation for the HTPB-type propellant and for the minimum smoke-type propellant are listed in Table 21. These are the same propellants, liner, and insulators as used in Phase I, Task 1. Compositions of these materials are given in Tables 1 and 2.

Aging Plan

The 16-week aging program is displayed in Table 22. Also listed on that table are the tests performed with each of the five types of samples for the two aging programs. Each of the aging programs followed the same aging plan.

Aging Data

Aging of the two bond systems at 165°F was carried out for a period of 16 weeks. Tests as listed in the aging plan were performed and the

TABLE 21

COMPOSITION OF BOND SAMPLES

(Phase I, Task 3)

HTPB Type Propellant/Liner/Insulation Samples

Insulation: TI-R300 (0.200 inch)

Liner: TL-H755A (0.040 inch)

Propellant: TP-H8279

Minimum Smoke Type Propellant/Liner/Insulation Samples

Insulation: TI-R701 (0.200 inch)

Liner: TL-H763A (0.040 inch)

Propellant: TP-Q7029

TABLE 22

AGING PLAN - PHASE I, TASK 3

| Sample Type | Age Time at 165°F, Weeks | | | | | |
|---|---|---|---|---|---|---|
| | 0 | 2 | 4 | 8 | 12 | 16 |
| 1) Composite Adhesion (18) | 3 | 3 | 3 | 3 | 3 | 3 |
| 2) Liner Tensile (18) | 3 | 3 | 3 | 3 | 3 | 3 |
| 3) Liner/Propellant Peel (18) | 3 | 3 | 3 | 3 | 3 | 3 |
| 4) Liner/Insulation Peel (18) | 3 | 3 | 3 | 3 | 3 | 3 |
| 5) Composite Peel (12) | 2 | 2 | 2 | 2 | 2 | 2 |

Tests at each age time:

1) 3 Samples - Tensile Adhesion at 77°F

2) 3 Samples - Tensile at 77°F on Liner

3) 3 Samples - Peel Strength at 77°F

4) 3 Samples - Peel Strength at 77°F

5) 1 Sample - Hardness Profile
- Gel/Sol Separation on Liner
- Gel/Sol Separation on Propellant as a Function of Distance from Liner Interface
- FTIS on Gel and Sol Fractions

1 Sample - Sectioned for FTIS on Propellant at Selected Locations from Interface with Liner.
- FTIS on Liner

results of HTPB propellant/liner/insulation tests are displayed in Table 23, while those tests of the minimum smoke propellant system are given in Table 24.

Gradient hardness of a composite bond sample for the HTPB bond system was also measured. This composite bond specimen consists of the insulation as a first layer, liner cured on top of insulation, and then propellant cast to a depth of approximately 0.75 inch on top of the liner. This specimen was sectioned vertically through the layers and the hardness of all materials measured using a penetrometer. Gradient hardness data are presented in Appendix C.

Gel fraction of the binders in the HTPB propellant bond system were also measured. The bond specimen described above was used in this test also. Samples of insulation, liner, and propellant were taken and a gel/sol separation of the binder in these materials made. Propellant was sectioned by distance from the liner and the gel fraction of each segment of propellant measured. These gel fraction data are also presented in Appendix C.

The principle objective in performing these mechanical property, hardness, and gel fraction tests was to gather information for correlation to infrared peak height changes. Correlations among mechanical properties, gel fraction, hardness, and time are of interest, of course, but were not the principle concern of the project. An analysis was made of those correlations and this analysis is presented in Appendix C. Correlations among mechanical properties, chemical properties, and infrared properties of the propellant, liner and insulation are presented in the next section of this report.

Correlations among mechanical properties, hardness, gel fraction, and time for the minimum smoke propellant bond system are presented in Appendix D. Also included in that appendix is a tabulation of the gradient hardness data for insulation, liner, propellant composite bond samples. These hardness data were obtained through the use of a penetrometer and a composite bond sample as described above. Propellant gel fraction was also measured and these data are presented in Appendix D. Correlations among the minimum smoke propellant bond system properties and the infrared characteristics of the minimum smoke propellant gel fraction are presented and discussed in the next section of the report.

## Data Analysis

### HTPB Propellant

Propellant for the infrared analysis presented here was taken from the composite bond specimen and the propellant was microtomed to specific thicknesses measured from the liner/propellant interface. Distances at which samples were taken for IR analysis were as follows: 0.00 inch, 0.01 inch, 0.02 inch, 0.06 inch, 0.15 inch, and 0.4 inch. IR data for these propellant samples were acquired using the procedure described in Appendix B.

A typical infrared spectrum of whole propellant, TP-H8279, is given in Figure 20. Arrows on that figure point to infrared peaks which are associated with the propellant binder and which were observed to undergo change

TABLE 23

TEST RESULTS, HTPB PROPELLANT/LINER/INSULATION
165°F BOND AGING

| Age Time (Wks) | Type Sample | Peel (pli) | Failure Mode | Test Temp. (°F) |
|---|---|---|---|---|
| 0 | Liner-to-Insulation | > 73.2 | Tab broke | 77 |
| 2 | | > 79.0 | Tab broke | 77 |
| 4 | | > 48.6 | Tab broke | 77 |
| 8 | | > 46.6 | Liner pulled from screen | |
| 12 | | > 45.5 | Tab broke | 77 |
| 16 | | > 26.1 | Tab broke | 77 |
| 0 | Propellant-to-Liner | 29.0 | Prop. & Liner | 77 |
| 2 | | 15.7 | Propellant | 77 |
| 4 | | 11.1 | Propellant | 77 |
| 8 | | 9.1 | Propellant | 77 |
| 12 | | 7.1 | Propellant | 77 |
| 16 | | 8.2 | Propellant | 77 |
| | | Max. Stress (psi) | | |
| 0 | Composite[(a)] | 110.7 | Propellant | 77 |
| 2 | | 104.0 | Propellant | 77 |
| 4 | | 138.0 | Propellant | 77 |
| 8 | | 127.0 | Propellant | 77 |
| 12 | | 145.0 | Propellant | 77 |
| 16 | | 146 | Propellant | 77 |
| | | Ult. Stress (psi) | Ult. Strain (%) | |
| 0 | Liner, Tensile[(b)] | 446 | 344 | 77 |
| 2 | | 574 | 150 | 77 |
| 4 | | 721 | 153 | 77 |
| 8 | | 647 | 79 | 77 |
| 12 | | 788 | 127 | 77 |
| 16 | | 770 | 137 | 77 |

(a) Crosshead speed: 0.2 in/min
(b) Crosshead speed: 20.0 in/min

TABLE 24

TEST RESULTS, MINIMUM SMOKE PROPELLANT/LINER/INSULATION

| Age Time (Wks) | Type Sample | Peel, pli | Failure Mode | Test Temp. (°F) |
|---|---|---|---|---|
| 0 | Liner-to-insulation | >48.5 | Tab broke. | 77 |
| 2 | | >51.0 | Liner pulled from screen. | 77 |
| 4 | | >48.7 | Liner pulled from screen. | 77 |
| 8 | | >42.7 | Liner pulled from screen. | 77 |
| 12 | | >23.7 | Liner pulled from screen. | 77 |
| 16 | | >35.7 | Liner pulled from screen. | 77 |
| 0 | Propellant-to-Liner | 26.0 | Propellant | 77 |
| 2 | | 44.3 | Propellant | 77 |
| 4 | | 42.5 | Propellant | 77 |
| 8 | | 41.7 | 30% Prop.; 70% Bond. | 77 |
| 12 | | 30.6 | 40% Prop.; 60% Bond. | 77 |
| 16 | | 14.1 | 40% Prop.; 60% Bond. | 77 |
| | | Max. Stress (psi) | | |
| 0 | Composite [(a)] | 65 | Propellant | 77 |
| 2 | | 67 | Propellant | 77 |
| 4 | | 61 | Propellant | 77 |
| 8 | | 55 | Propellant | 77 |
| 12 | | 43 | Top came off. | 77 |
| 16 | | 46 | Propellant | 77 |
| | | Ult. Stress (psi) | Ult. Strain (%) | |
| 0 | Liner, tensile [(b)] | 239 | 369 | 77 |
| 2 | | 328 | 249 | 77 |
| 4 | | 388 | 198 | 77 |
| 8 | | 405 | 167 | 77 |
| 12 | | 400 | 150 | 77 |
| 16 | | 408 | 130 | 77 |

[(a)] Crosshead Speed = 0.2 in/min.

[(b)] Crosshead Speed = 20.0 in/min.

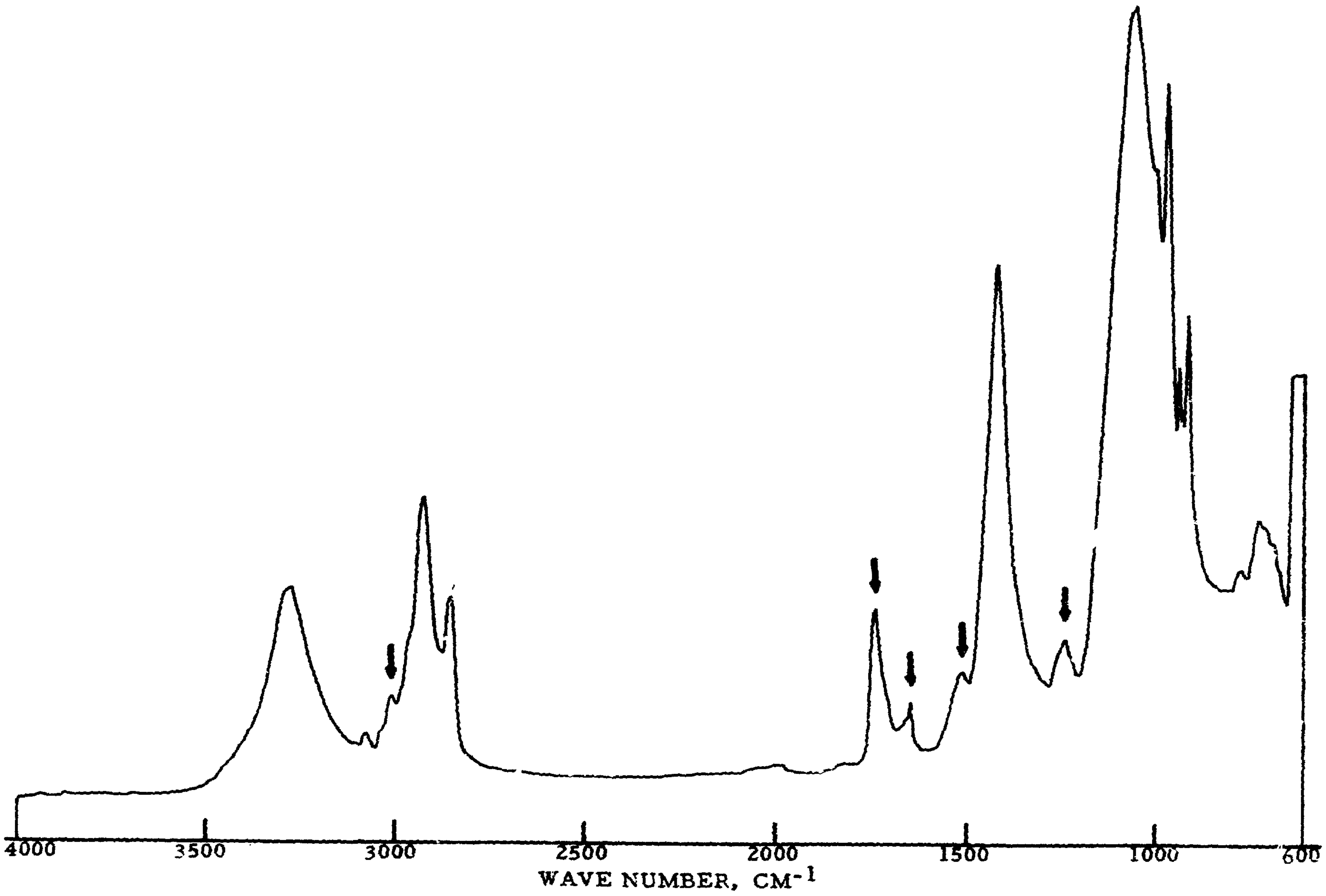


Figure 20. Typical IR Spectrum of Whole TP-H8279 Propellant.

with age time and age temperature. These peaks are located at the following wave numbers: 3008, 1734, 1641, 1513, and 1239. Changes to the IR peak height with time and with changes in the characteristics and properties of the bond are presented in the following figures. Figure 21 shows the change in height of the peak at 3008 $cm^{-1}$ with distance from the liner at various time intervals and it clearly shows that this peak varies both as a function of distance from the liner interface and as a function of time at 165°F. This is an unsaturation peak and shows that unsaturation decreases as the liner is approached, and the magnitude of the change in unsaturation increases with time at 165°F.

Figure 22 is a plot of the change of peak height at 1734 $cm^{-1}$ with distance from the propellant/liner interface at various age times. This peak is characteristic of the plasticizer, DOA, and shows that the concentration of DOA decreases as the interface between propellant and liner is approached; also, that the quantity of DOA decreases as time increases.

Figure 23 is a correlation between the height of the peak at 1641 $cm^{-1}$ with distance from the propellant/liner interface at various time intervals. This peak at 1641 $cm^{-1}$ is an unsaturation peak; however, it does not show the clear-cut change in unsaturation with approach to the interface that the peak at 3008 showed. This peak at 1641 $cm^{-1}$ is rather small and may be influenced by other factors that do not influence the peak at 3008 $cm^{-1}$. Certainly this correlation is not as strong as the correlation found with the peak at 3008 $cm^{-1}$.

Figure 24 relates the change in this unsaturation peak at 1641 $cm^{-1}$ to gel fraction in the propellant at a distance of 12 to 18 mm from the interface between the liner and propellant. There is a correlation there, but it is obviously not an exceedingly strong correlation. A review of the gel fraction data versus aging time in Appendix C will reveal that gel fraction of the propellant at this location in the propellant with time was a much stronger correlation than the correlation of unsaturation peak at 1641 $cm^{-1}$ with gel fraction.

Figure 25 relates height of the peak at 3008 $cm^{-1}$ to peel strength of the propellant/liner bond. A review of the propellant to liner peel strength versus aging time plot found in Appendix C will show that the peel strength changed as a curvilinear function of aging time, not as a straight line function. The correlation between the peak at 3008 $cm^{-1}$ and propellant to liner peel strength is quite good and follows the peel strength aging time data quite well. This is a <u>very</u> strong correlation.

<u>HTPB Liner - TL-H755A</u>

Infrared spectra used in this analysis and in the correlation of IR data with bond properties were taken of the sol fraction of liner. Liner was from the composite bond specimen where there is a layer of insulation, liner, and propellant. Correlations, then, among IR data and bond data mean the bond data must be from the composite bond specimen. The aging chemistry of liner itself may be slightly different from that taking place in the aging of liner where it is "sandwiched" between propellant and insulation.

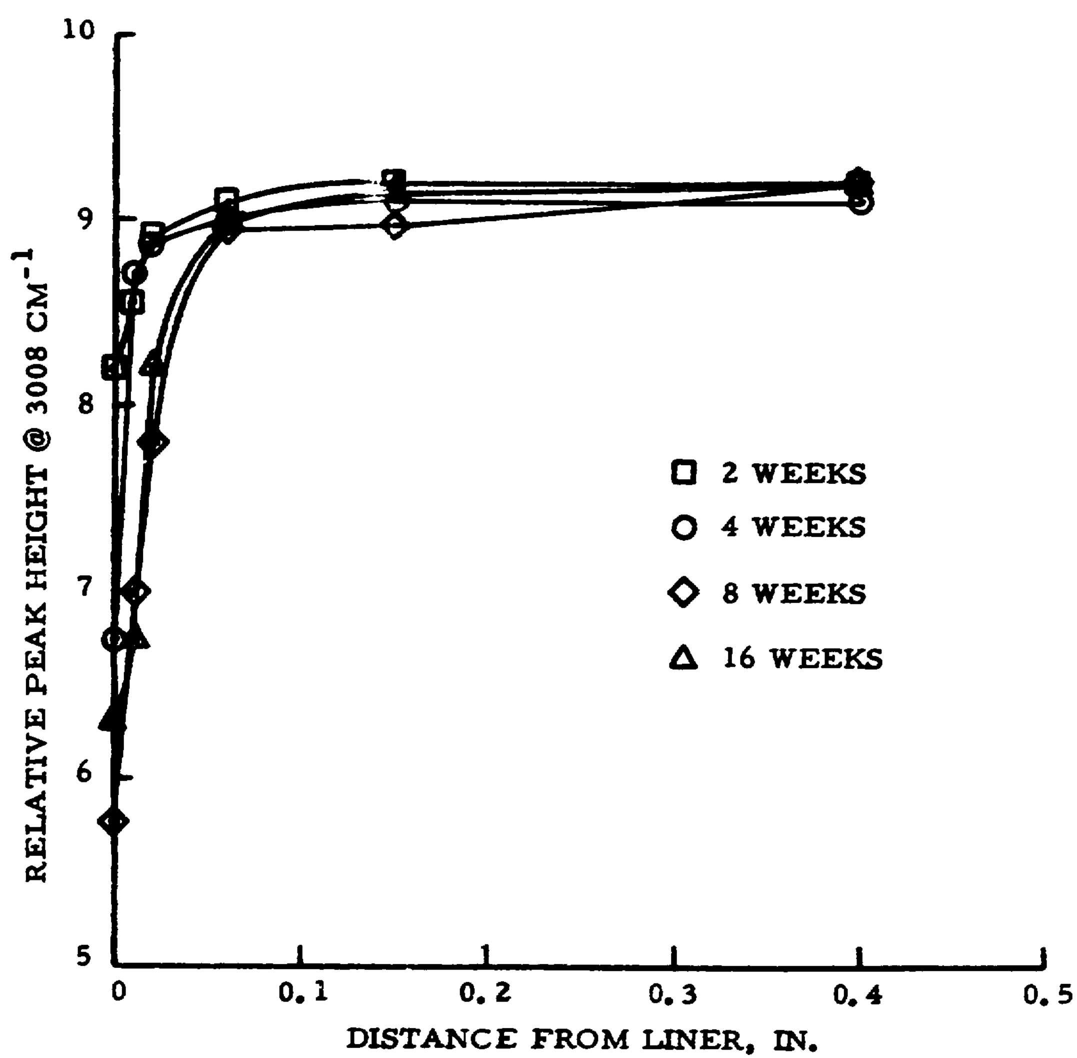


Figure 21. Correlation of Peak at 3008 $cm^{-1}$ with Distance from Liner Interface. TP-H8279 Propellant.

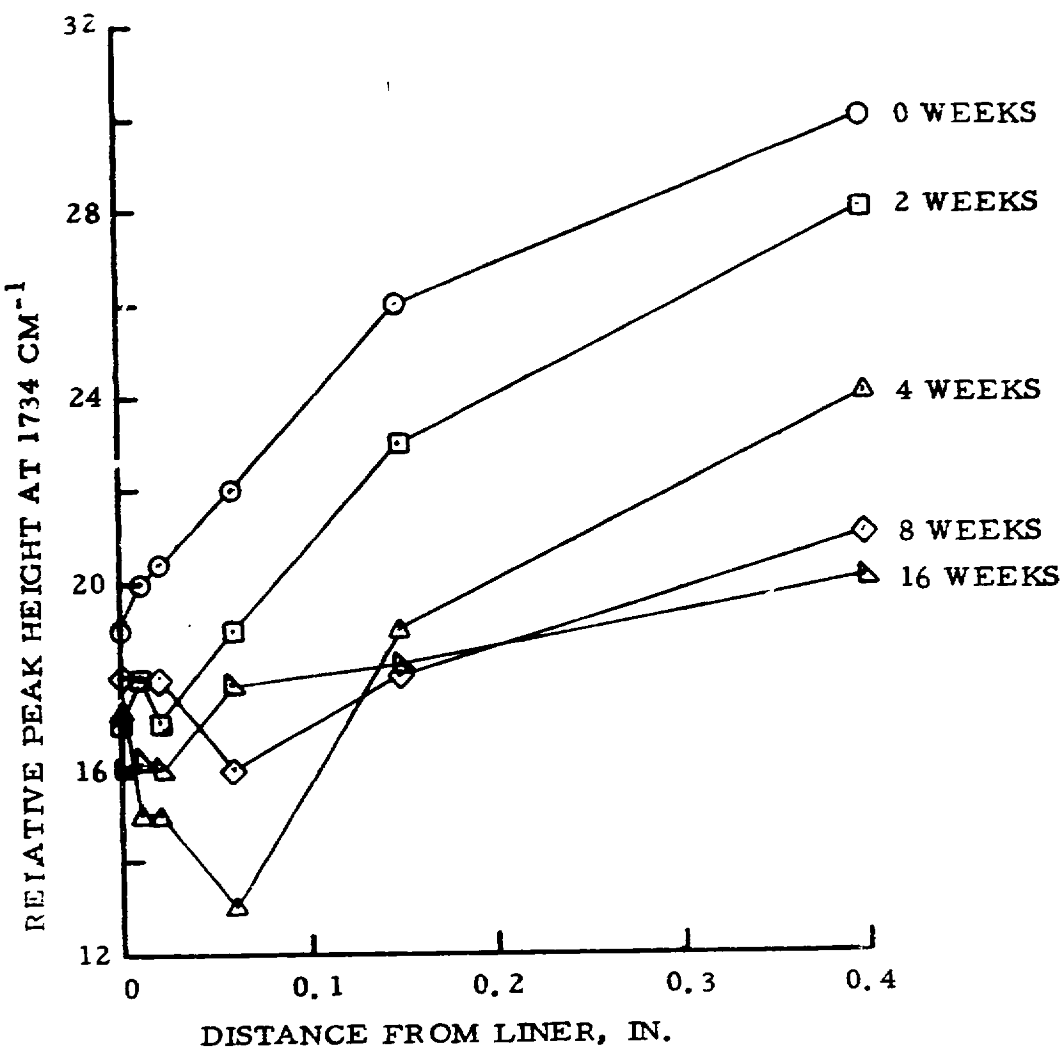


Figure 22. Change in Peak Height at 1734 cm$^{-1}$ with Time and Distance from Liner. TP-H8279 Propellant.

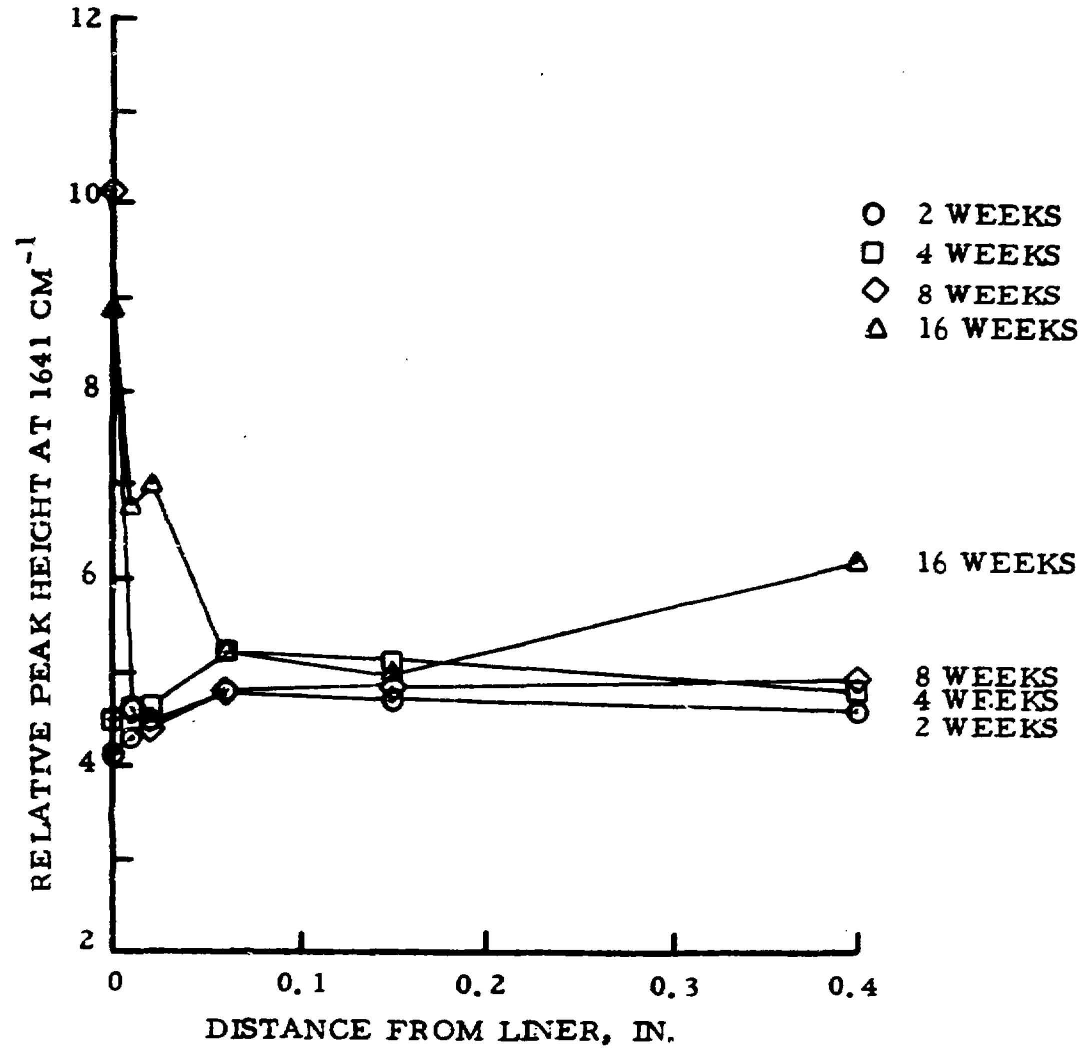


Figure 23. Change in Peak Height at 1641 $cm^{-1}$ with Time and Distance from Liner. HTPB Propellant.

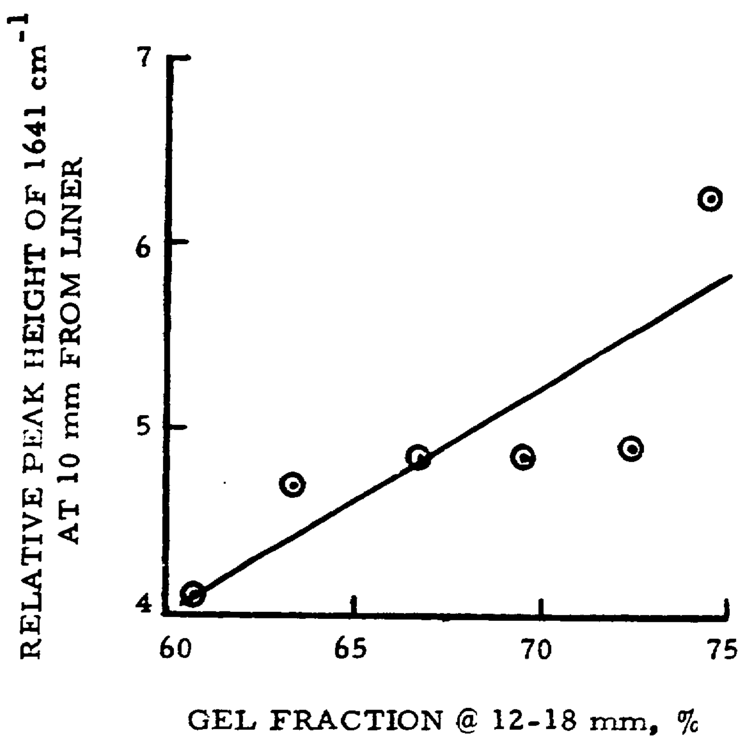


Figure 24. HTPB Propellant Correlation of Gel Fraction and Absorbance at 1641 $cm^{-1}$.

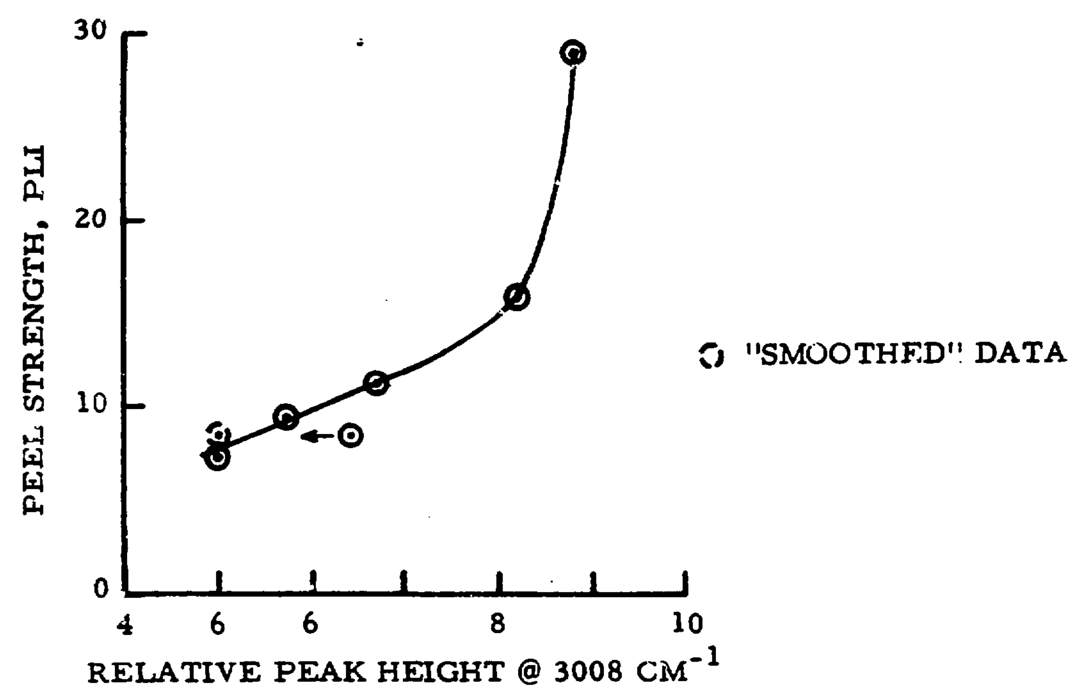


Figure 25. Correlation Between Propellant/Liner Peel Strength and Peak Height at 3008 $cm^{-1}$ at the Interface. HTPB Propellant.

Figures 26 and 27 are IR spectra of the sol fraction from TL-H755A liner. Figure 26 is sol fraction of the liner at zero time before the start of aging, while Figure 27 is of the sol fraction of the liner after 16 weeks of aging at 165°F. Table 25 is a listing of correlation coefficients for various peak heights in the infrared spectra of the sol fraction of liner and the various properties of liner including its hardness and gel fraction. Even though the IR spectra are of sol fractions from the composite tensile adhesion sample, the overall aging chemistry may bear close enough resemblance in the liner in this sample to a piece of liner aged separately from propellant and insulation that there may be correlations between the IR spectra and the tensile properties of the liner. Such was the case when a relative peak height of the sol at 969 $cm^{-1}$ was correlated with tensile stress of the aging liner. The correlation coefficient was not particularly good (-0.64), but the plot of the data revealed that the correlation coefficient was poor only because of one data point; and this was for the 12-week data. All other data points fell on a straight line and correlated exceedingly well. That is shown on Figure 28. Figure 29 relates relative peak height at 915 $cm^{-1}$ to aging time at 165°F and shows that this peak, representative of vinyl unsaturation in the binder of the liner, changes very uniformly with aging time, showing a steady, uniform decrease in peak height as time increases.

Tensile stress of the liner was found to relate well to relative peak height at 915 $cm^{-1}$. Data shown in Table 25 reveal that this correlation has a coefficient of -0.667; however, a plot of the data shown in Figure 30 reveals that the correlation is quite strong except for 16-week data.

Figure 31 relates height of the peak at 1747 $cm^{-1}$ to propellant/liner peel strength. This peak in the infrared is characteristic of DOA and it then relates the peel strength to the migration of DOA from the propellant into the liner. The correlation is an inverse one and has a coefficient of 0.91. It reveals to us that as DOA moves into the liner, the propellant-to-liner peel strength increases. Figure 32 shows much the same data in that it relates the propellant/liner peel strength to changes in the height of the peak at 2962 $cm^{-1}$. This peak is also characteristic of DOA and the correlation coefficient for this relationship is -0.92.

From these correlations, it can be concluded that the infrared spectrum of the sol fraction of liner will be useful in identifying mechanical properties of the bond between liner and propellant.

TI-R300 Insulation

Insulation aged as a part of the composite samples was submitted to a gel/sol separation test. Data concerning the amount of gel and sol have already been presented. The discussions here concern the infrared spectra of the sol fractions and correlation of the various peaks in those infrared spectra with the mechanical properties of the bond system which involves the insulation.

The sol fraction for each of the extractions was dissolved in carbon tetrachloride to a volume of 25 ml in a volumetric flask. Spectra were made from the solution in a 1 mm cell. Typical spectra for the sol fractions are displayed in Figures 33 and 34; Figure 33 being the insulation sol fraction at 0 weeks' aging and Figure 34 being sol fraction of the insulation after 16 weeks of aging at 165°F.

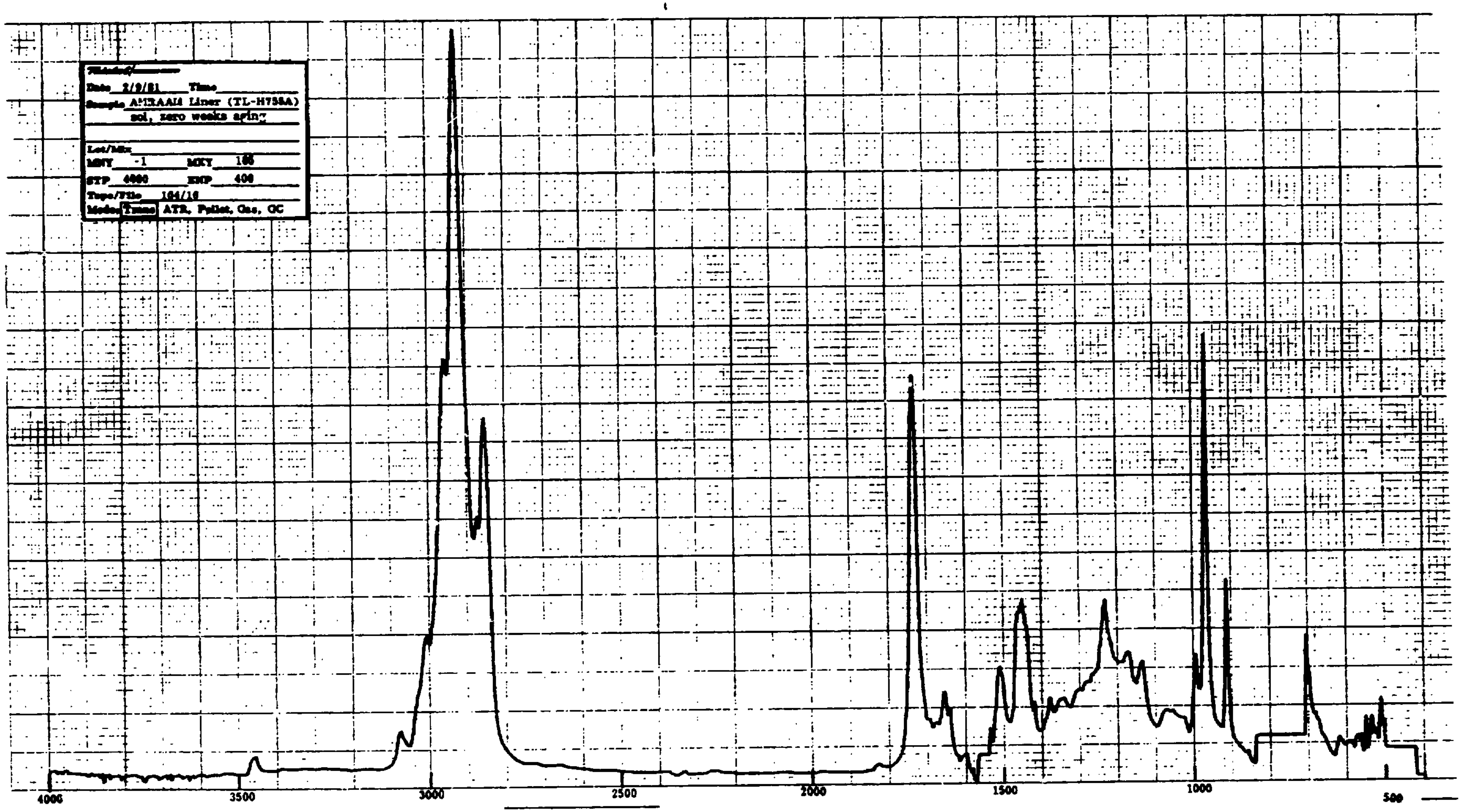


Figure 26. IR Spectrum of TL-H755A Liner Sol Fraction at Start of Aging.

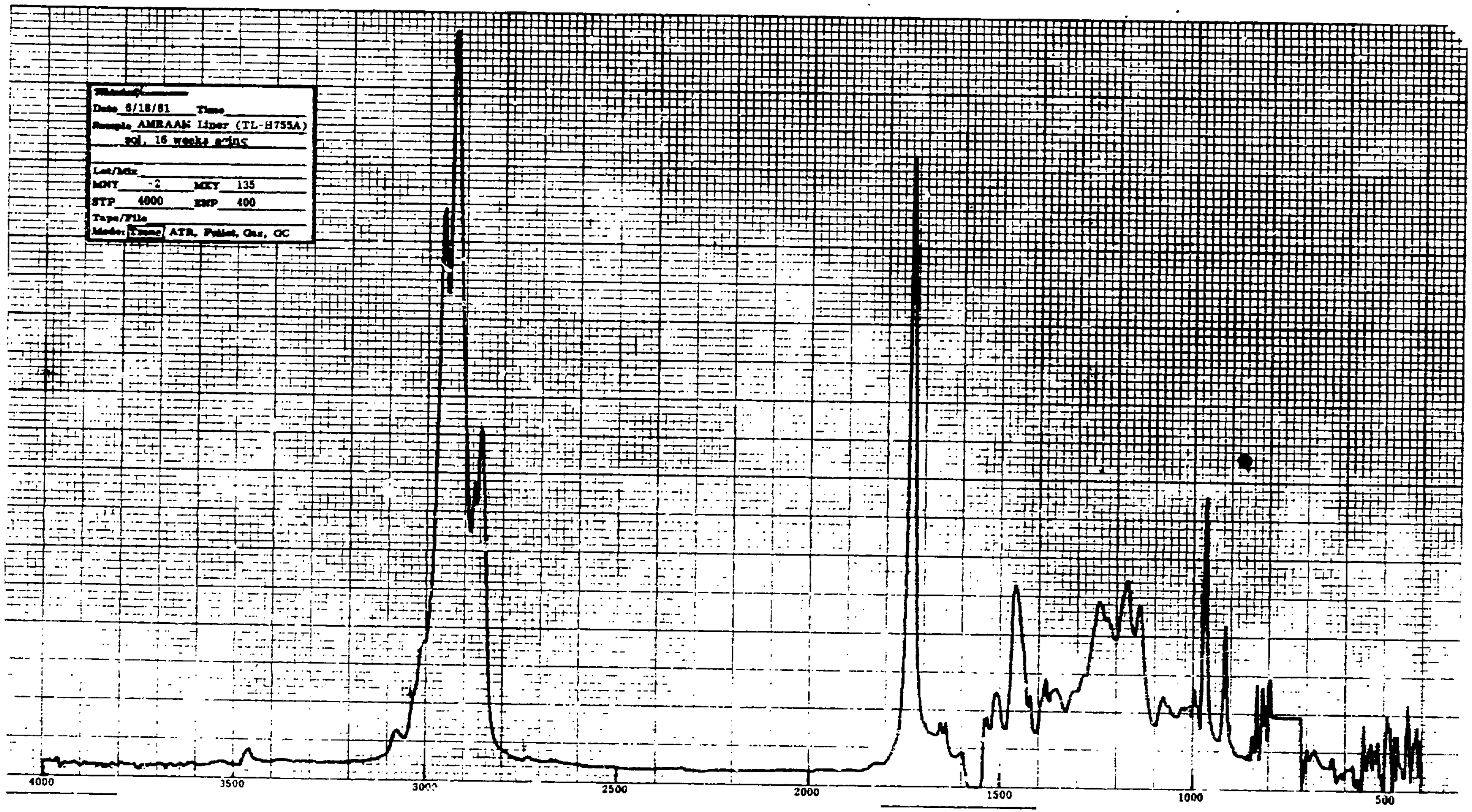


Figure 27. IR Spectrum of TL-H755A Liner Sol Fraction at End of Aging.

TABLE 25

CORRELATION COEFFICIENTS: PEAK HEIGHTS AND LINER PROPERTIES

| Wave No., $cm^{-1}$ | Liner-to-Insulation Peel | Liner-to-Propellant Peel | Composite Tensile Adhesion | Liner Tensile Stress | Liner Tensile Strain | Hardness | Gel Fraction |
|---|---|---|---|---|---|---|---|
| 915 | 0.770 | 0.601 | -0.631 | -0.667 | 0.445 | 0.189 | -0.710 |
| 969 | 0.752 | 0.625 | -0.621 | -0.638 | 0.546 | 0.340 | -0.684 |
| 996 | 0.402 | 0.073 | -0.150 | -0.051 | 0.089 | -0.193 | -0.211 |
| 1062 | 0.067 | -0.389 | 0.059 | 0.199 | -0.521 | -0.567 | 0.224 |
| 1077 | -0.831 | -0.861 | 0.814 | 0.904 | -0.724 | -0.615 | 0.855 |
| 1173 | -0.905 | -0.937 | 0.822 | 0.900 | -0.841 | -0.561 | 0.936 |
| 1286 | -0.260 | -0.389 | 0.099 | 0.245 | -0.439 | -0.157 | 0.498 |
| 1382 | -0.687 | -0.621 | 0.478 | 0.539 | -0.625 | -0.331 | 0.723 |
| 1421 | 0.031 | -0.049 | -0.375 | -0.229 | -0.285 | 0.067 | 0.276 |
| 1641 | -0.509 | -0.198 | 0.713 | 0.439 | 0.066 | 0.065 | -0.020 |
| 1737 | -0.906 | -0.905 | 0.818 | 0.905 | -0.782 | -0.533 | 0.934 |
| 2738 | -0.129 | -0.271 | 0.361 | 0.391 | -0.106 | -0.249 | 0.128 |
| 2857 | 0.695 | 0.326 | -0.494 | -0.431 | 0.173 | -0.105 | -0.480 |
| 2877 | -0.803 | -0.801 | 0.639 | 0.764 | -0.731 | -0.472 | 0.905 |
| 2930 | -0.424 | -0.848 | 0.429 | 0.670 | -0.921 | -0.854 | 0.796 |
| 2962 | -0.867 | -0.920 | 0.765 | 0.886 | -0.830 | -0.583 | 0.959 |
| 3011 | 0.493 | 0.073 | -0.335 | -0.237 | -0.104 | -0.291 | -0.228 |

AMRAAM LINER SOL
TP-H1755A

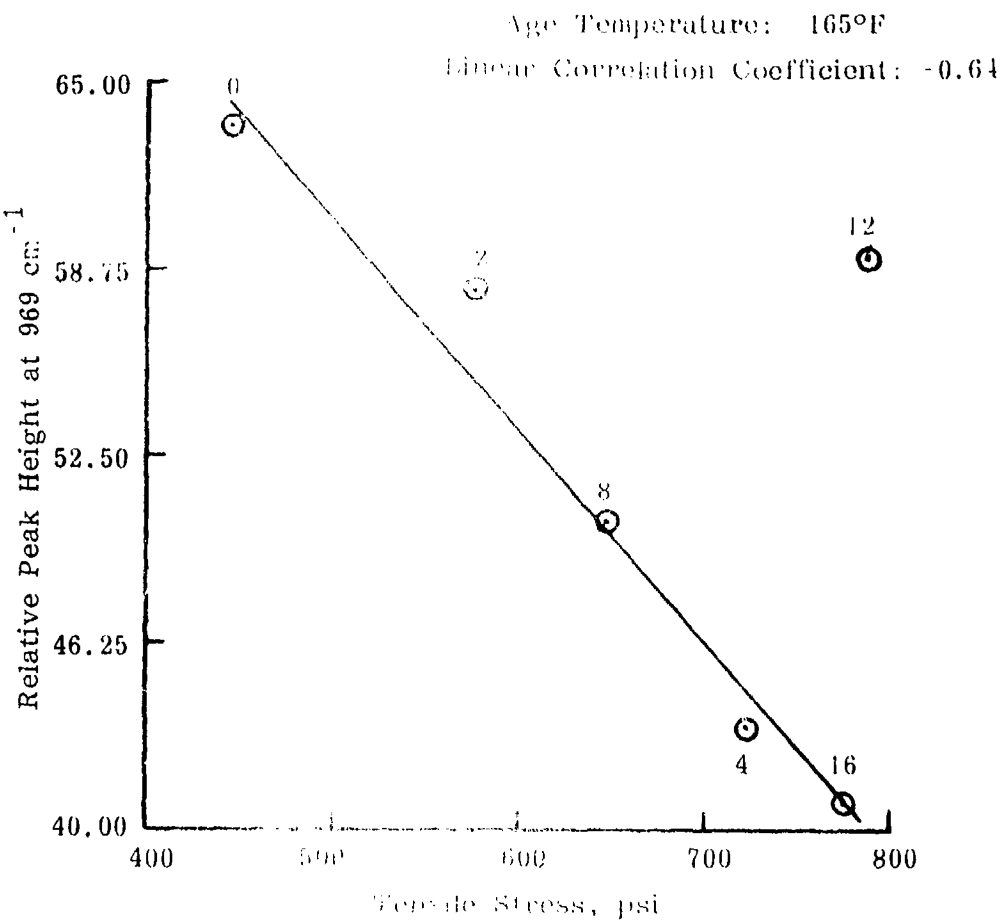


Figure 28. Correlation Between Peak Height at 969 cm$^{-1}$ and Liner Tensile Stress.

AMRAAM LINER SOL

TL-H755A

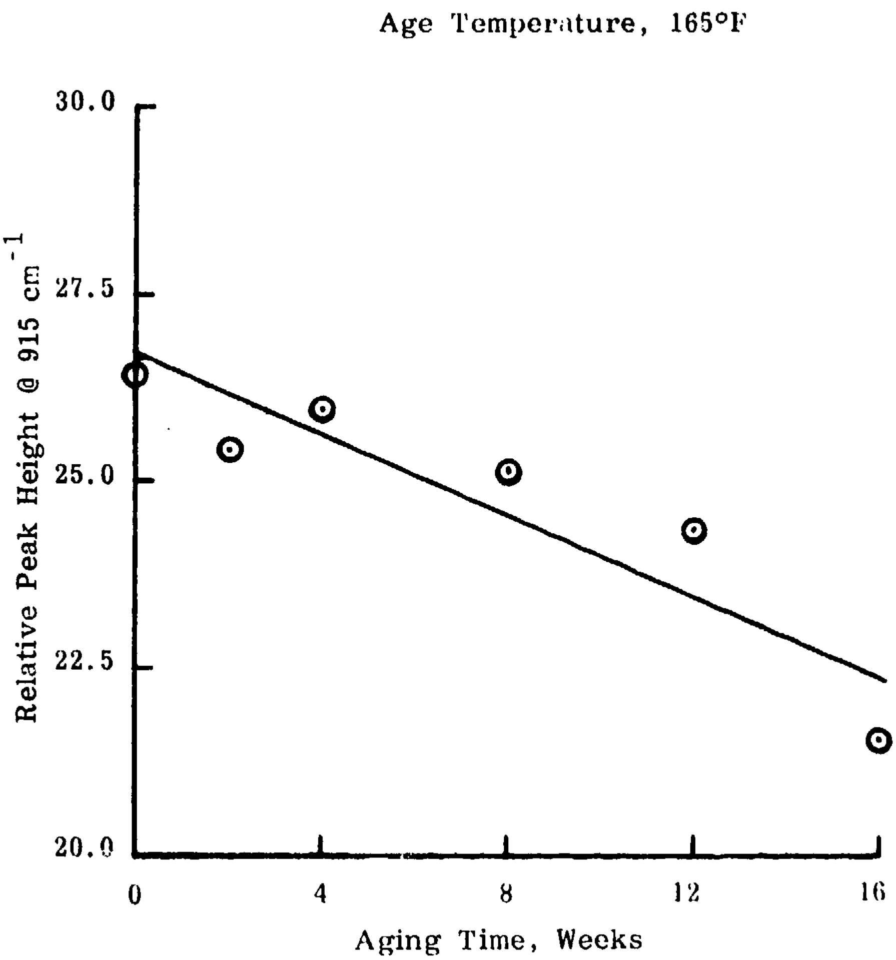


Figure 29. Change in Peak at 915 $cm^{-1}$ With Age Time.

AMRAAM LINER SOL

TL-H755A

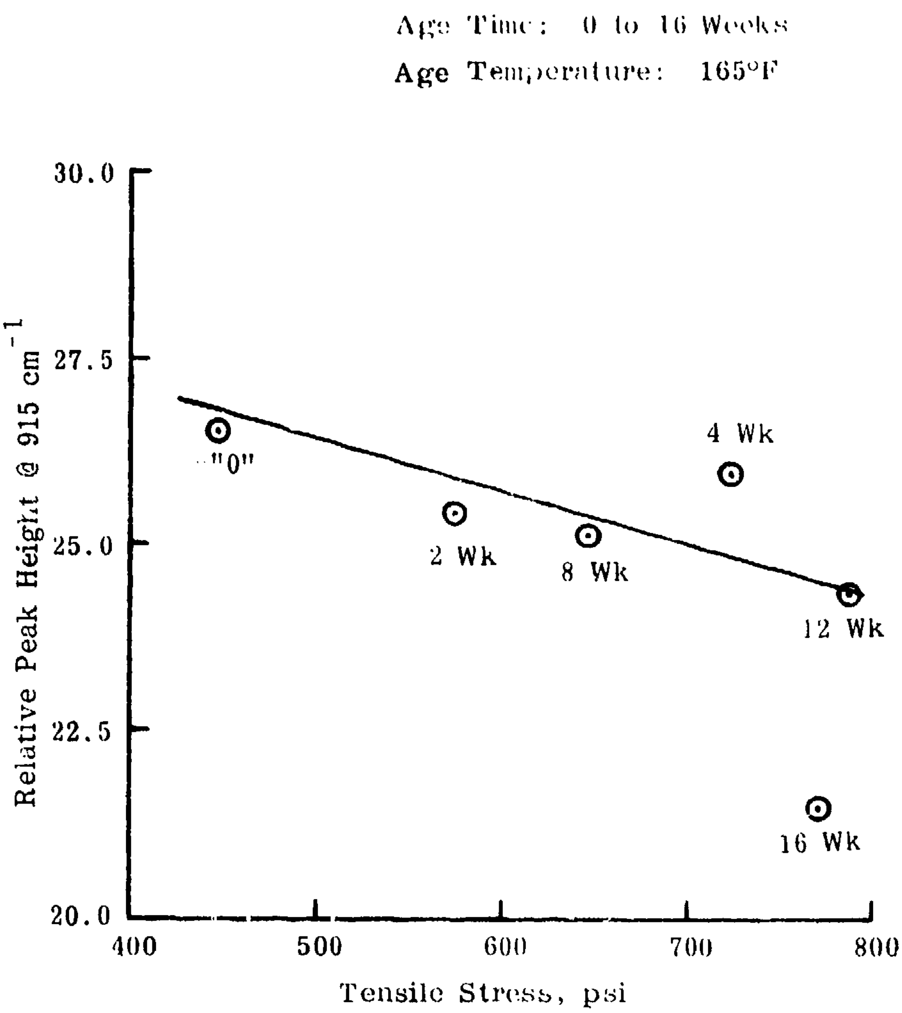


Figure 30. Correlation Between Peak Height at 915 $cm^{-1}$ and Liner Tensile Stress.

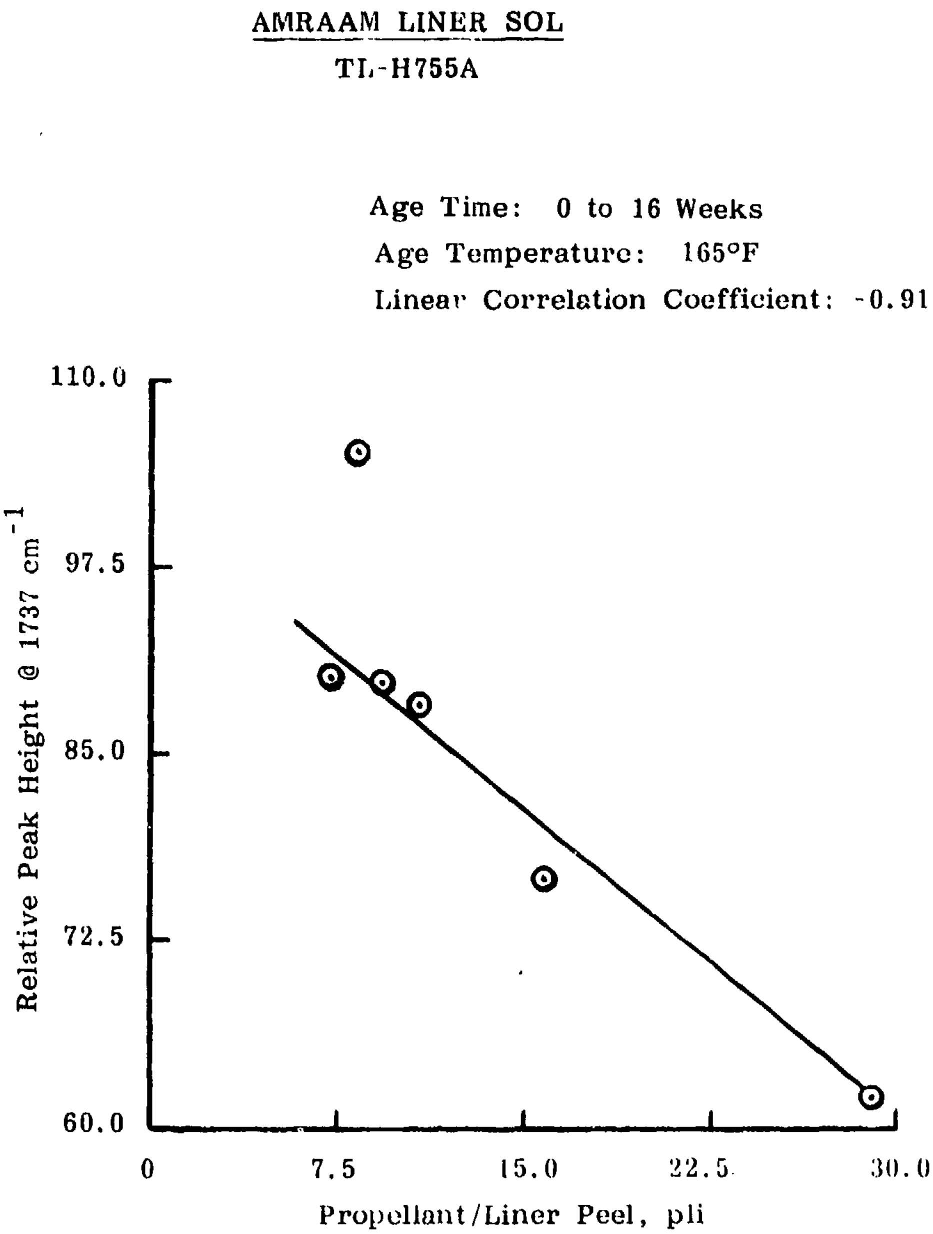


Figure 31. Correlation Between Peak Height at 1737 $cm^{-1}$ and Propellant/Liner Peel.

AMRAAM LINER SOL

TL-H755A

Age Time: 0 to 16 Weeks

Age Temperature, 165°F

Linear Correlation Coefficient: -0.92

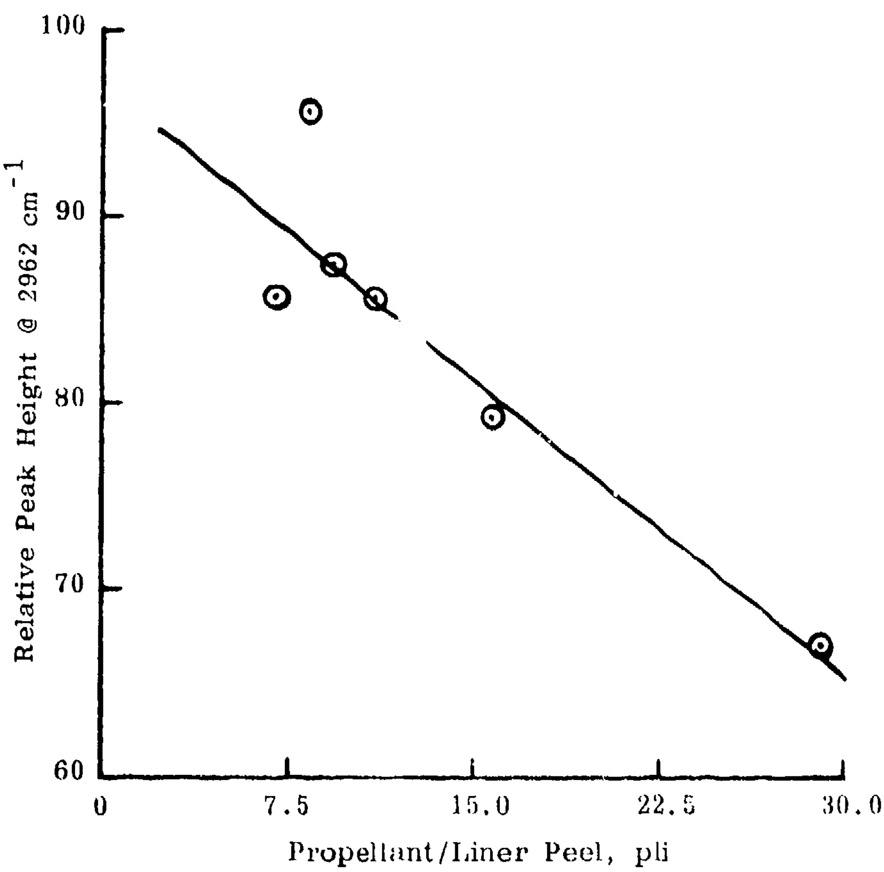


Figure 32. Correlation Between Peak Height at 2962 $cm^{-1}$ and Propellant/Liner Peel Strength.

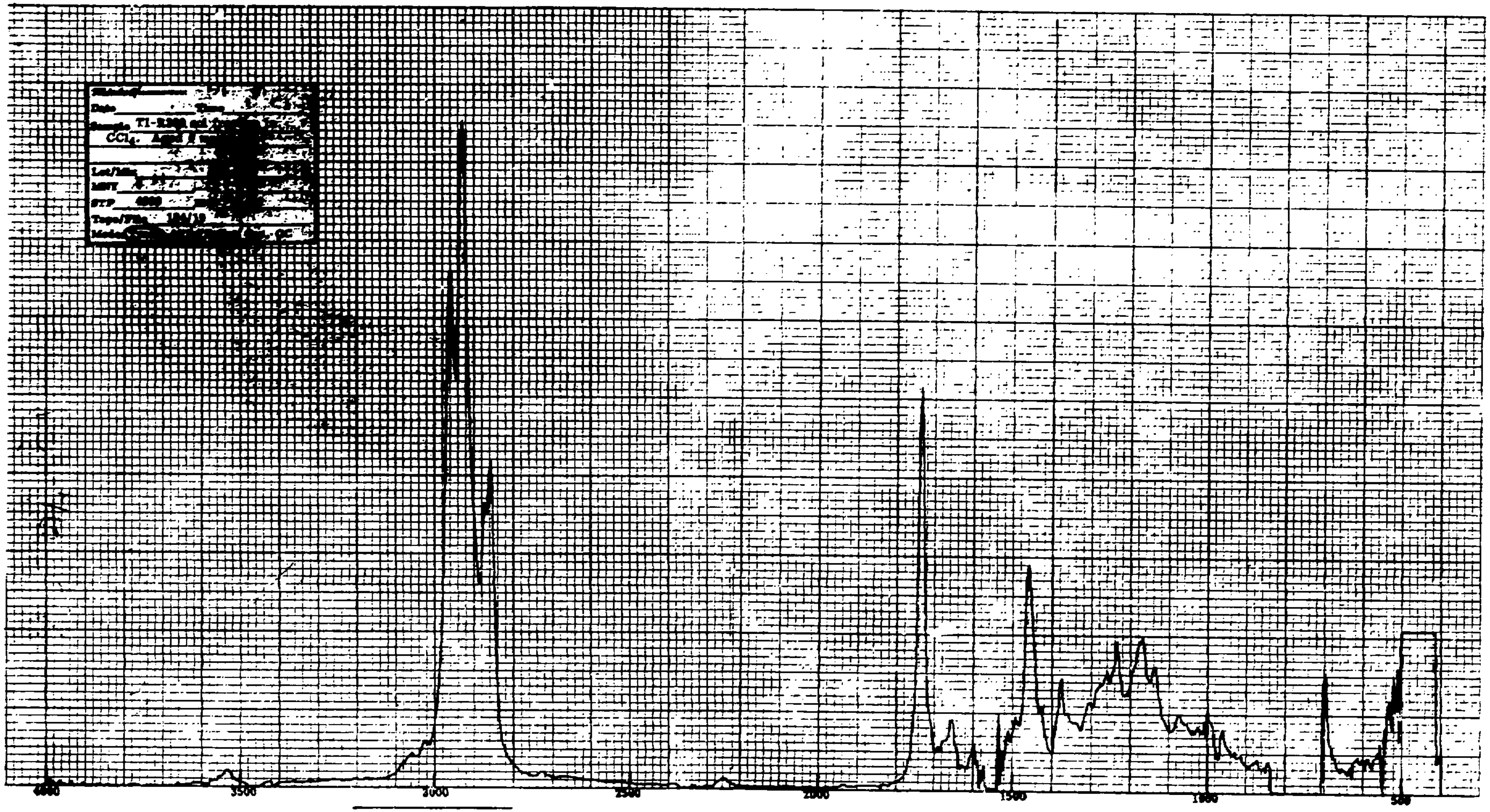


Figure 33. Infrared Spectrum of TI-R300 Insulation Sol Fraction. Aged 0 Weeks.

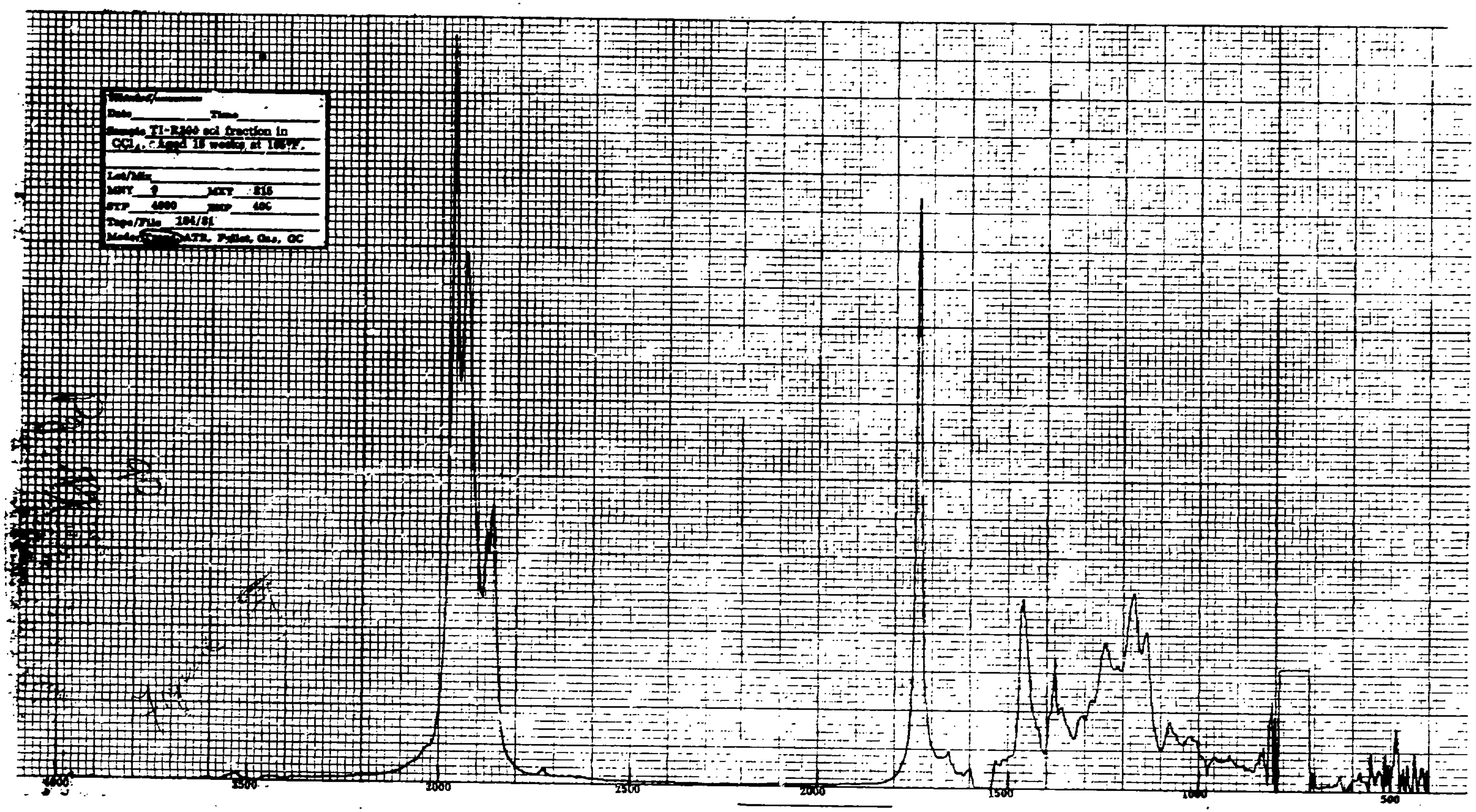


Figure 34. Infrared Spectrum of TI-R300 Insulation Sol Fraction. Aged 16 Weeks at 165°F.

An interesting observation in these two spectra is that the strongest peaks (outside of the region 2800 to 3000 $cm^{-1}$) are DOA peaks. The strong peak at 1734 $cm^{-1}$ is characteristic of DOA. The three peaks in the region 1140 to 1240 $cm^{-1}$ are also characteristic of DOA. The peak located at 1460 $cm^{-1}$ is a CH peak and is present in almost every organic material; i.e., it would be present in DOA and in the soluble portion of polyisoprene. In the 2800 to 3000 $cm^{-1}$ region, there is one peak, that located at 2960 $cm^{-1}$, that has grown considerably from 0 time to 16 weeks. That peak is characteristic of DOA. Other peaks in that region are characteristic of DOA and the soluble portion of polyisoprene.

Correlation of the change of infrared peaks in the sol fraction of the insulation with time reveal that there are only three peaks that furnished a good correlation. All three of these peaks are characteristic of DOA, which says in effect that the most outstanding change taking place in insulation during this aging period was the absorption of DOA from the liner and, of course, the ultimate source of DOA is the propellant. The fact that the 0 aging time insulation sol fractions show presence of DOA is nothing more than a reflection of the fact that 0 time for this spectrum was not 0 time for migration. Migration begins at the time the propellant was cast against the liner. These samples, of course, were in cure for seven days at 145°F and it was some time period after that before the insulation gel/sol separation test was run. During all of this time, DOA obviously was migrating out of propellant through the liner and into the insulation.

There were three peaks in these spectra which correlated quite well with time and they were the peaks at 1737, 1380, and 2734 $cm^{-1}$. All three peaks are characteristic of DOA. The peak at 1737 $cm^{-1}$ is the carbonyl group in the DOA, while the peak at 1380 $cm^{-1}$ is a $CH_2$ deformation peak which is present in DOA, while the peak at 2734 $cm^{-1}$ is quite small and is an overtone of the 1380 $cm^{-1}$ peak. In spite of the fact that the peak at 2734 is very small, it responds quite well to time and correlates well with the movement of DOA. This peak is present in the spectrum of DOA. These correlations are displayed in Figures 35, 36, and 37.

Of the physical properties measured during the bond aging portion of Phase I, two of the samples involved insulation...the composite adhesion sample (a composite of insulation/liner/propellant) and the liner/insulation peel sample. Since the infrared spectra are of the sol fraction, the correlation of these spectra applies only to the properties displayed by aging the composite adhesion samples. The liner/insulation peel samples were not exposed to propellant, therefore, the spectra of the insulation sols so heavily loaded with DOA cannot be correlated in a meaningful manner with the results of the liner/insulation peel tests. The correlation of the peaks at 1737, 2734, and 1380 $cm^{-1}$ with composite tensile adhesion showed strong correlations. The peak at 1380 versus tensile adhesion is plotted on Figure 38 and reveals that there was a correlation coefficient here of 0.88. Because all failures in the composite tensile adhesion tests were located in the propellant, this correlation is nothing more than a measure of the amount of DOA coming out of the propellant and the effect of this DOA migration on the tensile strength of the propellant.

TI-R300 INSULATION SOL

CHANGE IN PEAK AT 1737 $CM^{-1}$ WITH AGE TIME

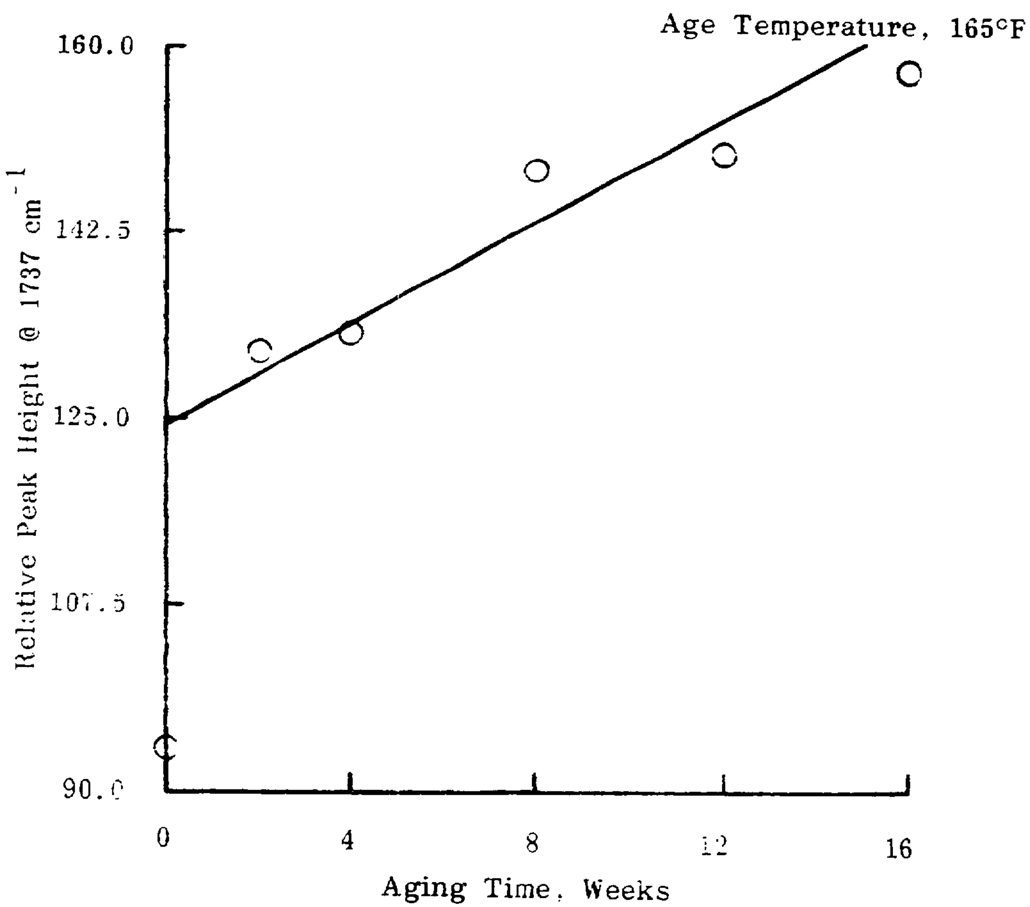


Figure 35.

TI-R300 INSULATION SOL

CHANGE IN PEAK AT 1380 $CM^{-1}$ WITH AGE TIME

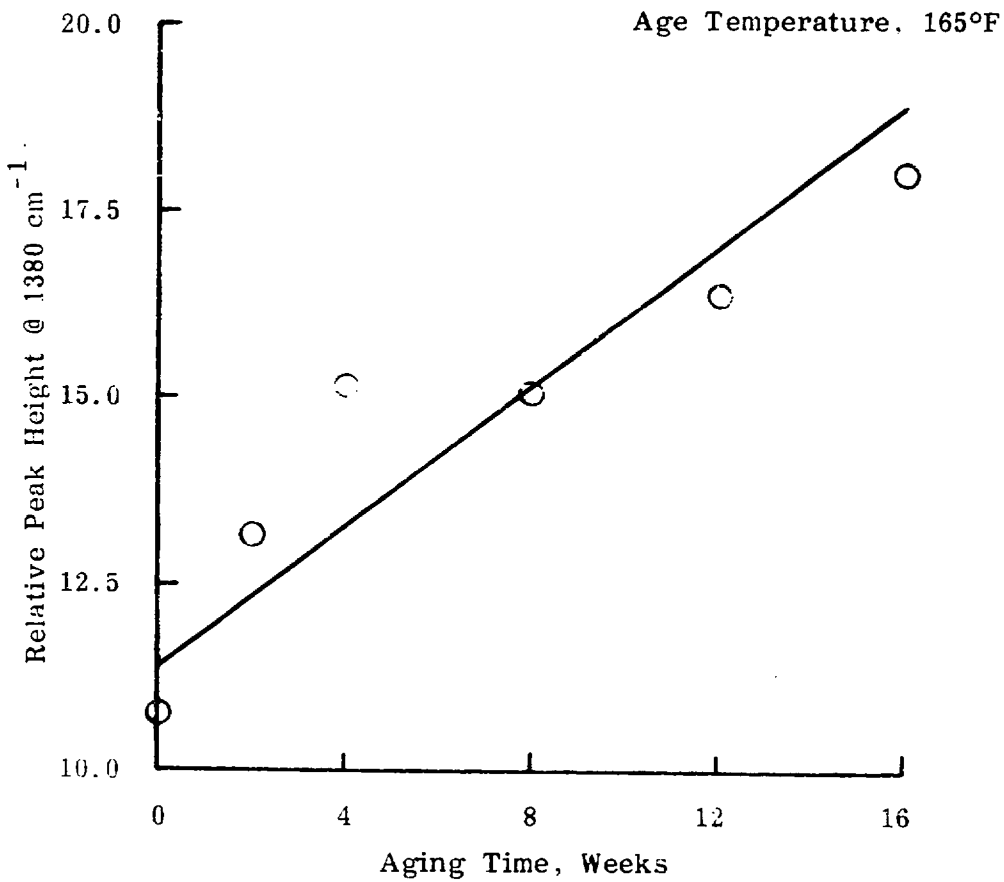


Figure 36.

## TI-R300 INSULATION SOL

## CHANGE IN PEAK AT 2734 $CM^{-1}$ WITH AGE TIME

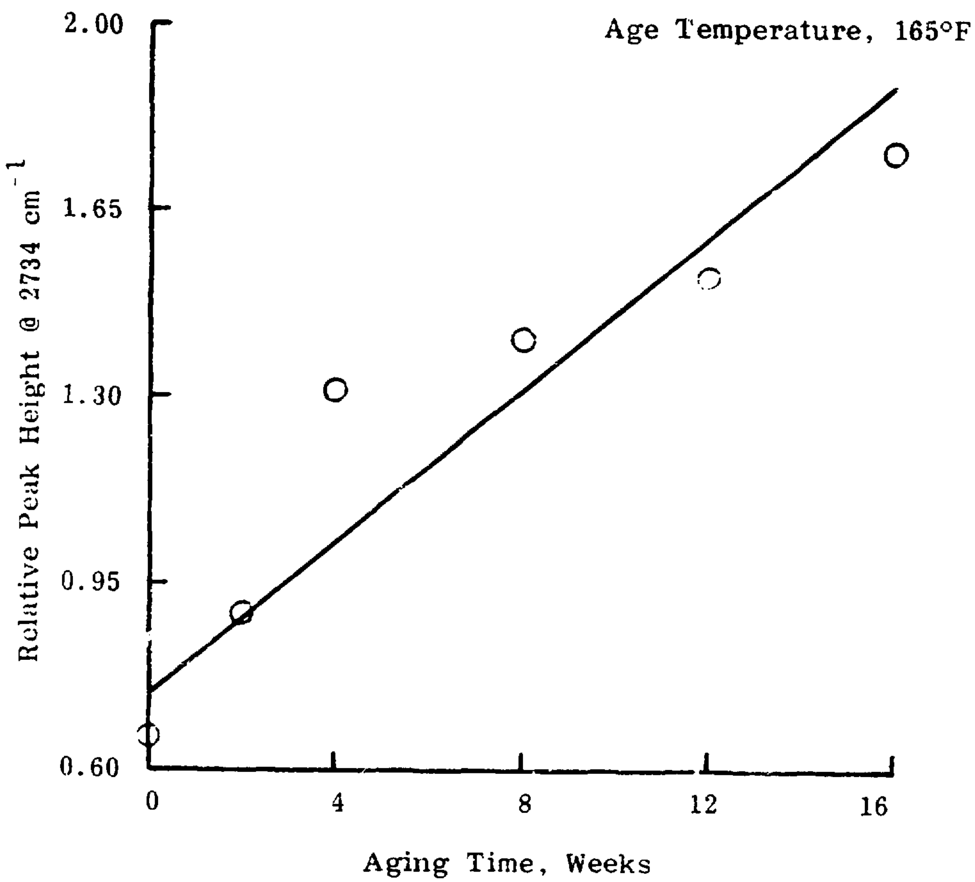


Figure 37.

TI-R300 INSULATION SOL

CORRELATION BETWEEN PEAK HEIGHT AT 1380 $CM^{-1}$ AND COMPOSITE TENSILE ADHESION

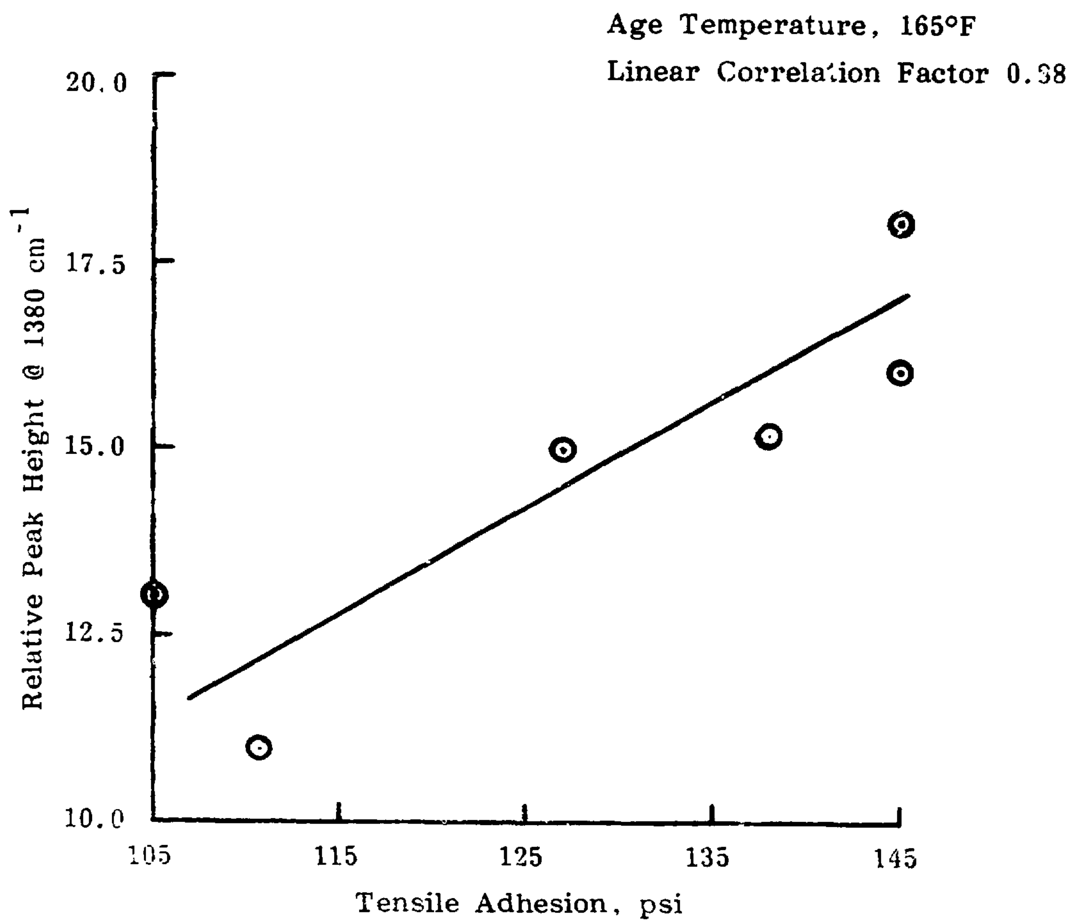


Figure 38.

The quantity of DOA in the sol fraction also correlated quite well with the quantity of sol fraction. This is displayed in Figure 39 using the peak at 1737 $cm^{-1}$ and gel fraction. This correlation, of course, is an inverse one and has a quite high correlation factor, -0.93.

There is a small peak located at 1656 $cm^{-1}$ which is indicative of unsaturation in the binder of the polyisoprene insulation. Variation in the height of this peak with time and with liner-to-insulation peel strength is quite strong. Figure 40 shows the variation in peak height with time, while Figure 41 shows the variation of this peak with liner-to-insulation peel strength. The correlation coefficient for the relationship shown in Figure 41 is 0.997. This relationship is strong enough that it can be used to identify peel strength from the IR spectrum of the insulation sol fraction. An equation for this relationship is shown on Figure 41.

Minimum Smoke Propellant Gel Fraction

Infrared spectra of the gel fraction of the minimum smoke propellant, TP-Q7029, were made. Samples of the propellant from the composite adhesion specimen were cut at discrete distances from the liner/propellant interface and the samples extracted in a gel/sol separation procedure. Distances from the liner/propellant interface were: 0.00 in., 0.02 in., 0.04 in., 0.06 in., 0.10 in., 0.20 in., 0.30 in., and 0.50 in. After extracting the propellant samples overnight with acetone, they were dried; and an IR spectrum of each sample gel fraction made. Our general procedure for extracting and drying samples is given in Appendix B, Page 183.

A typical infrared spectrum of the gel fraction at zero time and 0.0 in. from the interface is presented in Figure 42, while the spectrum of the gel fraction of the minimum smoke propellant after 16 weeks of aging at 165°F is given in Figure 43. Note on Figure 43 that several of the peaks have an arrow above them. These arrows designate peaks which changed in height during the aging of the minimum smoke propellant. Changes in peak heights at each of the interfacial distances for each test interval were compared to the various bond properties. Significant correlations were found for propellant taken at the liner interface and 0.02 inch away from that interface. Propellant adjacent to the liner gave the best correlations and those are the ones presented here. Two peaks, one located at 1521 $cm^{-1}$ and one located at 1726 $cm^{-1}$, were found to have a correlation to changes in propellant/liner bond strength.

Figure 44 shows the correlation between the peak at 1521 $cm^{-1}$ and propellant-to-liner peel strength. A strong correlation is displayed here.

Figure 45 shows the correlation between the peak at 1726 $cm^{-1}$ and gel fraction of the propellant. The peak at 1726 $cm^{-1}$ in minimum smoke propellant is probably characteristic of the urethane linkage in the binder of the propellant. This same peak was found to correlate with propellant/liner/insulation composite tensile stress, as displayed in Figure 46 and with propellant/liner peel strength, as displayed in Figure 47.

TI-R300 INSULATION SOL

CORRELATION BETWEEN PEAK HEIGHT AT 1737 $CM^{-1}$ AND GEL FRACTION

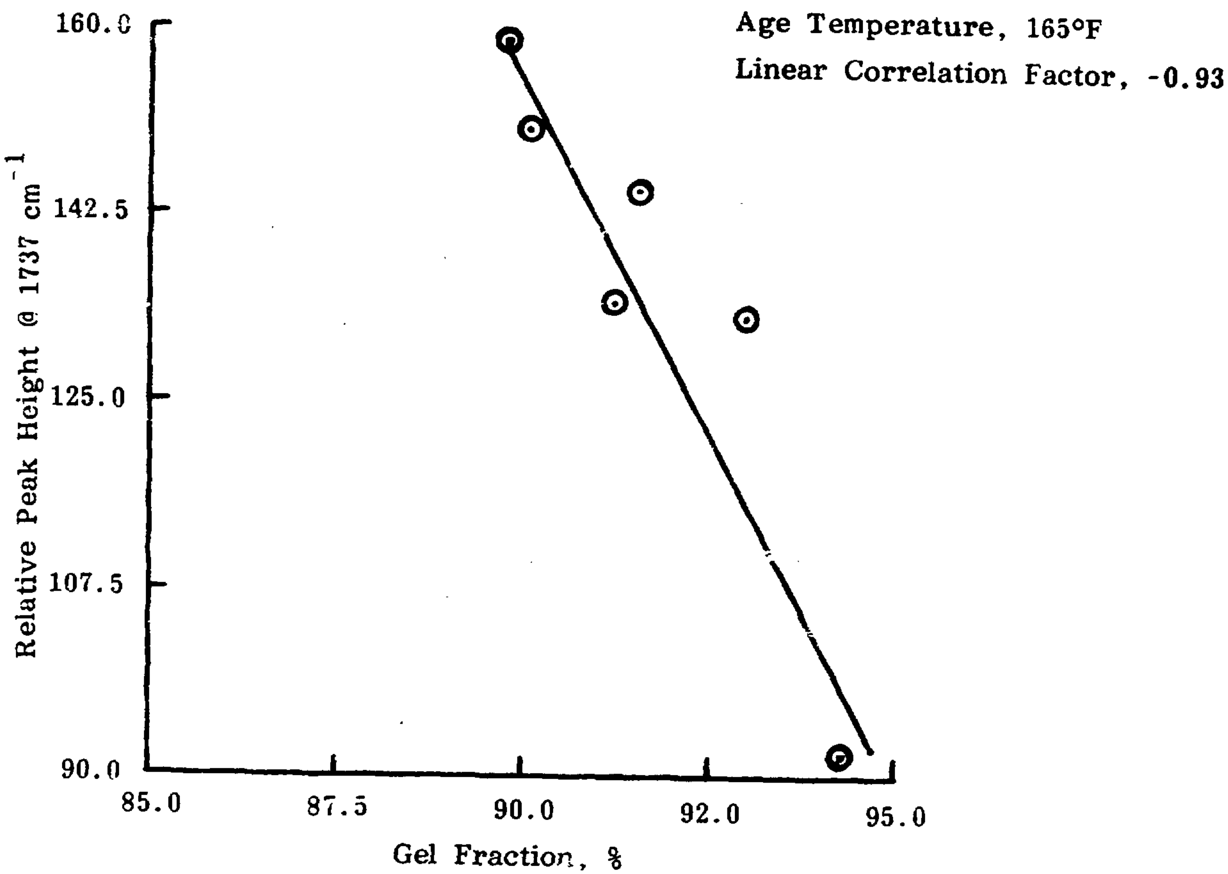


Figure 39.

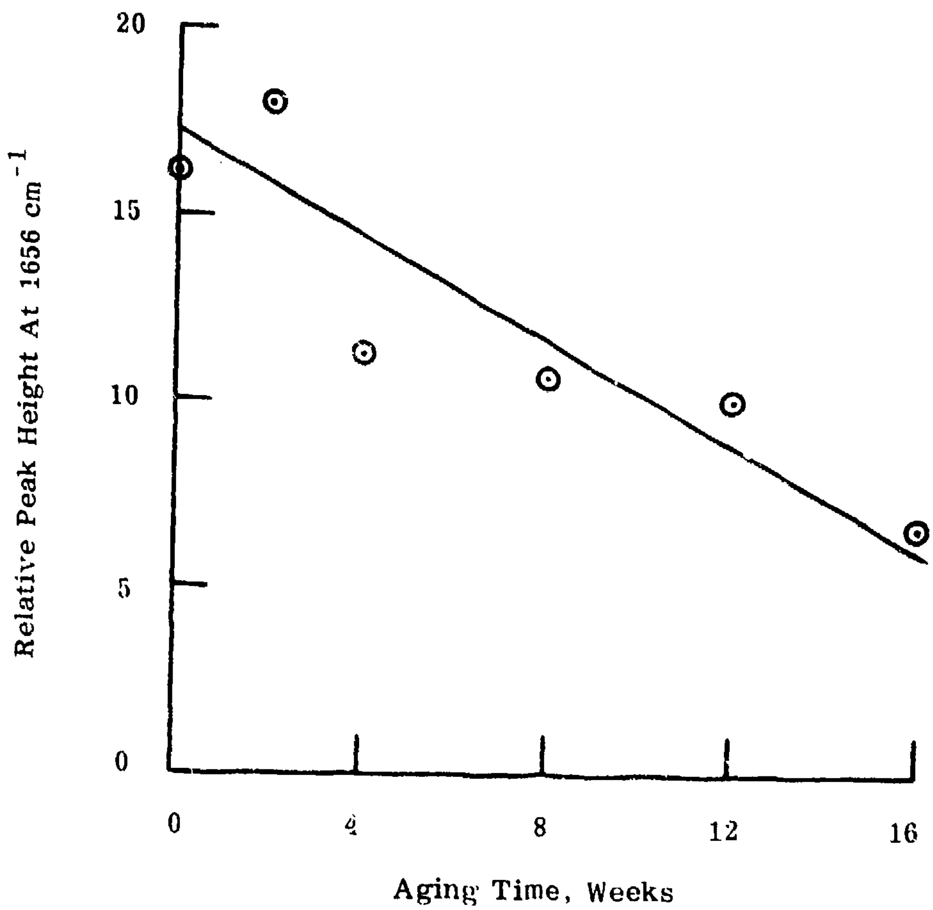


Figure 40. Variation with Time of Peak at 1656 $cm^{-1}$ in Sol Fraction of TI-R300 Aged 0 to 16 Weeks.

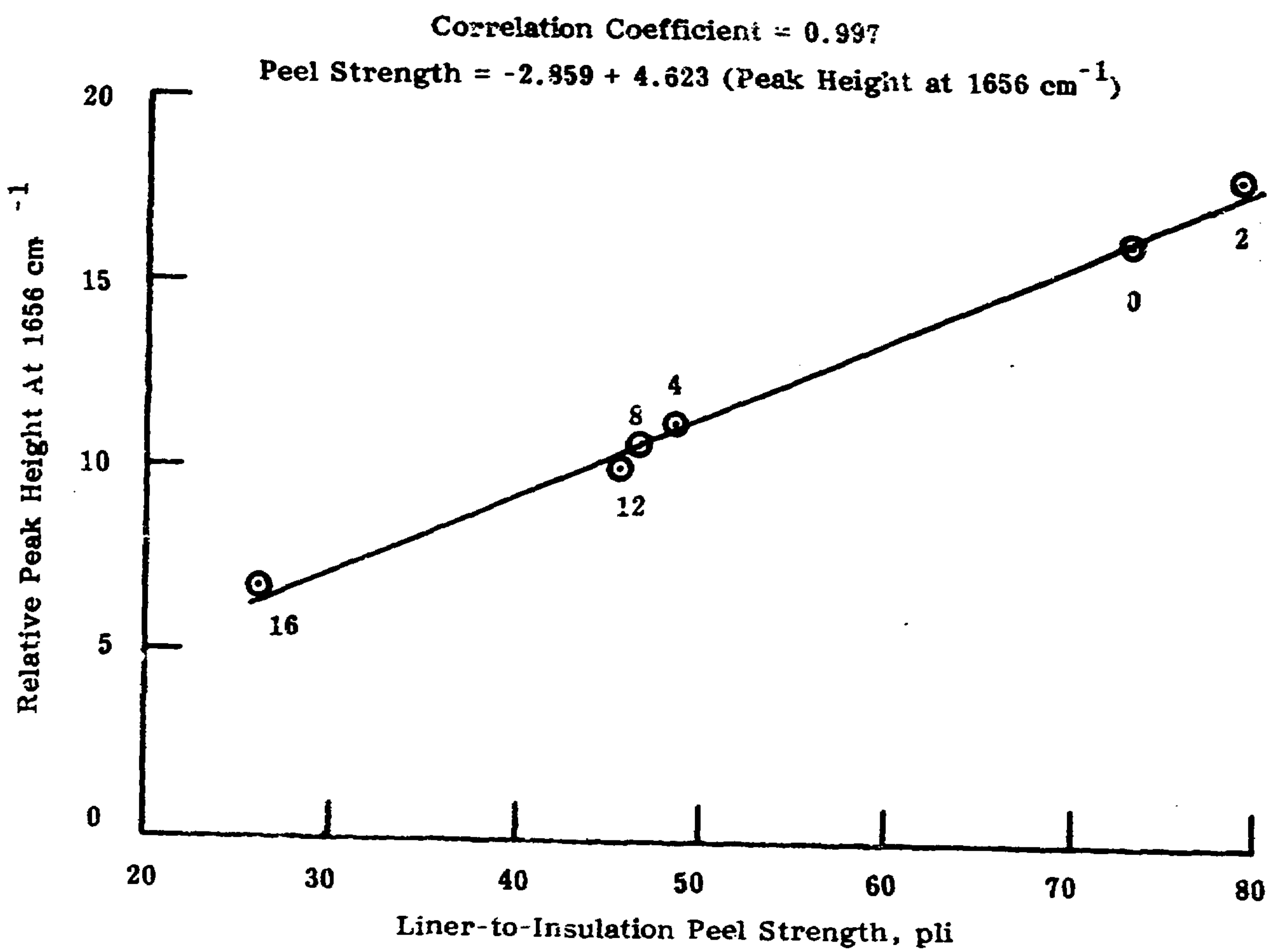


Figure 41. TI-R300 Insulation Sol Aged 0 To 16 Weeks At 165°F.

Figure 42. Minimum Smoke Propellant (TP-Q7029), Gel Fraction. Aged 0 Weeks.

0.00 INCH FROM LINER

0 WEEKS AT 165°F

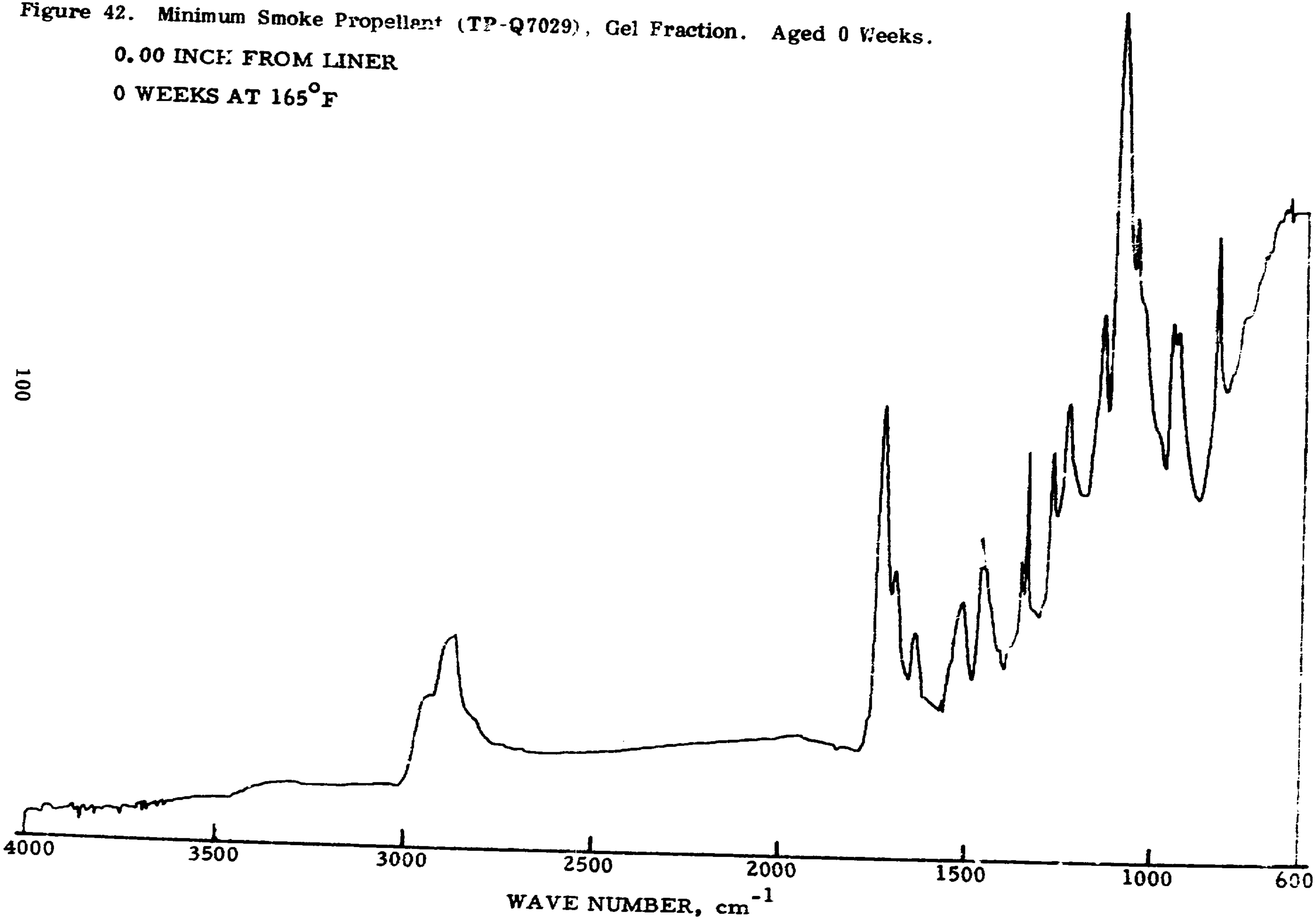

Figure 43. Minimum Smoke Propellant (TP-Q7029), Gel Fraction. Aged 16 Weeks.

0.00 INCH FROM LINER

16 WEEKS AT 165°F

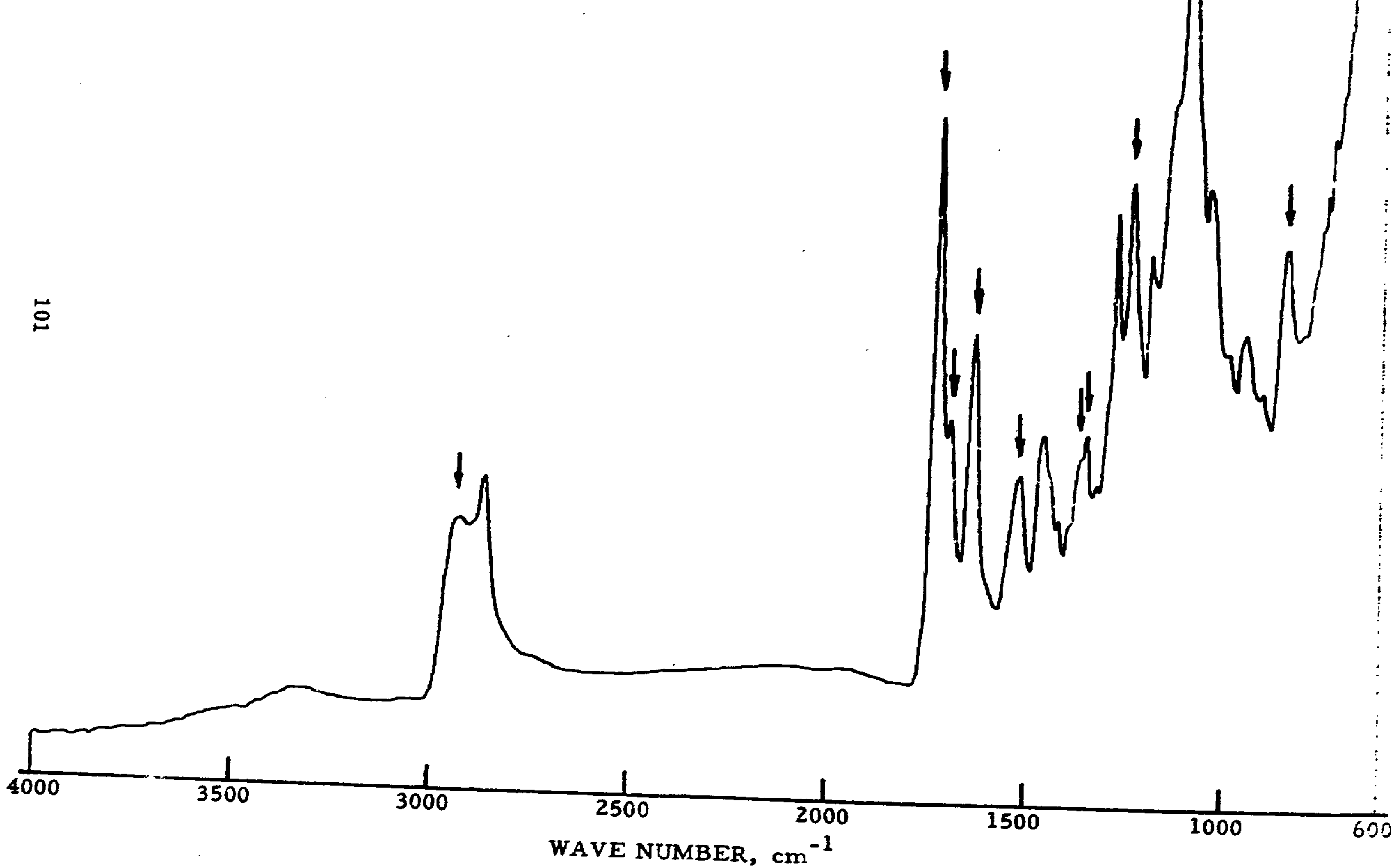

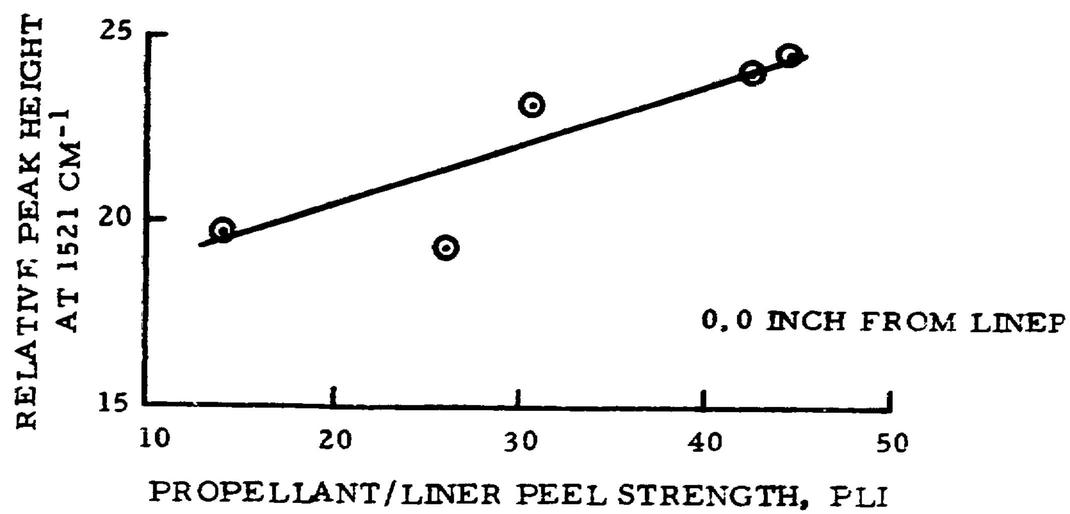


Figure 44. Minimum Smoke Propellant Correlation Between Propellant/Liner Peel and Peak at 1521 $cm^{-1}$.

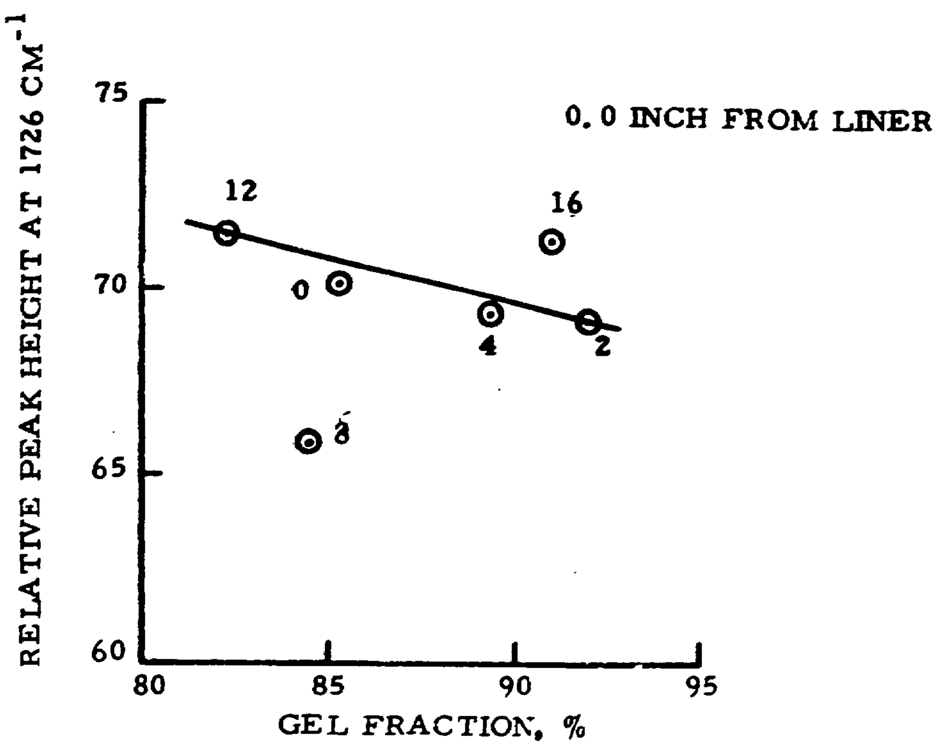


Figure 45. Minimum Smoke Propellant Correlation Between Gel Fraction and Peak at 1726 cm$^{-1}$.

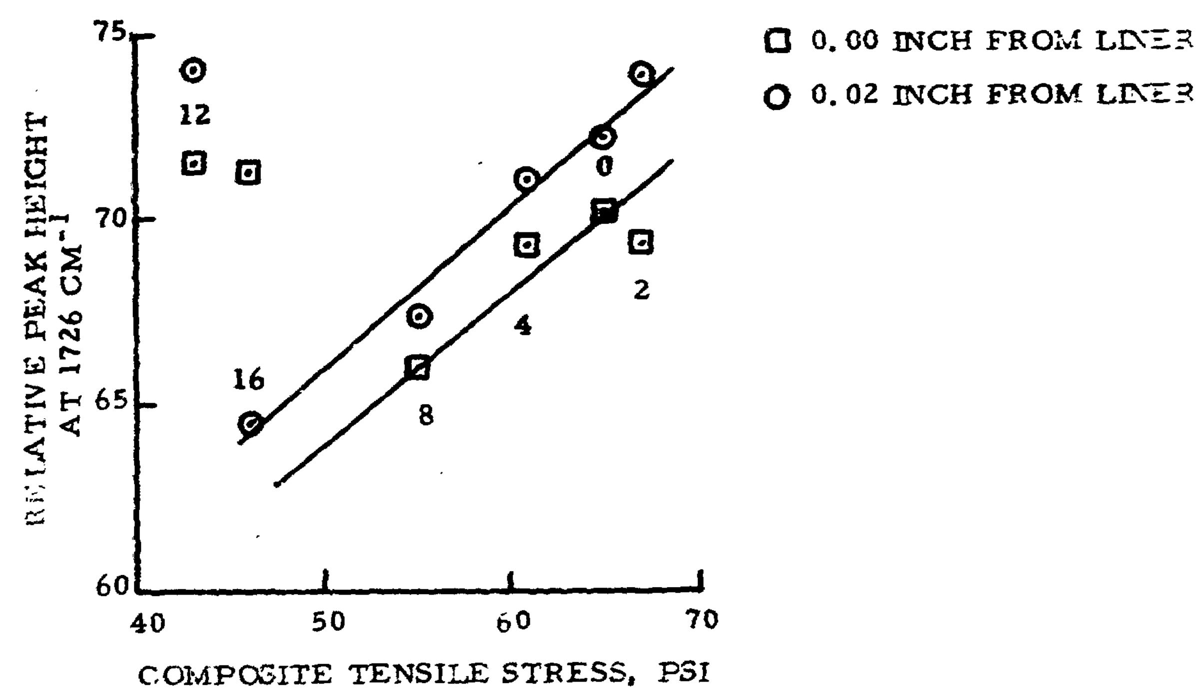


Figure 46. Minimum Smoke Propellant Correlation Between Composite Tensile Stress and Peak at 1726 cm$^{-1}$.

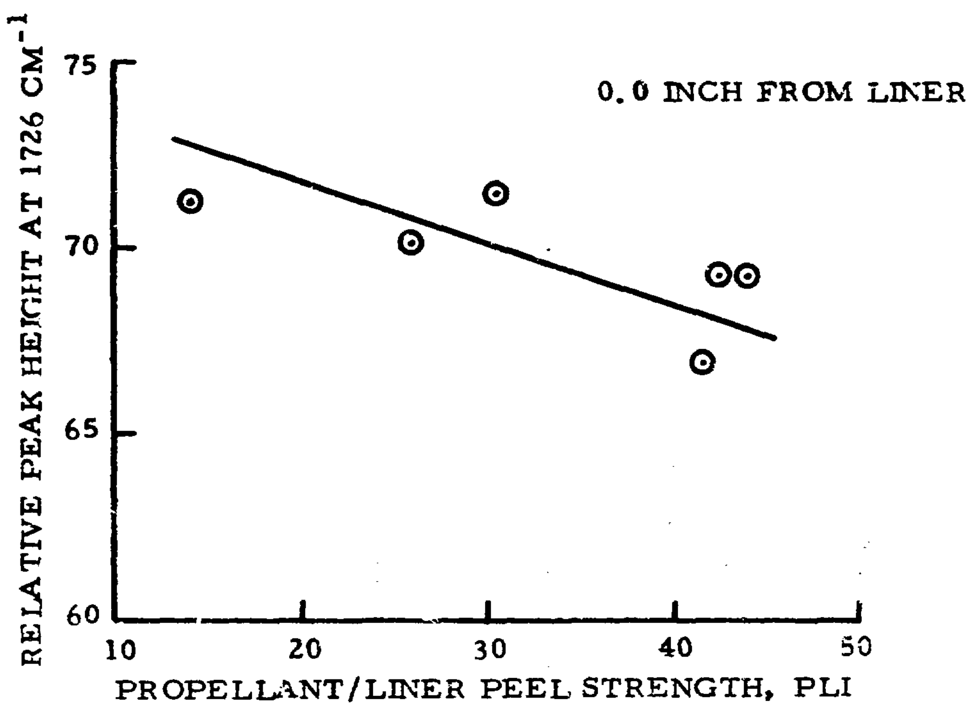


Figure 47. Minimum Smoke Propellant Correlation Between Propellant/Liner Peel and Peak at 1726 $cm^{-1}$.

Conclusions from Phase I Work

Following are the general conclusions which were drawn based upon the work of Phase I.

1) Sample preparation procedures were established.

2) IR data acquisition procedures were established.

3) IR of whole liner and insulation were determined not to be quantitatively useful.

4) IR of sol fraction was determined to be quantitatively excellent.

5) The best IR data for propellant/liner bond studies comes from propellant near the bond line.

6) No useful information was derived from IR of whole minimum smoke propellant.

7) IR of gel fraction of minimum smoke propellant was determined to be quantitatively useful.

8) HTPB propellant: Propellant/liner peel test was most useful.

9) Minimum smoke propellant: Propellant/liner peel was good - composite adhesion was good.

10) For HTPB propellant (AP/urethane), the best IR information is at 3008 $cm^{-1}$.

11) For minimum smoke propellant gel fraction (urethane), the best IR information is at 1726 and 1521 $cm^{-1}$.

## PHASE II - SERVICE LIFE

### Task 1 - Future Properties Programming

#### Summary of Programs

The principal goal of the computer programming portion of this project has been two-fold: (1) To identify propellant and bond mechanical properties from IR spectral data, and (2) predict what propellant or bond mechanical properties will be at a future time at some selected storage temperature. We started this project with two computer programs, E490 and E410. The E490 program accepted the IR spectral data from magnetic tape, computed normalized spectra, tabulated peak heights, and then performed certain correlation operations using input from computer program E410. Computer program E410 accepted propellant mechanical properties data, along with the aging time and temperature parameters associated with those data. It then tabulated the data and put them on magnetic tape so they would be available to the E490 program.

The functions of these two computer programs have remained basically the same through our continued programming efforts; however, some of the specific functions have changed. Old functions have been dropped, new functions added so that the entire package is better organized, easier to use, and performs its operations in a way that is more convenient to the user.

Table 26 summarizes the input and output of the set of programs for the Bondline Infrared Spectroscopy project. The first program described in Table 26 is E490 and the input to this program is the IR spectra as supplied on the magnetic tape from the FTS-10 infrared spectrophotometer. The output of E490 is a tabulation of normalized peak heights, and this tabulated data set is also deposited on disc for use by other computer programs.

The second of the computer programs is E572. This program is for regression analysis and uses component parts of a Thiokol program (E023). E572 has as input the spectral peak data from E490 and the bond aging data from program E410. The output of the program is a gression analysis showing the interrelationship among spectral peak heights and the propellant and/or bond properties. Mechanical properties are presented as functions of spectral peak heights. Simple and multiple linear correlations are calculated for a variety of transformations on each of the variables.

The third program presented on Table 26 is E410. This program has remained basically unchanged from the earlier version. Its input is mechanical property data (whether it be bond or propellant data) and the time and temperature associated with each of the mechanical properties. The output of program E410 is a tabulation of mechanical properties at the associated time and temperature. This entire data set is also stored on disc where it is readily available for use by the other computer programs in this set.

The fourth computer program listed in Table 26 is E571 and is concerned with the computation of activation energy for use in the Arrehenius equation. Input to this program is the peak height data from

TABLE 26

SUMMARY OF PROJECT COMPUTER PROGRAMS

| INPUT | PROGRAM NAME | OUTPUT |
|---|---|---|
| IR spectra, on mag tape | E490 | 1) Tabulation of normalized peak heights.<br>2) Data set (1) on disc. |
| Peak heights and bond mechanical properties (or propellant mechanical properties) | E572<br>(Regression) | 1) Mechanical properties as a function of spectral peak heights. Includes simple and multiple linear correlation, and a variety of transformations on each variable. |
| Mechanical Properties (bond or propellant), time and temperature | E410 | 1) Tabulation of mechanical properties at associated time and temperature.<br>2) Data set (1) on disc. |
| Peak height data (E490), time and temperature (E410) | E571<br>(Activation Energy) | 1) Activation energy based on peak height changes at any selected wave numbers.<br>2) Reaction rate constants at any selected temperature (not just aging program temperatures). |
| Equations from REGS; and activation energy and reaction rate constant from ACT | E575<br>(Prediction) | 1) Identification of propellant or bond mechanical properties from spectral data.<br>2) Prediction of mechanical properties at any future time at any temperature. |

program E490 and the time and temperature data associated with those infrared peak heights from program E410. The output of program E571 is the activation energy for the propellant based on peak height changes at any selected wave number. Another output is the reaction rate constant at any selected temperature, not just the temperatures in the aging program used to derive the peak height data.

The fifth and last program in the Table 26 summary is E575. This program has as its input the equations from the E572 program and the activation energy and reaction rate constants from program E571. The output of E575 is to identify the propellant or bond mechanical properties from the spectral date such that the actual mechanical property testing of the propellant does not have to take place, but that the properties can be derived based upon the infrared spectrum of the propellant. The second output from this program will be a prediction of mechanical properties and/or bond properties at any future time at any temperature.

The interrelationship among these five computer programs is displayed graphically in Figure 48. It shows the total input to this group of computer programs, the output from each program and how that output is used to arrive at the Bondline project objectives of: (1) Identifying propellant and bond properties from IR data, and (2) the prediction of propellant mechanical properties or bond properties at some future time.

More information on the functioning of each program follows. A detailed description of how to use each program will be found in "User's Manual for Bondline Infrared Spectroscopy Code" by R. J. Schorr.

E410 - Propellant Properties Computer Program Description

Program E410 is designed to create and maintain a permanent dataset for solid propellant mechanical and other properties from test data punched on cards. Once established, this dataset will be utilized for input to E571 and E572 computer programs along with the data set generated by E490.

This FORTRAN code consists of two parts, a main and a subroutine called RENAME. The main program creates the initial dataset and lists the data contained in the file. RENAME is designed strictly for updating or accessing an existing propellant file. No computations are performed on the data. The data is strictly read from cards and written to disc or tape.

The generated dataset may contain a maximum of a 100 logical records, each record corresponding to all the test data for one specimen. The data is unformatted, single precision, and written in the following sequence: Record number, aging time, aging temperature, test temperature, followed by ten (10) propellant properties; the same way it is listed on the print-out. The first six properties have been predefined as:

1) Modulus (PSI)
2) Strain at Break (%)
3) Strain at Maximum Stress (%)

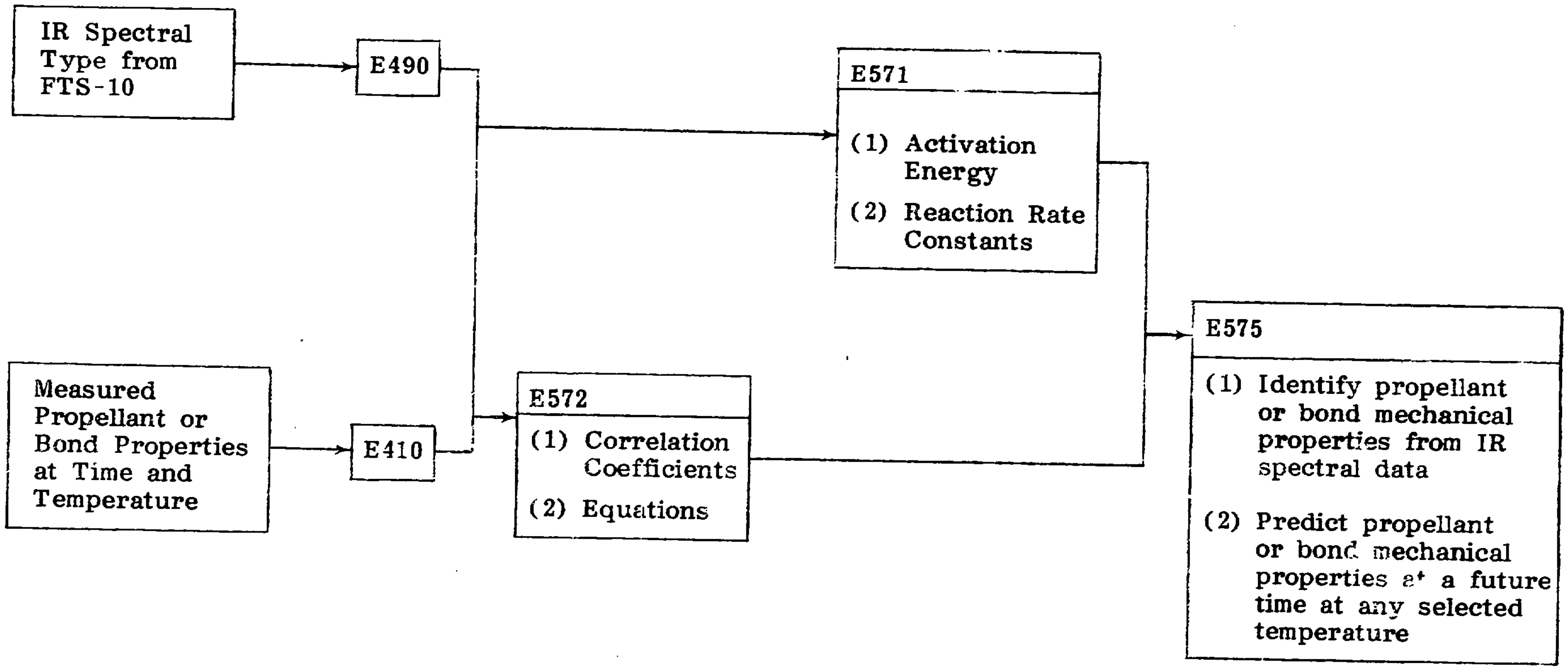


Figure 48. Interrelationships Among Project Computer Programs.

4) Maximum Stress (PSI)

5) Strain Energy Density (psi)

6) Strain Endurance (%)

The remaining four (4) properties may be anything the user wishes.

## E490 - IR Data Reduction Computer Program Description

The primary function of program E490 is to read infrared spectral data on Digilab FTS-10 tape and extract from it a set of infrared peak heights which are significant and can be compared to sets of peak heights from other FTIS spectra. For each infrared spectrum on an FTS-10 tape, a set of peak heights can be written to a permanent tape or disc file.

E490 can operate in one of two modes. The first time E490 is executed in a test series, it is run in the CREATE mode, generating a new dataset on tape 27. In subsequent runs involving related spectra, E490 is run in the UPDATE mode in which an existing dataset is read as tape 26, added to, and written to a new dataset on tape 27.

The following table illustrates how data from n FTIS files are stored on tape.

| Logical Record | Type | Data |
|---|---|---|
| 1 | Real | Normalization peak height; APMX |
| 2 | Integer | Number of IR absorbances/FTIS file-NPEAKS |
| 3 | Integer | Dataword of each IR absorption-NDAWD() |
| 4 | Real | Wave number of each IR absorption-WAVENO() |
| 5 | Integer | Logical sequence number for this spectral file |
| | Alpha | FTIS tape number-TAPENO |
| | Integer | FTIS file number-NFIL |
| | Real | IR peak heights for each absorption-HGT() |
| n | Integer | Logical sequence number for this spectral file |
| | Alpha | FTIS tape number-TAPENO |
| | Integer | FTIS file number-NFIL |
| | Real | IR peak heights for each absorption-HGT() |

## E571 - Activation Energy Computer Program Description

Because IR absorption is related to the quantity of a chemical specie in a propellant, changes in IR absorption with respect to time should be related to the reaction rate of those species. From knowledge of a reaction rate, we can predict what the IR absorption will be in the future.

Program E571 serves two functions, the second one being a continuation of the first. These two functions are:

1. Determine the linear relationships between any propellant property listed in the propellant property file and the IR absorptions listed in the E490 generated dataset. It was intended that IR absorptions would typically be a variable in this relationship; however, any two variables may be used.

2. Determine first-order reaction rate constants and activation energies of reactions associated with changes in IR absorptions.

Since E571 is dependent on E410 and E490 for data input, it cannot be executed until both E410 and E490 have generated their respective datasets.

Prior to determining the linear relationship between two variables, any of several types of transformations may be performed on either one of both variables. The FORTRAN code contains a single subroutine TRNVAR which is called upon to perform those transformations.

The majority of the computations in E571 involve finding least square regression lines. The general algorithm for E571 is as follows:

1. Read input data specifying dependent and independent variable, transformations to be used, and on which records in propellant property and IR data files to find each observation for specified variables.

2. Read data from tape 25 (propellant property file) and tape 20 (IR data file).

3. Perform transformations:

   $$y = fn_1 \text{ (dependent var)}$$

   $$x = fn_2 \text{ (independent var)}$$

4. Calculate least square regression line,

   $$y = \beta_0 + \beta_1 x,$$

   the standard error of estimate, and the correlation coefficient.

5. Repeat step 2 - 4 for each IR absorption specified in input.

6. Repeat step 2 - 5 for another set of observations, if any exist.

7. If regression equation is

   $$\ln(\text{IR absorption}) = \beta_0 + \beta_1(\text{aging time})$$

   $$\beta_1 = \text{rate constant}$$

   and it has been determined for at least two sets of observations at different aging temperatures, continue.

8. Tabulate $\beta_1$ (rate constant) at each aging temperature for each IR absorption.

9. Calculate and list the least square regression line

$$\ln(\mathrm{abs}(\beta_1)) = E_A/R(1/T) + C$$

$T$ = aging temperature (°K)
$E_A$ = Activation Energy
$R$ = Gas constant

for each IR absorption.

10. Calculate and list $E_A$ for each IR absorption.

## E572 - Multiple Regression Computer Program Description

E572 is designed to generate two empirical equations from data in files generated by E410 and E490.

1. A multiple linear regression equation relating any propellant property in the mechanical property file to IR absorbances tabulated by E490.

$$fn(\text{property}) = \beta_0 + \beta_1 fn_1(A_1) + \beta_2 fn_2(A_2) + \beta_n fn_n(A_n) \quad (1)$$

$A_i$ = ith IR absorbance value
$fn_i$ = transformation for $A_i$

2. An equation relating a propellant property to a function of time obtained by substituting regression equations

$$fn_1(A_1) = \alpha_1 + \gamma_1 fn_1(\text{time})$$

$$fn_2(A_2) = \alpha_2 + \gamma_2 fn_2(\text{time})$$

$$fn_3(A_3) = \alpha_3 + \gamma_3 fn_3(\text{time})$$

$$\vdots$$

$$fn_n(A_n) = \alpha_0 + {}_n fn_n(\text{time}) \quad (2)$$

into equation (1), resulting in

$$fn(\text{property}) = C_0 + C_1 fn_1(\text{time}) + C_2 fn_2(\text{time}) + \ldots + C_n fn_n(\text{time}) \quad (3)$$

Since E572 is dependent on E410 and E490 for data input, it cannot be executed until both E410 and E490 have generated their respective datasets.

The FORTRAN code consists of a main program which does all the computations except for the transformations. These are handled by two subroutines called TRAN and UNTRAN. UNTRAN does the inverse transformations.

The general algorithm for E572 is as follows:

1. Read input data from a NAMELIST called INPUT.

2. Read tape 25 (propellant properties).

3. Read tape 27 (IR absorptions).

4. Perform transformations on variables.

5. List transformed variables for each observation.

6. Calculate and list simple linear correlation coefficients between each variable.

7. Enter coefficients for the independent variables (IR absorptions) into the regression equation (1) one at a time beginning with the most significant as determined by an F value test. With each coefficient going into the regression equation, calculate and list the F value along with the standard error of estimate associated with each coefficient and the standard error of estimate of the dependent variable.

8. After all the coefficients are entered, calculate and list the multiple linear correlation coefficient.

9. Calculate and list the predicted value of the propellant property along with the actual property for each observation.

10. Repeat steps 2 - 9 for other dependent variables (propellant properties) listed in input.

11. Determine the least square regression line (2) for each independent variable in equation (1). A transformation on time may be specified in INPUT by TIMTRN().

12. Substitute the relations determined in the previous step into equation (1) yielding equation (3).

E575 - Future Properties Computer Program Description

Program E575 uses data generated by E571 and E572 to predict future propellant properties at any time=t given a normalized infrared absorbance at time=0. E575 is a short program that calls no subroutines and neither uses nor generates datasets or tapes.

The general program algorithm is as follows:

1. Given a rate constant for a particular temperature and the activation energy (output from E571), determine the rate constants at the expected aging temperature for a particular infrared absorption using the Arrhenius equation:

$$\ln \frac{k_2}{k_1} = \frac{E_A}{R} \frac{(T_1 - T_2)}{(T_1 T_2)} \qquad (1)$$

$k_1$ = rate constant ($time^{-1}$) at temperature $T_1$ (°K)
$k_2$ = rate constant ($time^{-1}$) at temperature $T_2$ (°K)
E = Activation Energy (cals/mole)
R = Gas constant

If rate constants are available for more than one temperature, calculate $k_2$ for each and average the results.

2. Repeat step 1 for other pertinent infrared absorptions.

3. Given an infrared absorption $A_0$ at time=0, calculate the infrared absorption value $A_t$ at time=t using (pseudo) first order kinetics.

$$\ln A_t = -k_2 t + \ln A_0 \qquad (2)$$

4. Repeat step 3 for other pertinent infrared absorptions.

5. Given the regression equation relating propellant property to infrared absorptions (generated from E572), make the appropriate transformations on the infrared absorptions to give $fn_i(A_i)$ and predict fn(MP)* at time=t.

$$fn(MP) = \beta_0 + \beta_1 fn_1(A_1) + \beta_2 fn_2(A_2) + \ldots + \beta_n fn_n(A_n) \qquad (3)$$

6. The inverse function of fn(MP) is taken to get the value of the propellant property.

Rationale for Future Bond Property Prediction

The first step in the prediction of future bond properties of propellant/liner/insulation systems (can also be applied to all correlated physical properties) involves the acquisition of data characterizing the chemical structures in the infrared spectra that are changing with time. In order for the peak heights of each functional group between spectra to be compared quantitatively, all the spectra in a considered group must be normalized relative to one of the spectra in the group. The peak selected for normalizing is one which is least likely to change during the aging period, such as the saturated carbon-hydrogen absorption peak.

We will assume that the majority of the detected aging reactions are first order. The foundations of this assumption are the small range of change occurring in a given functional group during aging and the majority of components are at such a high percentage that their concentration may be

*MP = mechanical property.

considered constant. Also, the data agree with and support first order kinetics.

The rate of a first order reaction at any time at a constant temperature is directly proportional to the concentration $C_a$ of reactant A where

$$\frac{-dC_a}{dt} = K_1 C_a \qquad (1)$$

and $K_1$ is the specific rate constant. If "a" is the initial concentration of A, and "x" the decrease in concentration of A due to reaction up to time=t, then $C_a = a - x$ at time t,

$$\frac{-dC_a}{dt} = \frac{-d(a-x)}{dt} = \frac{dx}{dt}$$

and equation (1) becomes

$$\frac{dx}{dt} = K_1(a-x) \qquad (2)$$

Integrating equation (2) and rearrangements gives

$$\ln(a-x) = -K_1 t + \ln a \qquad (3)$$

In the bondline program, the peak heights from the spectral data are equivalent to "a-x" in equation (3). A plot of ln(a-x) versus t should yield a straight line in which the y intercept will be lna (peak height at zero age time) and the slope equals $-K_1$. By plotting the ln peak height data versus time for each of several aging temperatures, the specific rate constants for the peaks that change can be determined at each aging temperature.

The variation of rate constants with temperature can be represented by the Arrhenius equation

$$\frac{d\ln K}{dT} = \frac{Ea}{RT^2} \qquad (4)$$

where K is the reaction rate constant, T the absolute temperature, R the gas constant, and Ea the energy of activation. Integrating (4) we obtain

$$\ln K = \frac{-Ea}{RT} + C \qquad (5)$$

A plot of lnK against $\frac{1}{T}$ should be a straight line with

$$\text{slope} = \frac{-Ea}{R}$$

Using the rate constants determined for a given infrared peak at each aging temperature, we can calculate the activation energy Ea of each peak.

If we integrate equation (4) between the limits $K = K_1$ at $T = T_1$ and $K = K_2$ at $T = T_2$, then

$$\ln\frac{K_2}{K_1} = \frac{Ea}{R}\left(\frac{T_2 - T_1}{T_1 T_2}\right) \tag{6}$$

and as soon as Ea and a value of K at one temperature are known, K at another temperature may be calculated.

Remaining data necessary to predict future bond properties are a good correlation between measured bond properties and an infrared peak for which rate constants and activation energy have been derived. The relationship does not have to be linear, but may involve a transform applied either to the bond property or infrared peak height or both. These transforms may include

1 = log (x)

2 = $(x = \text{constant})^{\text{power}}$

3 = $\sqrt{x}$

4 = ln(x)

To calculate or predict a bond property value at some future time $t_n$ and at an aging temperature $T_n$, the following steps are followed:

a) The activation energy and one rate constant derived for the peak being used are entered in equation (6) to calculate the rate constant $K_n$ at temperature $T_n$.

b) The rate constant $K_n$, time t, and an initial absorbance value for the peak are entered in equation (3) to calculate the absorbance value at time $t_n$.

c) The derived absorbance value at time $t_n$ is entered into the equation relating peak height and the bond property to calculate the new bond property value at time $t_n$.

## Task 2 - Bond System Aging and Data Analysis

Two distinctly different bond systems were prepared, aged and tested during this task. One was based on an HTPB propellant and the other on a minimum smoke propellant.

### Preparation of Bond Samples for Aging

Materials used in the HTPB bond system are presented in Table 27. The propellant is TP-H8288; the liner is TL-H755A; while the insulation is TI-R701, an asbestos-free insulation. Compositions of all three materials are given in Table 27.

Samples for the minimum smoke propellant bond system are made up of propellant TP-Q7030, liner TL-H774A, and insulation TI-R701. Compositions of all three materials are presented in Table 28.

TABLE 27

## HTPB TYPE BOND SYSTEM AGING

Propellant: TP-H8288
Liner: TL-H755A
Insulation: TI-R701

### COMPOSITIONS

| | Material | Weight, % |
|---|---|---|
| TP-H8288 | R-45M/Mixed Antioxidant<br>DDI<br>DOA<br>HX-752 | 13.00 |
| | Ballistic Stabilizer | 1.00 |
| | RDX | 4.00 |
| | AP | 82.00 |
| TL-H755A | R-45M | 41.85 |
| | DDI | 12.15 |
| | HX-868 | 6.00 |
| | Carbon | 40.00 |
| TI-R701 | Polyisoprene Binder<br>Kevlar® Fiber Filler | |

TABLE 28

MINIMUM SMOKE TYPE BOND SYSTEM AGING

Propellant: TP-Q7030

Liner: TL-H774A

Insulation: TI-R701

| | Material | Weight, % |
|---|---|---|
| TP-Q7030 | Minimum Smoke Binder | 6.657 |
| | Nitrate Plasticizers | 22.843 |
| | Ballistic Additives | 3.000 |
| | Nitrate Oxidizers | 67.500 |
| TL-H774A | R-45HT | 45.526 |
| | DDI | 10.204 |
| | HX-868 | 4.000 |
| | Carbon | 40.000 |
| | Maleic Anhydride | 0.135 |
| | $\phi_3Bi$ | 0.135 |
| TI-R701 | Polyisoprene Binder | |
| | Kevlar® Fiber Filler | |

Two types of composite bond samples were prepared: Peel samples and composite adhesion samples. The composite adhesion sample consists of a 2-inch diameter disc of prevulcanized insulation positioned in a 2-inch diameter mold. Approximately 0.030 inch of liner is cured on top of the insulation and the propellant cast onto the liner. The peel specimen consists of a 2-inch by 4-inch section of prevulcanized insulation positioned at the bottom of a 2-inch by 2-inch by 1-inch mold with approximately 0.030 inch of liner cast on the insulation in a mold. When the liner has been cured, the propellant is cast on top of the liner to a depth of about 0.8-inch.

Aging Plan

The aging test matrix for the HTPB bond system is displayed in Table 29, while the aging test matrix for the minimum smoke-type bond system is given in Table 30. Shown on those two tables are the number and types of tests that were run at each of the time/temperature test intervals.

Aging Data

Bond Data

Tensile adhesion and peel strength for the HTPB propellant bond system are displayed in Table 31, while the data for the minimum smoke propellant bond system are displayed in Table 32. During the time these aging programs were in progress, a safety incident (not connected with this program) occurred which necessitated moving the HTPB bond aging samples from one 165°F oven to another. Two sets of samples were misplaced and never found; therefore, the 24 and 32-week data for 165°F aging are missing.

Tests of the minimum smoke propellant bond system were planned for only 16 weeks at 165°F. This plan was based on results of other aging programs wherein it was found that the stabilizer, MNA, was depleted after about 12 weeks at 165°F. With depletion of MNA, the propellant binder degraded very rapidly and whether the propellant could be tested became questionable. On Table 32, note that at 12 weeks of aging the peel strength of the bond system was almost nil. At 16 weeks of aging the peel sample literally fell apart when it was being placed in the test apparatus (Instron tensile tester).

Variation of the tensile adhesion of the HTPB propellant bond system with age time is displayed in Figure 49, while the variation of peel strength with age time at the various age temperatures is plotted in Figure 50. The response of the minimum smoke propellant bond system to aging time is shown on Figure 51 for the tensile adhesion and on Figure 52 for peel strength.

IR Data

IR spectra of the HTPB propellant in the bond samples were made at the propellant/liner bond interface and at 0.5 inch from the interface. Five spectra were made at each age time/temperature condition, each spectrum made of a separate sample. The five spectra at each time/temperature condition were electronically averaged and this average spectrum employed in the data correlations.

TABLE 29

HTPB

AGING TEST MATRIX

| Sample Type | Storage Condition | Storage Temp. (°F) | Testing Level At Storage Time, Wks 0 | 1 | 2 | 4 | 8 | 16 | 24 | 32 |
|---|---|---|---|---|---|---|---|---|---|---|
| Propellant/liner/insulation Composite Adhesion (Note 1) | Purged with $N_2$ | 77 | 1 | | | 1 | 1 | 1 | 1 | 1 |
| | | 100 | | | | 1 | 1 | 1 | 1 | 1 |
| | | 130 | | | | 1 | 1 | 1 | 1 | 1 |
| | | 165 | | 1 | 1 | 1 | 1 | 1 | 1 | 1 |
| Propellant/liner/insulation Peel Specimens (Note 2) | Purged with $N_2$ | 77 | 2 | | | 2 | 2 | 2 | 2 | 2 |
| | | 100 | | | | 2 | 2 | 2 | 2 | 2 |
| | | 130 | | | | 2 | 2 | 2 | 2 | 2 |
| | | 165 | | 2 | 2 | 2 | 2 | 2 | 2 | 2 |
| Propellant/liner insulation Composite Peel (Note 3) | Purged with $N_2$ | 77 | 3 | | | 3 | 3 | 3 | 3 | 3 |
| | | 100 | | | | 3 | 3 | 3 | 3 | 3 |
| | | 130 | | | | 3 | 3 | 3 | 3 | 3 |
| | | 165 | | 3 | 3 | 3 | 3 | 3 | 3 | 3 |

TEST LEVELS

Level 1: Composite bond tests at 77°F.
Level 2: Peel test at 77°F.
Level 3: Samples for infrared analysis of propellant at interface and 0.5 inch from the interface.

NOTES:

1) 3 samples per aging condition = 23 x 3 = 69

2) 3 samples per aging condition = 23 x 3 = 69

3) 1 sample per aging condition = 23 x 1 = 23

TOTAL: 161

TABLE 30

MINIMUM SMOKE

AGING TEST MATRIX

| Sample Type | Storage Condition | Storage Temp. (°F) | Testing Level At Storage Time, Wks | | | | | | | | |
|---|---|---|---|---|---|---|---|---|---|---|---|
| | | | 0 | 1 | 2 | 4 | 8 | 12 | 16 | 24 | 32 |
| Propellant/liner/insulation | Purged with | 77 | 1 | | | 1 | 1 | | 1 | 1 | 1 |
| Composite Adhesion | $N_2$ | 100 | | | | 1 | 1 | | 1 | 1 | 1 |
| (Note 1) | | 130 | | | | 1 | 1 | | 1 | 1 | 1 |
| | | 165 | | 1 | 1 | 1 | 1 | 1 | 1 | | |
| Propellant/liner/insulation | Purged with | 77 | 2 | | | 2 | 2 | | 2 | 2 | 2 |
| Composite peel | $N_2$ | 100 | | | | 2 | 2 | | 2 | 2 | 2 |
| (Note 2) | | 130 | | | | 2 | 2 | | 2 | 2 | 2 |
| | | 165 | | 2 | 2 | 2 | 2 | 2 | 2 | | |
| Propellant/liner/insulation | Purged with | 77 | 3 | | | 3 | 3 | | 3 | 3 | 3 |
| Composite Peel | $N_2$ | 100 | | | | 3 | 3 | | 3 | 3 | 3 |
| (Note 3) | | 130 | | | | 3 | 3 | | 3 | 3 | 3 |
| | | 165 | | 3 | 3 | 3 | 3 | 3 | 3 | | |

TEST LEVELS

Level 1: Composite bond tests at 77°F.
Level 2: Peel test at 77°F.
Level 3: Samples for infrared analysis of propellant gel fraction at interface and 0.5 inch from the interface.

NOTES:

1) 3 samples per aging condition = 22 x 3 = 66

2) 3 samples per aging condition = 22 x 3 = 66

3) 1 sample per aging condition = 22 x 1 = 22

TOTAL: 154

TABLE 31

## HTPB PROPELLANT BOND SYSTEM AGING

(Mix T-1161)

| Time (Weeks) | Age Temp. (°F) | Tensile Adhesion (psi) | Failure Mode | Peel (pli) | Failure Mode |
|---|---|---|---|---|---|
| 0 | 77 | 81.7 | Propellant | 3.3 | Propellant |
| 1 | 165 | 85.0 | Propellant | 8.0 | Propellant |
| 2 | 165 | 10[illegible].5 | Propellant | 12.6 | Propellant |
| 4 | 77 | 111.2 | Propellant | 8.9 | Propellant |
| | 100 | 100.5 | Propellant | 10.1 | Propellant |
| | 130 | 123.2 | Propellant | 9.8 | Propellant |
| | 165 | 108.2 | Propellant | 13.4 | Propellant |
| 8 | 77 | 88.6 | Propellant | 9.0 | Propellant |
| | 100 | 90.2 | Propellant | 7.8 | Propellant |
| | 130 | 94.9 | P, BL/P | 10.6 | Propellant |
| | 165 | 98.1 | BL/P | 12.0 | Bond & P |
| 16 | 77 | 75.7 | Propellant | 8.7 | Propellant |
| | 100 | 87.2 | BL/P | 8.5 | Propellant |
| | 130 | 99.8 | BL/P | 12.5 | BL/P |
| | 165 | 106.8 | BL/P | 5.3 | BL/P |
| 24 | 77 | 86.0 | Propellant | [illegible].8 | Propellant |
| | 100 | 98.0 | Propellant | 11.6 | Propellant |
| | 130 | 107.0 | Propellant | 33.9 | Propellant |
| | 165 | SAMPLES LOST | | | |
| 32 | 77 | 70.6 | Propellant | 9.7 | Propellant |
| | 100 | 88.5 | Propellant | 11.7 | Propellant |
| | 130 | 90.1 | Propellant | 3.2 | BL/P |
| | 165 | SAMPLES LOST | | | |

NOTES: P = propellant; BL = bond line.

TABLE 32

MINIMUM SMOKE PROPELLANT BOND SYSTEM AGING

(Mix X-27)

| Time (Weeks) | Age Temp. (°F) | Tensile Adhesion (psi) | Failure Mode | Peel (pli) | Failure Mode |
|---|---|---|---|---|---|
| 0 | | 47.7 | Propellant | 14.0 | Propellant |
| 1 | 165 | 41.8 | Propellant | 29.3 | Propellant |
| 2 | 165 | 50.8 | Propellant | 21.1 | Propellant |
| 4 | 77 | 52.2 | Propellant | 27.7 | Propellant |
| | 100 | 78.8 | Propellant | 26.1 | Propellant |
| | 130 | 71.1 | Propellant | 33.2 | Propellant |
| | 165 | 81.4 | Propellant | 14.3 | Propellant |
| 8 | 77 | 50.0 | Propellant | 30.5 | Propellant |
| | 100 | 45.4 | Propellant | >28.7 | P, PFF |
| | 130 | 54.4 | Propellant | >28.3 | P, PFF |
| | 165 | 69.3 | P, BL/P | 3.3 | TCP/L |
| 12 | 165 | 53.3 | Propellant | 2.3 | TCP/L |
| 16 | 77 | 57.2 | Propellant | >24.0 | Propellant |
| | 100 | 52.5 | Propellant | >26.9 | Propellant |
| | 130 | 62.3 | Propellant | 27.2 | Propellant |
| | 165 | 53.8 | NOT TESTED. | | |
| 24 | 77 | 91.0 | Propellant | 34.3 | Propellant |
| | 100 | 81.0 | Propellant | 31.9 | Propellant |
| | 130 | 100.0 | Propellant | 20.7 | Propellant |
| 32 | 77 | 43.4 | Propellant | 27.2 | Propellant |
| | 100 | 50.5 | Propellant | 32.6 | Propellant |
| | 130 | 44.5 | Propellant | 12.9 | Propellant |

NOTES: P = propellant; BL = bond line; PFF = propellant pulled from frame; TCP/L = thin coat of propellant at liner interface.

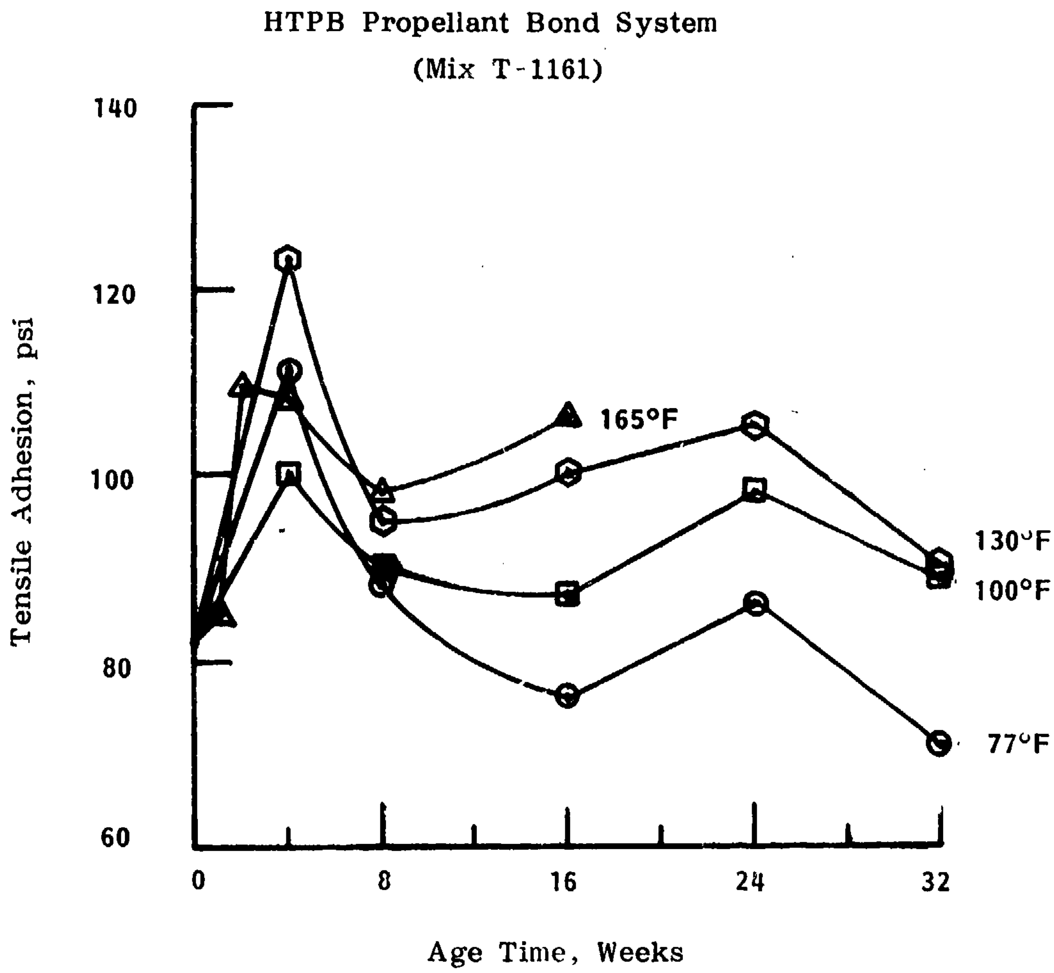


Figure 49. Variation in Tensile Adhesion with Time and Temperature.

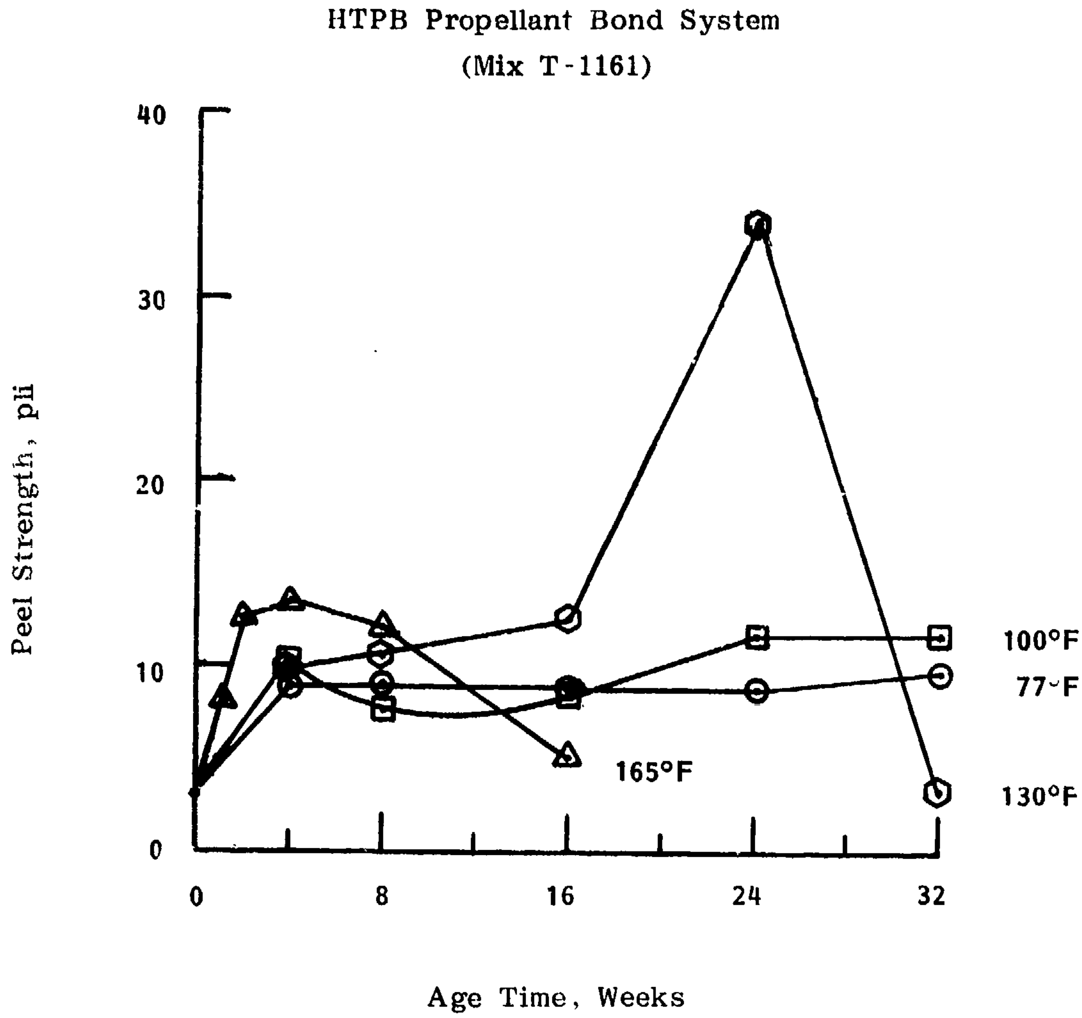


Figure 50. Variation of Peel Strength with Time and Temperature.

Minimum Smoke Propellant Bond System
(Mix X-27)

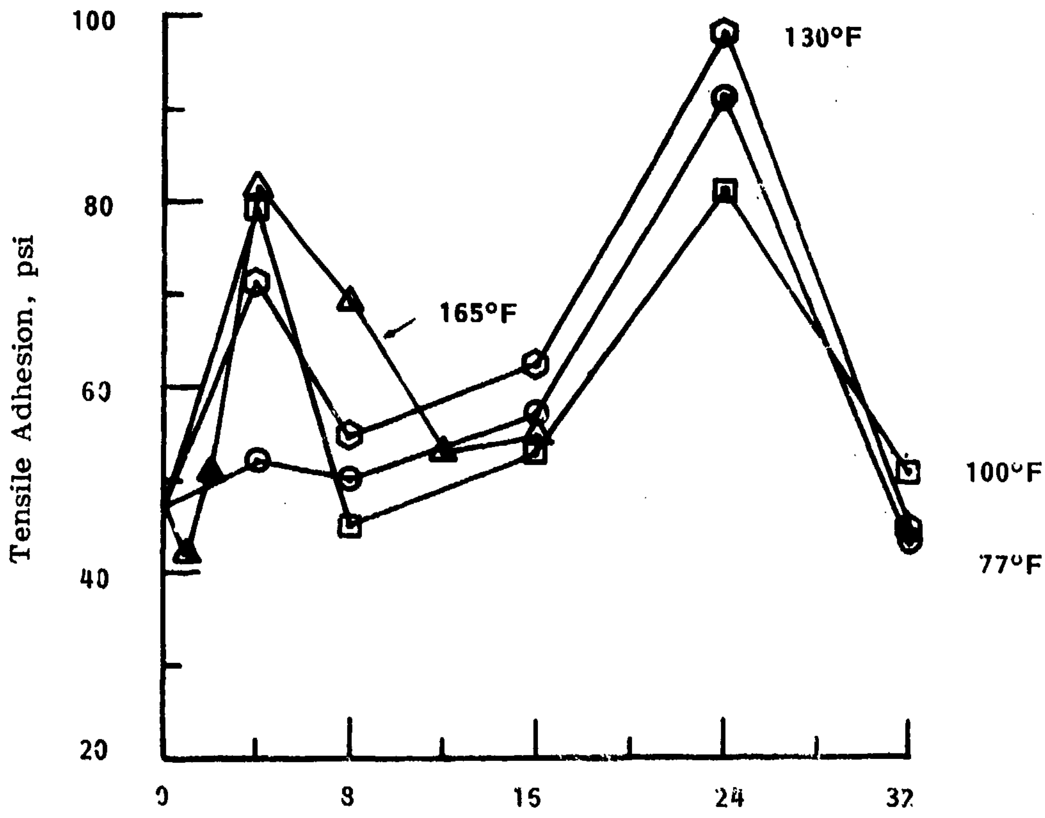


Figure 51. Variation of Tensile Adhesion with Time and Temperature.

Minimum Smoke Propellant Bond System
(Mix X-27)

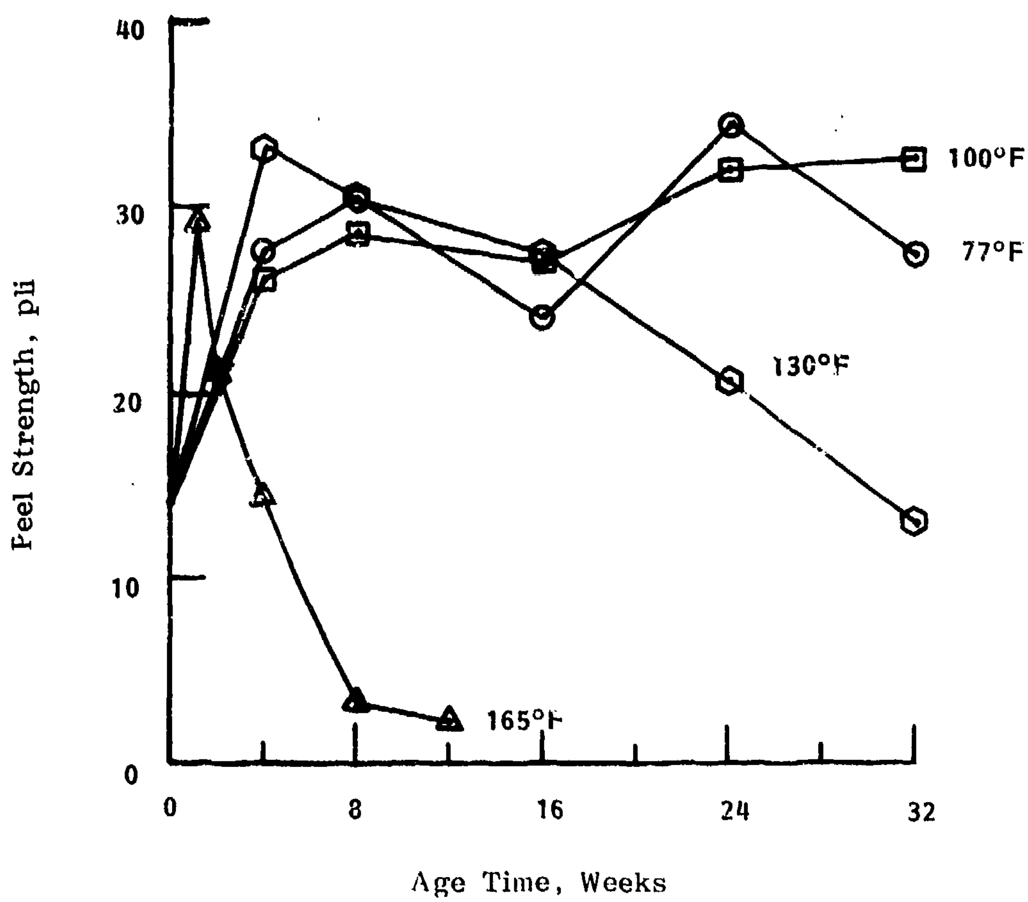


Figure 52. Variation of Peel Strength with Time and Temperature.

IR spectra of the minimum smoke propellant in the bond samples were made at the propellant/liner interface and at 0.5 inch from the interface. Three propellant samples were taken at each location at each time/temperature condition and the sol fraction removed by extraction with acetone. IR spectra were made of the remaining gel fraction. The three spectra at each time/temperature test interval were electronically averaged and this average spectrum employed in the data correlations.

Aging of the two bond systems was commenced the end of September, 1981; and early in November, 1981, before the IR analysis of the 4-week samples was run, the infrared spectrophotometer failed. Repair of the instrument was not effected totally until mid-April, 1982. Propellant samples for IR analysis collected during this 5-month period were frozen and their IR spectra made after mid-April. Some of the samples then were stored for 5 months before their spectra were made; this may have had some effect on the outcome of the IR peak height correlations with time/temperature and with bond properties.

## Analysis of TP-H8288 Data

### IR Data and Time/Temperature

IR spectra were made of TP-H8288 propellant at a liner/propellant interface and of samples taken from approximately 0.5 inch away from this interface. Typical IR spectra of propellant at these two locations are shown on Figure 53 for propellant 0.5 inch from the interface and Figure 54 for propellant near that liner interface. A common baseline data reduction technique was used for this propellant. The location of these common baseline areas is displayed in Figure 53. Also identified in Figure 53 is the source of each of the infrared peaks. Note that the spectrum is dominated by RDX and there are few peaks that are totally free of the influence of RDX. RDX does not change with age time the way the binder in the propellant changes; and, if the RDX did change, it probably would not have a really intense effect upon the mechanical properties of propellant (since it is only 4% of the propellant). Binder peaks located at 1440 and 1738 $cm^{-1}$ are free of the influence of RDX. The peak at 1738 is the principle peak of DOA, with some urethane influence in that peak. Binder peaks also appear in the 2800 to 3000 region of the spectrum and these peaks are free of the influence of RDX. Other peaks associated with the binder are cis unsaturation in the 720 $cm^{-1}$ region and trans unsaturation at 965 $cm^{-1}$.

Correlations will be presented first for propellant taken from the bond interface and then for propellant in the area 0.5 inch away from the bond interface. Table 33 shows the correlations of IR peak height and time for the propellant. Only those correlations stronger than 0.8 are quoted. A review of the data on Table 33 shows that at 165°F, there were correlations at several of the peaks and fewer correlations at 100° and 130°F. All of the peaks that correlated are in part attributable to RDX and this, then, says that the amount of RDX appearing at the ATR/IRE surface is varying with age time and age temperature which is, in reality, a correlation of propellant modulus with age time and temperature. Table 34 is the correlation of the natural logarithm of peak height and time for propellant taken near the bond interface. Again, the same peaks are correlating with time as were found in Table 33. Correlation

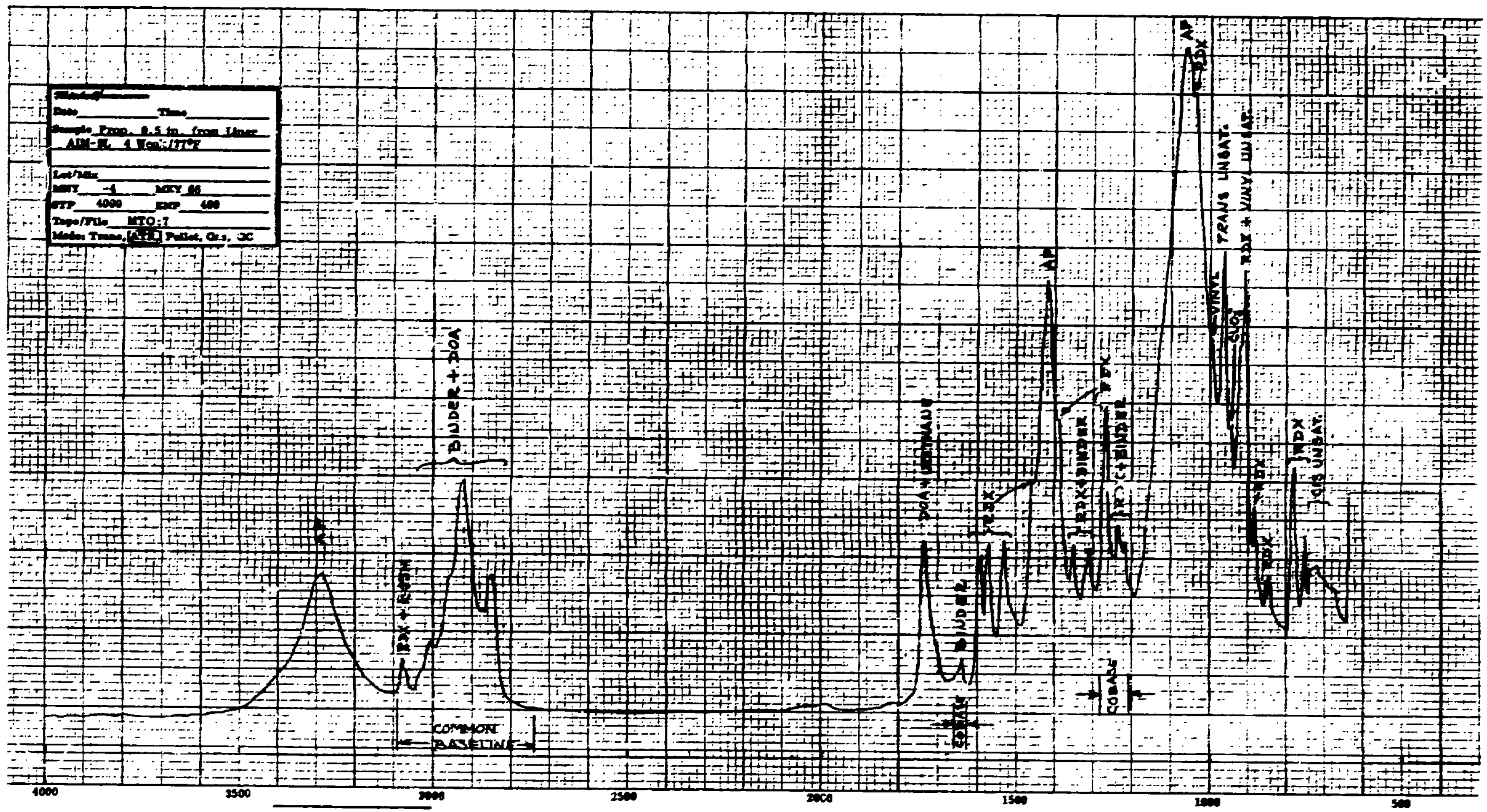


Figure 53. IR Spectra of TP-H8288 Propellant 0.5 Inch From Liner Interface.

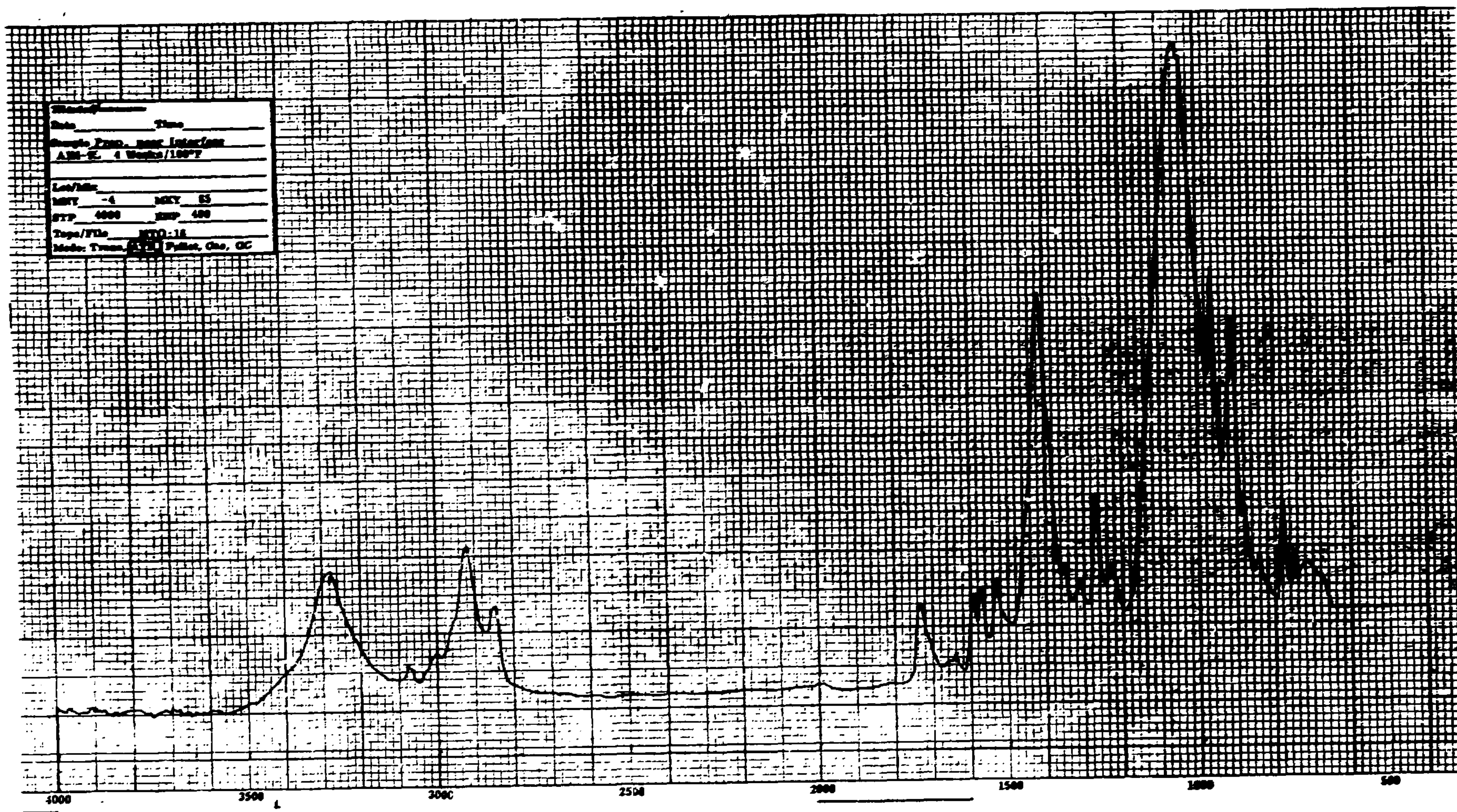


Figure 54. IR Spectra of TP-H8288 Propellant Near Interface With Liner.

## TABLE 33

### CORRELATION OF IR PEAK HEIGHT AND TIME, IR OF PROPELLANT AT BOND INTERFACE

| Wave No., $cm^{-1}$ | Correlation Coefficient at Age Temperature 77°F | 100°F | 130°F | 165°F |
|---|---|---|---|---|
| 2749.1 | | 0.9484 | 0.9548 | 0.9117 |
| 1532.7 | | | | -0.8013 |
| 1420.7 | | | 0.8642 | |
| 1312.6 | | | | -0.8970 |
| 1219.9 | | | | -0.8186 |
| 883.9 | | | | 0.8935 |
| 853.0 | | | | -0.8917 |
| 845.3 | | | | 0.8922 |

## TABLE 34

### CORRELATION OF IR ln PEAK HEIGHT AND TIME, IR OF PROPELLANT AT BOND INTERFACE

| Wave No., $cm^{-1}$ | Correlation Coefficient at Age Temperature 77°F | 100°F | 130°F | 165°F |
|---|---|---|---|---|
| 2749.1 | | 0.8547 | 0.9563 | 0.8552 |
| 1532.7 | | | | -0.8257 |
| 1420.7 | | | 0.8602 | |
| 1312.6 | | | | -0.9291 |
| 1219.9 | | | | -0.8250 |
| 883.9 | | | | -0.9166 |
| 853.0 | | | -0.8060 | -0.9438 |
| 845.3 | | | | -0.9126 |

NOTE:
Common baseline data reduction used for the following groups of peaks:

a) 3090 - 2740 $cm^{-1}$
b) 1660 - 1630 $cm^{-1}$
c) 1280 - 1205 $cm^{-1}$

coefficients are modified only slightly by taking the natural logarithm of the peak height. The variation of these peak heights with temperature where the peak height is a logarithm allows for the calculation of reaction rate con stant, and then these reaction rate constants can then be correlated against the reciprocal of temperature in an Arrhenius-type plot. The correlation of the log of the reaction rate constant with reciprocal of absolute temperature is given in Table 35. The peaks that correlated with variation in time also appear here, plus several others that did not appear in Tables 33 and 34. Principally, the peak occurring at 3007.9 $cm^{-1}$ is of interest because it is free of the influence of RDX. The correlation coefficient for reaction rate constant and reciprocal of absolute temperature is quite high.

Correlations of IR peak height with time for propellant taken from the area about 0.5 inch from the interface with the liner are revealed on Table 36. Peaks at 2876 and 2749 $cm^{-1}$ correlated strongly with variations in time, at the three higher age temperatures, but these peaks are extremely small as a review of Figure 53 will show. As a matter of fact, the peaks are so small that they do not even show on Figure 53. Therefore, we are left with one peak in this series (1737 $cm^{-1}$) which shows a strong correlation with time at three age temperatures. Changing to a natural logarithm of the IR peak height did not significantly change any of the correlations (see Table 37). Reaction rate constants (calculated from the logarithm of peak height and time) were correlated with 1/absolute temperature at which the reaction was occurring. These correlations are displayed in Table 38. Those data show the correlation for the peak at 1737.4 $cm^{-1}$ to be extremely high.

## IR Data and Bond Properties

Bond aging data presented earlier show that the adhesion and peel strengths of the bond system were not well-ordered functions of time at any of the aging temperatures. Because of loss of some samples, aging at 165°F was terminated at 16 weeks, so the data there are very limited and correlations will likewise be limited. Correlations at other temperatures are displayed on Tables 39 and 40 for propellant taken at the bond interface. Data on these two tables show that there are correlations in those parts of the infrared spectrum which are characteristic of the binder; namely, peaks occurring at 3007.9, 1737.4, and 1640.8 $cm^{-1}$. There is also a correlation with the peak occurring at 965 $cm^{-1}$ which is also a peak characteristic of the binder and free of influence of RDX. Again, only those correlation coefficients higher than 0.8 are given.

Correlation of IR peak height with peel and adhesion for propellant 0.5 inch from the interface is displayed in Tables 41 and 42, respectively. Correlations of IR peak height change with changes in peel strength at this distance from the interface are very sparse and show that there is little influence of propellant this far away from the interface on the peel strength of the bond system. IR peak height changes correlated with adhesion (Table 42) at this distance from the interface say that the strength of the propellant at this distance is probably characteristic of the propellant which failed in the adhesion test. Correlations were strong with the peak at 3007.6 $cm^{-1}$, which is a region of the IR spectrum that is free of the influence of RDX.

TABLE 35

CORRELATION OF ln REACTION RATE CONSTANT AND 1/TEMPERATURE

(TP-H8288 Propellant)*

| Wave No., $cm^{-1}$ | At Propellant/Liner Interface W/77°F Data | W/O 77°F Data |
|---|---|---|
| 3069.7 | -0.8977 | -0.8762 |
| 3007.9 | -0.9958 | -0.9991 |
| 2749.1 | -0.7450 | -0.1928 |
| 1652.4 | -0.5205 | 0.5896 |
| 1590.6 | -0.9259 | -0.9223 |
| 1351.2 | -0.5965 | -0.8470 |
| 1312.6 | -0.8979 | 0.9943 |
| 883.9 | -0.9325 | -0.9126 |
| 853.0 | | -0.9794 |

TABLE 36

CORRELATION OF IR PEAK HEIGHT AND TIME.

IR OF PROPELLANT 0.5 INCH FROM INTERFACE

(TP-H8288 Propellant)

| Wave No., $cm^{-1}$ | Correlation Coefficient at Age Temperature | | | |
|---|---|---|---|---|
| | 77°F | 100°F | 130°F | 165°F |
| 3069.7 | | 0.8729 | | 0.9564 |
| 2876.6 | | -0.8830 | -0.8960 | -0.9327 |
| 2749.1 | | 0.8422 | 0.9722 | 0.9176 |
| 1737.4 | | -0.9808 | -0.9800 | 0.8679 |
| 1590.6 | | | | 0.9447 |
| 1571.3 | | | | -0.8129 |
| 1420.7 | | | | 0.9556 |
| 1351.2 | | | | -0.8931 |
| 910.9 | | -0.9653 | | |
| 883.9 | | | | -0.8765 |

NOTE:
Common baseline data reduction used for the following groups of peaks:

a) 3090 - 1740 $cm^{-1}$
b) 1660 - 1630 $cm^{-1}$
c) 1280 - 1205 $cm^{-1}$

TABLE 37

CORRELATION OF ln IR PEAK HEIGHT AND TIME.

IR OF PROPELLANT 0.5 IN. FROM INTERFACE

(TP-H8288 Propellant)

| Wave No., $cm^{-1}$ | Correlation Coefficient at Age Temperature | | | |
|---|---|---|---|---|
| | 77°F | 100°F | 130°F | 165°F |
| 3069.7 | | 0.8593 | | 0.9505 |
| 2876.6 | | -0.8920 | -0.9001 | -0.9374 |
| 2749.1 | | 0.8902 | 0.9588 | |
| 1737.4 | | -0.9767 | -0.9756 | -0.8658 |
| 1590.6 | | | | -0.9518 |
| 1571.3 | | | | -0.8160 |
| 1420.7 | | | | 0.9346 |
| 1351.2 | | | | -0.9037 |
| 910.9 | | -0.9648 | | |
| 883.9 | | | | -0.8874 |

NOTE:
Common baseline data reduction used for the following groups of peaks:

a) 3090 - 2740 $cm^{-1}$
b) 1660 - 1630 $cm^{-1}$
c) 1280 - 1205 $cm^{-1}$

TABLE 38

CORRELATION OF ln REACTION RATE CONSTANT AND 1/TEMPERATURE

(TP-H8288 Propellant)

| Wave No., $cm^{-1}$ | 0.5 in. from Interface W/All Temps. | 0.5 in. from Interface W/O 77°F Data |
|---|---|---|
| 3077.4 | 0.6906 | -0.5796 |
| 3069.7 | -0.8740 | -0.9411 |
| 3007.9 | -0.5030 | -0.9489 |
| 2876.6 | -0.9766 | -0.9974 |
| 2749.1 | -0.9699 | -0.9622 |
| 1737.4 | -0.9649 | -0.9993 |
| 1652.4 | -0.7561 | -0.2326 |
| 1590.6 | -0.9393 | -0.8769 |
| 1571.3 | -0.7992 | -0.8216 |
| 1532.7 | -0.5322 | -0.9917 |
| 1420.7 | -0.6451 | -0.9274 |
| 1351.2 | -0.7295 | -0.8708 |
| 1312.6 | -0.8045 | -0.9832 |
| 1266.2 | 0.7640 | 0.8765 |
| 883.9 | -0.8543 | -0.8614 |
| 853.0 | | -0.8496 |
| 845.3 | | 0.8292 |
| 779.6 | -0.9926 | -0.9838 |
| 752.6 | -0.5439 | -0.7033 |

NOTE:
Common baseline data reduction used for the following groups of peaks:

a) 3090 - 2740 $cm^{-1}$
b) 1660 - 1630 $cm^{-1}$
c) 1280 - 1205 $cm^{-1}$

TABLE 39

CORRELATION OF IR PEAK HEIGHT AND PEEL.

IR OF PROPELLANT AT BOND INTERFACE

(TP-H8288 Propellant)

| Wave No., $cm^{-1}$ | Correlation Coefficient at Age Temperature 77°F | 100°F | 130°F | 165°F |
|---|---|---|---|---|
| 3069.7 | | | | -0.9368 |
| 2922.9 | | | 0.8690 | |
| 1737.4 | 0.9963 | | -0.7904 | |
| 1640.8 | | | 0.8174 | |
| 1420.7 | 0.8803 | | | |
| 1235.3 | | | 0.8619 | |
| 1219.9 | | | 0.8227 | |
| 965.0 | | | 0.8438 | |
| 910.9 | | | | -0.9770 |

NOTE:
Common baseline data reduction used for the following groups of peaks
a) 3090 - 2740 $cm^{-1}$
b) 1660 - 1630 $cm^{-1}$
c) 1280 - 1205 $cm^{-1}$

TABLE 40

CORRELATION OF IR PEAK HEIGHT AND ADHESION.

IR OF PROPELLANT AT BOND INTERFACE

(TP-H8288 Propellant)

| Wave No., $cm^{-1}$ | Correlation Coefficient at Age Temperature 77°F | 100°F | 130°F | 165°F |
|---|---|---|---|---|
| 3069.7 | | -0.8800 | | |
| 3007.9 | | 0.9103 | | |
| 2876.6 | -0.8844 | | | |
| 1590.6 | | | 0.9393 | |
| 1571.3 | | | 0.9838 | |
| 1532.7 | | 0.8357 | 0.8337 | |
| 1420.7 | | 0.8587 | | |
| 1351.2 | | | 0.8846 | |
| 1312.6 | | 0.8807 | 0.9305 | |
| 1266.2 | | 0.9249 | | |
| 1219.9 | | 0.8138 | | |
| 965.0 | | | | 0.8822 |
| 883.9 | | | 0.9163 | |
| 853.0 | | 0.8699 | 0.9728 | |
| 845.3 | | 0.9545 | | |
| 779.6 | | 0.8780 | | |
| 752.6 | | 0.8402 | | |

NOTE:
Common baseline data reduction used for the following groups of peaks:

a) 3090 - 2740 $cm^{-1}$
b) 1660 - 1630 $cm^{-1}$
c) 1280 - 1205 $cm^{-1}$

TABLE 41

CORRELATION OF IR PEAK HEIGHT AND PEEL
IR OF PROPELLANT 0.5 INCH FROM INTERFACE
(TP-H8288 Propellant)

| Wave No., $cm^{-1}$ | Correlation Coefficient at Age Temperature 77°F | 100°F | 130°F | 165°F |
|---|---|---|---|---|
| 1652.4 | | 0.8080 | | |
| 1640.8 | | | 0.8068 | |
| 1590.6 | -0.8308 | | | |
| 1061.6 | | | 0.9601 | |
| 725.6 | | -0.8982 | | |

TABLE 42

CORRELATION OF IR PEAK HEIGHT AND ADHESION
IR OF PROPELLANT 0.5 INCH FROM INTERFACE
(TP-H8288 Propellant)

| Wave No., $cm^{-1}$ | Correlation Coefficient at Age Temperature 77°F | 100°F | 130°F | 165°F |
|---|---|---|---|---|
| 3077.4 | | 0.8206 | | |
| 3007.6 | | 0.9436 | 0.9765 | |
| 2922.9 | | 0.9672 | 0.8507 | |
| 1590.6 | | | 0.9401 | |
| 1571.3 | | | 0.9121 | |
| 1532.7 | | 0.9668 | 0.9133 | |
| 1420.7 | | | -0.8651 | |
| 1351.2 | | 0.9129 | 0.9188 | |
| 1312.6 | | 0.9173 | 0.9131 | |
| 1266.2 | 0.8463 | 0.9904 | 0.9067 | 0.8350 |
| 1235.3 | | | | 0.9195 |
| 1219.9 | | 0.9109 | 0.8934 | |
| 965.0 | | | | 0.8617 |
| 910.9 | | | 0.8910 | 0.8829 |
| 883.9 | | | 0.8852 | |
| 853.0 | | 0.8955 | 0.9237 | |
| 845.3 | | 0.9791 | | |
| 779.6 | | 0.9222 | 0.8266 | |
| 752.6 | | 0.9304 | 0.9326 | |

NOTE:
Common baseline data reduction; used for the following groups of peaks:

a) 3090 - 2740 $cm^{-1}$
b) 1660 - 1630 $cm^{-1}$
c) 1280 - 1205 $cm^{-1}$

Following are our conclusions concerning the TP-H8288 bond system:

1) IR peak height changes correlate well with adhesion, but not well with peel.

2) Propellant remote from the bond interface correlates somewhat better than propellant at the interface. This may be caused by our inability to obtain propellant from precisely the same location in the interface region for all samples. Composition of propellant binder near the interface is highly dependent upon distance from the interface and as little as 0.1 mm (0.004 inch) may make a significant difference in the structure of the binder.

3) Propellant binder remote (13 mm; 0.5 inch) from the interface is of a more uniform composition and much less subject to drastic change with small changes in distance.

4) In the case of TP-H8288 propellant, adhesion is a better ordered measure of bond strength than is peel.

5) Bond strength as measured by peel and adhesion seems to be subject to uncontrolled variables and is a quality which does not show well-ordered variation with age time/temperature.

6) RDX covers up a great many of the binder peaks and so reduces the number of opportunities for finding correlations.

## Analysis of TP-Q7030 Data

### IR Data and Time/Temperature

Gel fraction of TP-Q7030 propellant was analyzed in the infrared using the techniques already described. A typical spectrum of this propellant is given in Figure . A review of the spectra in this series revealed to us that it would be advantageous to use the common baseline data reduction technique to improve the measurement of peak heights in certain areas of the spectrum. These areas are shown in Figure 55. Peaks of statistical significance for relating peak height change to bond property changes are those at a wave number of less than 1800 $cm^{-1}$. The 2500 to 3500 $cm^{-1}$ region contains only the peak that was used for normalization (2860 $cm^{-1}$) and one other peak (2930 $cm^{-1}$), which did not have a significant relationship to changes in bond properties.

Spectra were made [illegible] the gel fraction propellant taken at the liner interface and at 0.5 inch from the interface.

Correlations were made of the infrared spectra and time. Several peaks in the infrared spectra of the propellant gel fraction correlated quite well with time, indicating that these peaks were changing in a regular, predictable fashion. These correlations are revealed in Table 43. Taking the natural logarithm of the peak height and correlating that with changes in time did not significantly alter any of these correlations. These latter correlations are displayed in Table 44. In both of these tables, only those correlations where the coefficient was equal to or greater than 0.8 are listed.

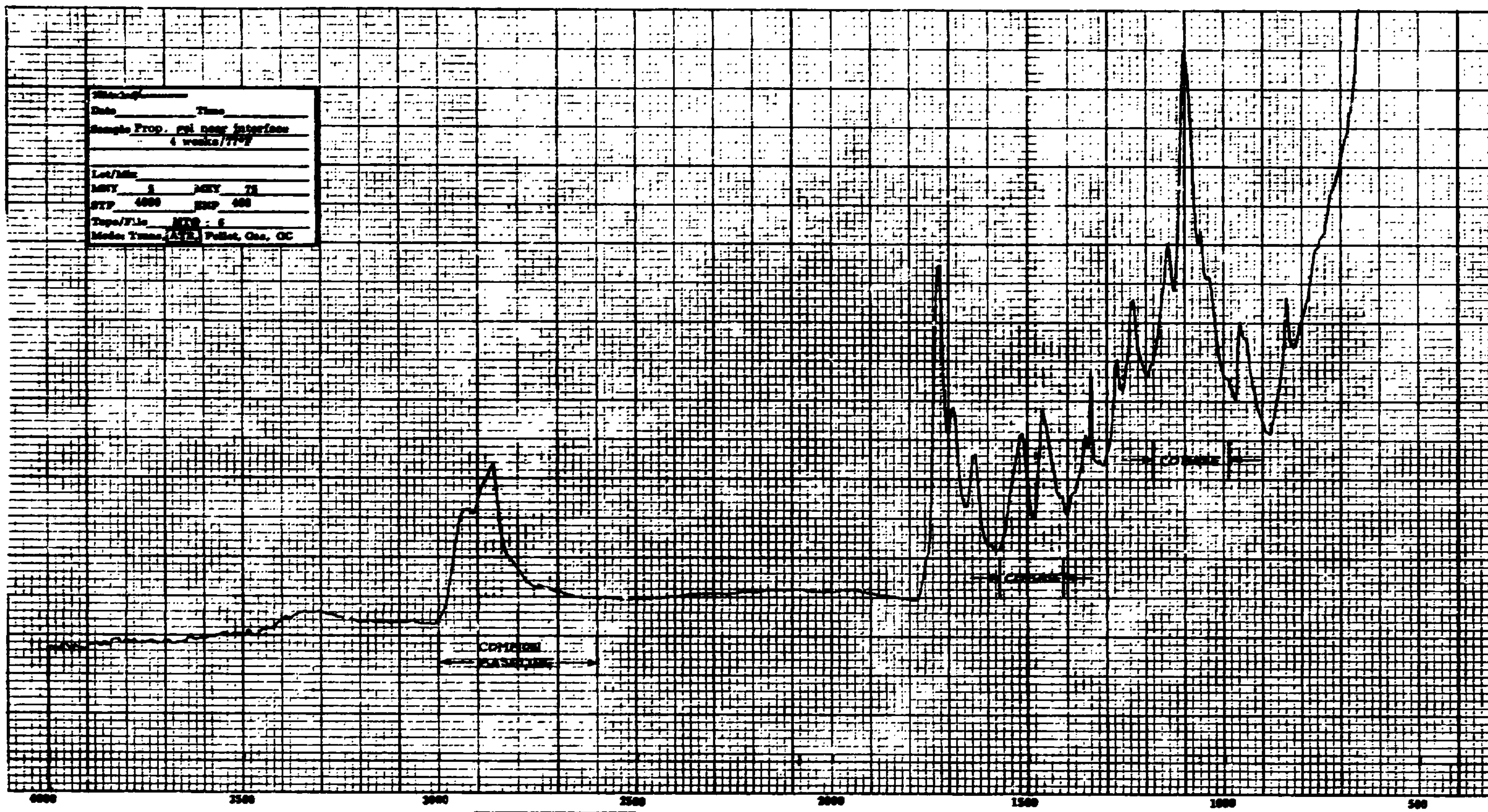


Figure 55. Infrared Spectrum of the Gel Fraction of TP-Q7030 Propellant (Mix X-27).

## TABLE 43

## CORRELATION OF IR PEAK HEIGHT AND TIME IR OF PROPELLANT 0.5 INCH FROM INTERFACE

(TP-Q7030 Propellant)

| WAVE NO., $cm^{-1}$ | Correlation Coefficient at Age Temperature | | | |
|---|---|---|---|---|
| | 77°F | 100°F | 130°F | 165°F |
| 1563.6 | | | -0.8228 | |
| 1343.5 | | | 0.8479 | -0.9942 |
| 1235.3 | | | | 0.8442 |
| 1146.5 | | | | -0.9125 |
| 841.4 | | -0.8727 | | |

## TABLE 44

## CORRELATION OF ln IR PEAK HEIGHT AND TIME IR OF PROPELLANT 0.5 INCH FROM INTERFACE

(TP-Q7030 Propellant)

| WAVE NO., $cm^{-1}$ | Correlation Coefficient at Age Temperature | | | |
|---|---|---|---|---|
| | 77°F | 100°F | 130°F | 165°F |
| 1563.6 | | | -0.9096 | |
| 1343.5 | | | 0.8447 | -0.9791 |
| 1235.3 | | | | 0.8455 |
| 1146.5 | | | | -0.9261 |
| 957.3 | | | | -0.8359 |
| 841.4 | | -0.8724 | | |

NOTE:
Common baseline data reduction used for the following groups of peaks:

a) 3000-2600 $cm^{-1}$
b) 1570-1410 $cm^{-1}$
c) 1180-985 $cm^{-1}$

Reaction rate constants were calculated for the changes in peak height with changes in time for peaks at all locations and computations were made where the 77°F data were included and where the 77°F aging data had been eliminated. Correlation of the reaction rate constant with the reciprocal of temperature is displayed in Table 45. These data are, in fact, the Arrhenius-type plot of change in reaction rate constant with change in temperature, where temperature is expressed as the reciprocal of the absolute reaction temperature (°K).

Identical computer runs were made using the spectra of the gel fraction of propellant taken at the interface. Correlation of the infrared peak heights of propellant from this location with time is given in Table 46. Again, only those correlation coefficients >0.8 are listed. As can be seen on that table, there are several very strong correlations for changes in IR peak height with time. Conversion of the peak height data to the natural logarithm does, of course, permit the calculation of the reaction rate constants; and these correlations are displayed in Table 47. Note that there are no changes in the peaks that correlate with time and only slight changes in the magnitude of the correlations. With the reaction rate constants having been calculated using the natural log of peak height and time, we then ran the correlation between these reaction rate constants and the reciprocal of absolute reaction temperature. These correlations are displayed in Table 48. There are strong correlations at 1563 $cm^{-1}$ where the 77°F data have been eliminated. Elimination of the 77°F data is a reasonable thing to do because the reactions occurring at that temperature are slow and time has been insufficient for the reaction to proceed far enough for an accurate measurement.

## IR Data and Bond Properties

Peel and adhesion data accumulated during the aging of the minimum smoke propellant bond samples were correlated with the infrared spectra of the gel fraction of propellant taken at the bond interface and from propellant taken approximately 0.5 inch from the interface. Correlation coefficients for changes in peak height with changes in peel strength for propellant from 0.5 inch from the interface are given in Table 49. Several very strong correlations were found which indicate that peel may be a function of the strength of the propellant and the strength of the propellant can be measured at a distance of 0.5 inch from the interface. Only correlation coefficients of a magnitude of 0.8 or higher are presented in that table.

Table 50 is a correlation of changes in infrared peak height and changes in bond adhesion using propellant taken 0.5 inch from the interface.

Turning now to correlations of infrared peak height changes for propellant taken at the interface and changes in peel and adhesion, we find that on Table 51 there are some very strong correlations here for peel. Table 52 reveals that there are some strong correlations for changes in peak height of propellant taken from the interface and adhesion. As with propellant taken at 0.5 inch from the interface, we find the propellant at the interface has greater number of correlations for the parameter peel than for the parameter adhesion.

## TABLE 45

## CORRELATION OF ln REACTION RATE CONSTANT AND 1/TEMPERATURE

(TP-Q7030 Propellant)

| WAVE NO., $cm^{-1}$ | 0.5 In. From Propellant/Liner Interface W/O 77°F Data | W/77°F Data |
|---|---|---|
| 1517.2 | -0.4768 | |
| 1467.0 | -0.9495 | |
| 957.3 | -0.9745 | |
| 841.4 | -0.1474 | -0.5786 |

## TABLE 46

## CORRELATION OF IR PEAK HEIGHT AND TIME. IR OF PROPELLANT AT THE INTERFACE

| WAVE NO., $cm^{-1}$ | Correlation Coefficient at Age Temperature | | | |
|---|---|---|---|---|
| | 77°F | 100°F | 130°F | 165°F |
| 1563.6 | | | -0.8854 | -0.8832 |
| 1517.2 | | | -0.8019 | -0.8832 |
| 1277.8 | | | | 0.8732 |
| 957.3 | | -0.9566 | | |
| 841.4 | | -0.9158 | | |

NOTE:
Common baseline data reduction used for the following groups of peaks:

a) 3000-2600 $cm^{-1}$
b) 1570-1410 $cm^{-1}$
c) 1180-985 $cm^{-1}$

TABLE 47

CORRELATION OF ln IR PEAK HEIGHT AND TIME.

IR OF PROPELLANT AT INTERFACE

(TP-Q7030 Propellant)

| WAVE NO., $cm^{-1}$ | Correlation Coefficient at Age Temperature | | | |
|---|---|---|---|---|
| | 77°F | 100°F | 130°F | 165°F |
| 1563.6 | | | -0.9051 | -0.8698 |
| 1517.2 | | | -0.8020 | -0.8876 |
| 1277.8 | | | | 0.8898 |
| 957.3 | | -0.9201 | | |
| 841.4 | | -0.9244 | | |

TABLE 48

CORRELATION OF ln REACTION RATE CONSTANT

AND 1/TEMPERATURE

(TP-Q7030 Propellant)

| WAVE NO., $cm^{-1}$ | At Propellant/Liner Interface | |
|---|---|---|
| | W/O 77°F Data | W/77°F Data |
| 1563.6 | -0.9211 | -0.5384 |
| 1416.8 | -0.7177 | |
| 1235.3 | -0.6196 | -0.5817 |

NOTE:
Common baseline data reduction used for the following groups of peaks:

a) 3000-2600 $cm^{-1}$
b) 1570-1410 $cm^{-1}$
c) 1180-985 $cm^{-1}$

TABLE 49

CORRELATION OF IR PEAK HEIGHT AND PEEL.

IR OF PROPELLANT AT 0.5 IN. FROM INTERFACE

(TP-Q7030)

| WAVE NO., $cm^{-1}$ | Correlation Coefficients at Age Temperature | | | |
|---|---|---|---|---|
| | 77°F | 100°F | 130°F | 165°F |
| 1517.2 | | -0.8221 | | |
| 1343.5 | -0.8711 | | -0.9046 | 0.8935 |
| 1235.3 | | | | -0.9617 |
| 1146.5 | | | | 0.8812 |
| 1104.0 | 0.9772 | | | |
| 1042.2 | 0.8147 | | | |
| 957.3 | | | | 0.8130 |
| 841.4 | | -0.9475 | | |

TABLE 50

CORRELATION OF IR PEAK HEIGHT AND ADHESION.

IR OF PROPELLANT 0.5 IN. FROM INTERFACE

(TP-Q7030)

| WAVE NO., $cm^{-1}$ | Correlation Coefficient at Age Temperature | | | |
|---|---|---|---|---|
| | 77°F | 100°F | 130°F | 165°F |
| 1691.0 | 0.8080 | | | 0.8873 |
| 1416.8 | | -0.9438 | | |
| 1104.0 | | -0.8376 | | |
| 1061.6 | 0.9023 | | | |
| 841.4 | | | | 0.8728 |

NOTE:
Common baseline data reduction used for the following groups of peaks:
a) 3000-2600 $cm^{-1}$
b) 1570-1410 $cm^{-1}$
c) 1180-985 $cm^{-1}$

## TABLE 51

## CORRELATION OF IR PEAK HEIGHT AND PEEL.

## IR OF PROPELLANT AT INTERFACE

(TP-Q7030)

| WAVE NO., $cm^{-1}$ | Correlation Coefficient at Age Temperature 77°F | 100°F | 130°F | 165°F |
|---|---|---|---|---|
| 1563.6 | | | | 0.8252 |
| 1517.2 | | | 0.8120 | |
| 1277.8 | | | | -0.9442 |
| 1235.3 | 0.9524 | | | -0.8874 |
| 1104.0 | 0.8671 | -0.8143 | | |
| 1061.6 | 0.9247 | -0.8638 | | -0.8237 |
| 1042.2 | 0.9289 | | | -0.8329 |
| 957.3 | | -0.9111 | | |
| 841.4 | | -0.9210 | | |

## TABLE 52

## CORRELATION OF IR PEAK HEIGHT AND ADHESION.

## IR OF PROPELLANT AT INTERFACE

(TP-Q7030)

| WAVE NO., $cm^{-1}$ | Correlation Coefficient at Age Temperature 77°F | 100°F | 130°F | 165°F |
|---|---|---|---|---|
| 1691.0 | 0.9128 | 0.8375 | -0.8507 | |
| 1416.8 | | -0.8704 | -0.8354 | |
| 1146.5 | | | 0.8396 | |
| 1104.0 | | | | 0.8398 |
| 841.4 | | | | 0.8946 |

NOTE:
Common baseline data reduction used for the following groups of peaks:

a) 3000-2600 $cm^{-1}$
b) 1570-1410 $cm^{-1}$
c) 1180-985 $cm^{-1}$

## Prediction of Bond Strength

Following is an illustration of how the computer programs written for this project can be used in a very practical manner. Correlations with propellant at the interface and peel strength were calculated for a peak at 1235 $cm^{-1}$. All IR data and all peel strengths were used, regardless of the time and temperature of aging, so that the result of this correlation is an equation which relates peel strength to peak height and says, if one knows the height of the peak at 1235 $cm^{-1}$, then one knows the peel strength for that bond system. The equation resulting from this correlation is:

$$\text{Peel Strength} = 55.10 - 1.736 \times (\text{Peak Height @ } 1235 \text{ cm}^{-1}) \qquad (1)$$

Correlation coefficient for this is -0.5618. This represents 21 observations, so that is an acceptable correlation coefficient. Continuing with the correlation, we correlated that peak height with time and came up with an equation representing the change in the height of the peak with time and so, if one knows time, then one may calculate what the height of the peak at 1235 $cm^{-1}$ can be expected to be. The equation is:

$$(\text{Peak Height @ } 1235 \text{ cm}^{-1}) = 17.47 \times 0.04887 \text{ (Age Time in Weeks)} \qquad (2)$$

Substituting equation (2) into equation (1) yields an equation for predicting peel strength based upon time, where the constant and coefficient for the equation are derived from infrared data such that

$$\text{Peel Strength} = 53.62 - 0.08482 \text{ (Age Time in Weeks)} \qquad (3)$$

A second, stronger correlation was found by using a combination of the peaks at 1235 $cm^{-1}$ and 1563 $cm^{-1}$. Using the heights of the peaks at these two locations and the equation (4), given below, one can compute the peel strength of the propellant/liner bond.

$$\text{Peel Strength} = 42.82 + 3.863 \text{ (Pk. Hght. @ 1563)} - 1.439 \text{ (Pk. Hght. @ 1235)} \qquad (4)$$

Here, the correlation coefficient is 0.6569, which is significant at the 99% level. These data are plotted in Figure 56. With this equation, the standard error of estimating peel strength is 7.4 pli.

An Arrhenius equation for prediction of properties was made. Making this prediction of properties requires the following:

a) Peak height versus property (where the data are independent of age time and temperature).

b) In peak height versus time [at several aging temperatures, and the peak must be the same as in (a)].

c) From (b), calculate the reaction rate constants ($K_1$) at each of the aging temperatures.

d) From (c), calculate the energy of activation for that reaction.

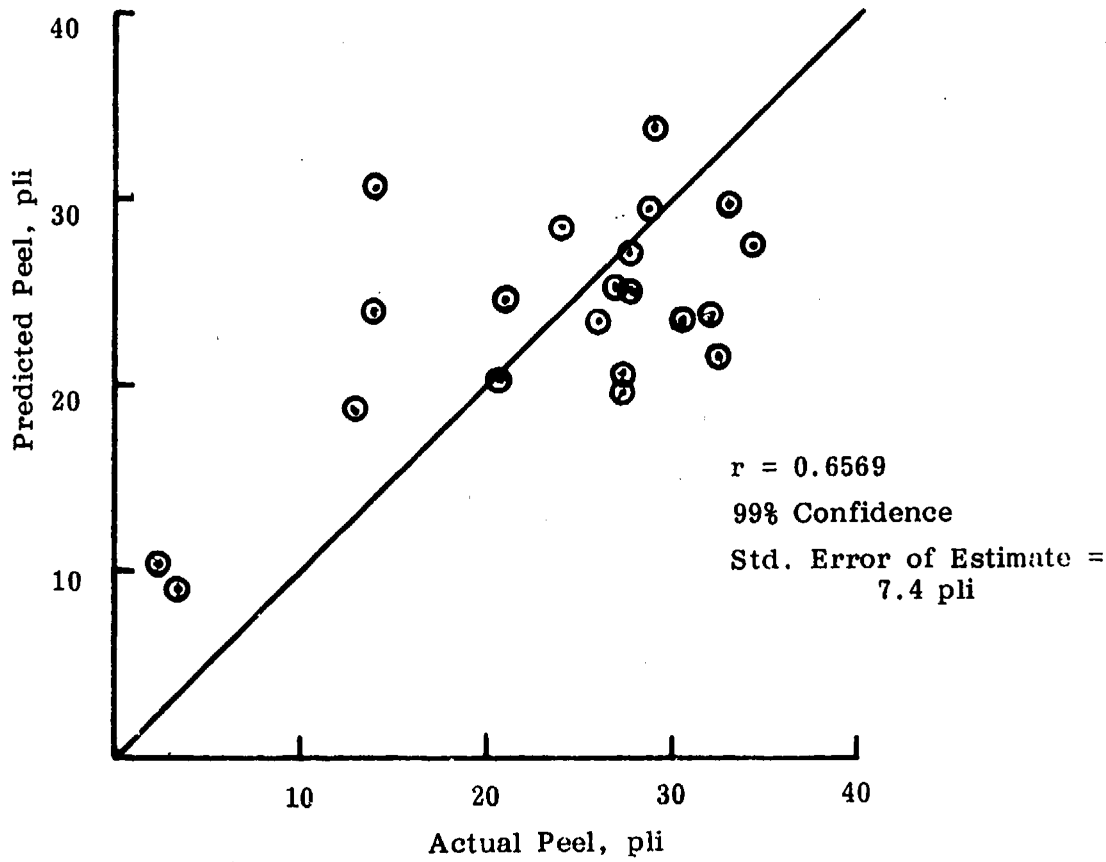


Figure 56 . Peel Strength as Identified from Peaks at 1563 and 1235 $cm^{-1}$.

e) From reaction rate constants, activation energy, compute a reaction rate constant for a selected aging temperature at which the prediction is desired. (This is the Arrhenius equation.)

f) Using the reaction rate constant ($K_1$), calculated in (e) and the coefficients in the $K_1$/log peak height relationship, then calculate the peak height at the selected aging time.

g) Using the peak height data from (f) and coefficients from the equation in (a), then calculate the value of the property at the selected age temperature and at some discrete time in the future. The computer program also will compute the property value at discrete time intervals up to a maximum of the selected time, whatever that time might be.

In making this prediction, as displayed in Table 53, information given to the computer included the starting time for the aging and the starting peak heights of the one or more peaks in question; in this case, the heights of the peaks at 1563 $cm^{-1}$ and 1235 $cm^{-1}$. Peak heights at 16 weeks of aging at 100°F were given and the computer program then proceeded to compute the peel strength of the propellant/liner bond at that particular time. The computer calculated that peel strength would be 25.24 pli. It was actually 26.9 pli at that time. Aging at 100°F proceeded through the full 32-week time period, which is 16 weeks from the start given in Table 53. At 16 weeks of aging, the computer calculated the peel would be 25.38; the actual peel strength at 32 weeks for 100°F aging was 32.6 pli. This is a reasonably good prediction of peel. Using the multiple correlation equation given as equation (4), the peel strength calculated from that for this 32-week aging at 100°F would be 21.5 pli. The prediction of peel strength from the Arrhenius equation is considerably more accurate than prediction of peel strength based solely upon IR data and its relationship with changes in mechanical properties. IR data, of course, used in the computation of reaction rate constant and reaction rate constants are, in turn, used in the computation of activation energy for the Arrhenius equation. But, by having activation energy calculated from more than one reaction rate constant, some of the variation in the IR data are eliminated, resulting in a more accurate prediction of peel strength. Overall, it can be said that the prediction is accurate, the computer program works, and the FTIS technique is applicable to the measurement of bond strength and to the prediction of bond strength.

## Analysis of MSL-303 Propellant Data

### Mechanical Properties and Time/Temperature

MSL-303 propellant was being aged in a separate project* and that aging had proceeded through 18 months when the infrared data accumulated during that aging were subjected to the analysis procedures and programs developed on the FTIS project and the Bondline Infrared Spectroscopy project. Aging temperatures for the MSL-303 propellant were 75°, 110°, 130°, 150°, 170°, and 190°F. Mechanical property data for the aging are displayed in Table 54.

*U. S. Army Missile Command, Contract DAAH01-82-C-A198.

TABLE 53

PREDICTED PEEL STRENGTH FOR 100°F AGING

(TP-Q7030 Propellant)

| TIME, Weeks | PROPERTY | IR PEAK | IR PEAK |
|---|---|---|---|
| 0.00 | 25.24 | 2.125 | 17.92 |
| 2.74 | 25.22 | 2.004 | 17.61 |
| 5.47 | 25.22 | 1.890 | 17.31 |
| 8.21 | 25.23 | 1.782 | 17.01 |
| 10.95 | 25.27 | 1.681 | 16.71 |
| 13.68 | 25.31 | 1.585 | 16.42 |
| 16.42 | 25.38 | 1.495 | 16.14 |
| 19.16 | 25.45 | 1.410 | 15.86 |
| 21.89 | 25.53 | 1.329 | 15.58 |
| 24.63 | 25.63 | 1.254 | 15.31 |
| 27.37 | 25.74 | 1.182 | 15.05 |
| 30.11 | 25.85 | 1.115 | 14.78 |
| 32.84 | 25.98 | 1.052 | 14.53 |
| 35.58 | 26.11 | .9917 | 14.28 |
| 38.32 | 26.24 | .9352 | 14.03 |
| 41.05 | 26.39 | .8820 | 13.79 |
| 43.79 | 26.54 | .8318 | 13.55 |
| 46.53 | 26.69 | .7844 | 13.31 |
| 49.26 | 26.85 | .7398 | 13.08 |
| 52.00 | 27.02 | .6976 | 12.85 |

TABLE 54

MSL-303 PROPELLANT - PERSHING P1a

| Aging Temp. (°F) | Property | Age Time, Months 0 | ½ | 1 | 2 | 3 | 6 | 12 | 18 |
|---|---|---|---|---|---|---|---|---|---|
| 75 | Max Stress, psi | 219.8 | 203.5 | 208.9 | 219.9 | 221.5 | 223.7 | 223.1 | 214.2 |
| | Strain @ Max Stress, % | 47.2 | 48.0 | 49.2 | 42.2 | 47.8 | 45.9 | 50.5 | 44.9 |
| | Ultimate Strain, % | 49.9 | 51.2 | 52.8 | 44.6 | 49.7 | 48.0 | 54.6 | 49.8 |
| | Modulus, psi | 1025.0 | 950.0 | 980.0 | 1027.0 | 1105.0 | 1038.0 | 937.0 | 1112.0 |
| 110 | Max Stress, psi | | 208.0 | 207.4 | 208.4 | 199.5 | 214.7 | 203.7 | 223.3 |
| | Strain @ Max Stress, % | | 49.6 | 52.1 | 48.4 | 48.9 | 47.3 | 49.0 | 46.6 |
| | Ultimate Strain, % | | 53.9 | 56.6 | 53.7 | 53.4 | 51.6 | 53.5 | 49.5 |
| | Modulus, psi | | 934.0 | 876.0 | 1016.0 | 926.0 | 950.0 | 950.0 | 1115.0 |
| 130 | Max Stress, psi | | 207.2 | 197.6 | 206.0 | 187.9 | 186.0 | 184.2 | 177.2 |
| | Strain @ Max Stress, % | | 51.5 | 50.6 | 51.3 | 54.0 | 49.5 | 50.7 | 54.1 |
| | Ultimate Strain, % | | 53.8 | 55.1 | 56.2 | 58.9 | 56.0 | 55.6 | 59.6 |
| | Modulus, psi | | 990.0 | 886.0 | 890.0 | 782.0 | 898.0 | 851.0 | 882.0 |
| 150 | Max Stress, psi | | 179.5 | 195.5 | 189.0 | 188.9 | 166.5 | 164.2 | 163.5 |
| | Strain @ Max Stress, % | | 50.2 | 55.1 | 52.2 | 52.5 | 56.4 | 47.4 | 48.5 |
| | Ultimate Strain, % | | 55.0 | 58.1 | 57.7 | 58.4 | 63.4 | 50.2 | 53.8 |
| | Modulus, psi | | 783.0 | 838.0 | 906.0 | 825.0 | 801.0 | 926.0 | 825.0 |
| 170 | Max Stress, psi | | 180.2 | 181.4 | 183.0 | 162.7 | 169.7 | 171.3 | 168.3 |
| | Strain @ Max Stress, % | | 53.4 | 54.1 | 54.9 | 49.4 | 49.1 | 46.5 | 40.6 |
| | Ultimate Strain, % | | 58.2 | 60.7 | 57.4 | 54.8 | 56.7 | 53.0 | 47.8 |
| | Modulus, psi | | 699.0 | 760.0 | 779.0 | 725.0 | 804.0 | 960.0 | 923.0 |
| 190 | Max Stress, psi | | 160.7 | 154.6 | 160.5 | 146.3 | 166.4 | 155.9 | 157.8 |
| | Strain @ Max Stress, % | | 55.9 | 47.7 | 50.7 | 32.9 | 36.8 | 35.0 | 20.2 |
| | Ultimate Strain, % | | 63.0 | 55.7 | 55.1 | 41.7 | 41.6 | 41.2 | 24.8 |
| | Modulus, psi | | 660.0 | 766.0 | 791.0 | 773.0 | 1004.0 | 858.0 | 1216.0 |

Plots of propellant modulus, strain at maximum stress, and maximum stress are shown in Figures 57, 58, and 59. These plots reveal that there is considerable scatter in the modulus data and in the stress data. The scatter is not as severe in the strain at max. stress data, but, nevertheless, only at elevated temperature does the strain at max. stress follow a trend that would permit a logical prediction of mechanical properties of the propellant based upon past aging experience.

IR Data and Time

Infrared spectra of the propellant were taken at each time/temperature test interval and the IR data stored on magnetic tape. Procedures used in accumulating the IR data were those that had been identified at the end of the FTIS project which are not exactly the same as used in the Bondline Infrared Spectroscopy project. However, the IR data are very good and do lend themselves to a good statistical analysis.

An infrared spectrum of MSL-303 propellant aged at 0 time is presented in Figure 60. This spectrum is typical of the spectra of HTPB family of propellants wherein ammonium perchlorate is used as the oxidizer. The strong ammonium perchlorate peaks occur near 3300, 1400, and 1000 wave numbers. These peaks are identified on Figure 60. Binder peaks in the HTPB propellant are those that remain and are unmarked on the figure. It was these binder peaks that were subjected to the rigorous infrared statistical analysis. Correlation of all IR peak heights with time and age temperature (see Table 55) revealed that there were a large number of peaks that were responding in an orderly fashion to changes in age at the various age temperatures. Some of these correlations indicate peak growth, some indicate peak decrease; they are shown by positive and negative correlations, respectively.

Taking the natural log of peak height and correlating it with time resulted in only minor changes in the correlation coefficients and those are displayed in Table 56. In this table, and in Table 55, only those correlation coefficients higher than 0.8 are listed.

The natural log of peak height at 911.5 $cm^{-1}$ and its variation with time and temperature are tabulated in Table 57. Reaction rate constants (for a first order reaction) were calculated for the reaction occurring at each age temperature that would have caused the change in the peak height at 911 $cm^{-1}$. This reaction rate constant is the slope of the line of a plot of natural log IR peak height versus time. These plots are shown in Figures 61 through 63 for the various aging temperatures.

Activation energy for this reaction can be calculated using the Arrhenius equation and the computer program previously described. Activation energy, when one includes all of the aging data, is -177.5 (given at the bottom of Table 57. However, since the 190°F aging data appear not to follow the same route as aging at the other five temperatures, these 190°F aging data were taken out of the correlation, and the activation energy then became 1059. If the 75°F aging data are also eliminated from consideration, then the activation energy is

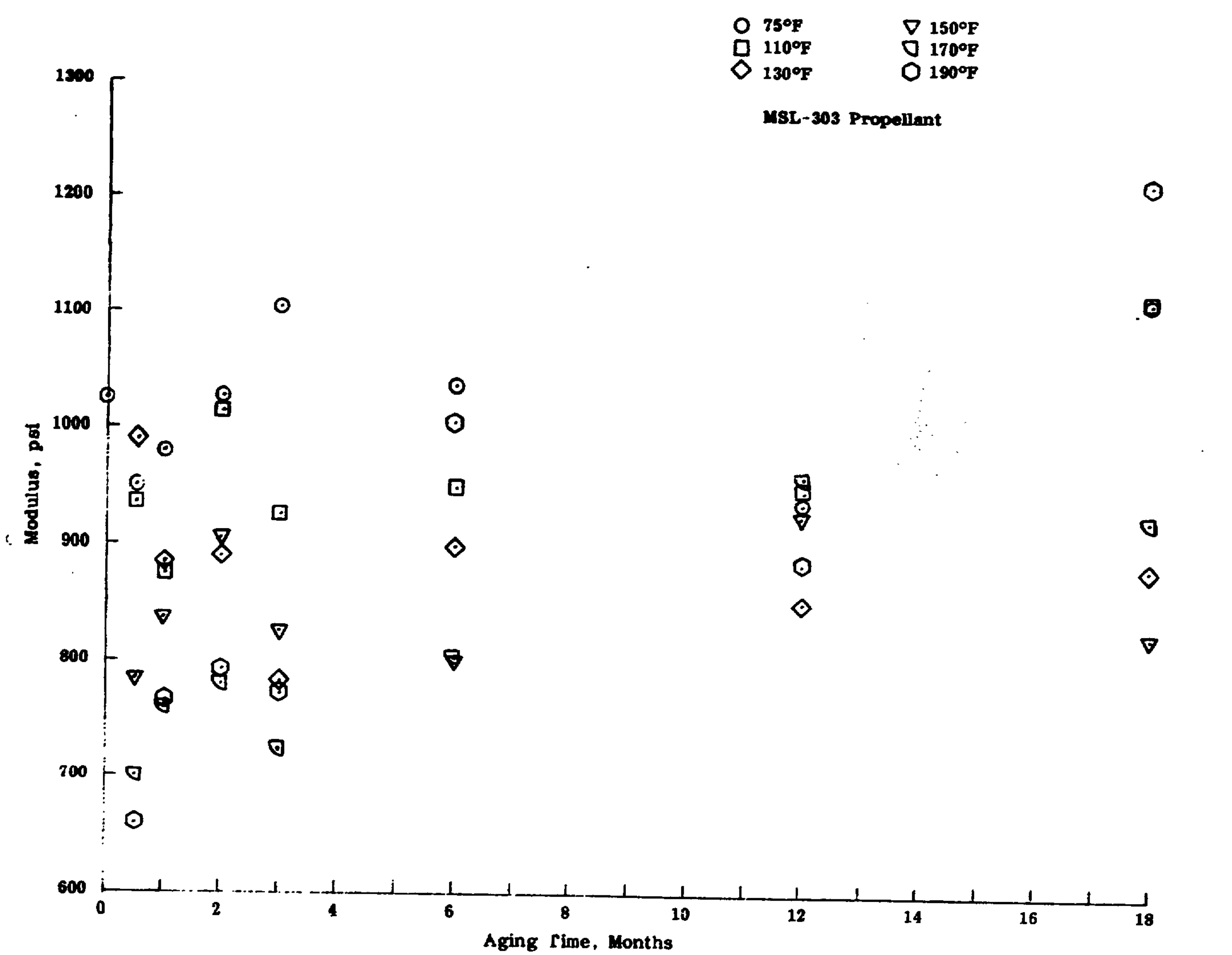


Figure 57. Variation in Modulus with Age Time (MSL-303).

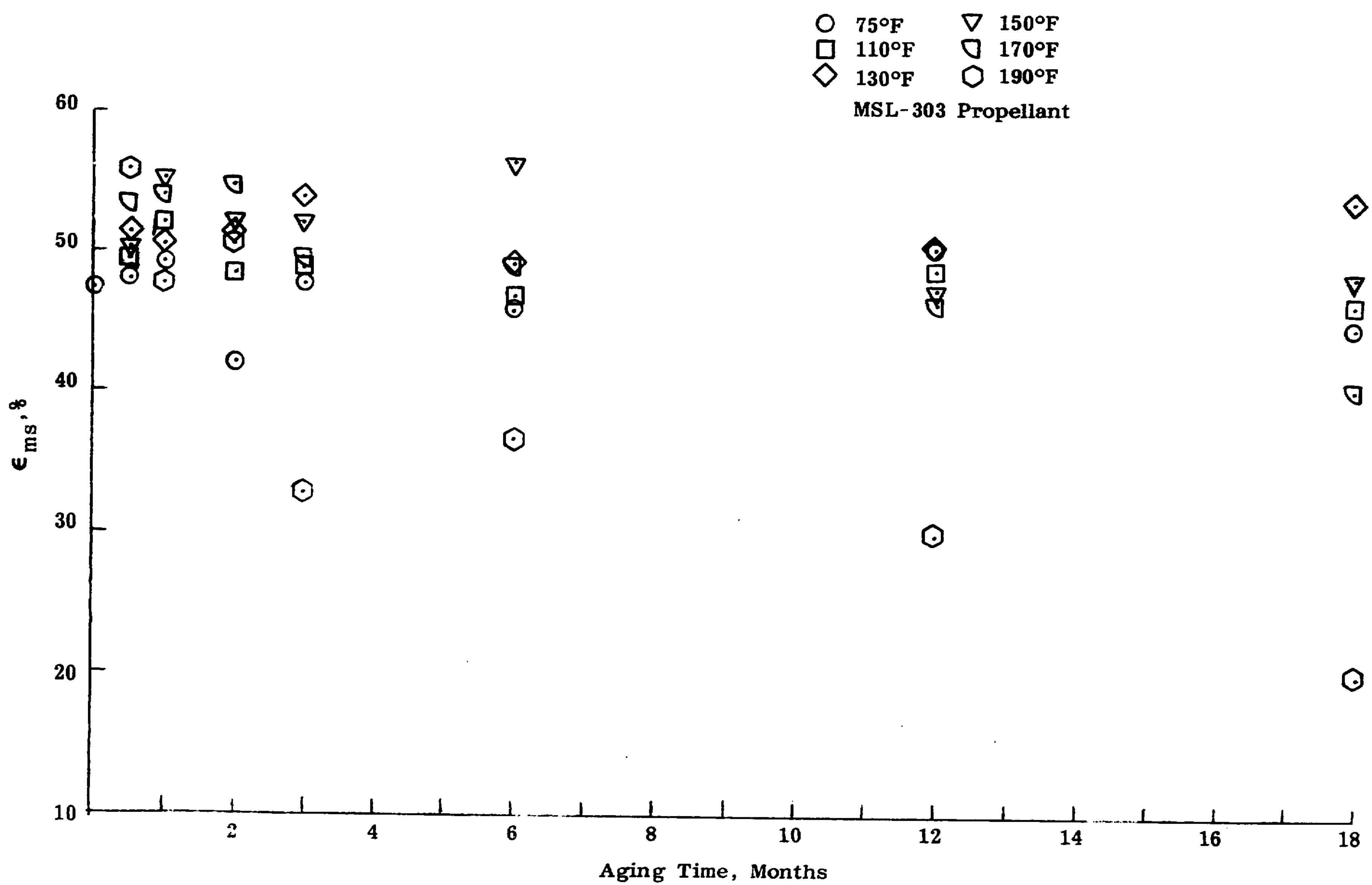


Figure 58. Variation in Strain at Max. Stress with Age Time (MSL-303).

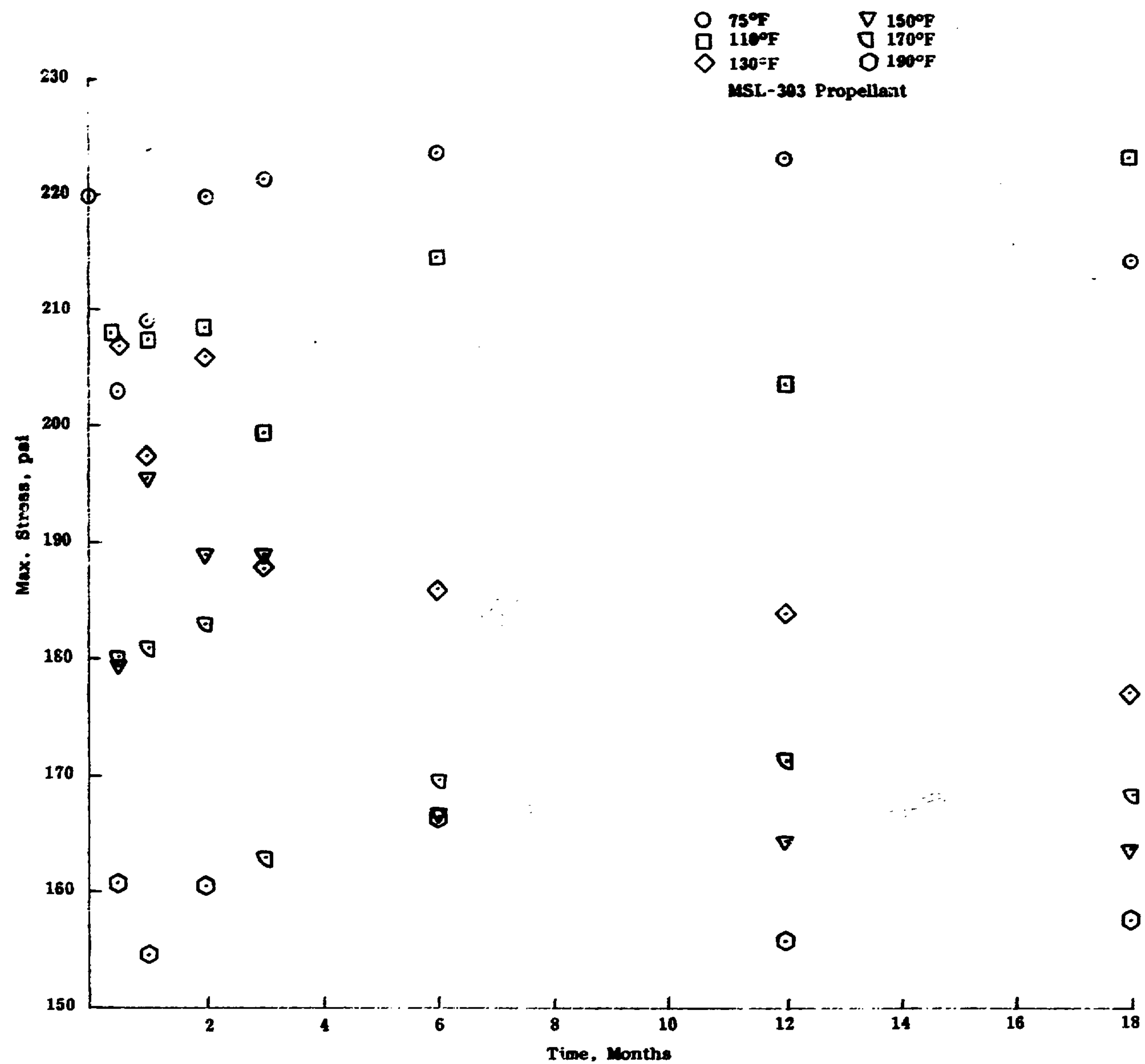


Figure 59. Variation in Max. Stress with Age Temperature (MSL-303).

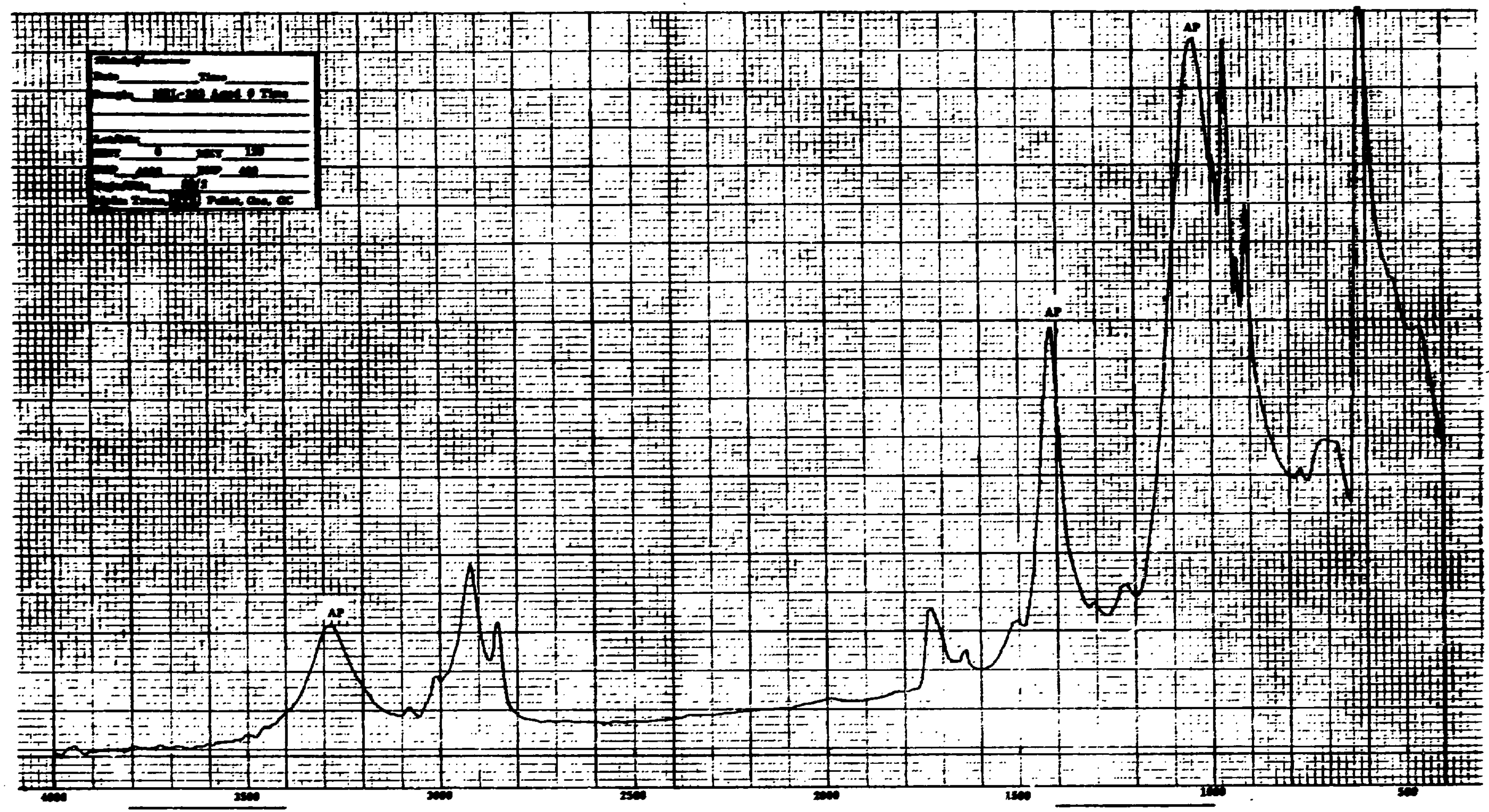


Figure 60. IR Spectrum of MSL-303 Propellant at Zero Age Time.

TABLE 55

CORRELATION OF IR PEAK HEIGHT AND TIME

(MSL-303 Propellant)

| Wave No., $cm^{-1}$ | Correlation Coefficient at Age Temperature | | | | | |
|---|---|---|---|---|---|---|
| | 75°F | 110°F | 130°F | 150°F | 170°F | 190°F |
| 3084.1 | -0.9519 | -0.9153 | -0.9463 | | | -0.9684 |
| 3014.5 | 0.9350 | 0.9335 | 0.8785 | | | 0.8732 |
| 2921.8 | -0.9170 | -0.8858 | -0.8015 | -0.8241 | -o.8324 | -0.8917 |
| 2736.2 | | | | 0.8286 | 0.8697 | |
| 1731.1 | -0.9643 | -0.8437 | -0.9021 | -0.9179 | -0.9538 | -0.9044 |
| 1305.8 | | 0.9329 | 0.9404 | | | 0.9232 |
| 1228.5 | -0.9133 | -0.8094 | | 0.9036 | -0.8605 | -0.8821 |
| 965.6 | -0.8194 | -0.9176 | -0.8172 | -0.9450 | -0.8551 | |
| 911.5 | -0.8609 | -0.9393 | -0.9016 | -0.9289 | -0.9117 | -0.8103 |
| 772.3 | | -0.8361 | -0.8350 | -0.8203 | -0.8879 | |
| 718.2 | | | | -0.8667 | | |

TABLE 56

CORRELATION OF ln IR PEAK HEIGHT AND TIME

(MSL-303 Propellant)

| Wave No., $cm^{-1}$ | Correlation Coefficient at Age Temperature | | | | | |
|---|---|---|---|---|---|---|
| | 75°F | 110°F | 130°F | 150°F | 170°F | 190°F |
| 3084.1 | -0.9556 | -0.9191 | -0.9501 | | | -0.9710 |
| 3014.5 | 0.9347 | 0.9307 | 0.8892 | | | 0.8773 |
| 2921.8 | -0.9155 | -0.8799 | | -0.8136 | -0.8226 | -0.8859 |
| 1731.1 | -0.9638 | -0.8388 | -0.8997 | -0.9196 | -0.9552 | -0.9116 |
| 1305.8 | | 0.9188 | 0.9367 | | | 0.9125 |
| 1228.5 | -0.9309 | -0.8114 | | -0.9006 | -0.8458 | -0.9036 |
| 965.6 | -0.8292 | -0.9411 | -0.8284 | -0.9474 | -0.8782 | |
| 911.5 | -0.8384 | -0.9276 | -0.9074 | -0.9236 | -0.9250 | -0.8016 |
| 772.3 | | -0.8681 | -0.8330 | -0.8263 | -0.8951 | |

## TABLE 57

### ln HEIGHT OF IR PEAK AT 911.5 $cm^{-1}$ AND ITS VARIATION WITH TIME AND TEMPERATURE

(MSL-303 Propellant)

| | Aging Temperature, °F | | | | | |
|---|---|---|---|---|---|---|
| Time, Mo. | 75 | 110 | 130 | 150 | 170 | 190 |
| 0 | 27.219 | | | | | |
| .5 | 26.629 | 28.275 | 28.209 | 30.018 | 27.064 | 29.357 |
| 1 | 28.457 | 27.483 | 28.579 | 29.786 | 26.669 | 22.176 |
| 2 | 26.165 | 27.811 | 27.011 | 30.219 | 28.568 | 26.912 |
| 3 | 28.729 | 29.598 | 28.546 | 28.083 | 29.154 | 29.759 |
| 6 | 28.201 | 25.443 | 29.749 | 29.200 | 28.449 | 24.757 |
| 12 | 9.871 | 11.783 | 10.932 | 11.139 | 10.430 | 12.023 |
| 18 | 13.689 | 11.851 | 11.338 | 11.665 | 9.636 | 16.002 |
| Correl. Coefficient | -0.8384 | -0.9376 | -0.9074 | -0.9236 | -0.9250 | -0.8016 |
| Reaction Rate Constant, $K_1$ | 0.05320 | 0.05950 | 0.06311 | 0.06507 | 0.07052 | 0.04144 |

| | | |
|---|---|---|
| Activation Energy, | All Data | -177.5 |
| | W/O 190°F | 1059 |
| | W/O 190°F & 75°F | 1066 |

## TABLE 58

### CORRELATION OF ln REACTION RATE CONSTANT ($K_1$) AND 1/TEMPERATURE

(MSL-303 Propellant)

| | Correlation Coefficient | | | |
|---|---|---|---|---|
| Wave No., $cm^{-1}$ | All Data | W/O 190°F Data | W/O 190°F & 75°F Data | Activation Energy W/O 190°F Data |
| 3084.1 | 0.2537 | 0.8143 | 0.4199 | -3952.9 |
| 3014.5 | 0.6830 | 0.9621 | 0.9953 | -2289.7 |
| 2921.8 | 0.6110 | 0.6873 | 0.4193 | -615.45 |
| 1731.1 | -0.4279 | -0.9359 | -0.7975 | 1941.4 |
| 1228.5 | -0.1274 | 0.8115 | 0.3159 | -1010.6 |
| 965.6 | 0.2218 | -0.8610 | -0.8156 | 1121.6 |
| 911.5 | 0.1018 | -0.9945 | -0.9834 | 1058.5 |
| 772.3 | | -0.7142 | 0.7796 | 6742.3 |

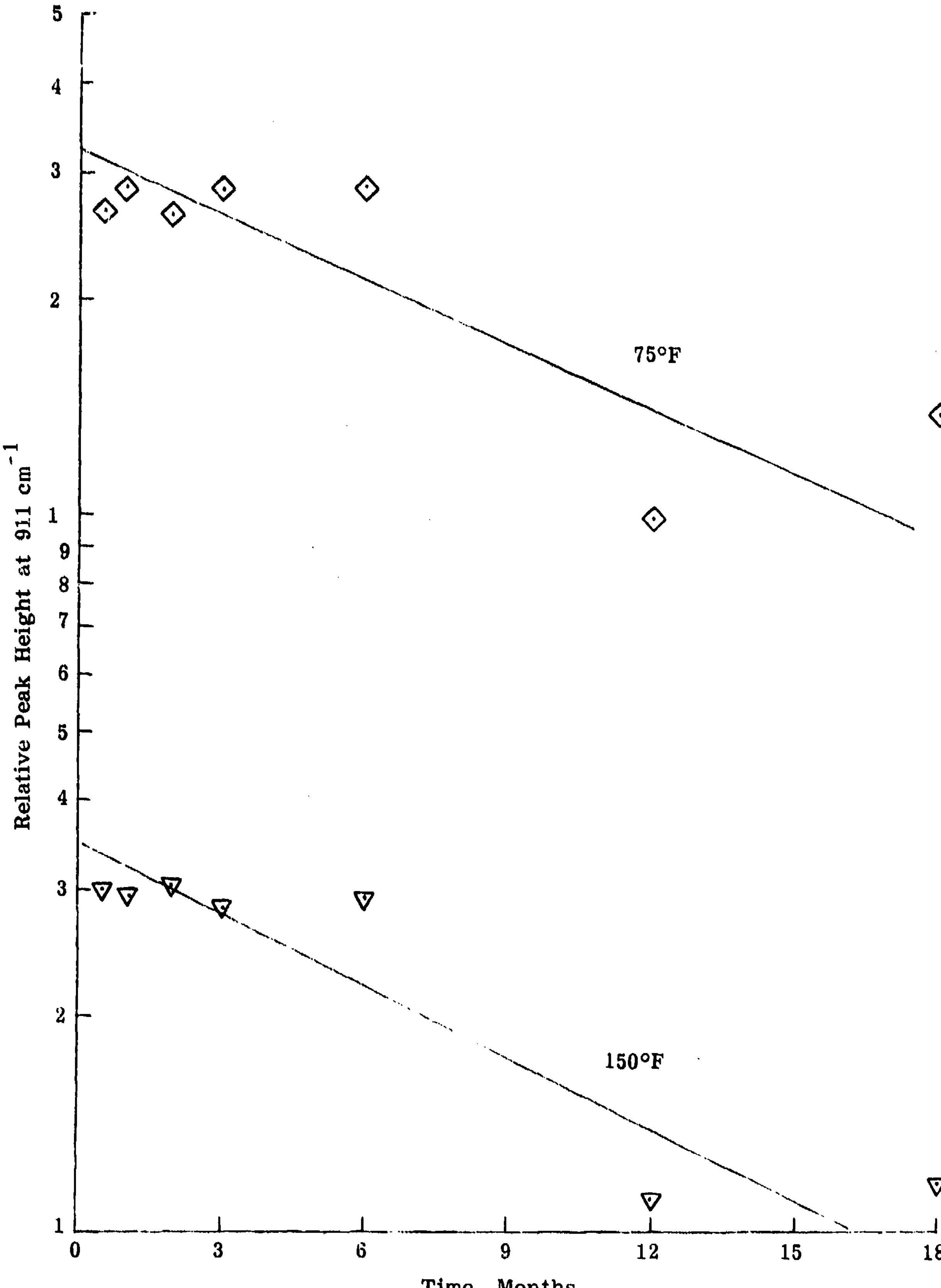


Figure 61. Variation in 911 $cm^{-1}$ Peak Height with Age Time at 75° and 150°F (MSL-303 Propellant)

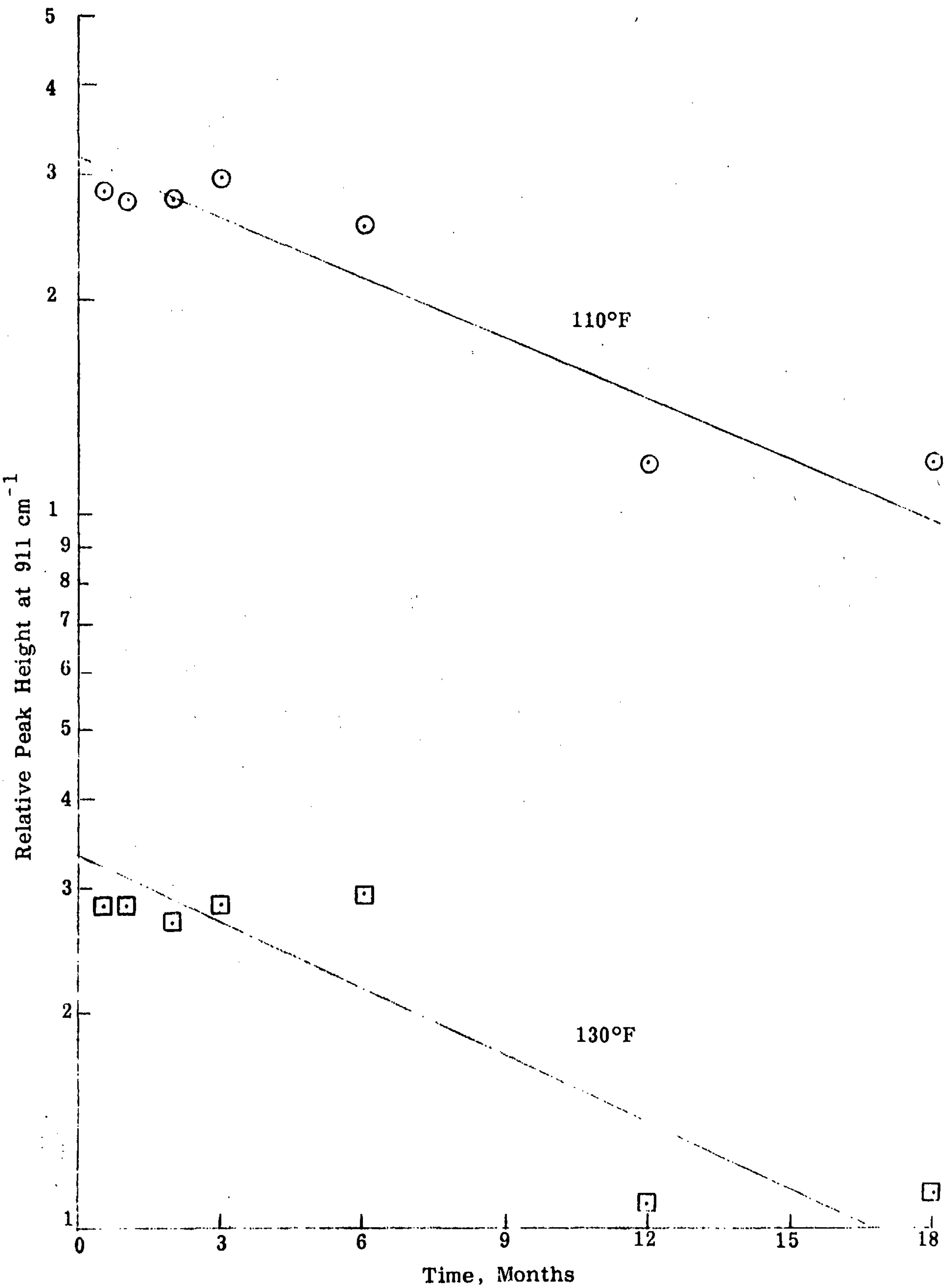


Figure 62. Variation in 911 $cm^{-1}$ Peak Height with Age Time at 110° and 130°F. (MSL-303 Propellant)

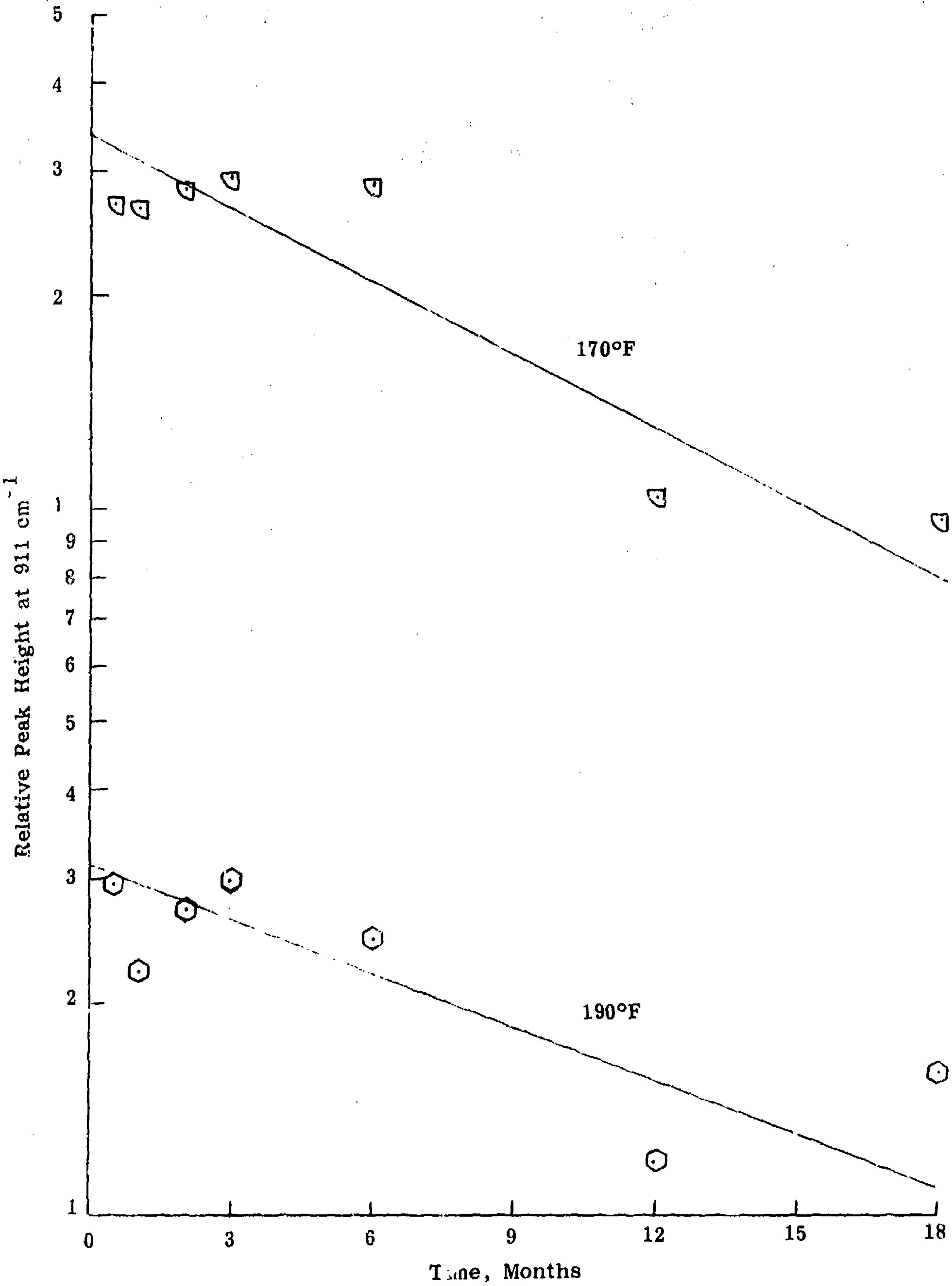


Figure 63. Variation in 911 $cm^{-1}$ Peak Height with Age Time at 170° and 190°F (MSL-303 Propellant)

1066...not much of a change. An activation energy plot of natural log reaction rate constant versus the reciprocal of absolute temperature (Figure 64) reveals why the 190°F data were eliminated from computation of activation energy. That 190°F data point is far from the line describing the other five reaction temperatures. Correlation coefficient for the correlation of reaction rate constant with the reciprocal of reaction temperature where all data are included is 0.1018; where the 190°F data are eliminated, then the correlation coefficient becomes -0.9945.

Correlation coefficients were calculated for the natural log reaction rate constant ($K_1$) and the reciprocal of the absolute reaction temperature. These data are displayed in Table 58. They show also that, where the 190°F aging data is eliminated, the correlations are all considerably enhanced.

Activation energy plots were prepared for others of the wave numbers shown in Table 58. Specifically, activation energy plots were made for 3014, 1638, 1506, and 965 $cm^{-1}$. These plots are shown in Appendix E.

IR Data and Mechanical Properties

Correlating IR peak height changes with propellant mechanical property changes did not reveal any strong correlations. This was totally expected when we realized that the IR peaks were correlating quite well with time, but that the mechanical properties of the propellant did not correlate with time or temperature in any way whatsoever. Under these conditions, IR peak height changes could not correlate strongly with propellant properties. Those correlations which were found are displayed in Table 59. Only those correlations where the coefficient was $\geq 0.8$ are listed.

With this total lack of correlation, it became of interest to see if the mechanical property data were smoothed such that they displayed a uniform response to time at a given temperature, would they then correlate well with IR changes. To that end, plots were made of strain at Max. stress and max. stress versus linear and log time. These data plots are given in Appendix E.

These smoothed mechanical property data were then correlated with changes in IR peak height and the results of that correlation for propellant stress are displayed in Table 60 and for correlations with strain at max. stress in Table 61. A review of those data reveals some very strong correlations between peak height changes and mechanical property mixes which confirms the fact that where mechanical property data are following a logical progression with time, the mechanical property changes can be identified by changes in the infrared spectra of the propellant. A typical plot of change in peak height is represented in Figure 65, where there is a plot of maximum stress versus relative peak height at 911 $cm^{-1}$. This plot is for two temperatures, 130° and 150°F. Correlation coefficients at both temperatures are exceedingly strong.

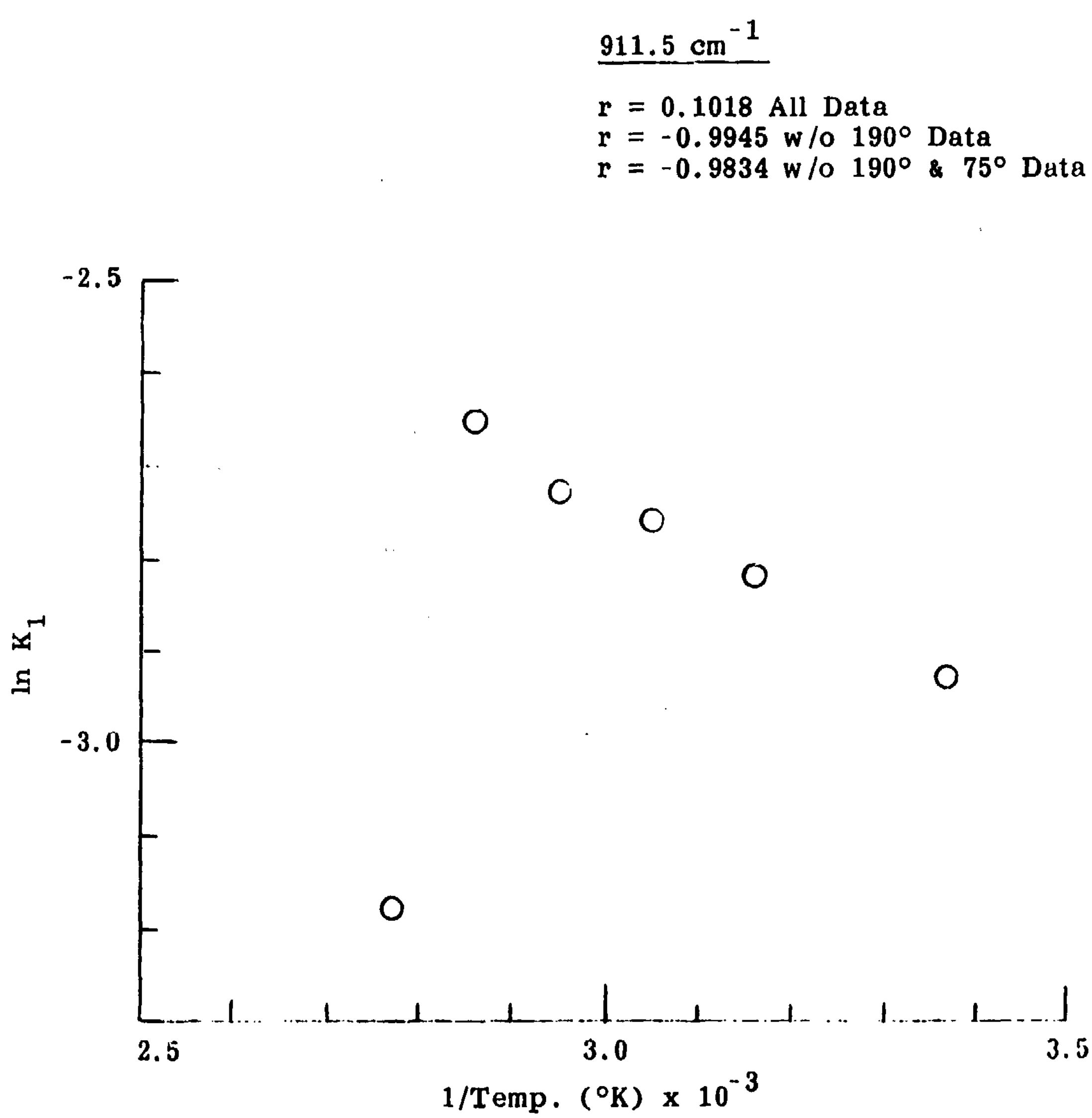


Figure 64. Activation Energy Plot for the Peak at 911 $cm^{-1}$.

TABLE 59

## CORRELATION OF IR PEAK HEIGHT AND PROPELLANT MODULUS, MAX. STRESS, AND STRAIN AT MAX. STRESS

(MSL-303)

| Wave No., cm$^{-1}$ | Correlation Coefficient at Age Temperature 75°F | 110°F | 130°F | 150°F | 170°F | 190°F |
|---|---|---|---|---|---|---|
| **MAX. STRESS** | | | | | | |
| 2736.2 | | | | -0.7934 | | |
| 1731.1 | | | 0.8632 | | | |
| **STRAIN AT MAX. STRESS** | | | | | | |
| 2921.8 | | | | 0.8035 | | |
| 2736.2 | | | | | -0.8820 | |
| 1731.1 | | | | | 0.8989 | |
| 1228.5 | | | | 0.7959 | | |
| 911.5 | | | | | 0.8114 | |
| 772.3 | | | | | 0.8941 | |
| **MODULUS** | | | | | | |
| 3084.1 | | | | | -0.9125 | |
| 3014.5 | | | | | 0.8482 | |
| 2921.8 | | | | | -0.9166 | |
| 1731.1 | | | | | -0.9503 | 0.7953 |
| 1228.5 | | | | | -0.9281 | |
| 965.6 | | | | | 0.8787 | |
| 911.5 | | | | | -0.9149 | |
| 772.3 | | | | | -0.8178 | |
| 718.2 | | | | | -0.8452 | |

## TABLE 60

## CORRELATION OF IR PEAK HEIGHT AND PROPELLANT STRESS

(MSL-303 Propellant)

| Wave No., $cm^{-1}$ | Correlation Coefficient 130°F | Correlation Coefficient 150°F | |
|---|---|---|---|
| 3084.1 | 0.8521 | | |
| 1731.1 | 0.9177 | 0.9684 | |
| 1414.1 | | 0.8578 | |
| 1305.8 | -0.8536 | | |
| 1228.5 | | 0.8602 | |
| 1042.9 | -0.8711 | | Correlations based on stress values read from a plot of stress versus log time. |
| 965.6 | | 0.8851 | |
| 934.7 | 0.8267 | 0.8334 | |
| 911.5 | 0.8068 | 0.8569 | |
| 772.3 | | 0.8049 | |
| 718.2 | | 0.8560 | |
| | | | |
| 3084.1 | 0.9475 | | |
| 3014.5 | -0.8771 | | |
| 2921.8 | 0.8042 | 0.8250 | |
| 2736.2 | | -0.8320 | |
| 1731.1 | 0.9036 | 0.9134 | |
| 1305.8 | -0.9415 | | |
| 1228.5 | | 0.9024 | |
| 1042.9 | -0.8795 | | Correlations based on stress values read from a plot of stress versus time. |
| 965.6 | 0.8187 | 0.9457 | |
| 934.7 | 0.9048 | 0.9264 | |
| 911.5 | 0.9031 | 0.9303 | |
| 772.3 | 0.8334 | 0.8244 | |
| 718 | | 0.8658 | |

TABLE 61

## CORRELATION OF IR PEAK HEIGHT AND STRAIN AT MAX. STRESS

(MSL-303)

| Wave No., $cm^{-1}$ | Correlation Coefficient 150° | 170° | 190° |
|---|---|---|---|
| 3084.1 | | | 0.8544 |
| 1731.1 | 0.9570 | 0.9291 | 0.9063 |
| 1228.5 | 0.8287 | | |
| 965.6 | 0.8114 | | |
| 911.5 | 0.8071 | | |
| 772.3 | 0.8007 | 0.8451 | |
| 718.2 | 0.8878 | | |

Correlations based on strain data taken from a plot of strain versus log time.

| Wave No., $cm^{-1}$ | Correlation Coefficient 150° | 170° | 190° |
|---|---|---|---|
| 3084.1 | | | 0.9682 |
| 3014.5 | | | -0.8725 |
| 2921.8 | 0.8221 | | 0.8911 |
| 2736.2 | -0.8279 | -0.8787 | |
| 1731.1 | 0.9247 | 0.9313 | 0.9033 |
| 1305.8 | | | -0.9234 |
| 1228.5 | 0.8994 | 0.8209 | 0.8811 |
| 965.6 | 0.9406 | 0.8296 | |
| 934.7 | 0.9192 | 0.8811 | 0.8394 |
| 911.5 | 0.9247 | 0.8885 | 0.8088 |
| 772.3 | 0.8265 | 0.8661 | |
| 718.2 | 0.8693 | | 0.8039 |

Correlations based on strain data taken from a plot of strain versus time.

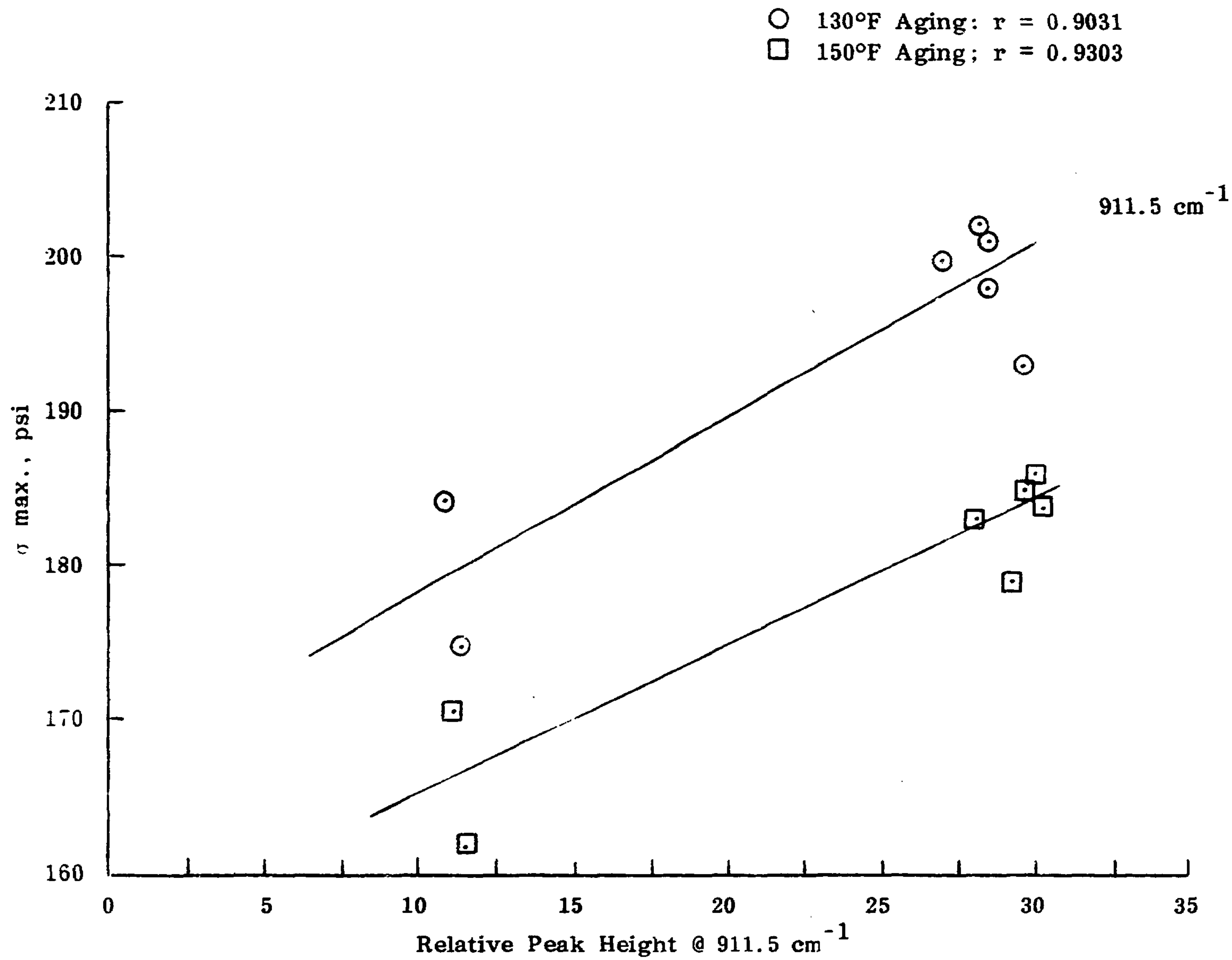


Figure 65. Correlation of Max. Stress with Peak at 911 $cm^{-1}$ (MSL-303).

# CONCLUSIONS AND RECOMMENDATIONS

## CONCLUSIONS

Following are the general conclusions from the work of this project.

1) Sample preparation procedures for IR spectra were established.

2) IR data acquisition procedures were established for use on an FTS-10 IR spectrophotometer.

3) IR of whole HTPB liner and insulation were determined not to be quantitatively useful. IR of sol fractions were determined to be quantitatively excellent.

4) No useful information was derived from IR of whole minimum smoke propellant.

5) IR of gel fraction of minimum smoke propellant was determined to be quantitatively useful.

6) Quality of the correlations between IR peak height changes with bond property changes is as dependent upon accurate measurement of bond properties as upon accurate measurement of IR properties.

7) IR measurements are more accurately made than bond property measurements.

8) IR peaks having the strongest correlations with bond properties must be determined for each bond system studied.

9) Computer programs written for the project are invaluable aids in data reduction, data correlations and prediction of bond properties.

## RECOMMENDATIONS

1) Using the technology developed in this project and in the FTIS project, develop the procedures for on-site inspection of rocket motors.

2) Using IR procedures developed in this project, identify the chemical mechanism of aging of minimum smoke propellant.

3) Using IR procedures developed in this project, identify the chemical mechanism of aging of HTPB type propellants.

4) Apply the developed technology and computer programs to the aging and service life prediction of propellants and bond systems to be employed in production rocket motors.

# APPENDIX A

## CORRELATION OF SPECTRAL CHANGES WITH SAMPLE LOCATION

## APPENDIX A

## CORRELATION OF SPECTRAL CHANGES WITH SAMPLE LOCATION

At the beginning of Phase I, Task 1 samples were made of HTPB and minimum smoke propellant bond systems and these samples were aged at 77° and 170°F. The purpose of these samples was to determine whether changes in the propellant near the bond line could be observed in the infrared spectru. After 3 months of aging at the two temperatures, the HTPB samples were tested and those data were reduced and analyzed. Changes in the spectra of the HTPB propellant at selected locations in the spectrum and at varying distances from the liner/propellant interface were examined and the data are plotted on Figures A-1 through A-8. Data plotted in these figures resulted from the testing of samples that did not have the mold release agent between the liner and the propellant. Spectra were also made of the propellant from those samples which did contain the mold release and it was found that the mold release had no influence upon the spectral changes that were observed.

Figure A-1 is a plot of the change in the peak height at 3009 $cm^{-1}$ versus distance from the liner, and shows that the magnitude of this peak decreases drastically the closer the sample is to the propellant/liner interface. This peak is indicative of the amount of unsaturation in the binder. Figure A-2 is a plot of the peak at 1737 $cm^{-1}$ and shows that this peak also decreases as the liner/propellant interface is approached. This absorbance is indicative of the amount of plasticizer in the propellant. Figure A-3, a plot of the absorbance at 1640 $cm^{-1}$, shows the same phenomenon as the other two. This peak is also indicative of the amount of unsaturation in the propellant. Both Figure A-1 and Figure A-3 show that there is a decrease in the total unsaturation as the propellant/liner interface is approached. Figure A-4 is a plot of the absorbance at 1243 $cm^{-1}$. Data there are quite scattered close to the propellant/liner interface and, overall, show no change with respect to distance from the propellant/liner interface.

Figures A-5 through A-8 are plots of amplitude at the same wave numbers versus distance from the propellant/liner interface, where the propellant has been aged 3 months at 170°F. Generally, they show the same effects as the 3 months' 77°F storage condition only the effects are more severe. Again, on Figure A-8, the peak at 1243 $cm^{-1}$ has not shown an overall change with distance from the liner. However, in general, the magnitude of that peak is less than the magnitude of that peak where the aging took place at 77°F temperature.

Conclusions that can be drawn from these data are listed below.

1) The average infrared absorptions at 1243 $cm^{-1}$ away from the propellant/liner interface were lower in the samples aged at 170°F than those at ambient storage. The structural source of this peak has not yet been identified, but the data indicate its concentration is decreasing at high-temperature aging.

2) The trans and cis unsaturation peaks at 965 and 911 $cm^{-1}$ show no meaningful trends in infrared intensities between ambient and 170°F aging after 3 months. Their location on the side of an ammonium perchlorate peak hinders their quantitative measure.

3) The presence of a mold release at the propellant/liner interface in one set of samples shows no effect on propellant spectra when compared to the samples without mold release.

4) The unsaturation (-CH) peak at 3008 $cm^{-1}$ exhibited an average decrease in value in the samples aged at 170°F compared to ambient storage in both samples with and without mold release.

5) The DOA peak at 1737 $cm^{-1}$ showed a gradient in all samples due to DOA migration from the propellant into the liner. The extent of migration is greater in the samples aged at 170°F.

6) The average value of the unsaturation peak at 1640 $cm^{-1}$ is slightly higher in the samples aged at 170°F compared to ambient storage. One would have expected a decrease in this peak at the higher temperature as further crosslinking occurs. The observed increase may be the result of an aging product which absorbs in the infrared near the 1640 $cm^{-1}$ unsaturation peak.

7) The propellant near the propellant/liner interface was hard and brittle in all samples but more so at 170°F. Because the samples were hard, poor contact was made with the IRE surface and the amplitudes of their spectra were quite low compared to samples further into the propellant. Therefore, it is quite difficult to make a quantitative judgement on the changes occurring in the propellant at this location.

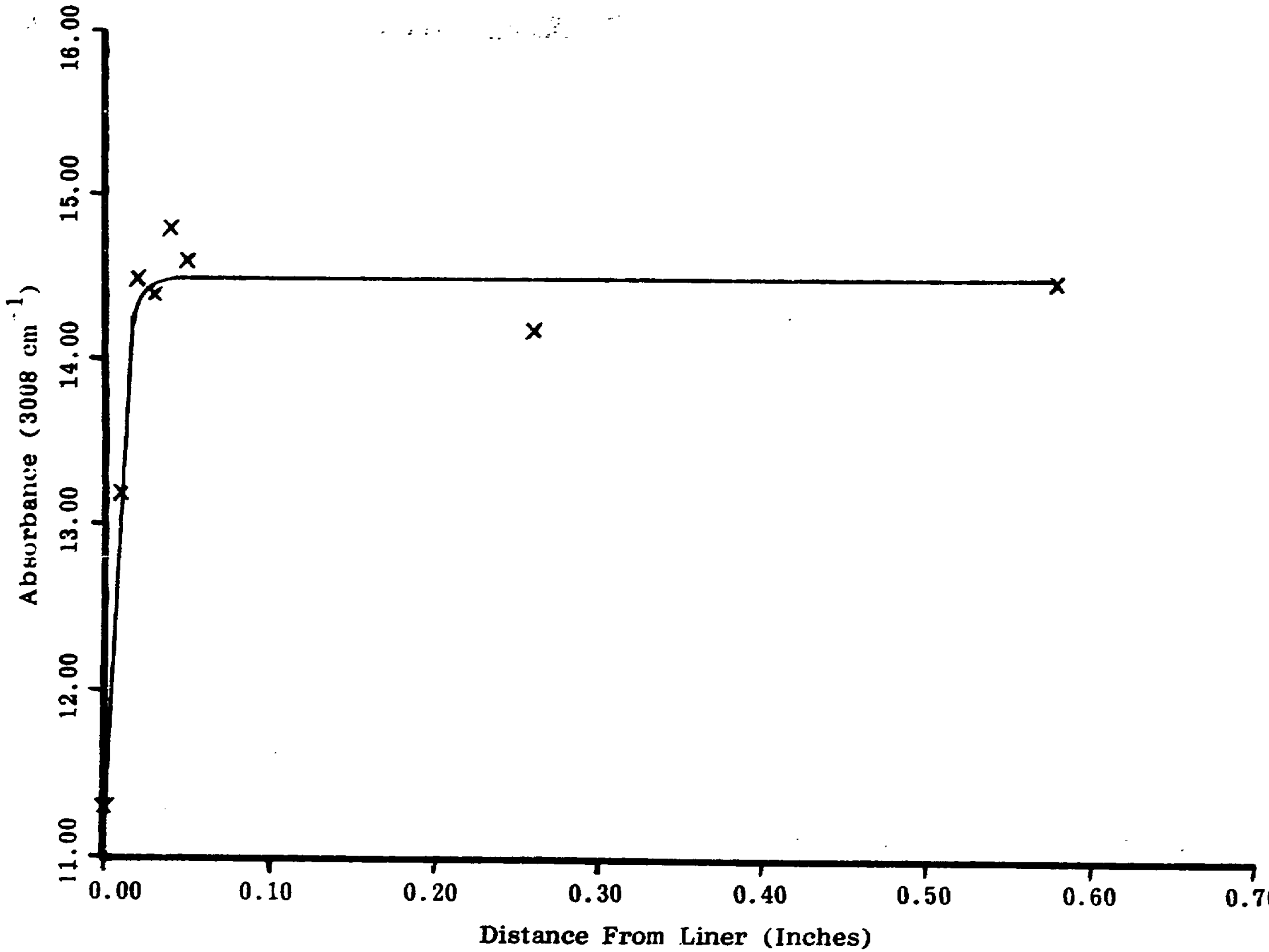


Figure A-1. Absorbance at 3008 cm$^{-1}$ As A Function of Distance Into the Propellant From the Liner Interface. Sample Aged 3 Months @ 77°F.

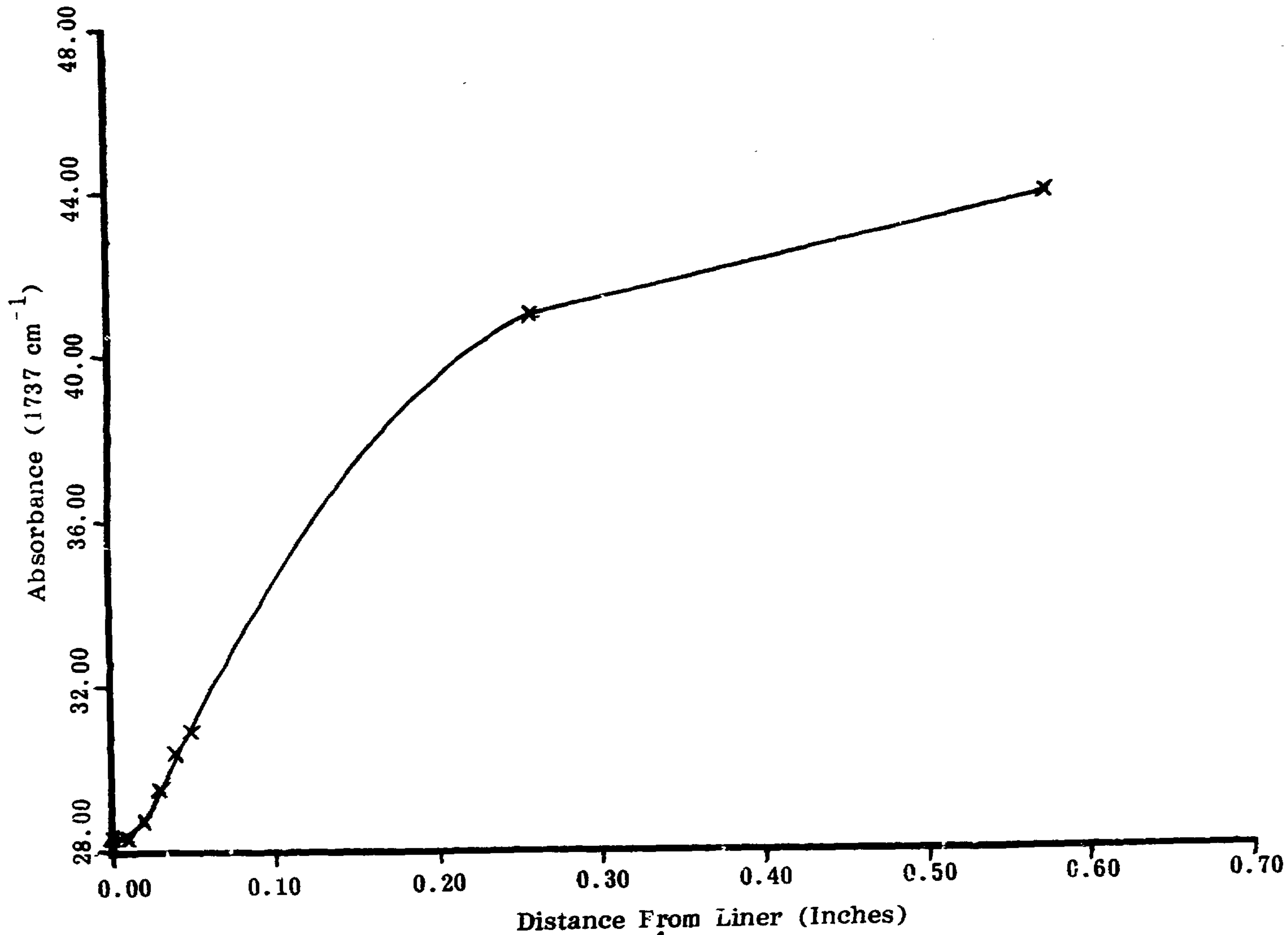


Figure A-2. **Absorbance at 1737 cm$^{-1}$ As a Function of Distance Into the Propellant From the Liner Interface. Sample Aged 3 Months @ 77°F.**

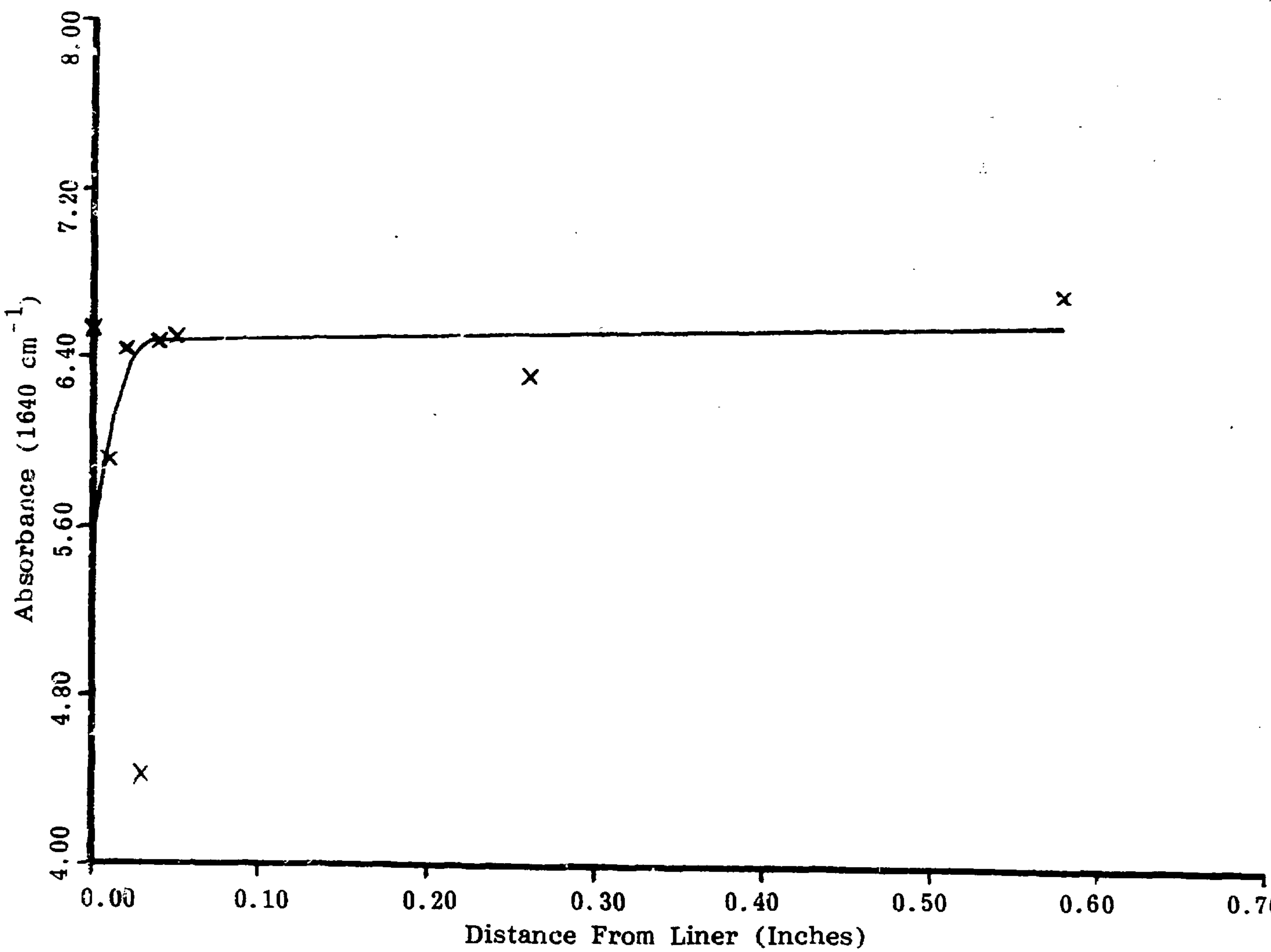


Figure A-3. Absorbance at 1640 cm$^{-1}$ As A Function of Distance Into the Propellant From the Liner Interface. Sample Aged 3 Months @ 77°F.

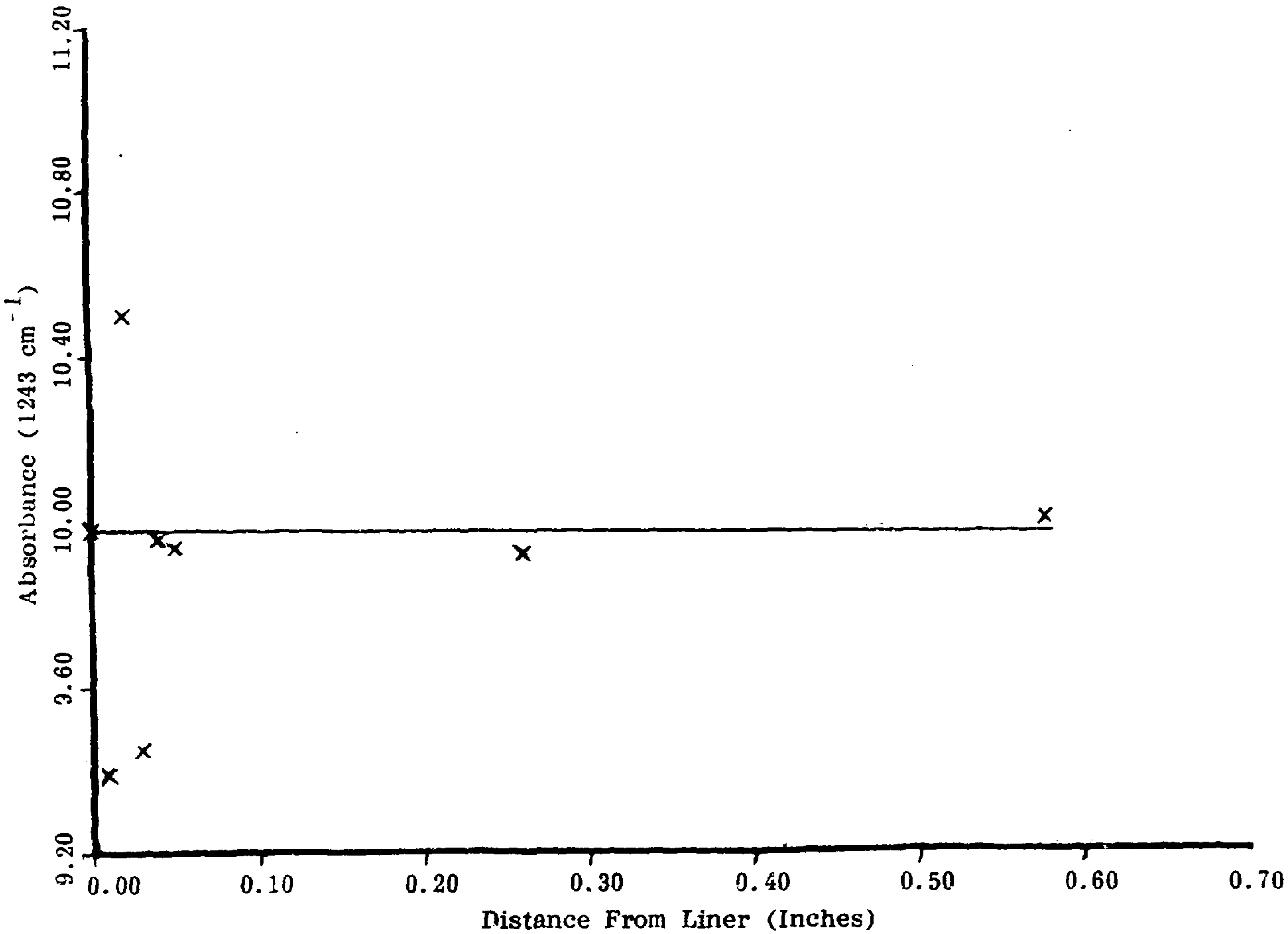


Figure A-4. Absorbance at 1243 cm$^{-1}$ As a Function of Distance Into the Propellant From the Liner Interface. Sample Aged 3 Months @ 77$^{o}$F.

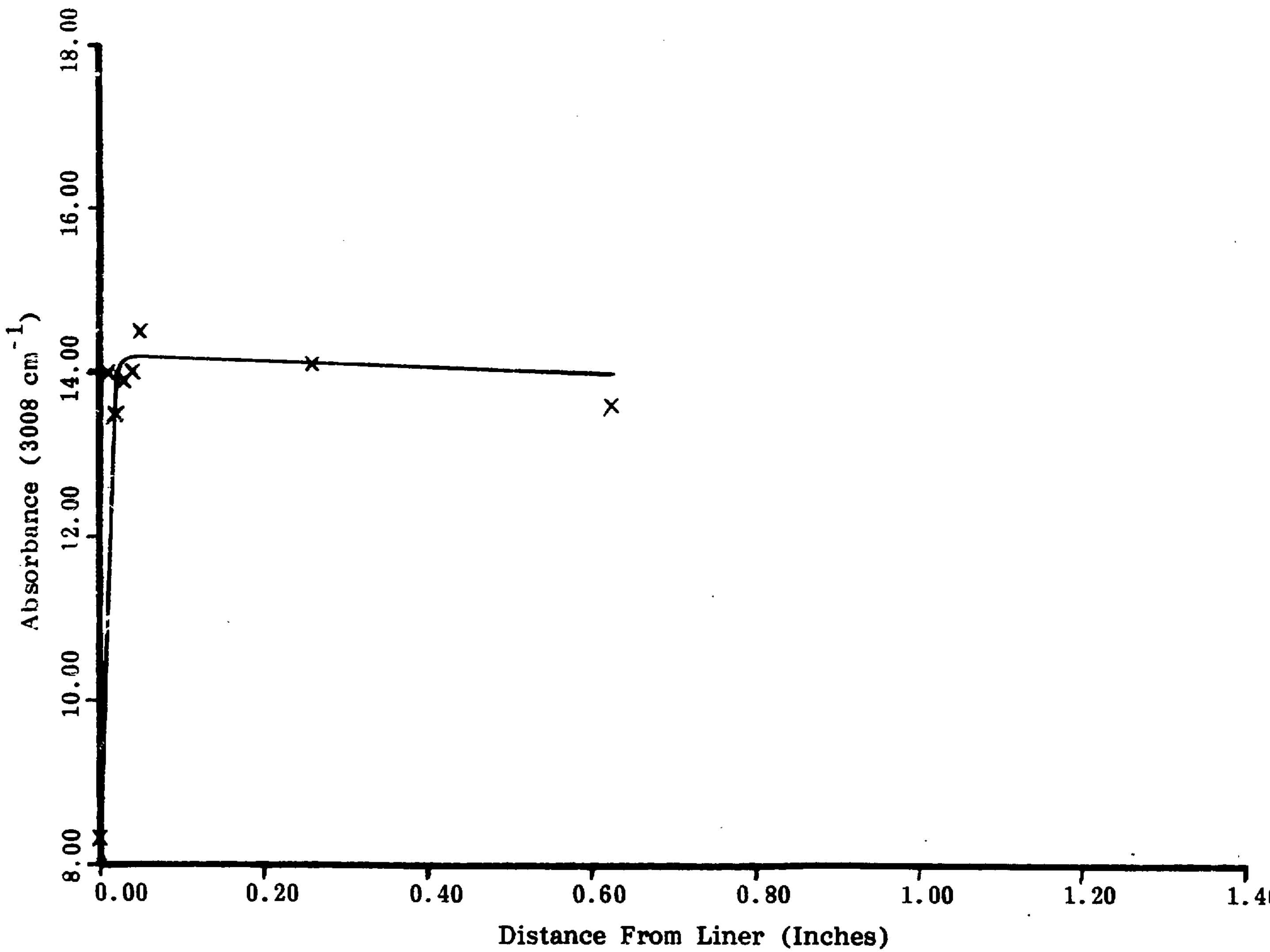


Figure A-5. Absorbance at 3008 $cm^{-1}$ As A Function of Distance Into the Propellant From the Liner Interface. Sample Aged 3 Months @ 170°F.

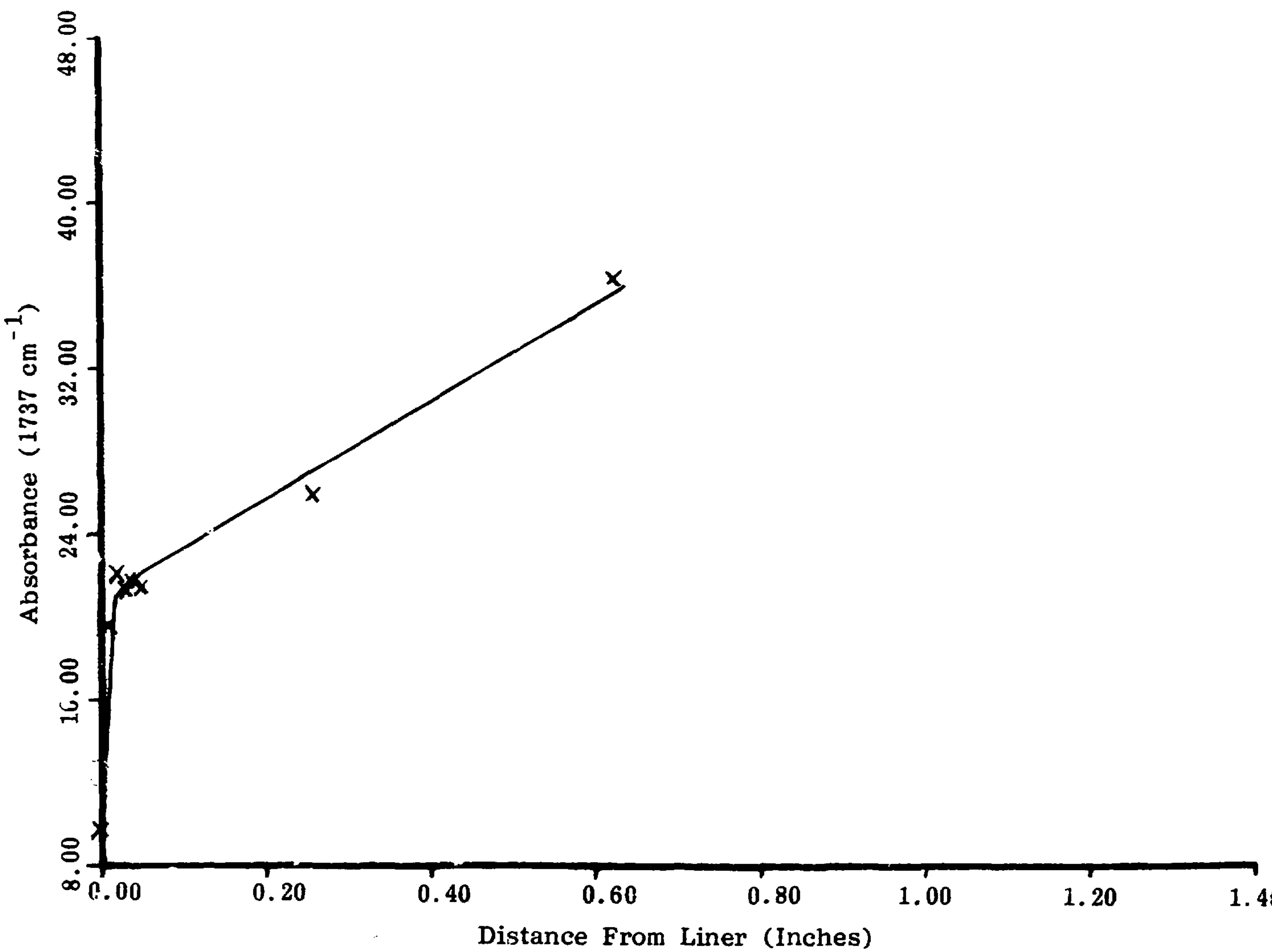


Figure A-6. Absorbance at 1737 $cm^{-1}$ As A Function of Distance Into the Propellant From the Liner Interface. Sample Aged 3 Months @ 170°F.

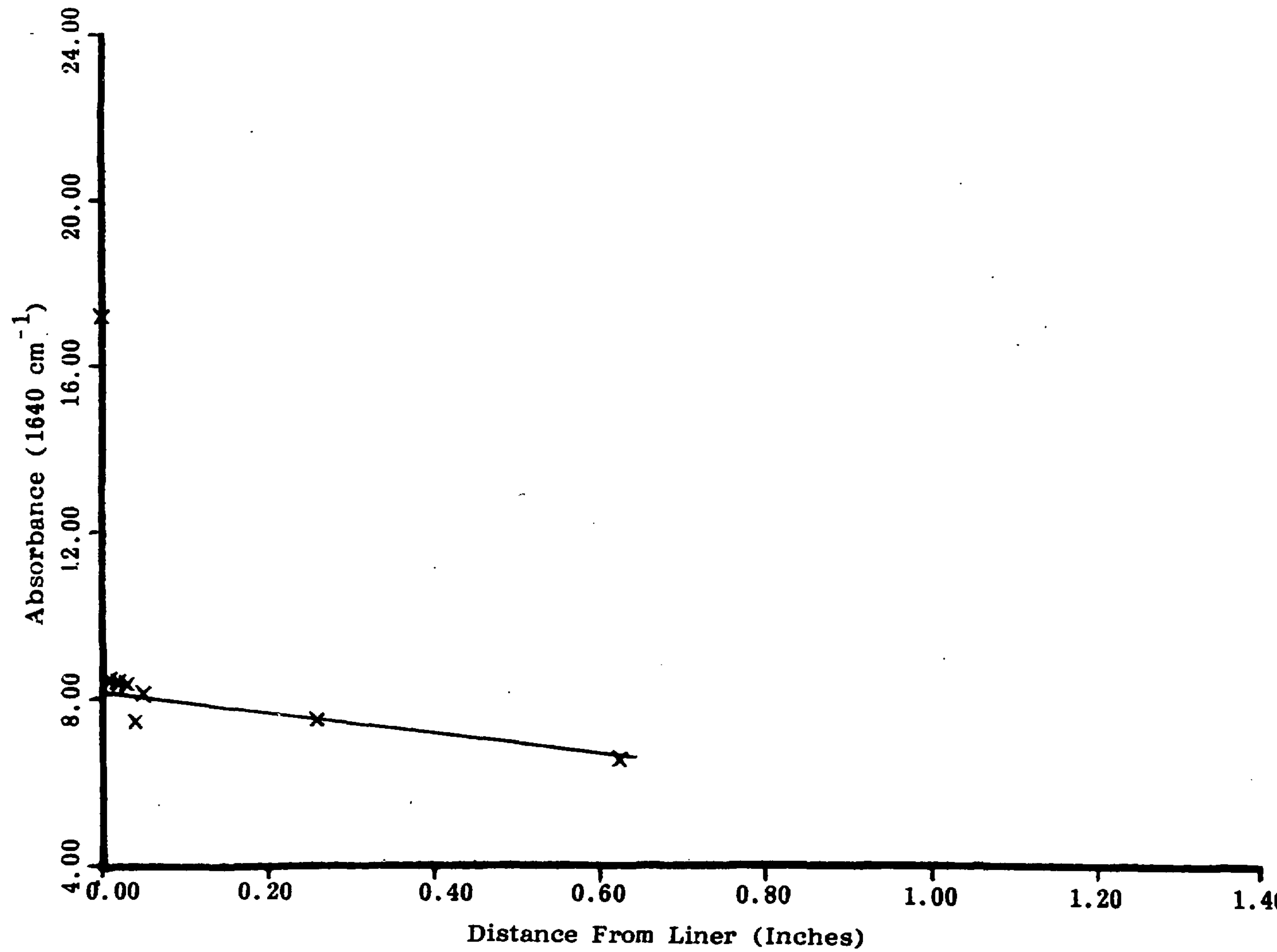


Figure A-7. Absorbance at 1640 $cm^{-1}$ As A Function of Distance Into the Propellant From the Liner Interface. Sample Aged 3 Months @ 170°F.

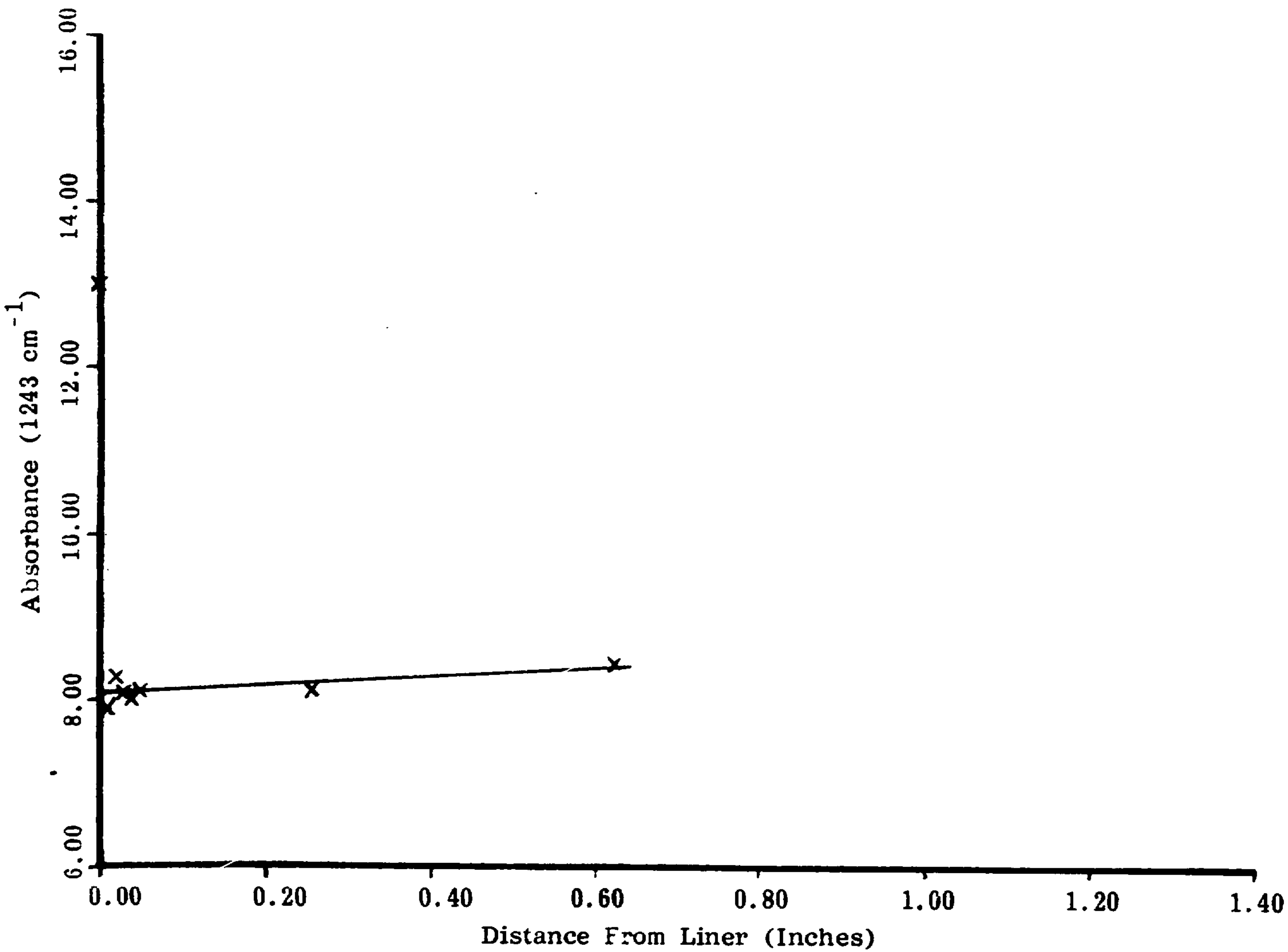


Figure A-8. Absorbance at 1243 cm$^{-1}$ As A Function of Distance Into the Propellant From the Liner Interface. Sample Aged 3 Months @ 170°F.

# APPENDIX B

## INFRARED TESTING PROCEDURES

## HTPB PROPELLANT BONDLINE INFRARED TESTING PROCEDURE

Composite adhesion (two-inch) bond samples were taken from the aging environments at the time intervals specified in the program plan for infrared analysis. The two-inch square of propellant, along with the liner and insulation is removed from the composite assembly with an X-acto knife. The removed square of propellant, liner, and insulation is cut into five equal sections perpendicular to the plane of the liner. Each of these sections is approximately one by five centimeters. A razor blade is pushed down the plane of the liner, separating the insulation and part of the liner from the propellant. Each propellant section is placed in a microtome cutting apparatus and the blade adjusted to carefully remove the residual liner from the propellant surface. A 10-mil slice of propellant is cut at the propellant-liner interface and also at 0.5 inch from the interface. The propellant slices from each location are divided with a razor blade into a pair, 0.5 by 5 centimeters. Each pair is mounted against a zinc selenide prism (50 x 5 2 mm, $\theta = 45°$) with the side closest to the interface against the prism and placed in a Harrick variable angle ATR set at an angle of 60°. The ATR unit is mounted in a Digilab FTS-10 spectrophotometer. After the sample is placed in the ATR unit, 15 minutes is allowed for propellant cold flow, then 1000 scans are collected, computed and compared to a reference spectrum to produce an absorbance spectrum for each of five pairs from the interface and five pairs at 0.5 inch from the interface. Collection of 1000 scans requires 20 minutes using the following parameters:

| | |
|---|---|
| DPM | P |
| GRR | -1 |
| NSS | 1000 |
| RES | 4 |
| SEN | 1 |
| UDR | 2 |
| WDS | SP |
| ZFF | 1 |

After each sample is run, the zinc selenide prism is held with tweezers and washed with methylene chloride, ethanol, and again with methylene chloride from a squeeze bottle. Still holding the prism with tweezers, it is dried with a hot air drier and remounted, holding the prism with lens paper.

The absorbance spectrum of each sample (five at interface, five at 0.5 inch) are recorded on magnetic tape. The five spectra at each location are later averaged using the arithmetical capabilities of the FTS-10's computer.

The averaged spectra are transferred from magnetic tape to the IBM computer (or equivalent) which normalizes and tabulates the spectral peaks for quantitative comparison using the "E490" program.

Bond data were obtained on aged samples taken at the same time intervals as the spectra samples. The bond data are submitted and recorded in the computer using the "E410" program.

The spectral data and bond data are correlated using programs "EREG" and "E572" to determine reaction rate constants, activation energies and correlation coefficients.

## MINIMUM SMOKE PROPELLANT BONDLINE INFRARED TESTING PROCEDURE

Composite adhesion (two-inch) bond samples were taken from the aging environments at the time intervals specified in the program plan for infrared analysis. The two-inch square of propellant, along with the liner and insulation is removed from the composite assembly with an X-acto knife. The removed square of propellant, liner, and insulation is cut into three equal sections perpendicular to the plane of the liner. Each of these sections is approximately 1.6 by 5 centimeters. A razor blade is pushed down the plane of the liner, separating the insulation and part of the liner from the propellant. Each propellant section is placed in a microtome cutting apparatus and the blade adjusted to carefully remove the residual liner from the propellant surface. A 20-mil slice of propellant is cut at the propellant-liner interface and also at 0.5 inch from the interface. The slices from a given location are placed in an alundum Soxhlet thimble (34 x 100 mm) and extracted 24 hours with 200 milliliters of acetone. The residual gel is removed, laid on a teflon pad, covered with another teflon pad, and dried under vacuum (approximately 10 mm) for 24 hours at 120°F.

The dried gel from each location is cut and pieced to cover both sides of a zinc selenide prism (50 x 5 x 2 mm, $\theta = 45°$) and placed in a Harrick variable angle ATR set at an angle of 60°. The ATR unit is mounted in a Digilab FTS-10 spectrophotometer. After the sample is placed in the ATR unit, 15 minutes is allowed for cold flow, then 1000 scans are collected, computed and compared to a reference spectrum to produce an absorbance spectrum for each of three pairs from the interface and three pairs at 0.5 inch from the interface. Collection of 1000 scans requires 20 minutes using the following parameters:

| | |
|---|---|
| DPM | P |
| GRR | -1 |
| NSS | 1000 |
| RES | 4 |
| SEN | 1 |
| UDR | 2 |
| WDS | SP |
| ZFF | 1 |

After each sample is run, the zinc selenide prism is held with tweezers and washed with methylene chloride, ethanol, and again with methylene chloride from a squeeze bottle. Still holding the prism with tweezers, it is dried with a hot air drier and remounted, holding the prism with lens paper.

The absorbance spectrum of each sample (three at interface, three at 0.5 inch) are recorded on magnetic tape. The three spectra at each location are later averaged using the arithmetical capabilities of the FTIS computer.

The averaged spectra are transferred from magnetic tape to the IBM computer (or equivalent) which normalized and tabulates the spectral peaks for quantitative comparison using the "E490" program.

Bond data was obtained on aged samples taken at the same time intervals as the spectra samples. These bond data are submitted and recorded in the computer using the "E410" program.

The spectral data and bond data are correlated using programs "EREG" and "E572" to determine reaction rate constants, activation energies and correlation coefficients.

# APPENDIX C

## CORRELATIONS AMONG MECHANICAL PROPERTIES, HARDNESS, GEL FRACTION AND TIME FOR HTPB BOND SYSTEM AGED 16 WEEKS

Bond of liner to insulation continued to decline over the entire 16-week aging and this is shown by the plot on Figure C-1. Propellant-to-liner peel strength also declined over the 16-week time period with its decline being about the same order of magnitude as the decline seen in the liner-to-insulation peel strength. All failures in the propellant-to-liner bond strength over the 16-week time period are shown on Figure C-2. Figure C-3 is a plot of the response of composite bond tensile strength to time at 165°F. The plot shows that the data are quite scattered. Composite bond strength increased with time; and, since all failures were in the propellant, one must conclude that the adhesive bond is a function of the stress level of the propellant immediately adjacent to the liner. Stress and strain changes in the liner itself are plotted on Figure C-4. The data show a considerable amount of scatter in the stress level of the liner while the strain of the liner appears to change more uniformly.

Gradient hardness of the insulation, liner, and propellant as measured in the composite bond samples is shown in Table C-I. A plot of the response of liner and insulation to age time at 165°F is given on Figure C-5. Insulation underwent a slow but uniform softening during the 16-week age period while hardness of liner, after an initial hardening at 2 weeks, was essentially constant throughout the remaining 14 weeks of aging. Hardness of the propellant as a function of distance from the liner is plotted on Figure C-6. From about 3 mm distance from the liner out to 15 mm from the liner, the propellant undergoes relatively little change. These data are plotted at the top of Figure C 6. For that plot, the data at locations from 3 to 15 mm from the liner were averaged and plotted, with the upper and lower extremes from this average shown for each time period as a vertical bar on either side of the average value. Most of the change in the propellant took place in the distance from 0.5 to 2.5 mm from the liner. The greatest total change took place closest to the liner, with the propellant undergoing a steady hardening for the first 8 weeks and from that time to 16 weeks there was relatively little change in hardness. The more remote from the liner, the less the total change in hardness of the propellant.

Gel fraction changes of the binder in insulation, liner, and propellant are given in Table C-II. These data are plotted on Figure C-7. Insulation underwent relatively little change in its gel fraction during the 16-week time period. The greatest change took place in the first 4 weeks. The same can be observed for the liner, where the greatest change took place within the first 4 weeks, but the liner gained in gel fraction where the insulation declined in gel fraction. From about 4 weeks to the end of the aging program at 16 weeks, the liner changed relatively little. Changes in the gel fraction of the propellant were most noticeable close to the liner. Gel fraction of propellant at the 0 to 3 mm distance from the liner underwent a considerable increase during the first 8 weeks of aging with comparatively little change from then to the end of the 16-week aging period. Propellant more remote from the liner, i.e., from 3 out to 18 mm from the liner, all behaved approximately the same. The major changes in the gel fraction of the propellant binder in this region occurred during the first 4 weeks of aging with a marked decline in the rate of change from 4 weeks out to 16 weeks of aging.

A correlation was found between propellant hardness (as measured by penetrometer) and the peel strength of the liner and propellant. Because the liner/propellant bond always fails in the propellant, it was of interest to see whether this peel strength would correlate with hardness of the propellant; and, in fact, it does as can be observed on Figure C-8. Since the hardness data are somewhat scattered, a second plot was made of th hardness of the propellant

0.5 mm from the liner using data that had been smoothed and then plotted on Figure C-6. This plot of the smoothed hardness data versus propellant-to-liner peel strength is given on Figure C-9.

The correlation of gel fraction in the liner and gel fraction in the propellant 0 to 3 mm away from the liner proved to correlate well with propellant-to-liner peel strength. A plot of these data is given on Figure C-10.

Gel fraction of the liner also proved to correlate well with the ultimate strain of the liner, and, although there was a correlation between ultimate stress of the liner and liner gel fraction, it was not as good. These data are plotted on Figure C-11.

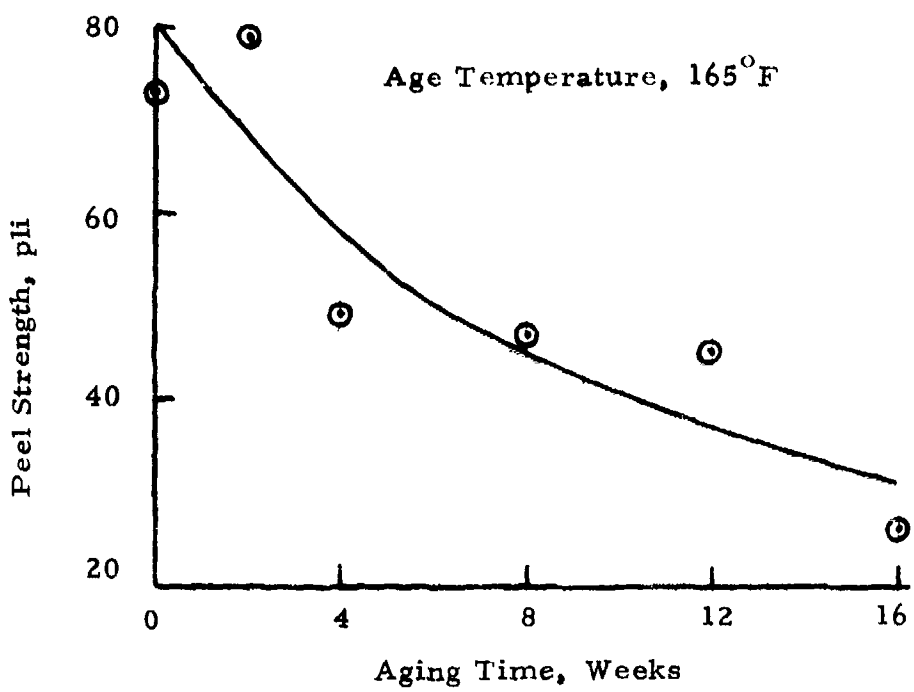


Figure ·-1. Liner-to-Insulation Peel Strength.

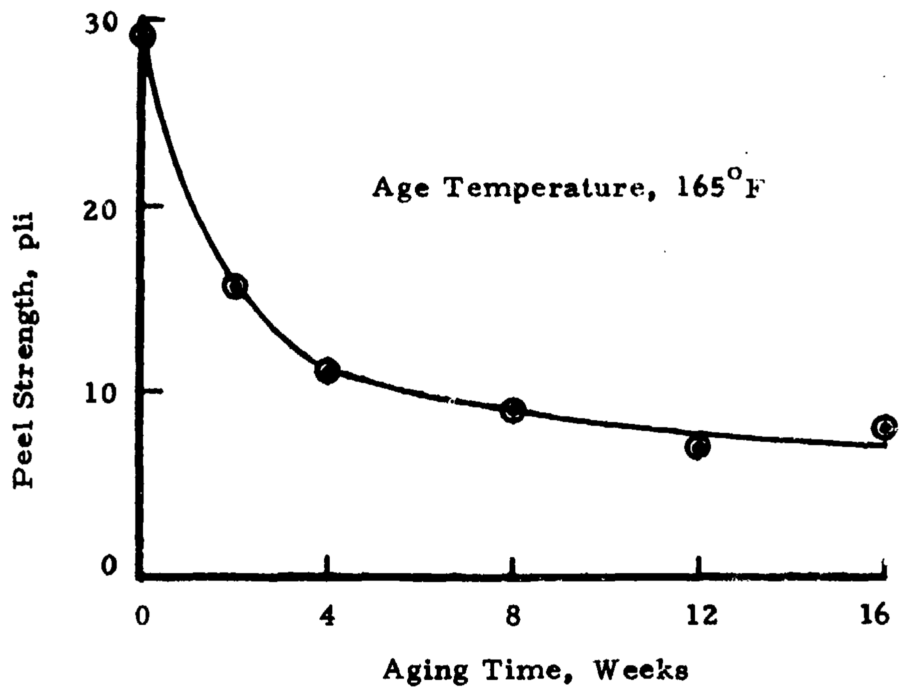


Figure C-2. Propellant-to-Liner Peel Strength.

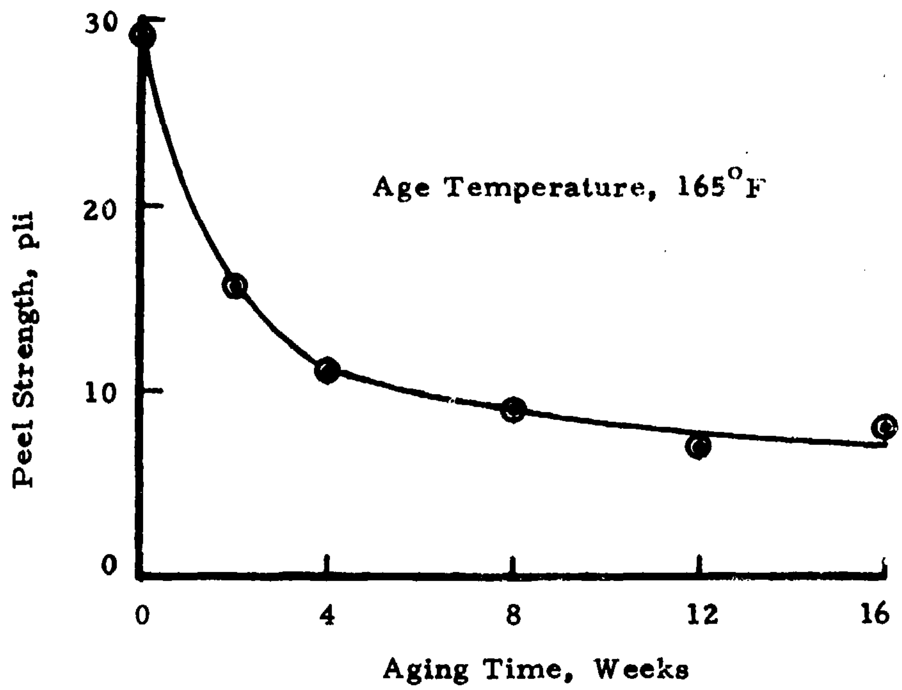


Figure C-2. Propellant-to-Liner Peel Strength.

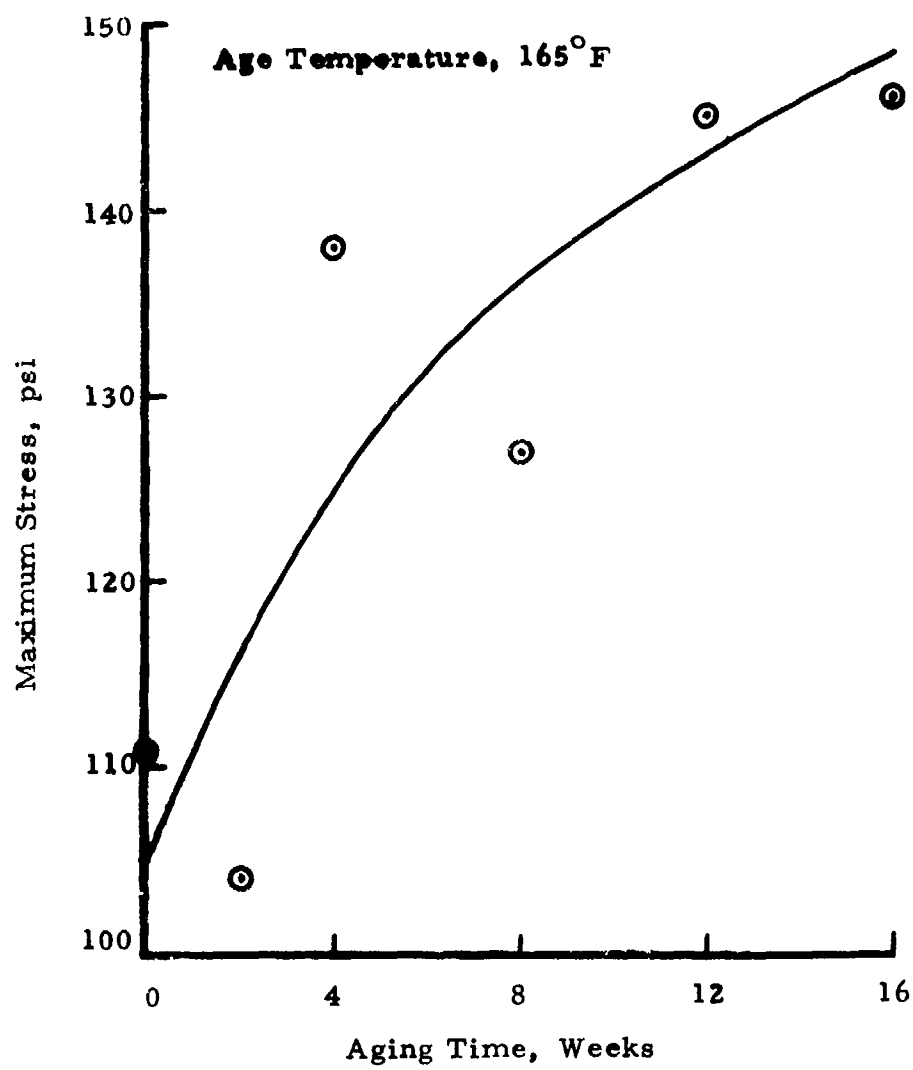


Figure C-3. Composite Bond Tensile Strength.

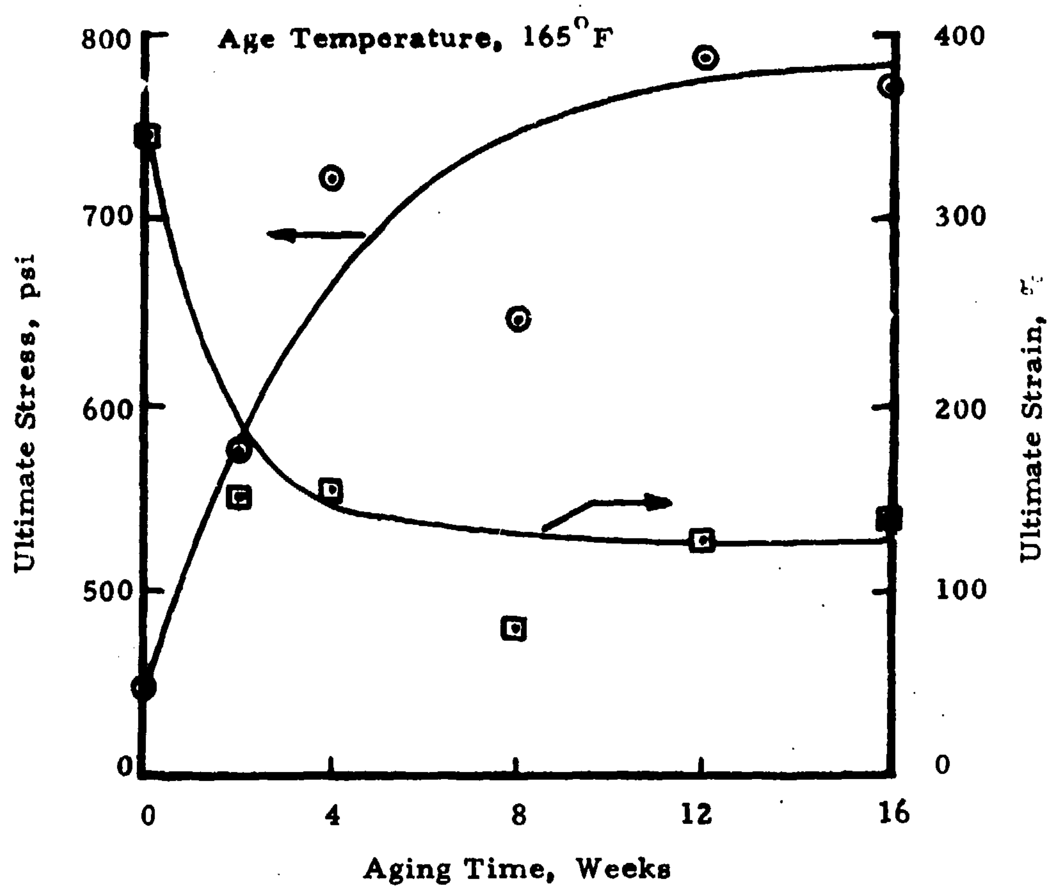


Figure C-4. TL-H755A Liner Tensile Properties.

TABLE C-1

GRADIENT HARDNESS OF INSULATION/LINER/PROPELLANT

(Measurement by Penetrometer)

Propellant: TP-H8279 (18Q-782)
Liner: TL-H755A (RL-05740)
Insulation: TI-R300 (Lot 7023)

| Age Time Weeks | Insulation | Liner | Distance From Liner, mm | | | | | | | | | | |
|---|---|---|---|---|---|---|---|---|---|---|---|---|---|
| | | | 0.5 | 1.0 | 1.5 | 2.0 | 2.5 | 3.0 | 4.0 | 5.0 | 7.0 | 10.0 | 15.0 |
| 0 | 4.0 | 30.0 | 20.0 | 25.5 | 29.0 | 28.0 | 33.5 | 35.0 | 33.5 | 33.5 | 31.0 | 34.5 | 35.0 |
| 2 | 5.5 | 20.5 | 15.5 | 19.5 | 25.0 | 23.5 | 30.0 | 34.0 | 31.0 | 29.5 | 33.0 | 35.0 | 38.0 |
| 4 | 4.5 | 21.0 | 12.0 | 14.0 | 30.0 | 30.0 | 32.5 | 31.5 | 31.5 | 31.0 | 31.0 | 30.0 | 29.5 |
| 8 | 6.5 | 23.0 | 12.0 | 19.5 | 22.0 | 25.5 | 25.5 | 23.0 | 25.5 | 28.0 | 28.0 | 23.5 | 28.5 |
| 12 | 8.1 | 20.5 | 18.0 | 17.0 | 23.5 | 24.0 | 28.0 | 24.5 | 22.0 | 23.0 | 24.5 | 25.0 | 27.5 |
| 16 | 7.5 | 24.0 | 17.5 | 18.5 | 23.5 | 24.5 | 25.0 | 23.0 | 24.0 | 26.5 | 27.0 | 20.5 | 22.5 |

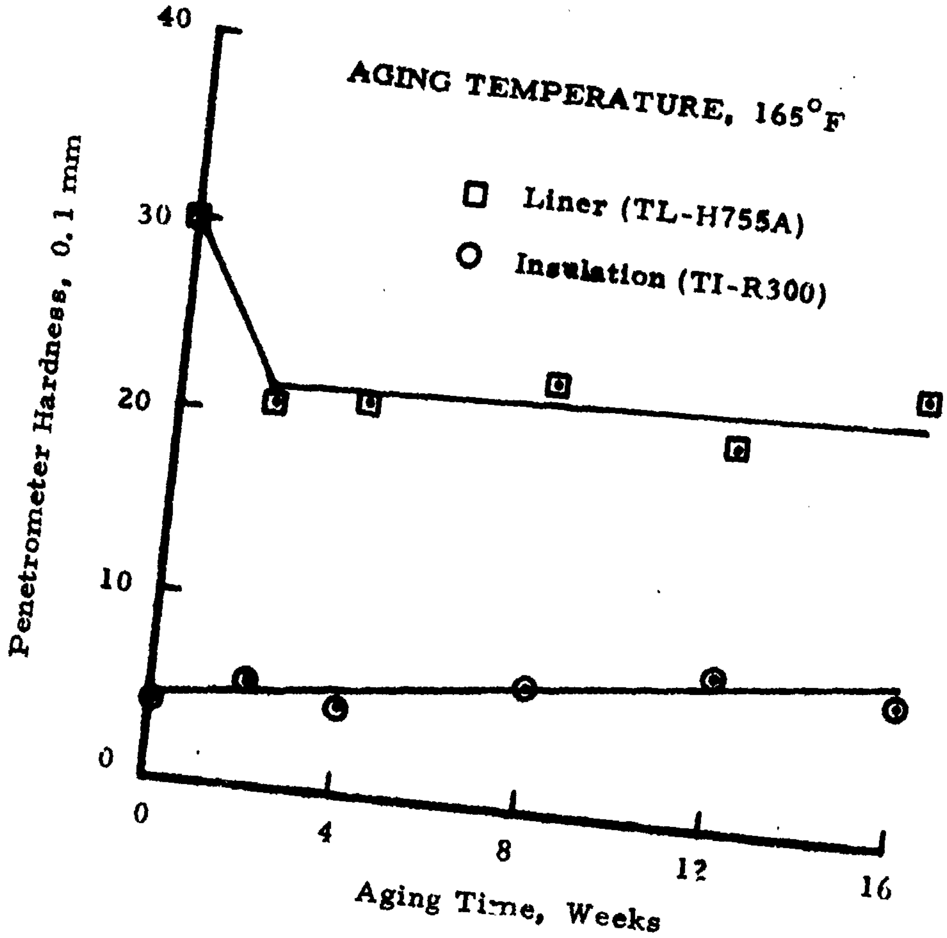


Figure C-5. Liner and Insulation Hardness As A Function of Age Time at 165°F.

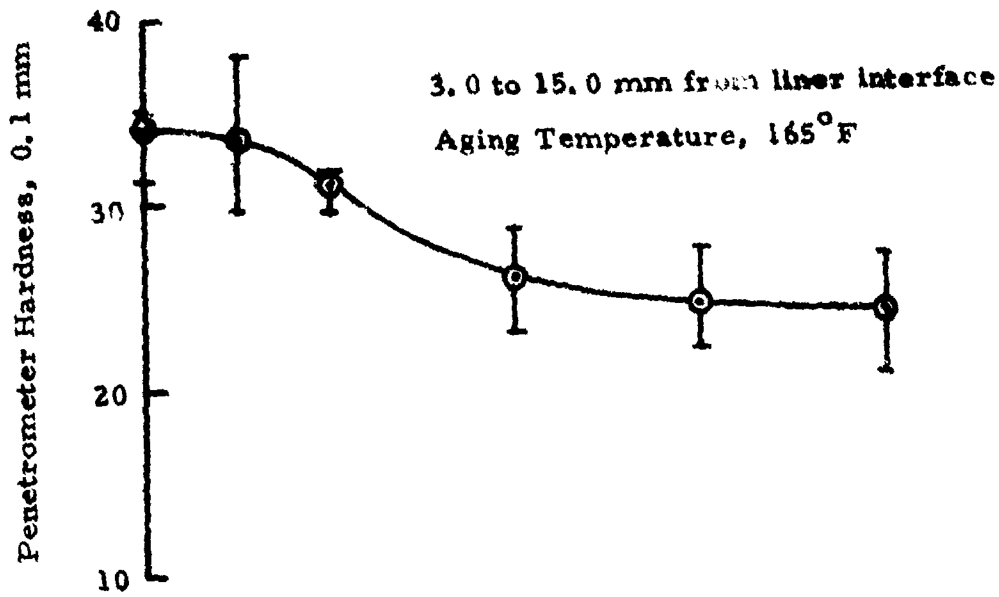


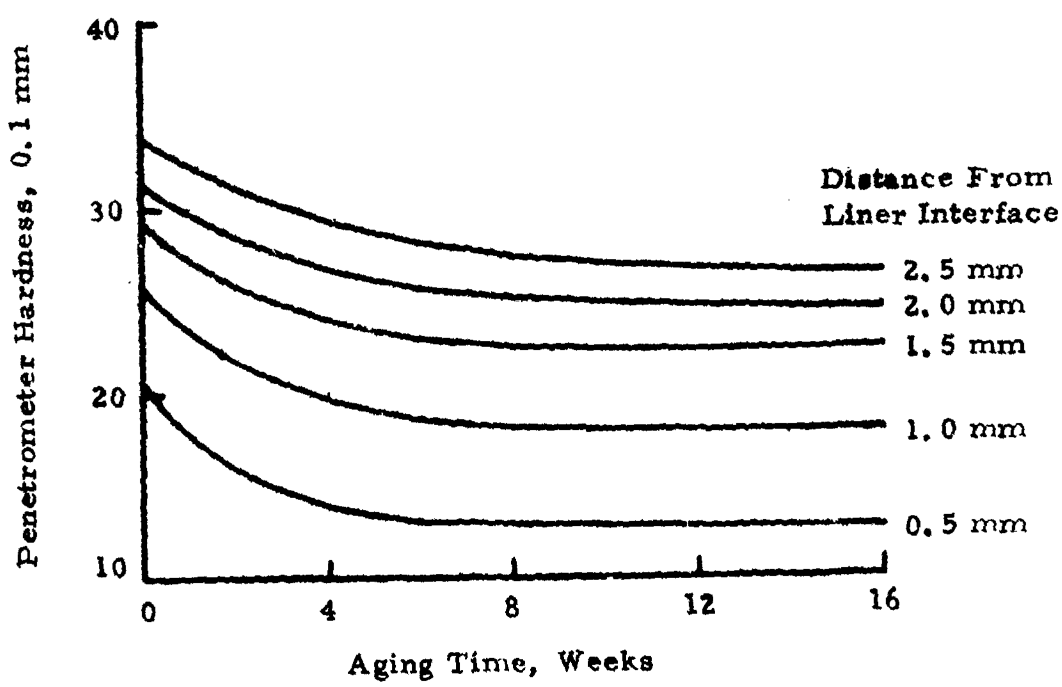


Figure C-6. Propellant Hardness As A Function of Distance From Liner and Aging Time.

TABLE C-2

GEL FRACTION OF BINDERS IN THE HTPB PROPELLANT BOND SAMPLES

(Age Temp. 165°F)

| Age Time, Weeks | Insulation | Liner | Binder Gel in Propellant (Distance From Liner) | | | | | | |
|---|---|---|---|---|---|---|---|---|---|
| | | | 0-3 mm | 3-6 mm | 6-9 mm | 9-12 mm | 12-15 mm | 15-18 mm | 18-21 mm |
| 0 | 94.24 | 78.14 | 64.30 | 62.21 | 61.28 | 60.78 | 60.90 | 60.35 | 57.93 |
| 2 | 93.05 | 83.06 | 67.72 | 64.85 | 64.11 | 63.71 | 63.65 | 63.23 | 62.86 |
| 4 | 91.60 | 83.20 | 72.16 | 69.58 | 68.47 | 67.17 | 66.82 | 66.35 | --- |
| 8 | 91.22 | 84.43 | 75.00 | 71.53 | 71.19 | 70.02 | 69.75 | 69.24 | --- |
| 12 | 90.05 | 84.07 | 74.82 | 73.01 | 72.60 | 71.94 | 71.99 | 72.86 | --- |
| 16 | 89.82 | 85.49 | 76.35 | 73.61 | 73.80 | 73.56 | 74.04 | 74.62 | --- |

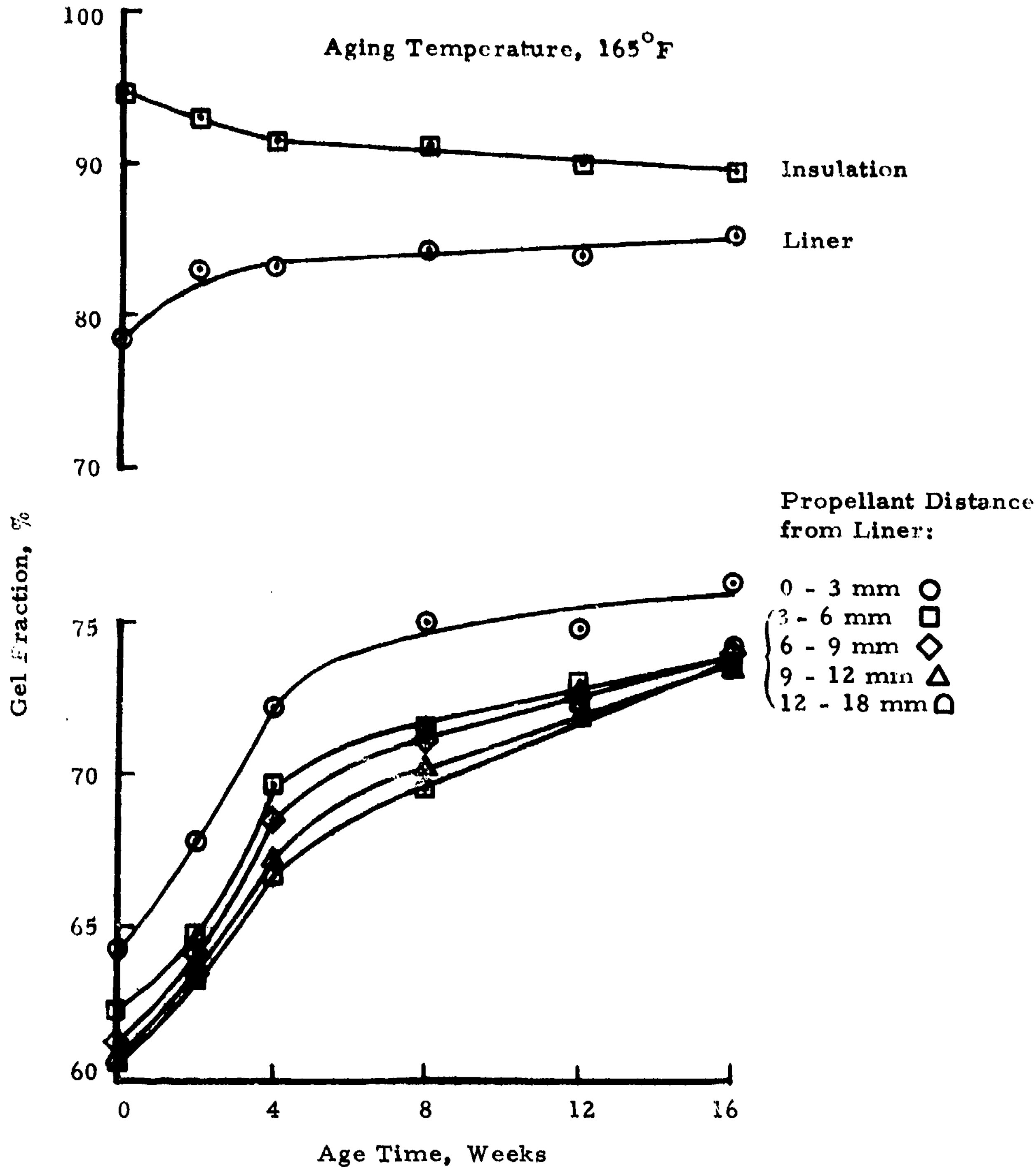


Figure C-7. Gel Fraction As A Function of Age Time.

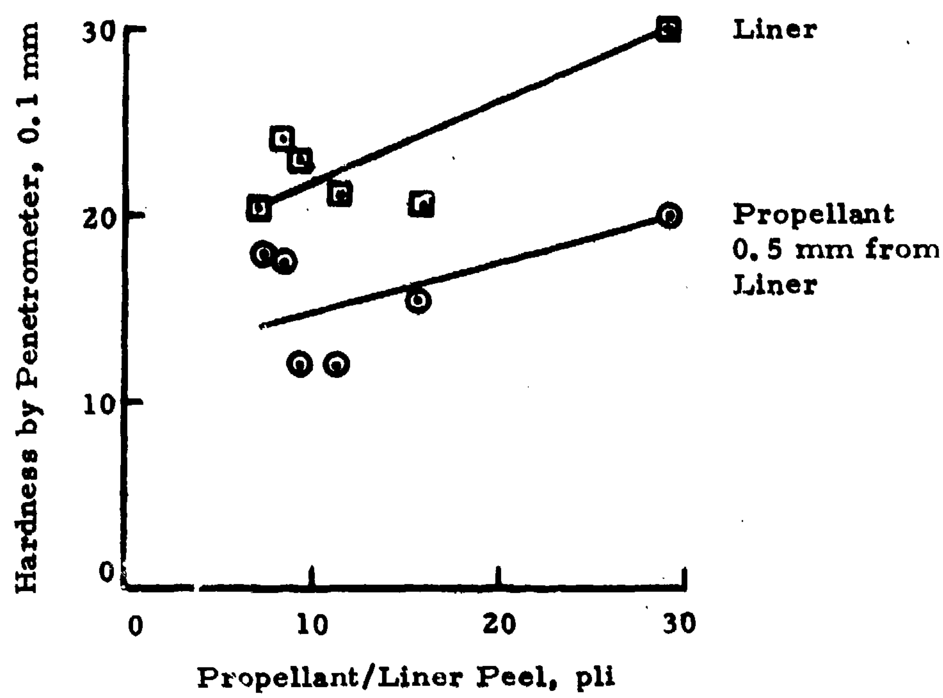


Figure C-8. Correlation Between Hardness and Peel Strength of Liner and Propellant.

NOTE: Hardness data smoothed, taken
from Figure 6.

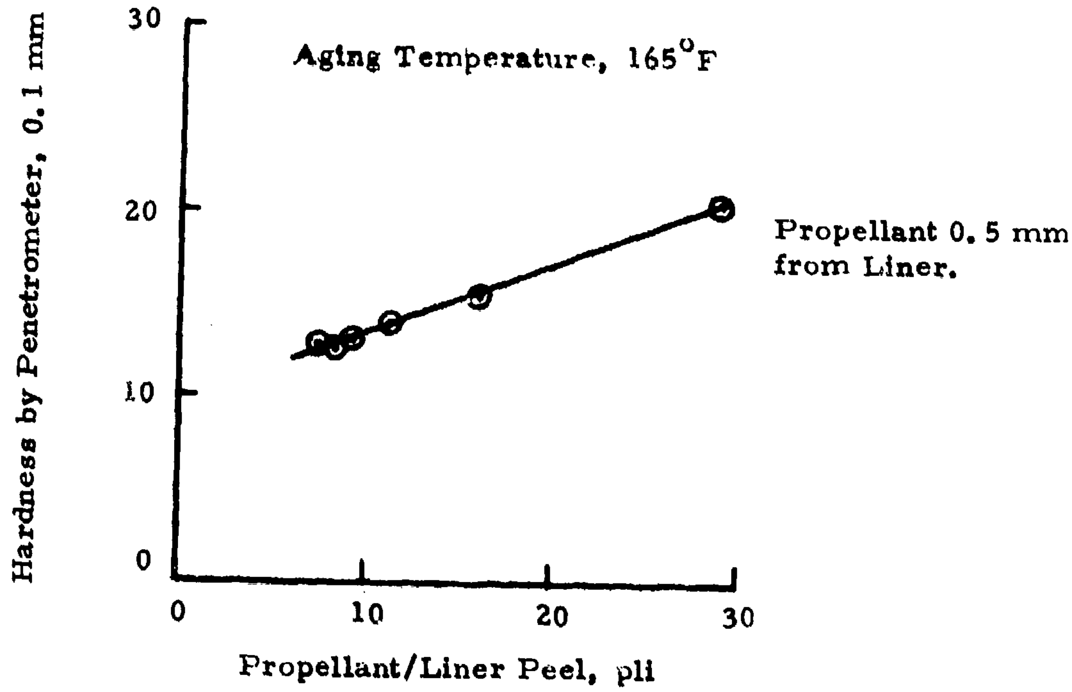


Figure C-9. Correlation Between Propellant Hardness and Propellant/Liner Peel Strength.

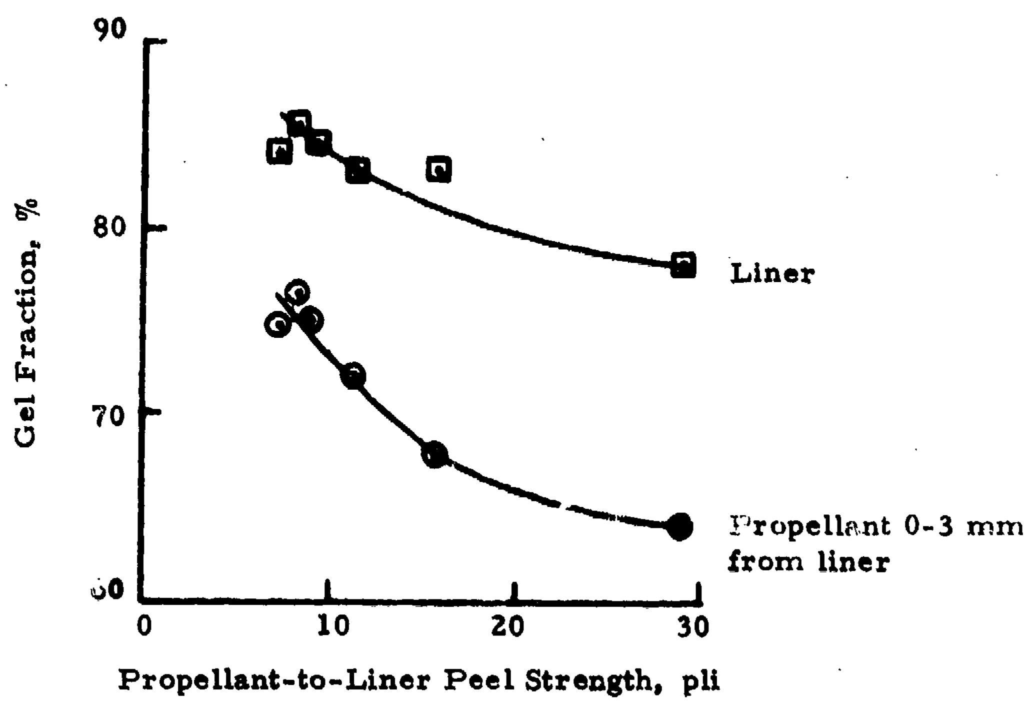


Figure C-10. Correlation of Gel Fraction and Propellant/Liner Peel Strength.

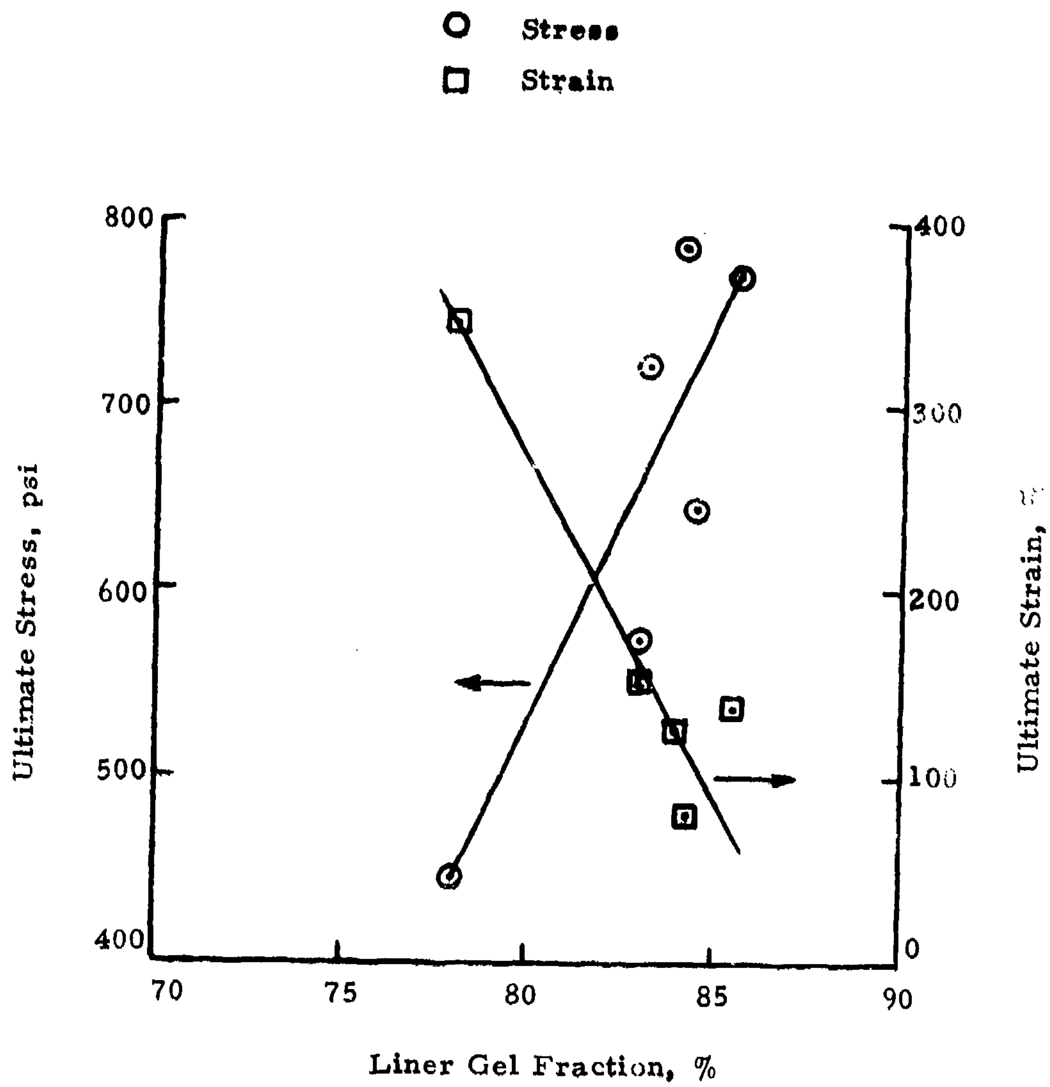


Figure C-11. Correlation Between Liner Gel Fraction and Stress and Strain.

## APPENDIX D

## CORRELATIONS AMONG MECHANICAL PROPERTIES, HARDNESS, GEL FRACTION AND TIME FOR MINIMUM SMOKE PROPELLANT BOND SYSTEM AGED 16 WEEKS

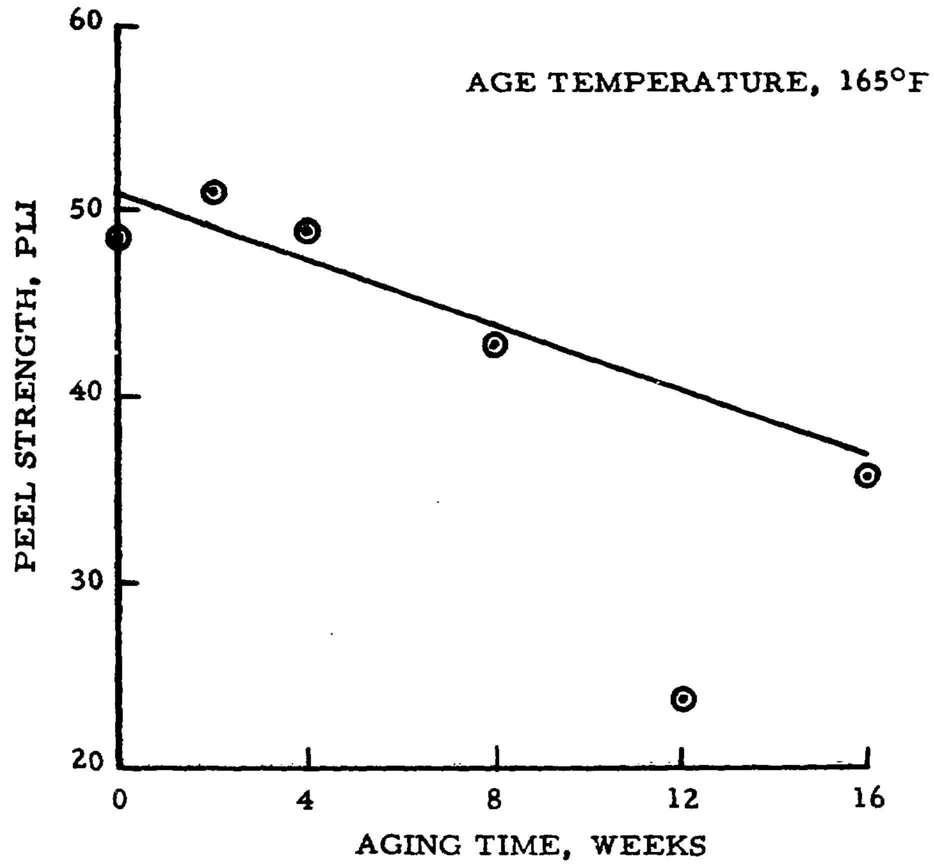


Figure D-1. Minimum Smoke Propellant Liner-to-Insulation Peel Strength

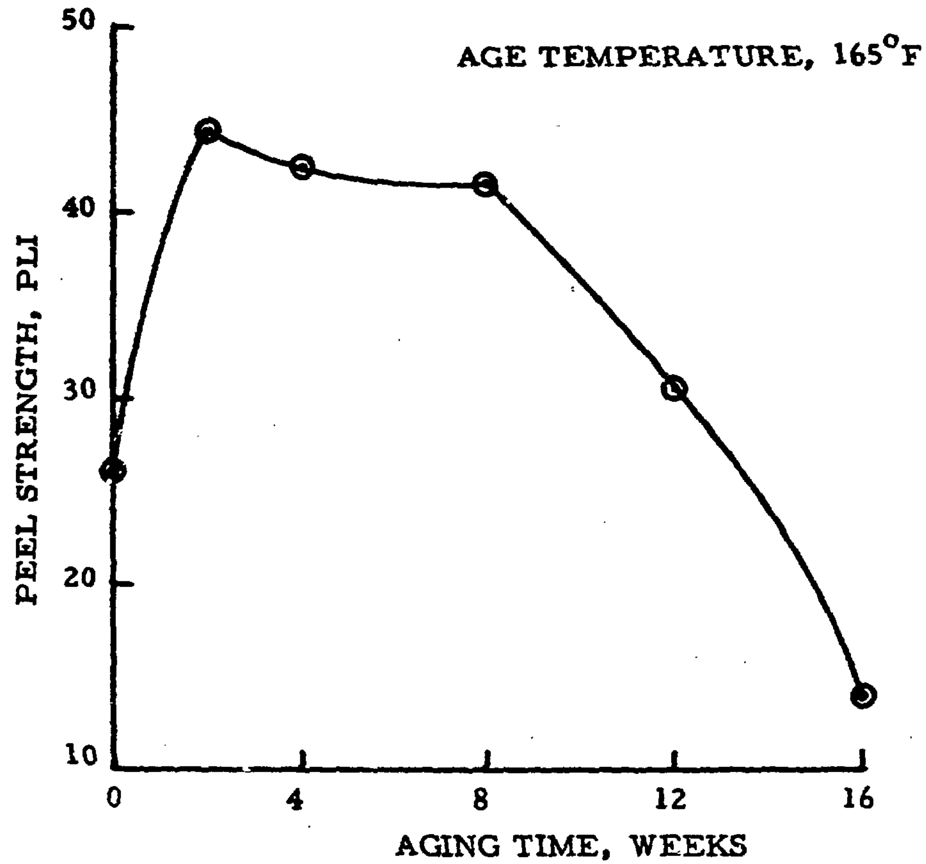


Figure D-2. Minimum Smoke Propellant Propellant-to-Liner Peel Strength

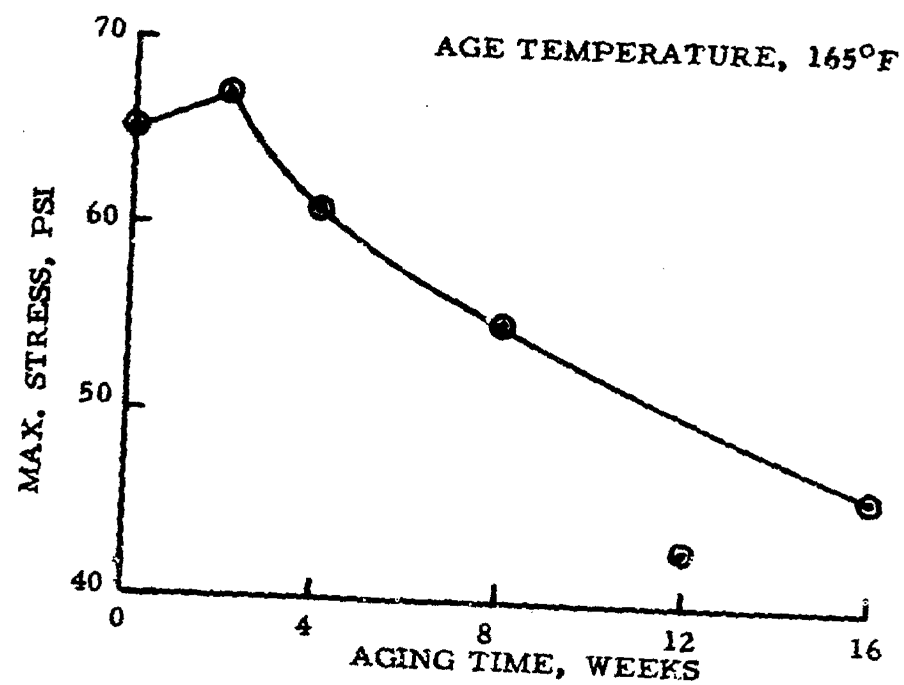


Figure D-3. Minimum Smoke Propellant Composite Bond Tensile Strength

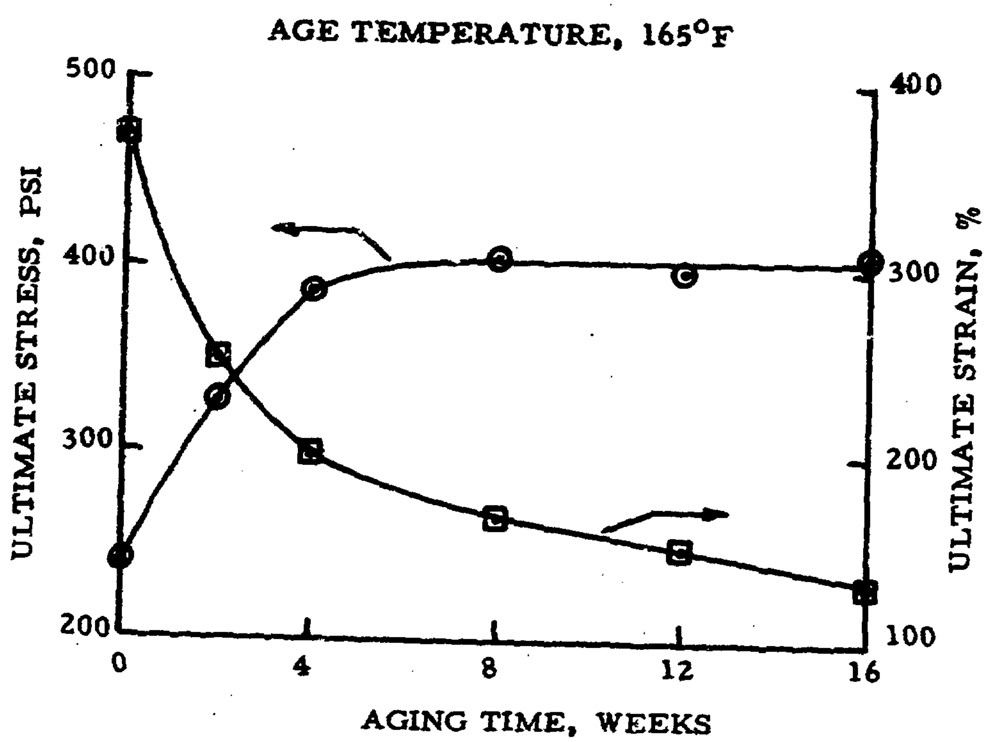


Figure D-4. Minimum Smoke Propellant TL-H774 Liner Tensile Properties

TABLE D-1

## GRADIENT HARDNESS OF INSULATION/LINER/PROPELLANT

(Measurement by Penetrometer)

Propellant: TP-Q7029 (18Q-819)
Liner: TL-H774 (RL-05764)
Insulation: TI-R701 (Lot 6017)

| Age Time Weeks | Insulation | Liner | Distance From Liner, mm | | | | | | | | | | |
|---|---|---|---|---|---|---|---|---|---|---|---|---|---|
| | | | 0.5 | 1.0 | 1.5 | 2.0 | 2.5 | 3.0 | 4.0 | 5.0 | 7.0 | 10.0 | 15.0 |
| 0 | 6.0 | 37.0 | 72.5 | 81.5 | 75.5 | 77.5 | 75.5 | 77.5 | 77.0 | 81.0 | 84.5 | 84.5 | N/A |
| 2 | 9.5 | 31.0 | 78.5 | 82.5 | 83.0 | 80.0 | 76.0 | 80.0 | 81.5 | 81.0 | 87.0 | 86.0 | N/A |
| 4 | 11.0 | 33.0 | 88.0 | 89.0 | 88.5 | 91.5 | 92.5 | 90.5 | 91.5 | 94.0 | 98.0 | 97.0 | 104.0 |
| 8 | 9.5 | 27.5 | 88.5 | 93.5 | 89.5 | 90.0 | 89.0 | 91.0 | 89.0 | 90.5 | 95.5 | 94.0 | 98.0 |
| 12 | 7.0 | 25.0 | 93.0 | 101.5 | 104.5 | 105.0 | 103.0 | 106.0 | 102.5 | 109.5 | 107.5 | 107.5 | 111.0 |
| 16 | 4.5 | 17.0 | 86.5 | 92.5 | 93.0 | 94.0 | 93.0 | 92.0 | 91.0 | 91.0 | 92.5 | 96.5 | 101.5 |

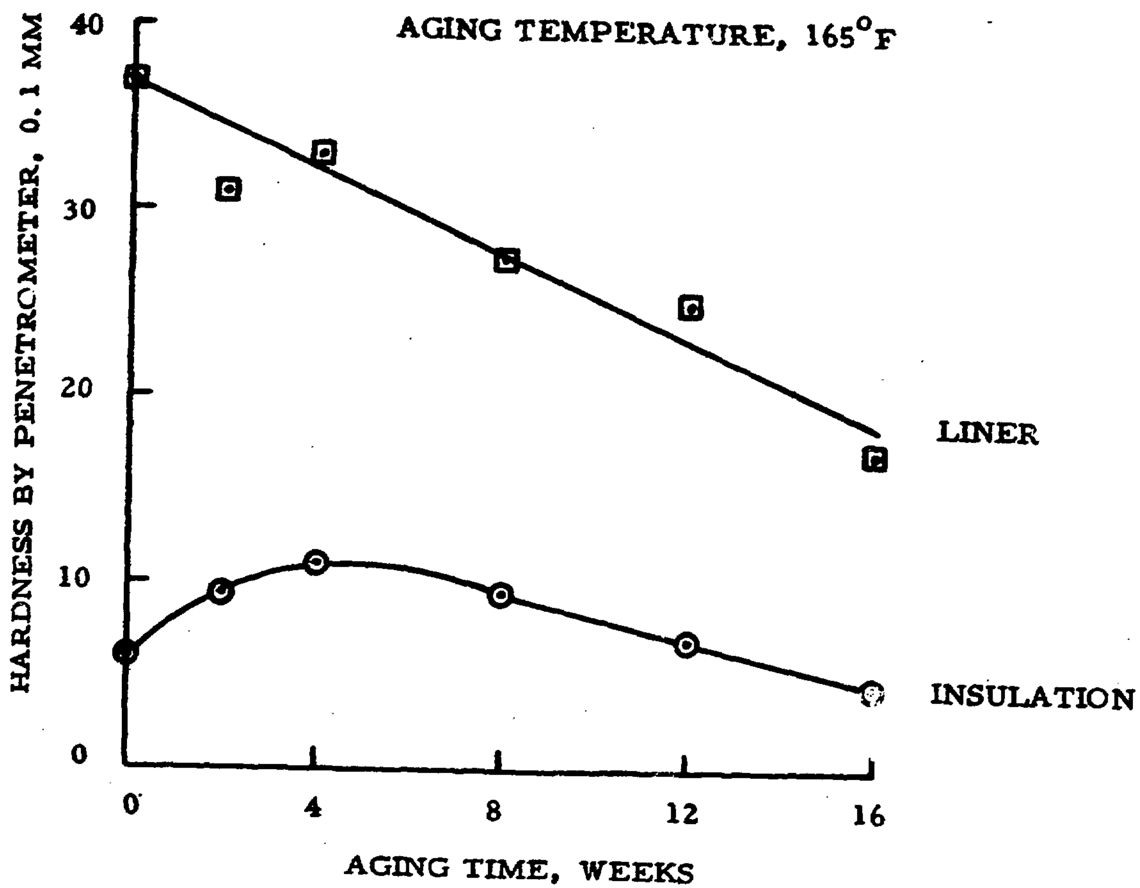


Figure D-5. Minimum Smoke Propellant Liner and Insulation Hardness

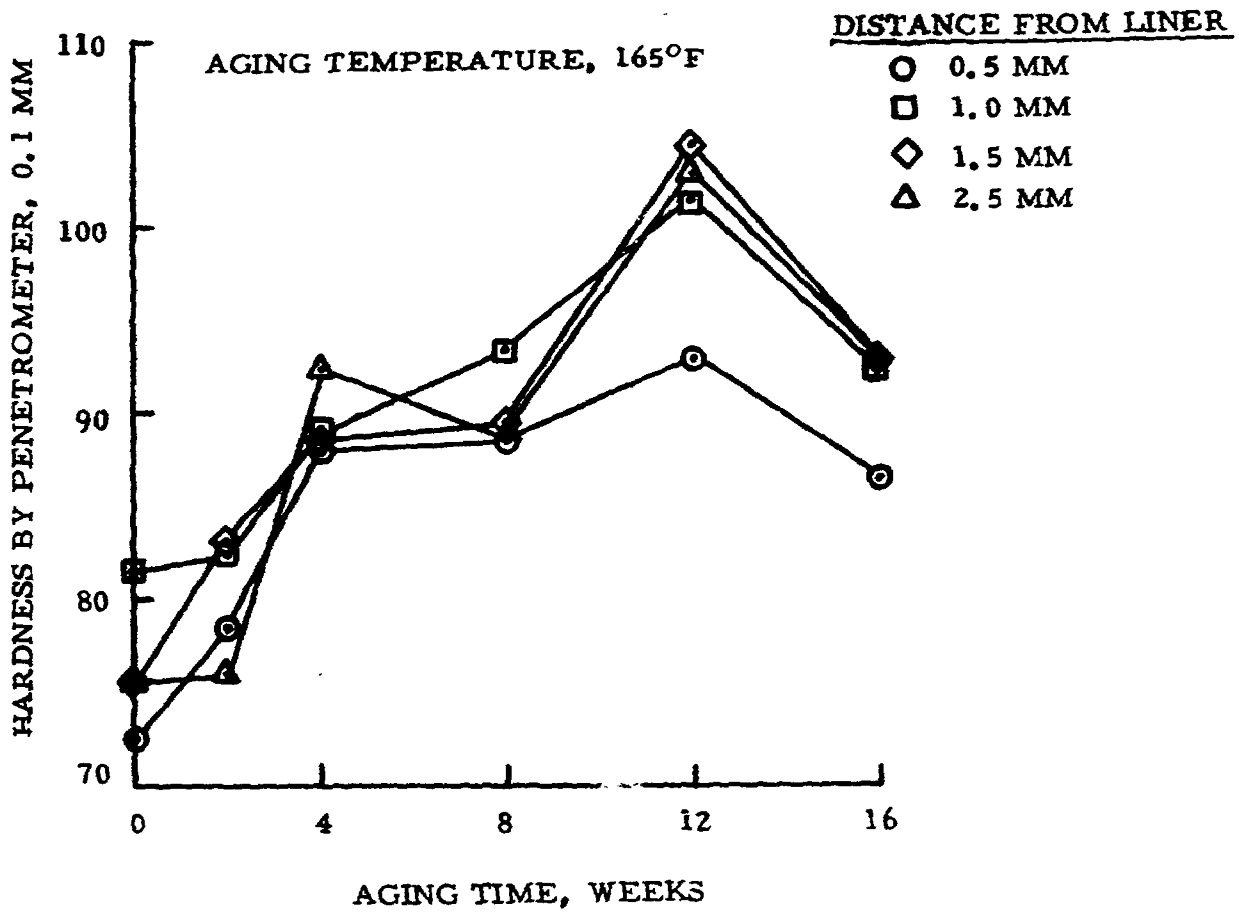


Figure D-6. Minimum Smoke Propellant - Propellant Hardness

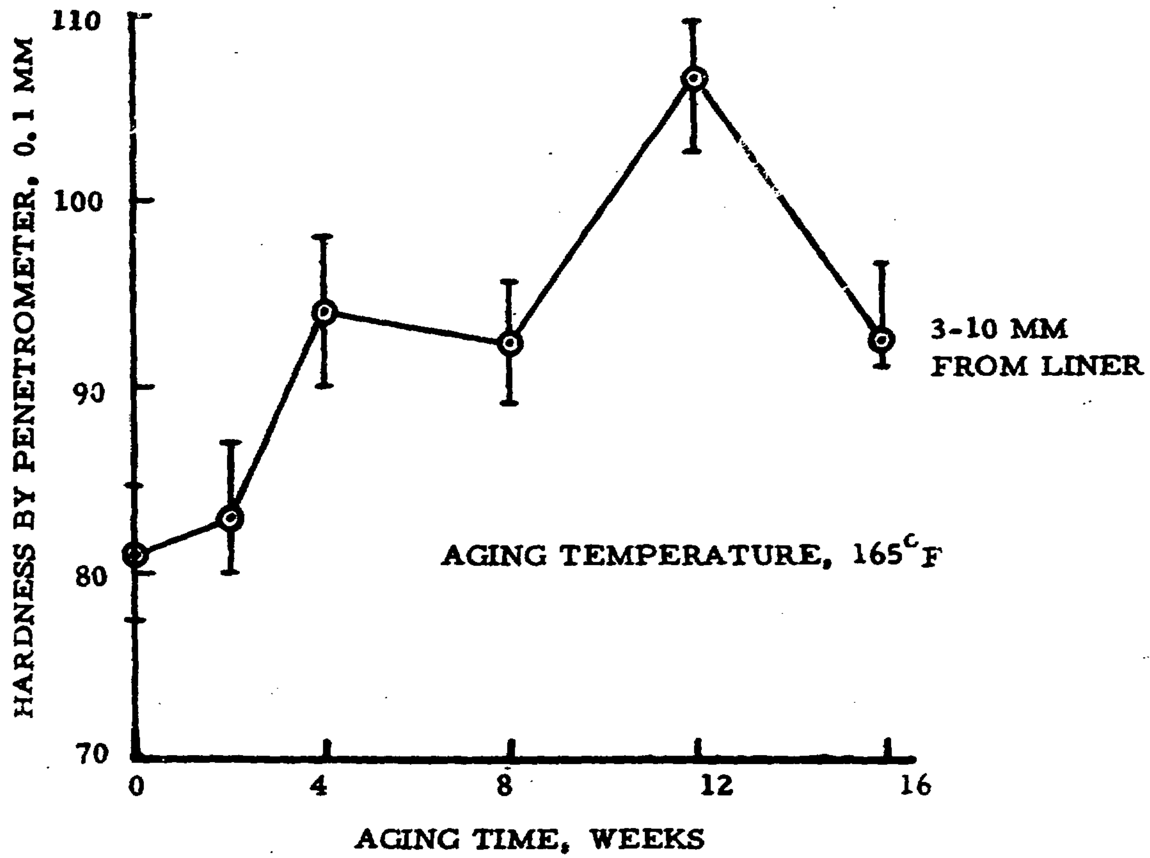


Figure D-7. Minimum Smoke Propellant - Propellant Hardness

TABLE D-2

MINIMUM SMOKE PROPELLANT BINDER GEL FRACTION

| AGE TIME, WEEKS | PROPELLANT BINDER GEL (%) AT DISTANCE FROM LINER, IN. | | | | | | | |
|---|---|---|---|---|---|---|---|---|
| | 0.00 | 0.020 | 0.040 | 0.060 | 0.100 | 0.200 | 0.300 | 0.500 |
| 0 | 85.26 | 86.12 | 88.13 | 88.70 | 91.13 | 65.84 | 84.12 | 87.41 |
| 2 | 91.99 | 88.70 | 89.99 | 91.85 | 90.27 | 93.28 | 89.84 | 90.70 |
| 4 | 89.27 | 85.12 | 89.13 | 87.89 | 88.13 | 86.55 | 87.98 | 84.98 |
| 8 | 84.55 | 97.14(?) | 89.56 | 89.70 | 86.41 | 88.41 | 93.71(?) | 85.26 |
| 12 | 82.26 | 81.83 | 81.55 | 81.97 | 83.55 | 82.40 | 81.97 | 81.12 |
| 16 | 90.99 | 88.70 | 86.70 | 88.98 | 88.41 | 87.41 | 87.55 | 84.12 |

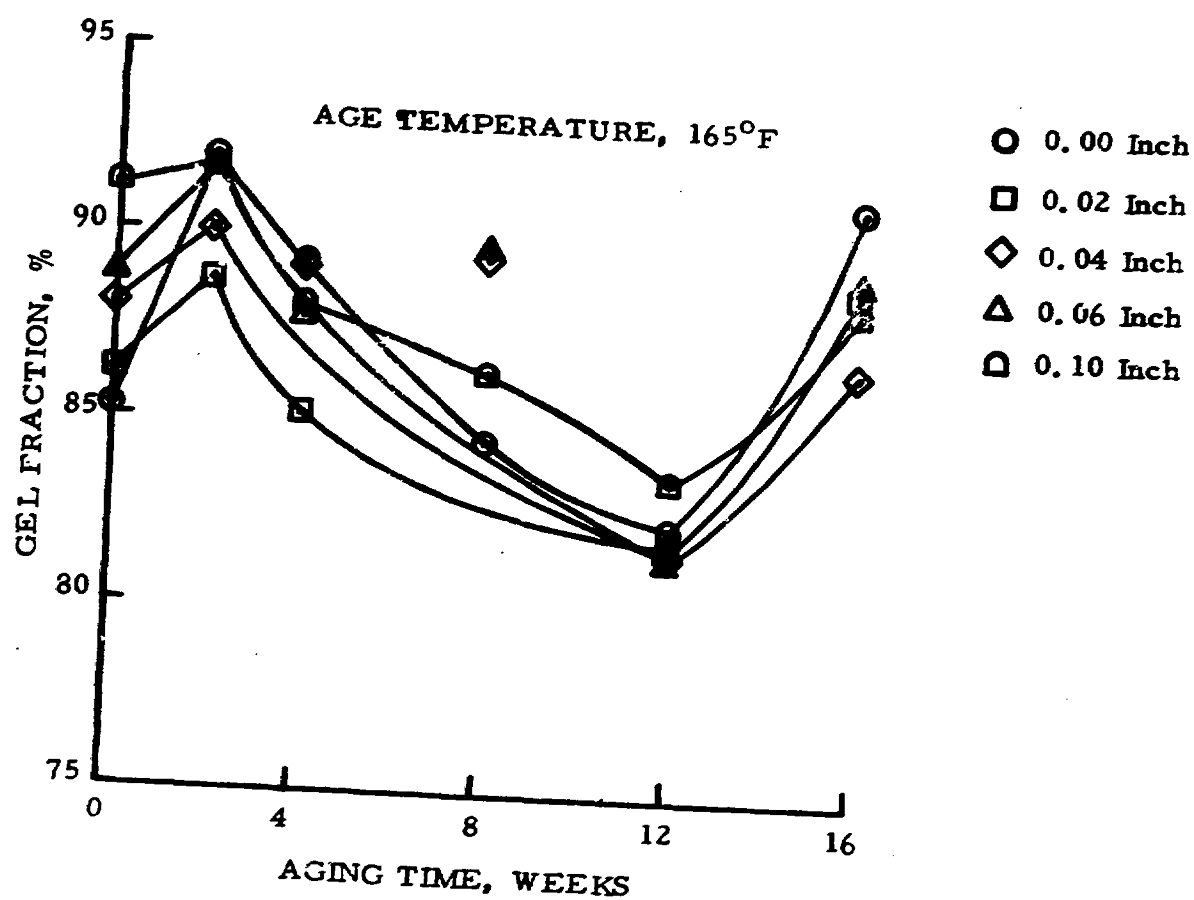


Figure D-8. Minimum Smoke Propellant Change in Propellant Gel Fraction with Time and Distance from Liner Interface

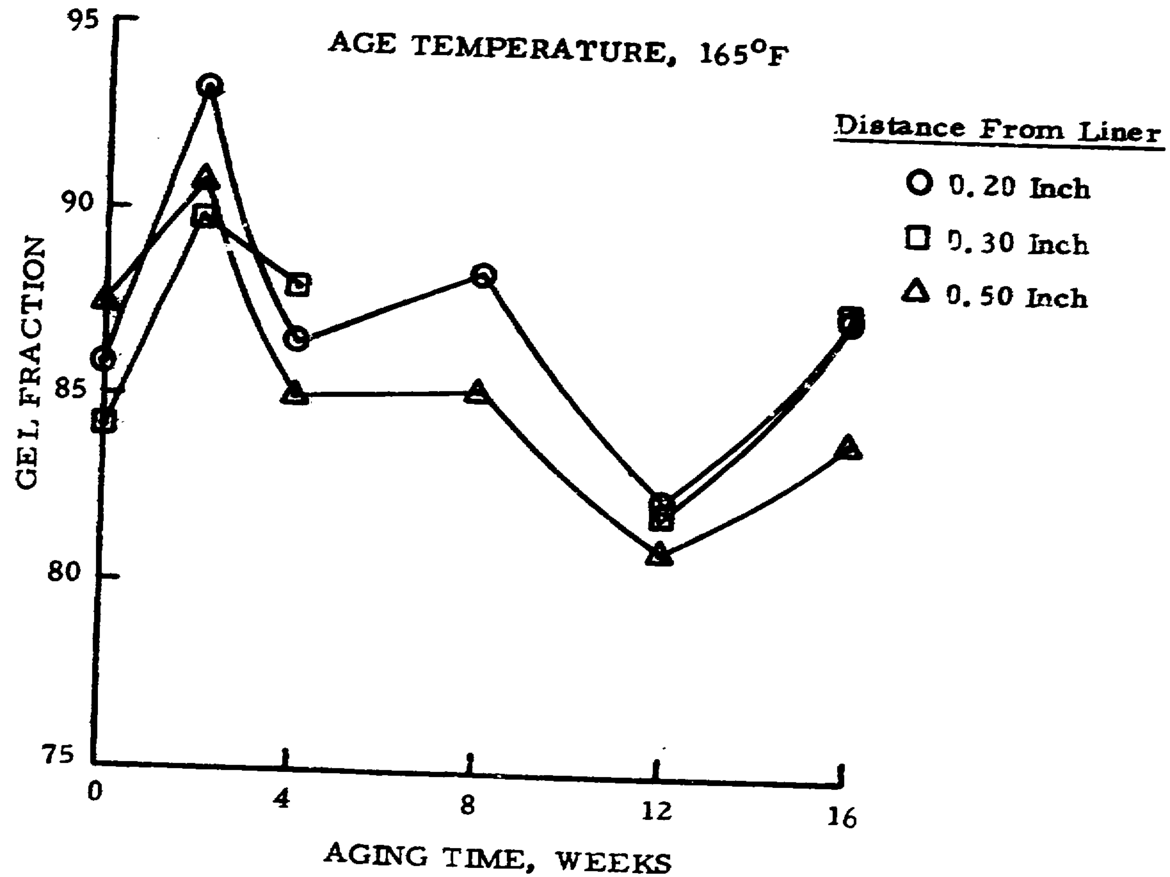


Figure D-9. Minimum Smoke Propellant Change in Propellant Gel Fraction with Time and Distance from Liner Interface

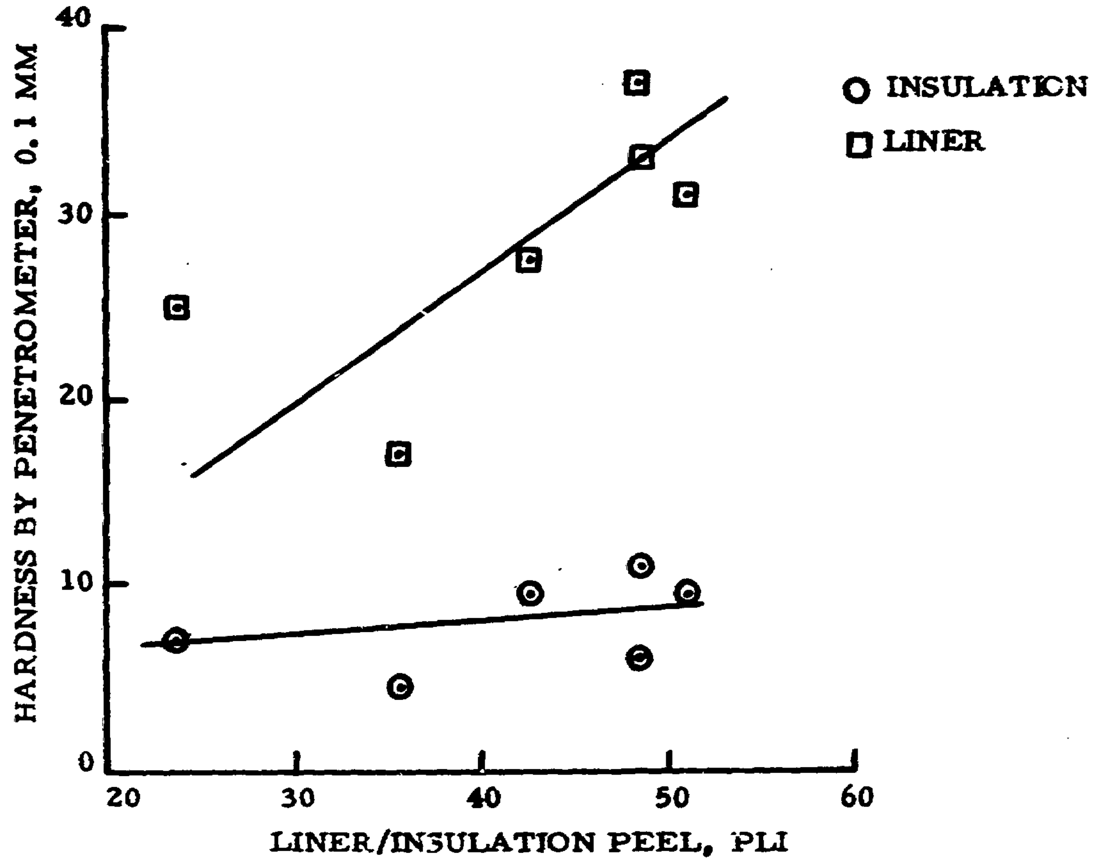


Figure D-10. Minimum Smoke Propellant Correlation Between Hardness and Liner/Insulation Peel Strength

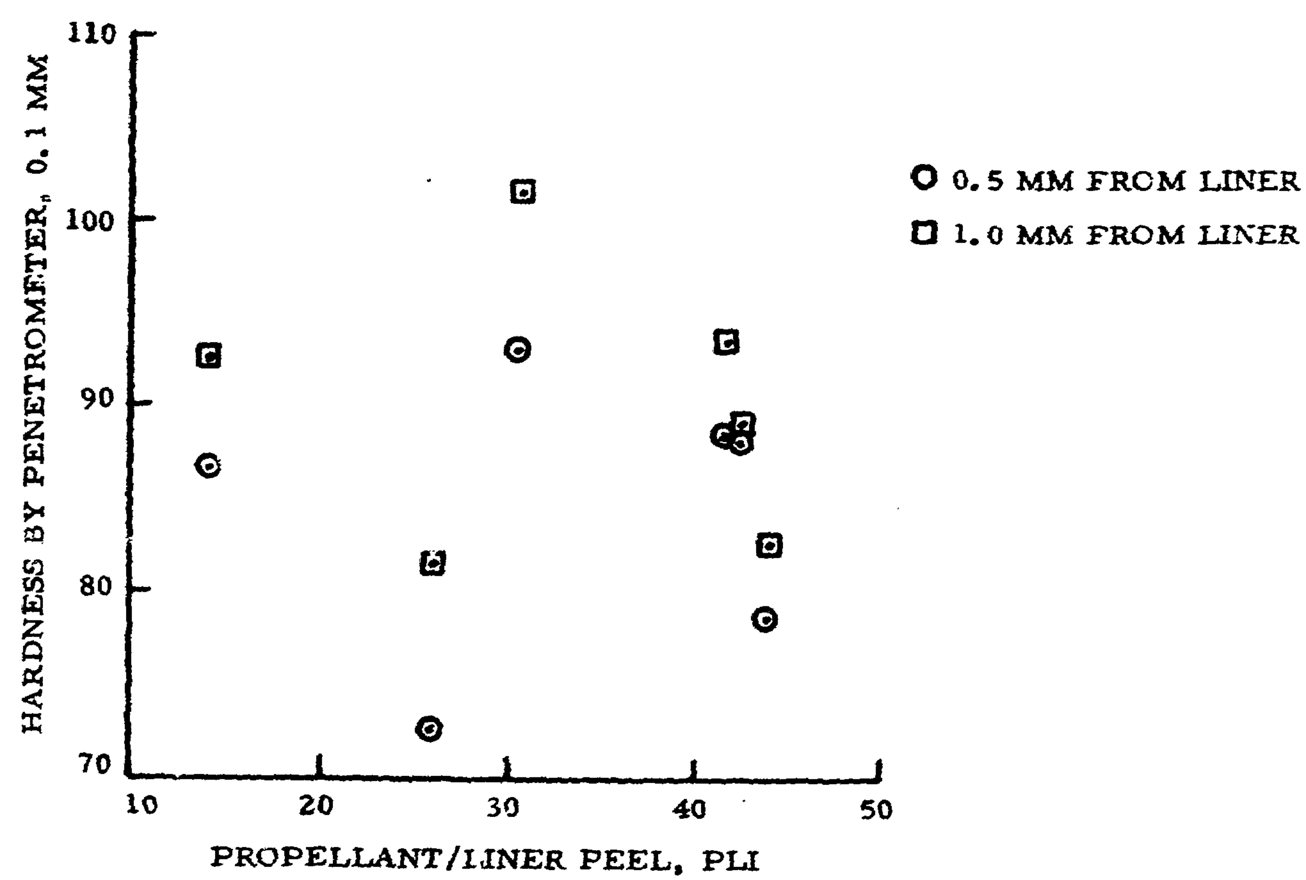


Figure D-11. Minimum Smoke Propellant Correlation Between Propellant Hardness and Propellant/Liner Peel Strength

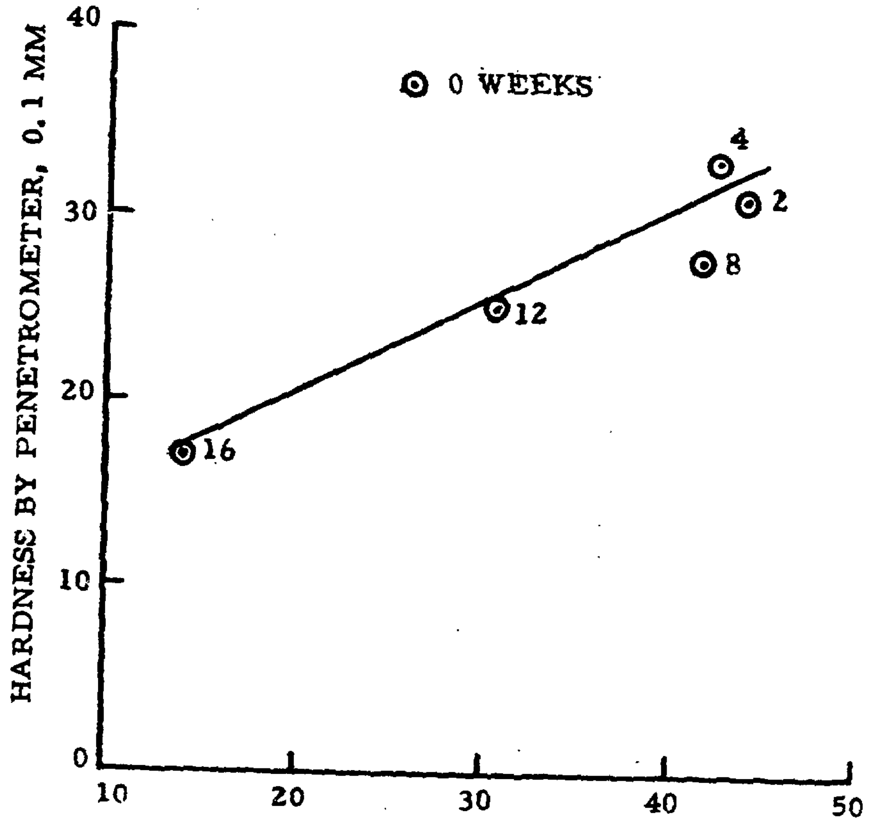


Figure D-12. Minimum Smoke Propellant Correlation Between Liner Hardness and Propellant/Liner Peel Strength

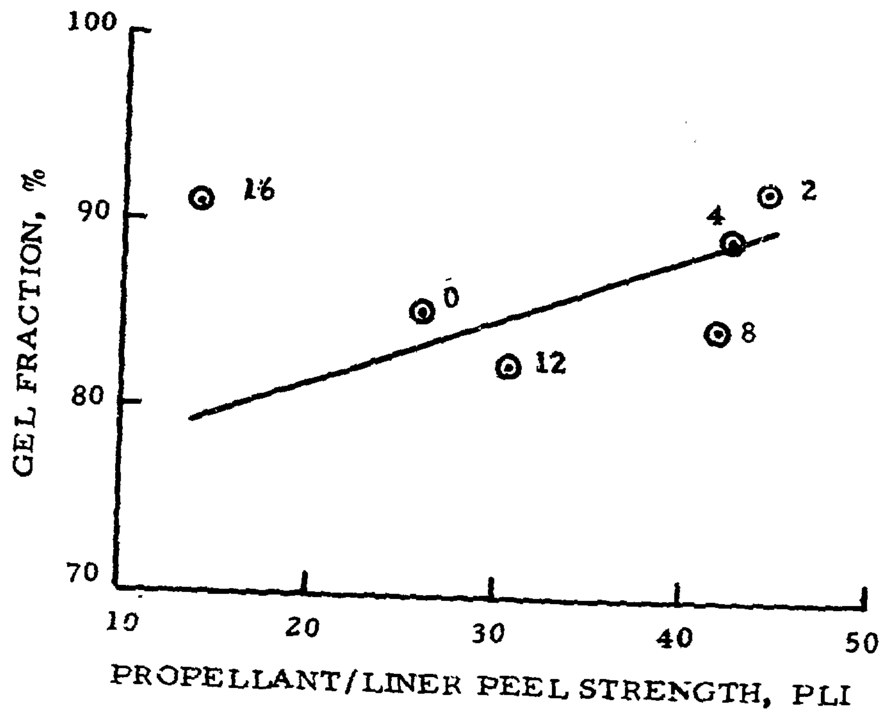


Figure D-13. Minimum Smoke Propellant Correlation of Propellant Gel Fraction at 0.00 In. From Liner with Propellant/Liner Peel Strength

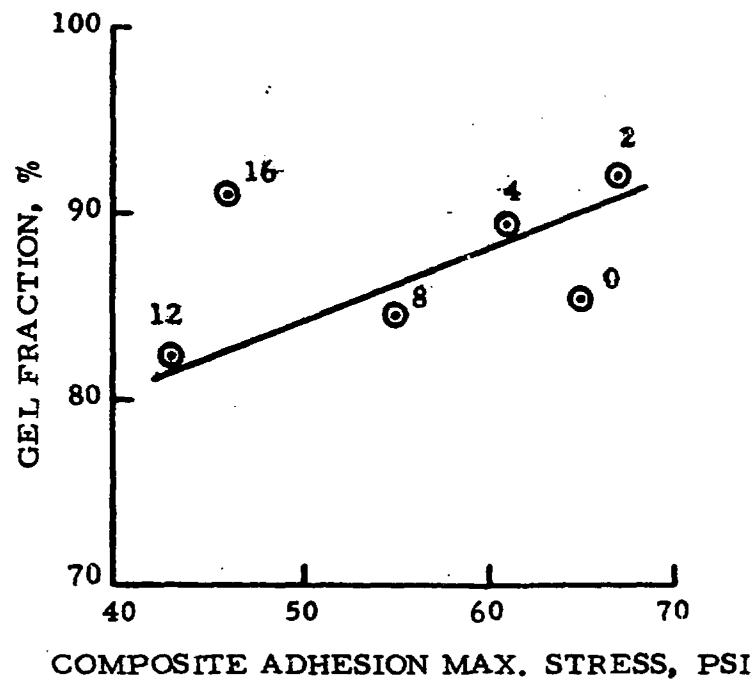


Figure D-14. Minimum Smoke Propellant Correlation of Propellant Gel Fraction at 0.00 In. From Liner with Composite Adhesion Max. Stress

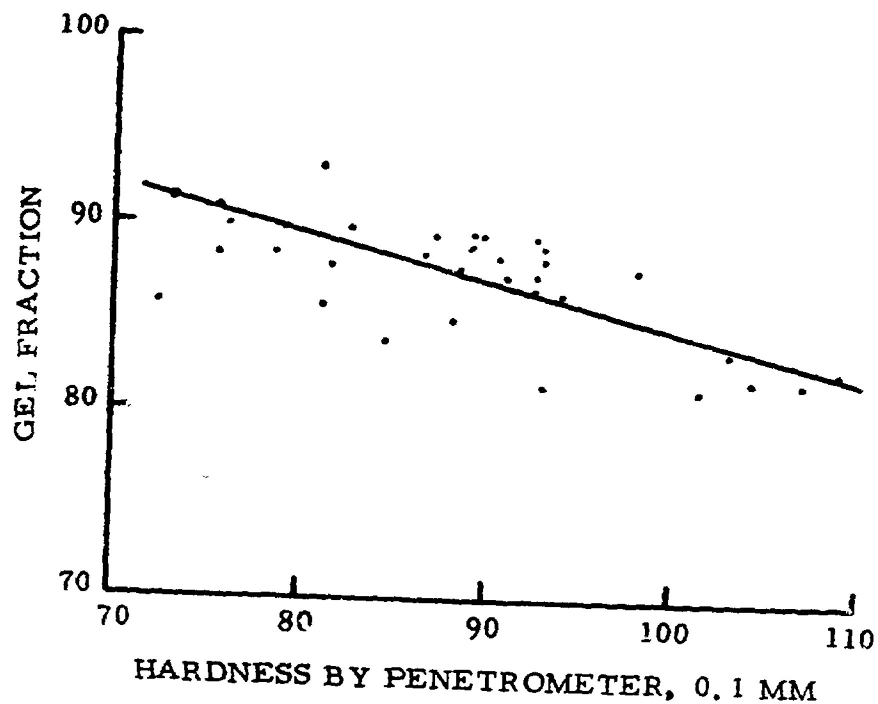


Figure D-15. Minimum Smoke Propellant Correlation of Gel Fraction with Hardness

# APPENDIX E

## DATA PLOTS FOR MSL-303 PROPELLANT

## ACTIVATION ENERGY PLOT

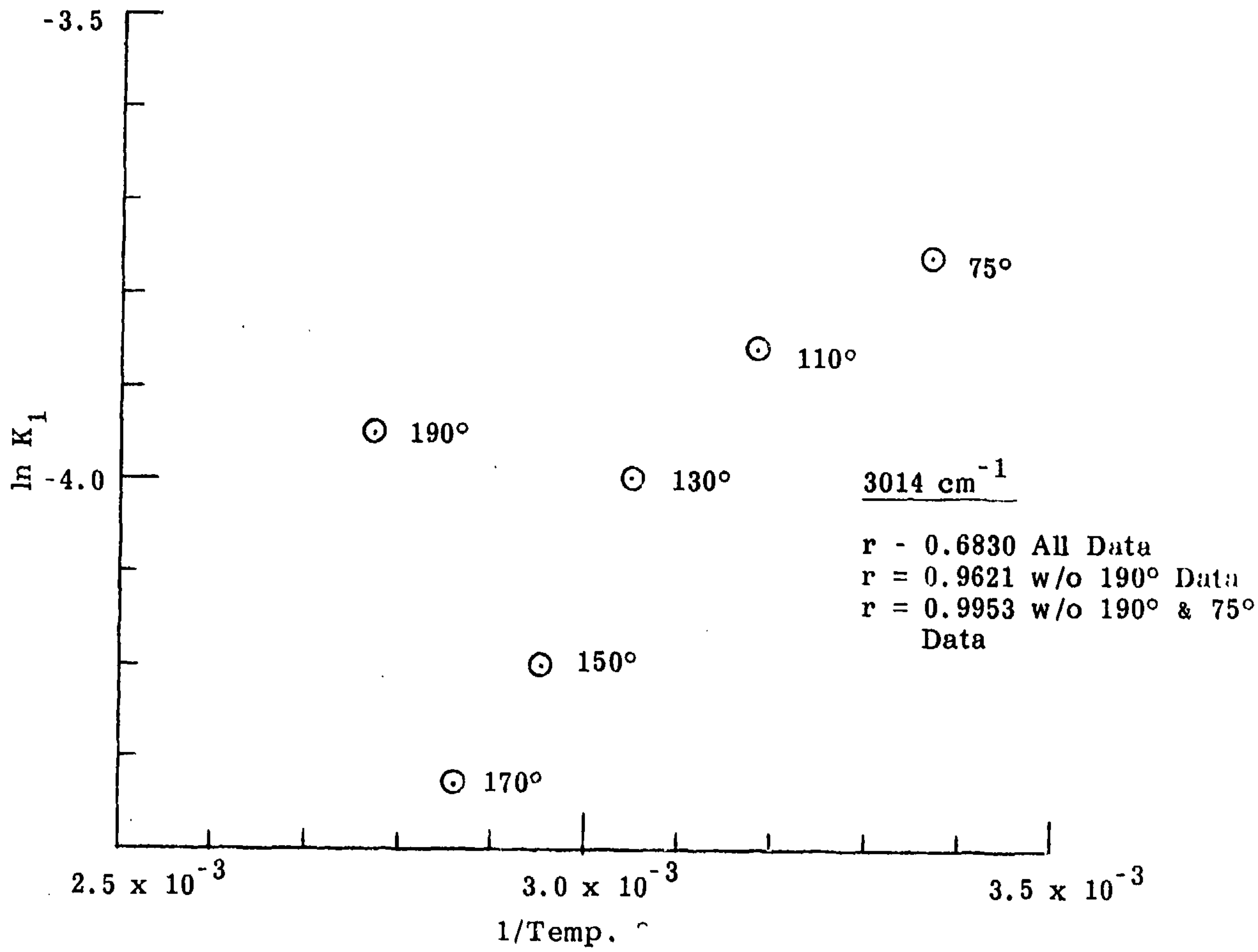


Figure E-1. Activation Energy Plot for the Peak at 3014 $cm^{-1}$.

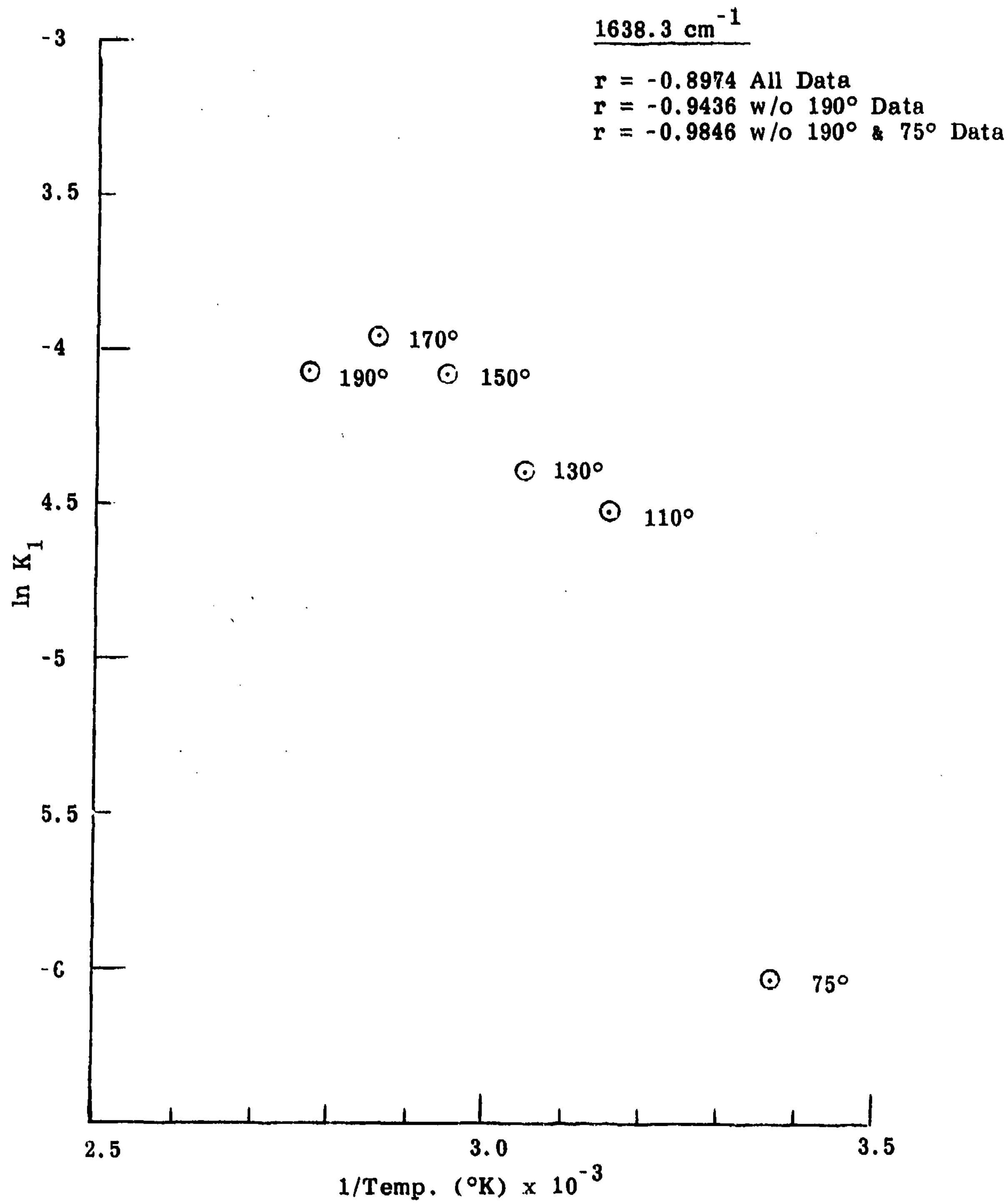


Figure E-2. Activation Energy Plot for the Peak at 1638.3 $cm^{-1}$.

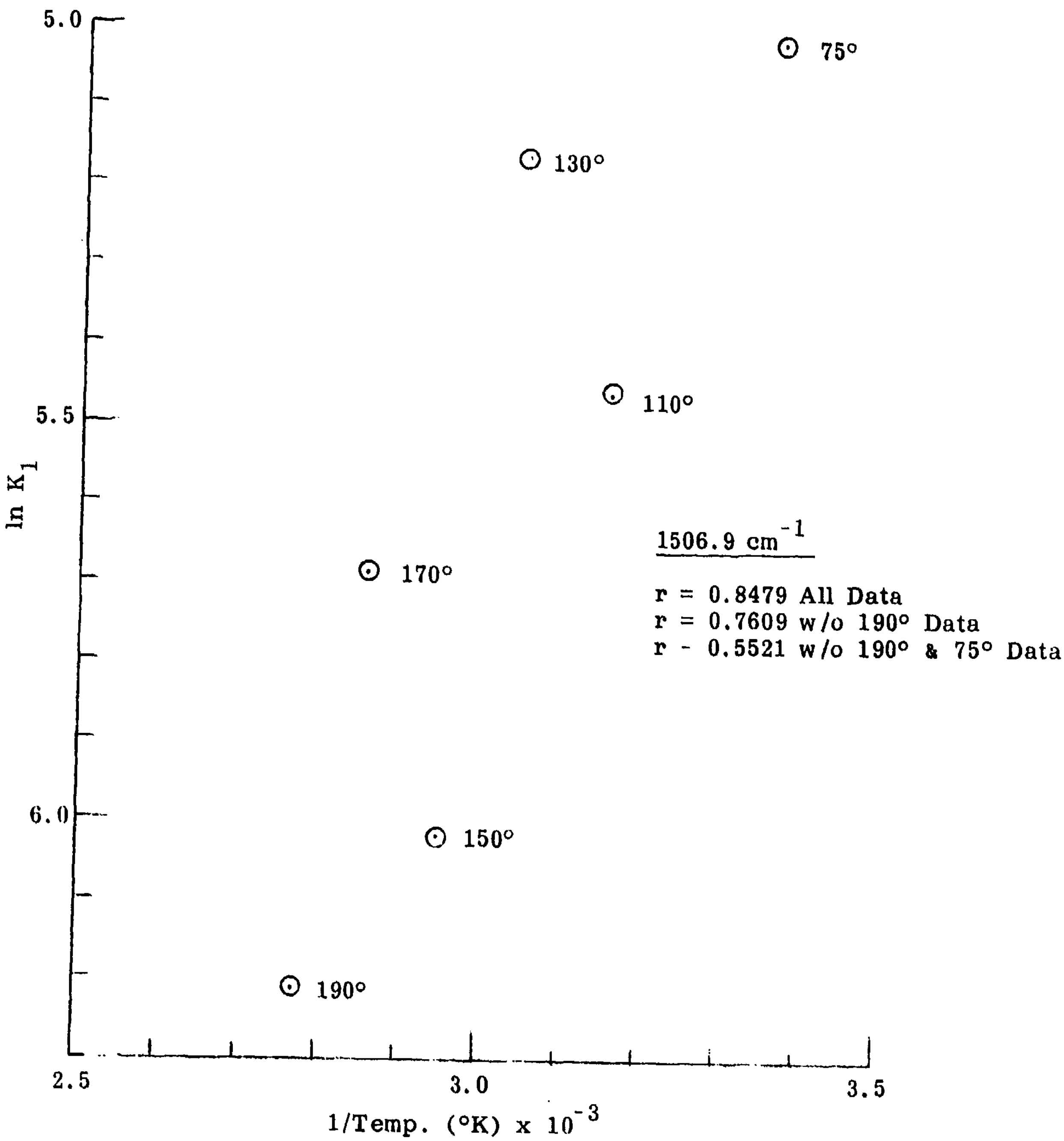


Figure E-3. Activation Energy Plot for the Peak at 1506.9 $cm^{-1}$.

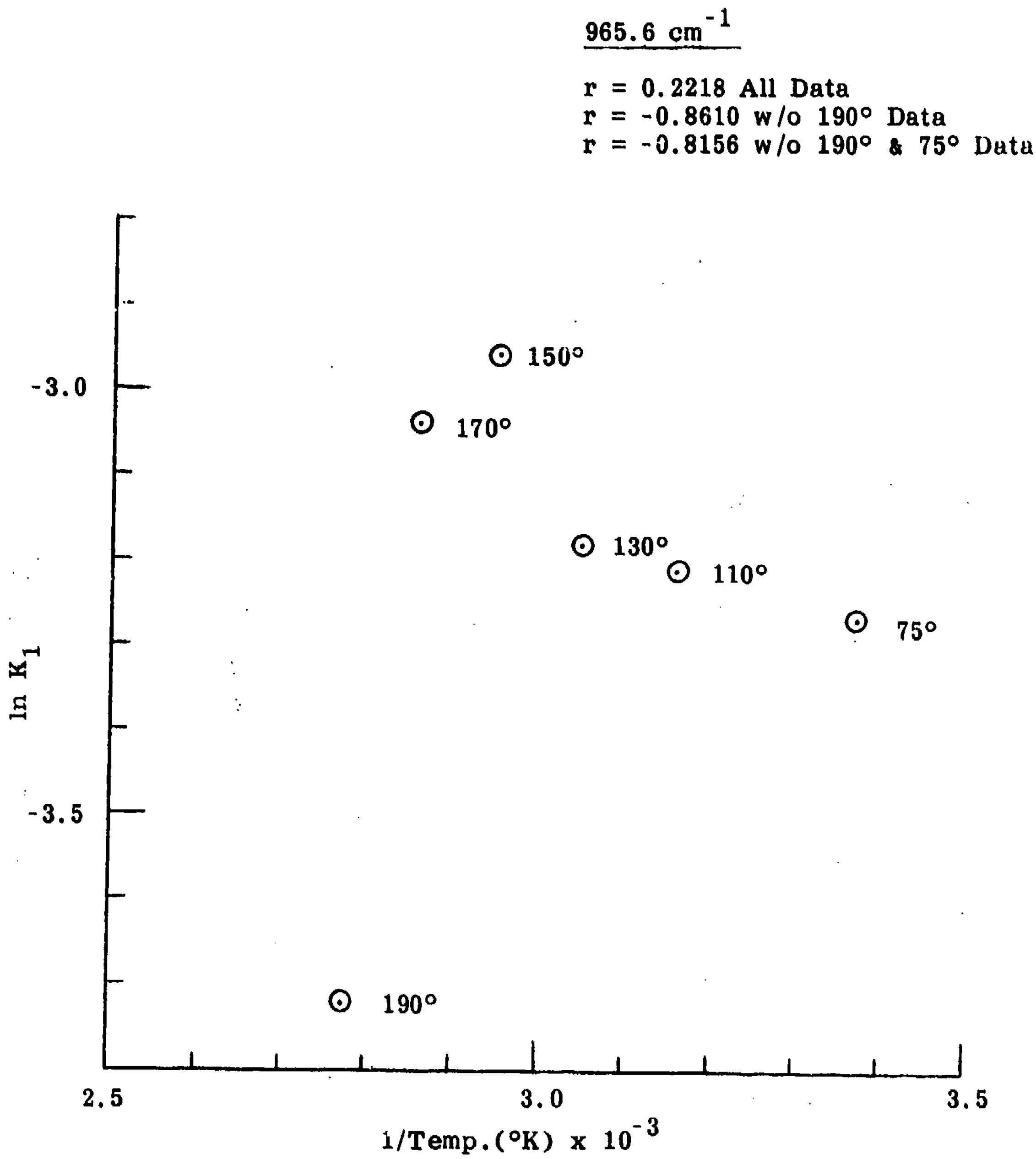


Figure E-4. Activation Energy Plot for the Peak at 965.6 $cm^{-1}$.

MSL-303

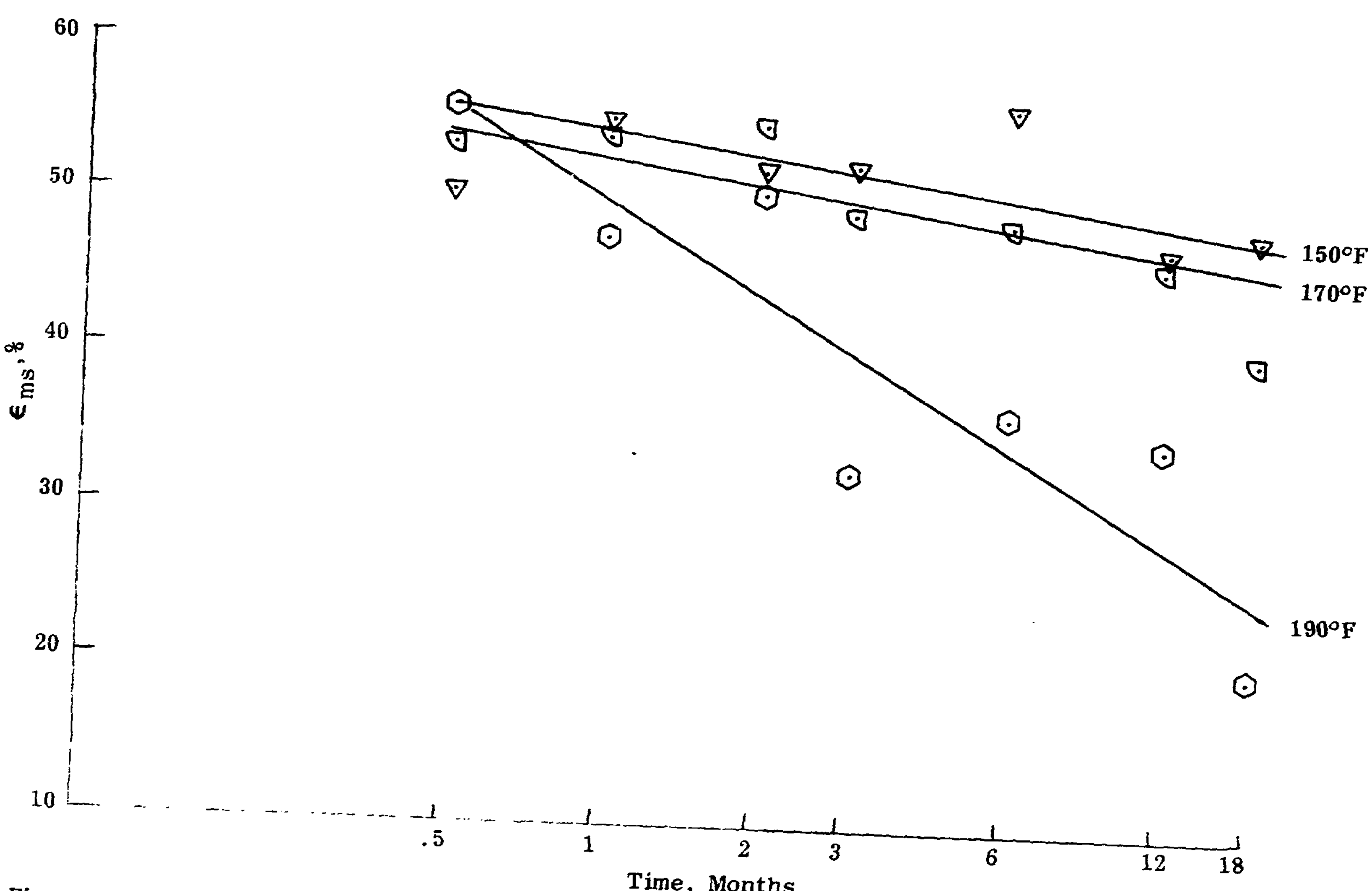


Figure E-5. Variation of Strain at Max. Stress with Log Age Time.

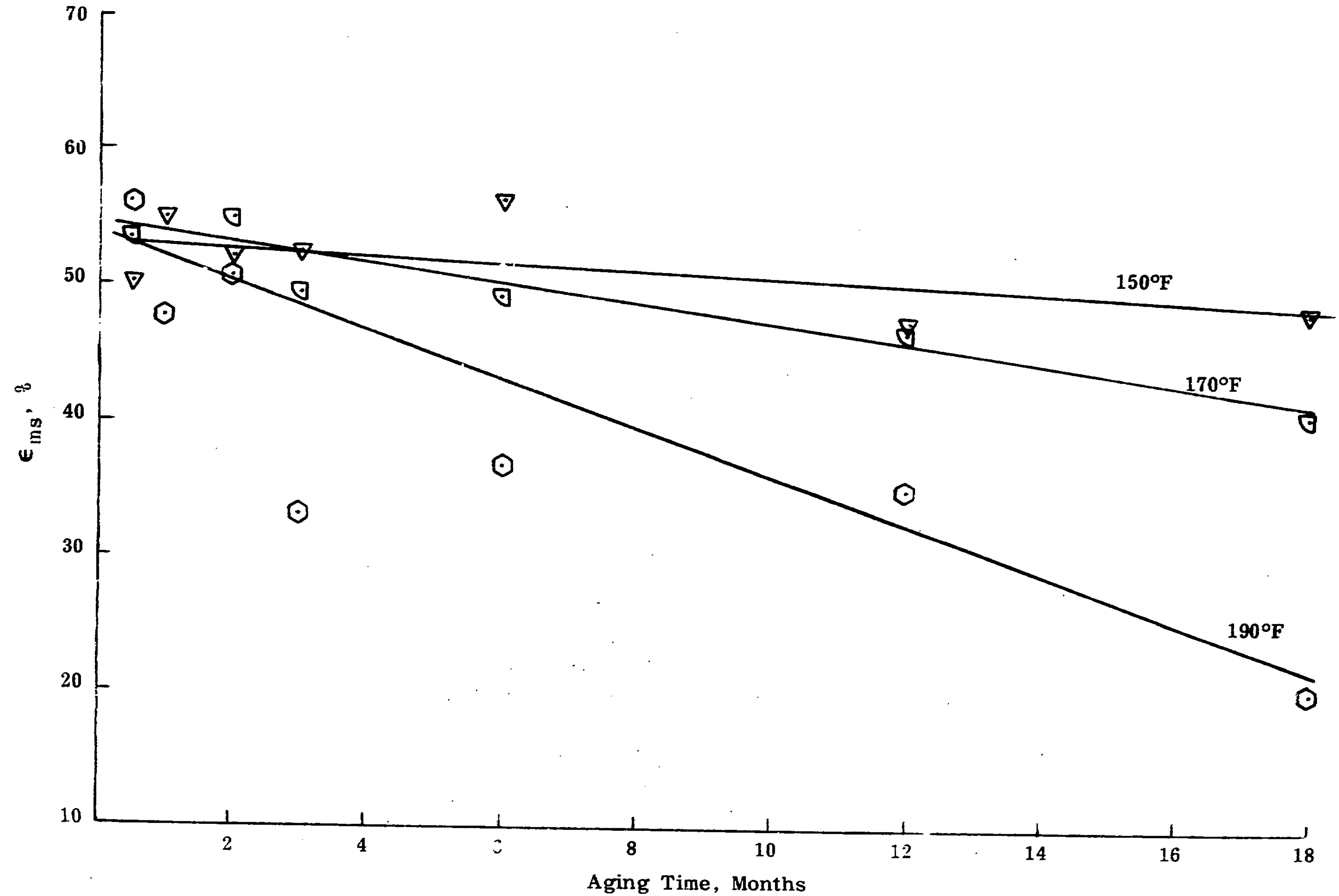


Figure E-6. Variation of Strain at Max. Stress with Age Time.

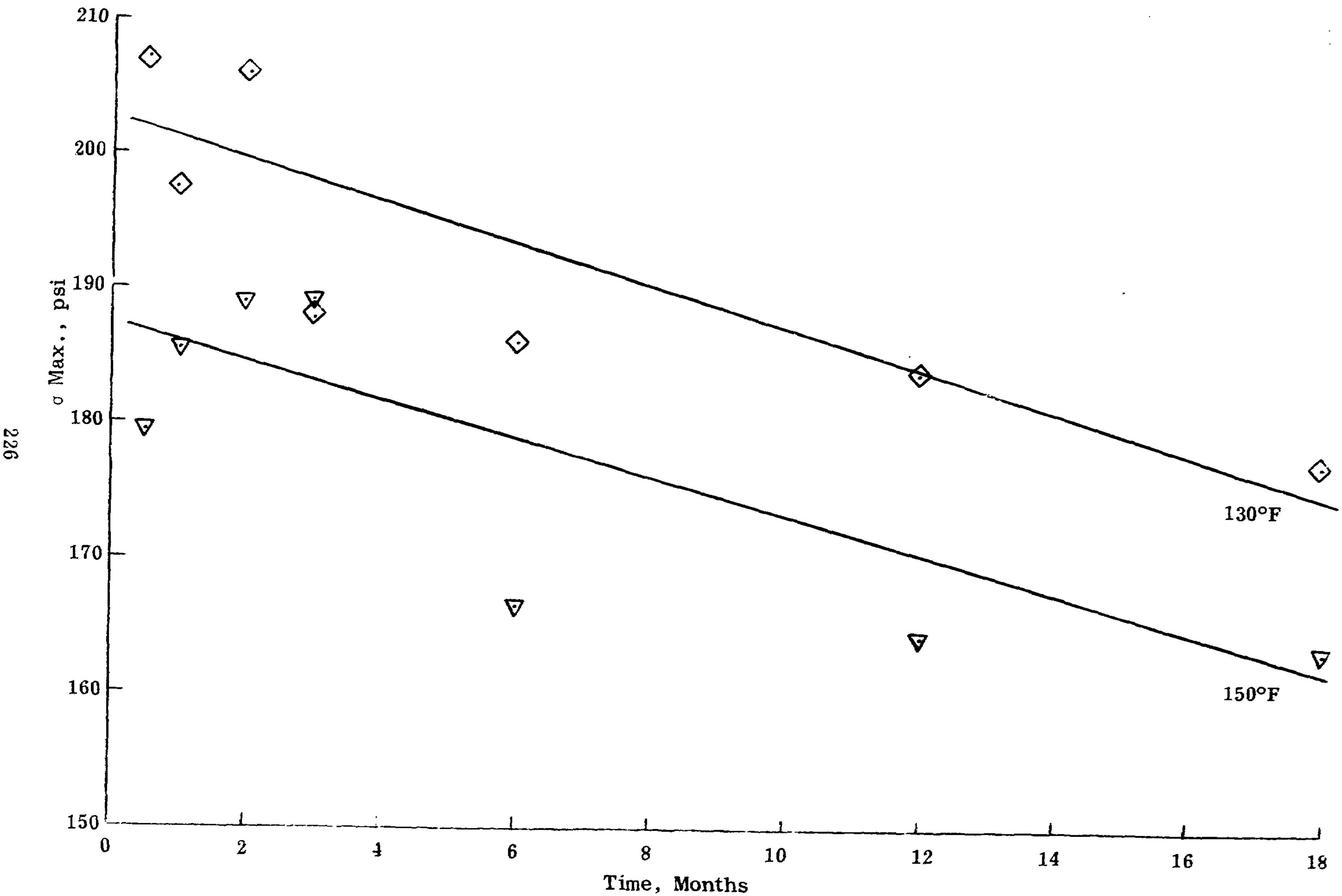

Figure E-7. Variation of Max. Stress with Age Time.

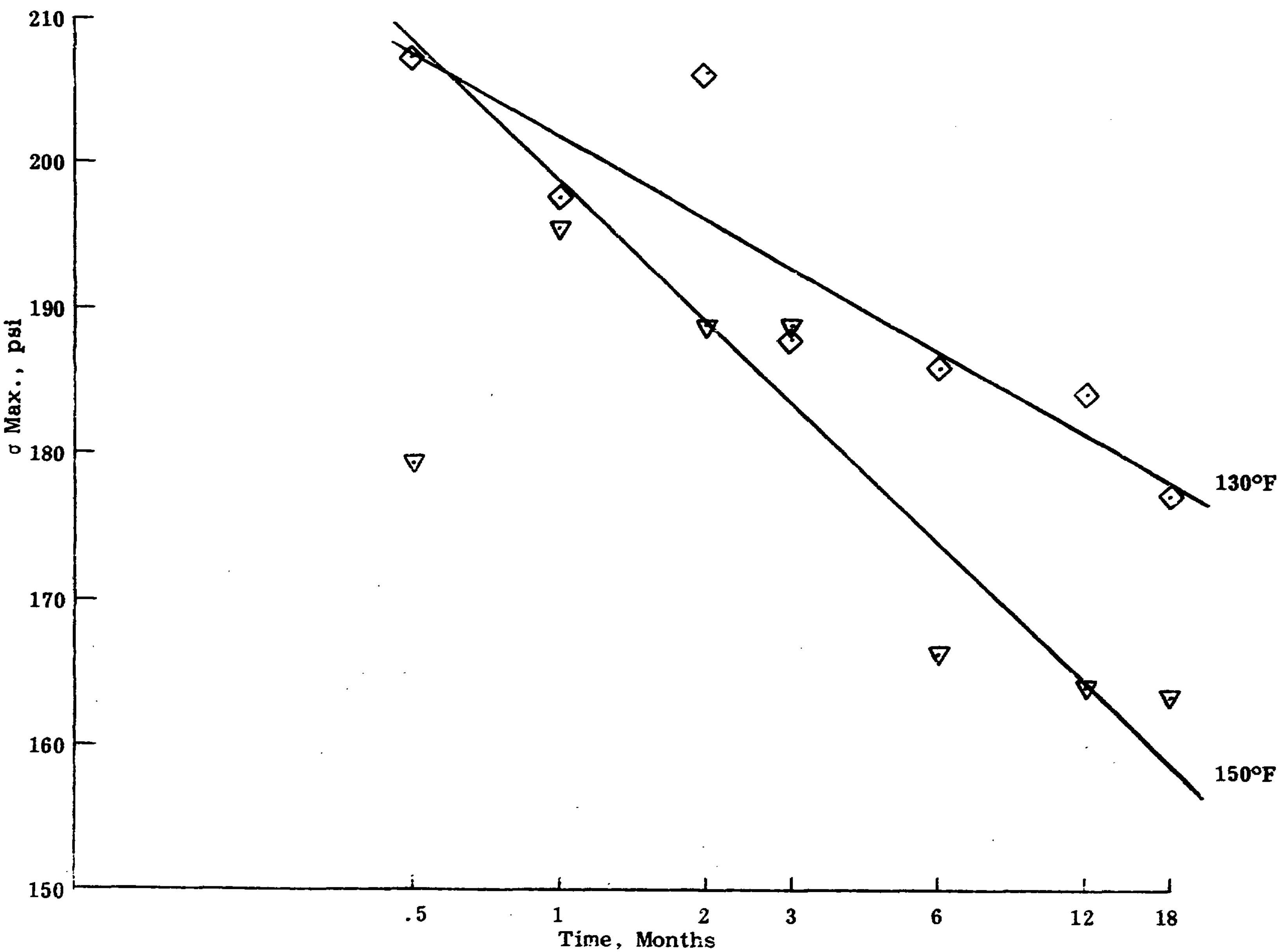


Figure E-8. Variation of Max. Stress with Log Age Time.